

PHYLOGENETIC RELATIONSHIPS WITHIN *COLUMNEA* SECTION  
*ANGUSTIFLORAE*: INSIGHTS INTO FORCES DRIVING SPECIATION

by

Lacie Janelle Schulte

A thesis

submitted in partial fulfillment  
of the requirements for the degree of  
Master of Science in Biology  
Boise State University

August 2012

© 2012

Lacie Janelle Schulte

ALL RIGHTS RESERVED

BOISE STATE UNIVERSITY GRADUATE COLLEGE

**DEFENSE COMMITTEE AND FINAL READING APPROVALS**

of the thesis submitted by

Lacie Janelle Schulte

Thesis Title: Phylogenetic Relationships within *Columnnea* Section *Angustiflorae*:  
Insights into Forces Driving Speciation

Date of Final Oral Examination: 01 June 2012

The following individuals read and discussed the thesis submitted by student Lacie Janelle Schulte, and they evaluated her presentation and response to questions during the final oral examination. They found that the student passed the final oral examination.

James F. Smith, Ph.D.	Chair, Supervisory Committee
Steven J. Novak, Ph.D.	Member, Supervisory Committee
Merlin White, Ph.D.	Member, Supervisory Committee
John L. Clark, Ph.D.	Member, Supervisory Committee

The final reading approval of the thesis was granted by James F. Smith, Ph.D., Chair of the Supervisory Committee. The thesis was approved for the Graduate College by John R. Pelton, Ph.D., Dean of the Graduate College.

## DEDICATION

To my parents, Don and Vickie, and my brother, Alex, for their unending support in all my endeavors. To Elizabeth Bader, for always encouraging me to spread my wings and fly.

## ACKNOWLEDGEMENTS

This thesis would not have been possible without the contributions and support of many people, but none were more important than my major advisor, Dr. James F. Smith. I would like to thank Jim first for giving me this opportunity despite my lack of experience in both botany and phylogenetics. His passion and expertise in both fields made the learning process much easier. I am grateful that Jim has pushed me out of my comfort zone to become a better scientist and writer. I cannot express how much his patience and guidance have meant to me throughout this whole process.

I would also like to thank my committee members for their assistance throughout this process: Dr. Stephen J. Novak for his insightful suggestions and explanations; Dr. Merlin White for his comments on brevity; and Dr. John L. Clark for his hours collecting plant material and knowledge of *Columnea* morphology.

This research was made possible by the many donations of plant material. Both Dr. James F. Smith and Dr. John L. Clark have spent countless hours collecting material, and the majority of specimens sampled came from their collections. I would also like to thank Larry Skog, Nancy and Jerry Kast, Bob Stewart, Bill Price, Carol Ann Bonner, Julie Mavity-Hudson, and Karen Cichocki, who have graciously donated plant material. In addition, I would like to thank the Selby Botanical Garden, Missouri Botanical Garden, Smithsonian Institute, National Herbarium of Colombia, University of the West

Indies, and Institute of Jamaica Herbaria for donating material and allowing us to photograph their specimens.

I was also given the opportunity to do field work in Jamaica. This field work would not have been possible without Keron Campbell and Judeen Meikle at the Institute of Jamaica. Keron and Judeen were gracious enough to accompany us into the field and help us find our way around Jamaica.

I would also like to thank my fellow lab members. Shandra Jeffries and Maggie Ooi made this thesis possible by helping gather molecular data, georeferencing herbarium specimens, and making work fun each and every day. Thank you also to Danielle Clay who helped me with lab techniques and made me feel welcome when I first arrived at Boise State and Patrick Kolar for all his help with GIS. I would also like to say thank you to the many individuals who have made my time at Boise State a memorable experience: Morgan Peters, Emma Wilson, Jessie Sherburne, Allison Korte, and many other friends and colleagues in the graduate program.

I must also acknowledge both Jane Wattrus and Gerald Cizadlo for their help in applying to the graduate program at Boise State. Without their initial encouragement and continued support, I would not have gone to graduate school.

No acknowledgement section would be complete without my family and friends. I am lucky to have an amazing support group across the country that has seen me through this entire process. I could not name them all, but I must say thank you to the people who heard me complain during the hard times but do not hear thank you enough: Mom and Dad, Al, Kathy and Randy, Linda and Jeff, Elizabeth, Kelly, and Caitie - thank you so much for all your love and support.

This research was made possible by funding from the National Science Foundation and the Gesneriad Society Elvin McDonald Research Endowment Fund. I would also like to thank the Gesneriad Society for awarding me the Student Travel Grant that allowed me to attend the 2011 Gesneriad Convention and meet so many of these Gesneriad enthusiasts who keep these plants growing and make Gesneriaceae research possible.

## ABSTRACT

Determining the specific factors that played a role in speciation previously took extensive resources that made such studies nearly intractable. Despite the difficulties presented by speciation studies, we are still interested in determining what forces drive the process of evolution to gain a better understanding of divergence among species. Advances in technology allow for a new approach to speciation studies, beginning with molecular phylogenetic analyses that identify the species within a monophyletic clade and generate a species-level phylogeny. Molecular data are an independent source of data and provide a phylogeny to map both morphological characters and ecological parameters. Identifying patterns among phylogenetic studies, morphological characters, and ecological variables highlight possible forces driving speciation.

Morphological characters have previously provided the foundation for phylogenetics. However, convergence among characters has made phylogenetic studies difficult based on morphology alone. Molecular phylogenetic analyses provide better insight into relationships across the family and as a result, better classification systems that are a reflection of ancestral evolutionary history rather than convergent evolution.

As the largest Neotropical genus in the family Gesneriaceae, with over 200 species, *Columnnea* has had a complex taxonomic history with classification systems based on morphological characters including vegetative, nectary, and floral characters. Most recent classification systems had classified the species of *Columnnea* into five

sections: sections *Columnnea*, *Collandra*, *Ortholoma*, *Pentadenia*, and *Stygnanthe*.

Section *Stygnanthe* encompassed eighteen species based on a similar floral morphology, characterized by small corollas that are slightly ventricose and constricted at the base, ranging in size from 1.4 to 5.2 cm in length.

A well-supported topology of the species of *Columnnea* can test the previous subgeneric classifications. The phylogenetic analyses presented here sampled 129 accessions representing 90 species within *Columnnea*. Of the 90 species included, fifteen of the eighteen species of *Stygnanthe* were sampled along with an additional three species, *Columnnea grisebachiana*, *C. moorei*, and *C. ulei*, which had not been placed in *Stygnanthe* but share a similar corolla morphology. Based on five chloroplast DNA (cpDNA) gene regions (*trnQ-rps16* spacer, *rpl32-trnL<sub>UAG</sub>* spacer, *rps16* intron, *trnS-G* spacer, and *trnH-psbA* spacer) and nuclear ribosomal internal transcribed spacers (ITS1 and ITS2, hereafter referred to as ITS) the results of this study indicated that the species of section *Stygnanthe* and the three additional species all with similar corolla morphologies, belong in three separate clades within *Columnnea*. Three of the species from *Stygnanthe* (*C. moesta*, *C. ultraviolacea*, and *C. xiphoidea*), including the type species and one of the additional species (*C. moorei*), were separated from the remaining twelve species of *Stygnanthe* that were tested. Because the type species (*C. moesta*) moved to another clade, most of the species of the former section *Stygnanthe* and one of the additional tested species (*C. ulei*) belong within section *Angustiflorae*. The other tested species, *C. grisebachiana*, fell out into a third separate clade. The results indicate that within *Columnnea* small corollas that are slightly ventricose and constricted at the base are the result of convergent evolution.

Molecular phylogenetic analyses with five cpDNA gene regions and ITS provided phylogenetic support for seven monophyletic clades within *Columnnea* but failed to resolve species-level relationships within clades. Additional molecular phylogenetic analyses were conducted to resolve species level relationships with 36 accessions, representing thirteen of fifteen species within *Angustiflorae*. The external transcribed spacer (ETS) was added to the sequences from the five cpDNA gene regions and ITS from the genus wide analysis to generate a well-resolved species level phylogeny. In addition, two low-copy nuclear gene regions, glyceraldehyde 3-phosphate dehydrogenase (*G3pdh*) and NADP-dependent isocitrate dehydrogenase (*idh*) were included to boost phylogenetic support of the major branching events within the section.

This study used these molecular phylogenetic analyses along with morphological characters and climatic variables to determine driving forces of speciation within section *Angustiflorae*. The species in section *Angustiflorae* have morphological variation and cover nearly the full geographic and climatic range of *Columnnea*, making speciation studies interesting and possible. Studying evolutionary and ecological parameters approaches speciation from a new angle, identifying patterns among phylogenetic studies, morphological characters, and ecological parameters. Correlation analyses between parameters identify possible forces that have driven evolutionary divergence by highlighting relationships between character states over the phylogenetic history. Character state shifts may indicate the larger forces that are driving evolutionary divergence. This study mapped fourteen morphological characters, phenology, and nineteen climate variables onto the species level phylogeny of *Angustiflorae*, and patterns were identified with ancestral state reconstructions and correlation analyses. Defining

patterns among morphological characters (including phenology) and climatic variables showed evidence for allopatric speciation, changes in photosynthetic ability, nectar robbing, pollinator shifts, and climate changes in temperature and precipitation as possible forces driving evolutionary divergence within *Angustiflorae*.

## TABLE OF CONTENTS

DEDICATION .....	iv
ACKNOWLEDGEMENTS .....	v
ABSTRACT .....	viii
LIST OF TABLES .....	xvi
LIST OF FIGURES .....	xvii
CHAPTER ONE: MOLECULAR PHYLOGENETIC ANALYSIS OF MAJOR CLADES IN THE GENUS <i>COLUMNEA</i> (GESNERIACEAE): A TEST OF THE MONOPHYLY OF SECTION <i>STYGNANTHE</i> .....	1
Abstract .....	1
Introduction .....	2
Materials and Methods .....	7
DNA Extraction, Amplification, and Alignment .....	7
Test of Incongruence .....	9
Phylogenetic Analyses .....	10
Results .....	11
DNA Amplification and Sequence Alignment .....	11
Test of Incongruence .....	13
Phylogenetic Analyses .....	13
Phylogenetic Tree Topology .....	14
Discussion .....	17

Topology of Relationships among <i>Columnnea</i> Species .....	17
Monophyly of Species .....	18
Section <i>Stygnanthe</i> .....	18
Section <i>Angustiflorae</i> .....	19
Unsampled Species .....	21
Jamaican Species .....	23
Morphological Homology.....	23
Taxonomic Treatment.....	25
LITERATURE CITED .....	30
CHAPTER TWO: SPECIES LEVEL PHYLOGENY OF SECTION <i>ANGUSTIFLORAE</i> IN <i>COLUMNEA</i> (GESNERIACEAE).....	50
Abstract.....	50
Introduction.....	51
Materials and Methods.....	53
DNA Extraction, Amplification, and Alignment.....	53
Test of Incongruence.....	60
Phylogenetic Analyses .....	60
Results.....	62
DNA Amplification and Sequence Alignment .....	62
Test of Incongruence.....	63
Phylogenetic Analyses .....	65
Phylogenetic Tree Topology: Full Data Set.....	66
Phylogenetic Tree Topology: Reduced Data Set .....	68
Analyses of Data Sets Including Indel Event Scores.....	69

Discussion.....	71
Data Partitions.....	71
Monophyly of Section <i>Angustiflorae</i> .....	72
Subclades within <i>Angustiflorae</i> .....	73
Discrepancies among Data Partitions .....	75
Unsampled Species .....	78
Taxonomic Treatment.....	79
LITERATURE CITED .....	103
CHAPTER THREE: DRIVING FORCES OF SPEC IATION WITHIN SECTION <i>ANGUSTIFLORAE</i> : MORPHOLOGICAL AND CLIMATE VARIABLES.....	129
Abstract.....	129
Introduction.....	130
Materials and Methods.....	135
Phylogenetic Analyses .....	135
Species Distributions .....	136
Morphological Characters.....	137
Climate Variables.....	139
Correlation Analyses.....	144
Results.....	146
Species Distributions .....	146
Morphological Characters.....	147
Climate Variables.....	148
Correlations.....	149
Discussion.....	150

Distribution and Speciation of Sister Species Pairs .....	151
Ancestral State Reconstructions of Climate using SEEVA and Simmap.....	152
Correlation Analyses.....	154
Forces Driving Speciation.....	162
LITERATURE CITED .....	167
APPENDIX A.....	198
Species and Voucher Specimen for Chapter One Phylogenetic Analyses .....	198
APPENDIX B .....	206
Species and Voucher Specimens for Chapter Two Phylogenetic Analyses .....	206
APPENDIX C .....	211
Latitude and Longitude Data for 493 Herbarium Collection Specimens .....	211
APPENDIX D.....	243
Extracted Environmental Data for All Herbarium Collection Specimens as Categorized by SEEVA Analyses.....	243
APPENDIX E .....	248
Maximum Likelihood Probability (MLP) and Bayesian Posterior Probability (BPP) Results from Ancestral State Reconstructions of Morphological Characters Using Both the Branch Length Model (BL) in Simmap 1.5 Analyses and Mk1 Model in Mesquite v. 2.75 Analyses for all Character States (Ch. State) .....	248
APPENDIX F.....	256
Bayesian Posterior Probability Results for Ancestral State Reconstructions of Climatic Variables Using the Branch Length Model in Simmap 1.5 Analyses for all Character States (Ch. State) .....	256

## LIST OF TABLES

Table 1.1 – History of <i>Columnea</i> Species Classifications .....	40
Table 1.2 – DNA Sequencing Results .....	43
Table 1.3 – Maximum Parsimony Results .....	44
Table 1.4 – Model Test Results .....	44
Table 2.1 – Results from Testing Seven Gene Regions to Determine the Ability to Resolve Species-level Relationships.....	111
Table 2.2 – Results for Ability of Two Low-copy Nuclear Gene Regions to Resolve Species-level Relationships within Section <i>Angustiflorae</i> .....	112
Table 2.3 – DNA Sequencing Results .....	113
Table 2.4 – Results of Scoring Indel Events.....	115
Table 2.5 – Maximum Parsimony Results .....	116
Table 2.6 – Model Test Results .....	117
Table 3.1 – Character State Definitions and Scores .....	175
Table 3.2 – Morphological and Climatic Variables not Used in Analyses.....	179
Table 3.3 – SEEVA Results.....	181
Table 3.4 – Results from the False Discovery Rate Test.....	185

## LIST OF FIGURES

- Figure 1.1 – *Columnnea katzensteiniae* (A), *C. tandapiana* (B), *C. isernii* (C), and *C. moesta* (D) demonstrating morphological characteristics. The arrow in plate A shows a ventricose corolla with slight swelling in the middle. Plates A and B are species in *Angustiflorae* that show the larger corolla lobes and less corolla pubescence compared to species in *Stygnanthe* pictured in plates C and D with smaller corolla lobes and more corolla pubescence. .... 45
- Figure 1.2 – Summary of maximum parsimony (MP), maximum likelihood (ML), and Bayesian inference (BI) partition model analyses mapped on BI partition analysis tree topology. Numbers above branches represent MP bootstrap (BS)/MLBS/BI posterior probability (PP). Bold branches are strongly supported in all three analyses (MPBS/MLBS > 75; PP > 95). Letters represent clades identified by Smith et al. (in review). Lines with dash dot dash pattern represent branches that collapse in either MP or ML analyses. Accessions in bold represent species that have a similar corolla morphology (tubular corolla with radially to subradially symmetric limbs) to species of section *Stygnanthe* sensu Smith (1994). The arrow represents the clade where *C. grisebachiana* was recovered (tree not shown), the third clade of species with radially to subradially symmetric tubular corolla. .... 47
- Figure 1.3 – The AWTY results from the comparison of the two Bayesian inference one model analysis runs. .... 48
- Figure 1.4 – The AWTY results from the comparison of the two Bayesian inference partition model analysis runs. .... 49
- Figure 2.1 – The Are We There Yet results from the comparison of the two Bayesian inference one model analyses of the full data set. .... 118
- Figure 2.2 – The Are We There Yet results from the comparison of the two Bayesian inference one model analyses of the reduced data set. .... 119
- Figure 2.3 – The Are We There Yet results from the comparison of the two Bayesian inference partition model analyses of the full data set. .... 120
- Figure 2.4 – The Are We There Yet results from the comparison of the two Bayesian inference partition model analyses of the reduced data set. .... 121

Figure 2.5 – Summary of maximum parsimony (MP), maximum likelihood (ML), Bayesian inference (BI) one model, and BI partition model analyses mapped onto the BI partition analysis tree topology for the full data set. Numbers above branches represent MP bootstrap (BS)/MLBS/BI one model posterior probability (PP)/BI partition model PP. Bold branches are strongly supported in all four analyses (BS > 75; PP > 95). Letters on the left of the tree represent the subclades within section *Angustiflorae* (A<sub>s</sub>, B<sub>s</sub>, C<sub>s</sub>, and D<sub>s</sub>). Letters on the far right represent clades identified by Smith et al. (in review) and Chapter One. Dotted lines represent branches that collapse in the MP analysis. Dashed and dotted lines represent branches that collapse in the MP and ML analyses. Asterisk indicates that the branch was not present in the MP analysis. Line with double strike through indicates that the branch was not present in the ML analysis. .. 122

Figure 2.6 – Summary of maximum parsimony (MP), maximum likelihood (ML), Bayesian inference (BI) partition model analyses model mapped on the BI partition analysis tree topology for the reduced data set. Numbers on branches represent MP bootstrap (BS)/MLBS/BI one model posterior probability (PP)/BI partition model PP. Bold branches are strongly supported in all four analyses (BS > 75; PP > 95). Letters on the left represent subclades in section *Angustiflorae* (A<sub>s</sub>, B<sub>s</sub>, C<sub>s</sub>, and D<sub>s</sub>). Letters on the far right represent clades identified by Smith et al. (in review) and Chapter One. Dashed and dotted lines represent branches that collapse in both MP and ML analyses. .... 123

Figure 2.7 – Distribution of *Columnea ambigua*, *C. angustata*, and *C. domingensis*. ... 124

Figure 2.8 – Distribution of *Columnea antiocana*, *C. crassicaulis*, and *C. orientandina*. ..... 125

Figure 2.9 – Distribution of *Columnea byrsina*, *C. colombiana*, and *C. suffruticosa*. ... 126

Figure 2.10 – Distribution of *Columnea katzensteiniae*, *C. manabiana*, *C. rileyi*, *C. ovatifolia*, and *C. tandapiana*..... 127

Figure 2.11 – Distribution of *Columnea spathulata*. ..... 128

Figure 3.1 – Ancestral State Reconstruction of Habit: Ancestral state reconstructions from Mk1 model and branch length reconstruction mapped onto a species level phylogenetic tree of section *Angustiflorae*. Character states are upright [0] – black, pendent [1] – white, and horizontal [2] – gray. Circles at extant taxa represent character state for species (Table 3.1). Pie charts at nodes represent the Bayesian posterior probabilities (BPP) and maximum likelihood probabilities (MLP) from ancestral state reconstructions. Nodes with only one pie chart have equal BPP and MLP values. Exact BPP and MLP values are available in Exact BPP and MLP

values are available in Appendix E. Numbers below branches represent branch lengths with size corresponding to branch length. Letters to right represent subclades within section *Angustiflorae* (Chapter Two). ..... 188

Figure 3.2 – Ancestral State Reconstruction of Leaf Isophylly: Ancestral state reconstructions from Mk1 model and branch length reconstruction mapped onto a species level phylogenetic tree of section *Angustiflorae*. Character states are anisophyllous [0] – black and isophyllous [1] – white. Circles at extant taxa represent character state for species (Table 3.1). Pie charts at each node on the left are the Bayesian posterior probabilities and pie charts on the right are the maximum likelihood probabilities from ancestral state reconstructions. Exact probabilities are available in Appendix E. .... 188

Figure 3.3 – Ancestral State Reconstruction of Lamina Surface Area: Ancestral state reconstructions from Mk1 model and branch length reconstruction mapped onto a species level phylogenetic tree of section *Angustiflorae*. Character states are 0.0-30.0 cm<sup>2</sup> [0] – black and > 30.0 cm<sup>2</sup> [1] – white. Circles at extant taxa represent character state for species (Table 3.1). Pie charts at each node on the left are the Bayesian posterior probabilities (BPP) and pie charts on the right are the maximum likelihood probabilities (MLP) from ancestral state reconstructions. Nodes with only one pie chart have equal BPP and MLP values. Exact probabilities are available in Appendix E. .... 189

Figure 3.4 – Ancestral State Reconstruction of Petiole Length: Ancestral state reconstructions from Mk1 model and branch length reconstruction mapped onto a species level phylogenetic tree of section *Angustiflorae*. Character states are 0.0-5.0 mm [0] – black, 5.0-20.0 mm [1] – white, and > 20.0 mm [2] – gray. Circles at extant taxa represent character state for species (Table 3.1). Pie charts at each node on the left are the Bayesian posterior probabilities and pie charts on the right are the maximum likelihood probabilities from ancestral state reconstructions. Exact probabilities are available in Appendix E. .... 190

Figure 3.5 – Ancestral State Reconstruction of Floral Bract Size: Ancestral state reconstructions from Mk1 model and branch length reconstruction mapped onto a species level phylogenetic tree of section *Angustiflorae*. Character states are 0.0-6.0 mm [0] – black, 6.0-13.0 mm [1] – white, and > 13.0 mm [2] – gray. Circles at extant taxa represent character state for species (Table 3.1). Pie charts at each node on the left are the Bayesian posterior probabilities and pie charts on the right are the maximum likelihood probabilities from ancestral state reconstructions. Exact probabilities are available in Appendix E. .... 190

Figure 3.6 – Ancestral State Reconstruction of Corolla to Calyx Ratio: Ancestral state reconstructions from Mk1 model and branch length reconstruction mapped onto a species level phylogenetic tree of section *Angustiflorae*. Character states are 0.0-2.5 [0] – black and > 2.5 [1] – white. Circles at extant taxa represent character state for species (Table 3.1). Pie charts at each node on the left are the Bayesian posterior probabilities and pie charts on the right are the maximum likelihood probabilities from ancestral state reconstructions. Exact probabilities are available in Appendix E. .... 191

Figure 3.7 – Ancestral State Reconstruction of Calyx Margin: Ancestral state reconstructions from Mk1 model and branch length reconstruction mapped onto a species level phylogenetic tree of section *Angustiflorae*. Character states are entire [0] – black and serrate [1] – white. Circles at extant taxa represent character state for species (Table 3.1). Pie charts at each node on the left are the Bayesian posterior probabilities and pie charts on the right are the maximum likelihood probabilities from ancestral state reconstructions. Exact probabilities are available in Appendix E. .... 191

Figure 3.8 – Ancestral State Reconstruction of Corolla Color: Ancestral state reconstructions from Mk1 model and branch length reconstruction mapped onto a species level phylogenetic tree of section *Angustiflorae*. Character states are yellow corolla [0] – black, red corolla [1] – white, purple corolla [2] – gray, and polymorphic for color [3] – stripes. Circles at extant taxa represent character state for species (Table 3.1). Pie charts at each node on the left are the Bayesian posterior probabilities and pie charts on the right are the maximum likelihood probabilities from ancestral state reconstructions. Exact probabilities are available in Appendix E. .... 192

Figure 3.9 – Ancestral State Reconstruction of Corolla Lobe Color: Ancestral state reconstructions from Mk1 model and branch length reconstruction mapped onto a species level phylogenetic tree of section *Angustiflorae*. Character states are same color as corolla [0] – black and different from corolla [1] – white. Circles at extant taxa represent character state for species (Table 3.1). Pie charts at each node on the left are the Bayesian posterior probabilities and pie charts on the right are the maximum likelihood probabilities from ancestral state reconstructions. Exact probabilities are available in Appendix E. .... 192

Figure 3.10 – Ancestral State Reconstruction of Phenology: Ancestral state reconstructions from Mk1 model and branch length reconstruction mapped onto a species level phylogenetic tree of section *Angustiflorae*. Character states are flowering continuously [0] – black, flowering from January to March [1] – white, and flowering from March to October [2] – gray. Circles at extant taxa represent character state for species (Table 3.1). Pie charts at each node on the left are the Bayesian posterior probabilities (BPP) and pie charts on the right are the maximum likelihood probabilities

(MLP) from ancestral state reconstructions. Nodes with only one pie chart have equal BPP and MLP values. Exact probabilities are available in Appendix E. .... 193

Figure 3.11 – Ancestral State Reconstruction of Annual Mean Temperature: Ancestral state reconstructions from branch length reconstruction using Simmap 1.5 mapped onto a species level phylogenetic tree of section *Angustiflorae*. Character states are < 18.667 °C [0] – black, 21.225-23.0 °C [1] – white, polymorphic [2] – gray, and < 21 °C [3] – stripes. Circles at extant taxa represent character state for species (Table 3.1). Pie charts at each node represent the Bayesian posterior probability values. Exact probabilities are available in Appendix F. .... 194

Figure 3.12 – Ancestral State Reconstruction of Temperature Seasonality: Ancestral state reconstructions from branch length reconstruction using Simmap 1.5 mapped onto a species level phylogenetic tree of section *Angustiflorae*. Character states are polymorphic [0] – black, 265.75-439.5 [1] – white, < 439.5 [2] – gray, and > 703.33 [3] – stripes. Circles at extant taxa represent character state for species (Table 3.1). Pie charts at each node represent the Bayesian posterior probability values. Exact probabilities are available in Appendix F. .... 194

Figure 3.13 – Ancestral State Reconstruction of Mean Temperature of Wettest, Driest, Warmest, and Coldest Quarters: Ancestral state reconstructions from branch length reconstruction using Simmap 1.5 mapped onto a species level phylogenetic tree of section *Angustiflorae*. Character states are < 18.85 °C [0] – black, polymorphic [1] – white, < 21.5 °C [2] – gray, and > 23.667 °C [3] – stripes for mean temperature of the wettest quarter; < 18.3 °C [0] – black, polymorphic [1] – white, < 20.98 °C [2] – gray, and > 22.633 °C [3] – stripes for mean temperature of the driest quarter; < 19.375 °C [0] – black, polymorphic [1] – white, < 21.85 °C [2] – gray, and > 23.9 °C [3] – stripes for mean temperature of the warmest quarter; < 18.133 °C [0] – black, polymorphic [1] – white, < 20.5 °C [2] – gray, and > 22.433 °C [3] – stripes for mean temperature of the coldest quarter. Though character states are different for each of the four bioclim variables represented on this tree, Bayesian posterior probabilities (BPP) were exactly the same for all four variables at all nodes and scores were the same for all extant species. Circles at extant taxa represent character state for species (Table 3.1). Pie charts at each node represent the BPP values. Exact probabilities are available in Appendix F. .... 195

Figure 3.14 – Ancestral State Reconstruction of Precipitation of Coldest Quarter: Ancestral state reconstructions from branch length reconstruction using Simmap 1.5 mapped a onto species level phylogenetic tree of section *Angustiflorae*. Character states are polymorphic [0] – black, < 382.0 mm [1] – white, > 382.0 [2] – gray, and 158.0-829.0 mm [3] – stripes. Circles

at extant taxa represent character state for species (Table 3.1). Pie charts at each node represent the Bayesian posterior probabilities values. Exact probabilities are available in Appendix F. .... 196

Figure 3.15 – Summary of Forces Driving Speciation within Section Angustiflorae: Pictures represent causes of speciation at each node and for individual species. An island represents allopatric speciation; the photosynthesis Z-scheme represents a shift in photosynthetic ability; a bee represents an adaptation to nectar robbing; a hummingbird represents a pollinator shift; a raincloud represents a shift in precipitation; and a sun represents a shift in temperature. .... 197

CHAPTER ONE: MOLECULAR PHYLOGENETIC ANALYSIS OF MAJOR CLADES  
IN THE GENUS *COLUMNEA* (GESNERIACEAE): A TEST OF THE MONOPHYLY  
OF SECTION *STYGNANTHE*

**Abstract**

The use of morphological characters to analyze evolutionary relationships of species, genera, and higher taxa within Gesneriaceae has been problematic, producing conflicting results because of convergence causing unrelated taxa to be classified together. Molecular phylogenetic analyses allow greater insights into relationships across the family, resulting in better classification systems that reflect the common ancestry of taxa rather than convergent evolutionary history. The taxonomic history of species considered *Columnnea*, the largest Neotropical genus in Gesneriaceae subfamily Gesnerioideae, has been problematic due to convergent morphology. The over 200 species of *Columnnea* have been placed in fourteen genera, with up to nine sections in *Columnnea*. Most recently, species of *Columnnea* have been classified in a single genus with five sections. *Stygnanthe*, one of the five sections in *Columnnea*, encompasses eighteen species based on floral morphology. However, molecular phylogenetic analyses have begun to deconstruct the five sections of *Columnnea*. The phylogenetic analyses presented here amplified 129 accessions representing 90 species for five chloroplast gene regions (*trnQ-rps16* spacer, *rpl32-trnL<sub>UAG</sub>* spacer, *rps16* intron, *trnS-G* spacer, and *trnH-psbA* spacer) and nuclear ribosomal internal transcribed spacers (ITS1 and ITS2) to build a well-supported topology that can test the previously proposed subgeneric

classifications. Fifteen species of section *Stygnanthe* and four species that share a similar floral morphology but had not been classified in *Stygnanthe* were included in molecular phylogenetic analyses to test the utility of floral form as an indicator of evolutionary history. The results indicate that classifying species of *Columnea* in five sections is not a real reflection of the evolutionary history; rather, there is support for seven monophyletic clades within the genus. There is also support that the species of section *Stygnanthe* and those that share a similar floral morphology belong in three separate clades, evidence that floral form is the result of convergent evolution within *Columnea*.

### **Introduction**

Historically, morphological characters provided the foundation for plant classification systems worldwide. Despite the apparent ease of assessing morphology, the underlying evolutionary and genetic homology of these phenotypic traits poses difficulties when evaluating characters in an evolutionary context. Without a critical evaluation to assess homology, convergence of phenotypic traits leads to flawed classification systems uniting unrelated taxa. Molecular methods have provided an alternative to morphological data, allowing for an easier assessment of homology and identification of phylogenetically informative characters while providing an independent source of data to build phylogenies.

Prior to the introduction of molecular methods, systematists had no alternative to morphological characters for building classification systems. As a result, many taxa that have not recently been revised lack the phylogenetic structure and support that molecular data provide. Many groups have been revised with molecular phylogenetic analyses. The temperate family, the former Scrophulariaceae, is just one example of an angiosperm

family that has recently undergone major reclassifications based on molecular data (Olmstead et al. 2001; Oxelman et al. 2005; Albach et al. 2005; Xia et al. 2009).

Gesneriaceae, the tropical counterpart to the former Scrophulariaceae, is one of many angiosperm families in need of molecular systematic revision. With over 3500 species distributed pantropically, this family is divided into two subfamilies: the almost exclusively Paleotropical Cyrtandroideae and nearly exclusively Neotropical Gesnerioideae (Weber 2004). Within the subfamily Gesnerioideae, the tribe Episcieae is easily delimited by a three-trace trilacunar node with split lateral bundles, generally superior ovaries and chromosome counts of  $x = 8$  or  $9$  (Wiehler 1983). *Columnea* L. is the largest genus within tribe Episcieae with over 200 species.

As the largest Neotropical genus in Gesneriaceae subfamily Gesnerioideae, *Columnea* has had a problematic taxonomic history, summarized in Table 1.1, with erroneous classification systems based on analogous rather than homologous morphological characters. The type species, *Columnea scandens* L., was first described by Linnaeus in 1753. Several more species were subsequently described and placed in other genera during the early 1800's. Most of these species were then combined by Hanstein (1854) to form the genus *Columnea*. He retained the generic status for both *Ortholoma* Benth. and *Collandra* Lem. and added four new genera (Hanstein 1854; Table 1.1). After a decade, Hanstein (1865) combined all the genera into a single genus, *Columnea*, and recognized each former genus as a subgenus with the exception of *Stygnanthe* J. Hanst (Table 1.1). Hanstein (1865) also added an additional subgenus, bringing the total number of subgenera to seven (Table 1.1). *Columnea* was reclassified by Fritsch (1894) who recognized the subgenera of Hanstein (1865) as sections and

considered *Trichantha* Hook. a separate genus from *Columnea*. Fritsch also combined the genera *Stygnanthe* and *Systolostoma* Benth. into *Columnea* and recognized each of them as sections (Fritsch 1894; Table 1.1). Morton (1971) and Morley (1974, 1976) each slightly altered the genus by recognizing different numbers of sections (Table 1.1). These classification systems relied predominantly on floral characters (Hanstein 1854, 1865; Fritsch 1894; Morton 1971; Morley 1974, 1976).

Wiehler (1973, 1983) questioned the utility of floral form, considering the corolla characteristics a reflection of pollinator selection activity rather than ancestral relationships. Wiehler (1973) proposed a reclassification of the family based on vegetative or nectary characteristics. Wiehler (1977, 1981) introduced the columneoid alliance by splitting the genus *Columnea* into four genera and adding a fifth genus *Bucinellina* Wiehler (Table 1.1).

However, Wiehler's (1977, 1981) classification system was controversial because *Columnea* was no longer considered a single genus. The presence of an opaque, white to pale colored berry fruit was an important unifying character and evidence for a single genus to encompass the species. Many researchers continued to treat *Columnea* as a single genus (Morley 1974, 1976; Smith 1991, 1994) including Kvist and Skog (1993) who combined Wiehler's five genera back into a single genus and recognized six sections (Table 1.1) that largely corresponded to Wiehler's (1977, 1981) genera.

Despite Wiehler's attempt to reorganize Gesneriaceae using characters that reflected ancestor descendent relationships, misinterpretations of homology among morphological characters have been prevalent within the family. Studies of groups within both Cyrtandroideae (Möller and Cronk 1997; Smith 1996; Smith et al. 1997,

1998; Mayer et al. 2003; Li and Wang 2007; Möller et al. 2009; Wang et al. 2010, 2011) as well as Gesnerioideae (Clark and Zimmer 2003; Smith et al. 2004; Roalson et al. 2005a, b, 2008; Woo et al. 2011; Clark et al. 2012) have shown evidence for varying relationships based on morphological versus molecular data, including species within *Columnea* (Smith et al. in review).

The first molecular phylogenetic analyses of *Columnea* were conducted by Smith and Sytsma (1994b, c) who studied Kvist and Skog's (1993) sections *Pentadenia* (Planch.) Hanst. and *Stygnanthe* using a combination of morphological characters and chloroplast DNA restriction site data. Although they did not have evidence for the monophyly of either of these sections, they were retained pending further molecular sampling. Smith (1994) recognized five sections within *Columnea*: sections *Pentadenia* and *Stygnanthe*, along with three others: sections *Columnea*, *Ortholoma*, and *Collandra* (Smith 1994; Table 1.1).

Since Smith and Sytsma (1994b, c), species of *Columnea* have been sampled in numerous DNA sequence based phylogenetic analyses (Smith and Carroll 1997; Smith 2000; Zimmer et al. 2002; Clark and Zimmer 2003; Clark et al. 2012) and have been recovered as either monophyletic or unresolved (Smith and Carroll 1997) among other closely related genera. However, none of those studies have provided sufficient phylogenetic resolution or support to test the subgeneric classification of *Columnea* (Smith and Carroll 1997; Smith 2000; Zimmer et al. 2002; Clark and Zimmer 2003; Clark et al. 2012).

Section *Stygnanthe* sensu Smith (1994) is one section that has lacked phylogenetic support for its monophyly. Smith (1994) placed eighteen species in section

*Stygnanthe* characterized as sublignose (rarely succulent) epiphytes with anisophyllous or slightly anisophyllous leaves, inflorescences of 1-12 flowers per axil, a calyx loosely clasping the corolla, and small corollas that are slightly ventricose (Figure 1.1) and constricted at the base ranging in size from 1.4 to 5.2 cm in length (Smith 1994). Previously, many of the species of section *Stygnanthe* were placed in genus *Pentadenia* by Wiehler (1973, 1977, 1981, 1983; Appendix A). Kvist and Skog (1993) then transferred most of the species to section *Stygnanthe* (Appendix A). Smith's (1994) section *Stygnanthe* moved some of Kvist and Skog's (1993) species into section *Pentadenia* and added others that had previously been untreated (Appendix A).

Molecular phylogenetic analyses have begun to resolve subgeneric relationships within *Columnea* (Smith et al. in review). Five chloroplast DNA (cpDNA) gene regions and nuclear ribosomal internal transcribed spacers, ITS1 and ITS2, show phylogenetic support for seven monophyletic clades within *Columnea* (Smith et al. in review) rather than five sections (Smith 1994; Table 1.1). The goal of this study to build on the study of Smith et al. (in review) to examine the relationships among species within *Columnea* to generate a well-supported phylogenetic tree to test the monophyly of the eighteen species in section *Stygnanthe* sensu Smith (1994).

Phylogenetic analyses were conducted to test the monophyly of section *Stygnanthe* sensu Smith (1994) using five cpDNA gene regions (*trnQ-rps16* and *rpl32-trnL<sub>UAG</sub>* spacers: both from Shaw et al. 2007; *rps16* intron: Oxelman et al. 1997; *trnS-G* spacer: Hamilton 1999; and *trnH-psbA* spacer: Clark et al. 2012), along with nuclear ribosomal internal transcribed spacers (ITS1 and ITS2, hereafter referred to as ITS;

Baldwin et al. 1995). These were chosen because previously they have resolved subgeneric clades within *Columnnea* with broad sampling (Smith et al. in review).

Previous data indicated that section *Stygnanthe* was not monophyletic. Smith et al. (in review) sampled twelve of the eighteen species within *Stygnanthe* and 68 species within *Columnnea*, represented by 93 accessions. This study included 40 accessions representing fifteen of the eighteen species of *Stygnanthe* sensu Smith (1994) and added an additional 22 species, sampling 90 species (129 accessions) in *Columnnea*. In addition, species that were not previously placed in *Stygnanthe* by Smith (1994), but share a similar tubular corolla with radially to subradially symmetric limbs were sampled: *Columnnea ulei*, *C. moorei*, and *C. grisebachiana*. *Columnnea ulei* and *C. moorei* were classified by Wiehler (1973) as *Trichantha* and considered members of section *Ortholoma* by Kvist and Skog (1993) and Smith (1994; Appendix A). *Columnnea grisebachiana* was previously classified in section *Pterygoloma* by Morley (1976).

## Materials and Methods

### DNA Extraction, Amplification, and Alignment

A complete list of samples and voucher specimens is in Appendix A. The ingroup included 129 accessions of *Columnnea* representing 90 species, based on morphology. These represent multiple individuals from each of Wiehler's (1983) segregate genera and the sections of Kvist and Skog (1993), with the exception that only one of the two species of *Bucinellina* was included (Appendix A). Outgroup samples included species of *Alloplectus*, *Corytoplectus*, *Crantzia*, *Drymonia*, *Glossoloma*, and *Neomortonia* (Appendix A) chosen based on a study of Episcieae by Clark et al. (2012).

DNA was extracted from silica-dried leaf material of one individual plant using Qiagen DNeasy plant mini kits (Valencia, California, U.S.A.) according to the manufacturer's instructions. Five cpDNA gene regions were chosen for amplification including the *trnQ-rps16* spacer (Shaw et al. 2007), *rpl32-trnL<sub>UAG</sub>* spacer (Shaw et al. 2007), *rps16* intron (Oxelman et al. 1997), *trnS-G* spacer (Hamilton 1999), and *trnH-psbA* (Clark et al. 2006). The sixth gene region used for this study was the nuclear DNA region ITS (Baldwin et al. 1995).

*Columnnea xiphoidea* had only herbarium leaf material available, making it difficult to amplify and sequence the DNA. Therefore, only two gene regions, *rpl32-trnL<sub>UAG</sub>* spacer and ITS, were amplified for *C. xiphoidea* following the same procedure as the silica-dried leaf material. *Columnnea xiphoidea* gene regions were analyzed separately from the six gene region combined analyses. The sequences for *rpl32-trnL<sub>UAG</sub>* spacer and ITS for the 129 accessions were combined, and the sequences from *C. xiphoidea*, for both gene regions, were added to the data set. The gene regions were combined into a single concatenated data set composed of two separate partitions and analyzed using maximum parsimony (MP) in PAUP\* v4.0 b10 (Swofford 2002).

All double-stranded DNA was amplified via polymerase chain reaction (PCR) following the methods of Smith et al. (1997). Sequences were obtained either through the methods described in Smith et al. (2004) or through Genewiz (Plainfield, New Jersey, U. S. A.) with chromatograms viewed and sequences edited and aligned by hand in PhyDE (<http://www.phyde.de/>).

Due to the different sequencing methods, each gene region had missing data at the beginning and end in the full alignment. Areas of missing data and ambiguous

alignments were excluded from phylogenetic analyses. Additionally, the alignment produced regions of ambiguity due to single base or microsatellite repeats. These repeats can be unambiguously aligned; however, the homology is uncertain. To test the impact of these single base and microsatellite repeats on phylogenetic analyses, I ran two additional MP analyses using PAUP\* v4.0 b10 (Swofford 2002), one with the repeats included and one with them excluded. To assess the utility of including single base and microsatellite repeats, the resolution and support within the tree was compared. If the repeats are homoplastic there will be less resolution and support within the tree due to increased homoplasy, which would be reflected in a reduced consistency index (CI; Kluge and Farris 1969).

The alignments also resulted in gaps to account for insertion or deletion (indel) events. The inclusion of indel events can be of phylogenetic significance (Simmons and Ochoterena 2000). Each indel event was scored as present or absent for all accessions. An additional data partition was then added to the end of the concatenated data set representing the score for each indel event (Lewis 2001). The data set that included the indel event scores was then analyzed separately using MP in PAUP\* v4.0 b10 (Swofford 2002).

### Test of Incongruence

The partition homogeneity test (Farris et al. 1994) was performed as implemented in PAUP\* v4.0 b10 (Swofford 2002) with 10,000 bootstrap replicates (using a heuristic search, simple addition, and no branch swapping). Because the cpDNA is a single non-recombining unit, the cpDNA gene regions were treated as a single partition. The ITS gene region was treated as a separate gene partition. As an additional measure of

congruence among partitions, bootstrap analyses were performed on each partition separately to assess areas of conflicting resolution and to determine if any conflict was strongly supported (Seelanen et al. 1997).

### Phylogenetic Analyses

Phylogenetic trees were estimated using MP, maximum likelihood (ML), and Bayesian inference (BI). Maximum parsimony analyses were performed using PRAP2 (Müller 2004) in conjunction with PAUP\* v4.0 b10 (Swofford 2002). Bootstrap support (BS) for nodes (Felsenstein 1985) was estimated with 1000 heuristic replicates using PRAP2 (Müller 2004). Descriptive statistics reflecting the amount of phylogenetic signal in the parsimony analysis were given by CI (Kluge and Farris 1969), retention index (RI; Farris 1989), and the resulting rescaled consistency index (RC; Farris 1989).

Maximum likelihood and BI analyses were performed using optimal substitution models suggested by Modeltest 3.6 (Posada and Crandall 1998). The Akaike information criterion (AIC), which allows non-nested models to be evaluated, was used as a selection criterion (Posada and Buckley 2004) for the cpDNA and ITS partitions separately and as a concatenated data set.

Substitution models were determined for both cpDNA and ITS partitions separately because two separate BI analyses were completed using MrBayes 3.1.1 (Huelsenbeck and Ronquist 2003). The first BI analysis, referred to as the one model analysis, was performed using a single model for all data (cpDNA and ITS). The second BI analysis, referred to as the partition model analysis, was performed with a separate model for each of the two data partitions.

All analyses were run with 4 to 1 heated chains, for ten million generations. Convergence was determined by viewing in Tracer v1.3 (Rambaut and Drummond 2005), and a burnin of 50,000 generations was discarded prior to sampling the posterior distribution for both BI analyses. Both of the BI analyses were repeated twice to ensure that parameter estimates converged to similar values. The separate runs were compared using the online version of Are We There Yet (AWTY; Nylander et al. 2008) as a means of determining if the separate chains approximated the same target distribution. The ML analysis was completed using GARLI v0.96 (Zwickl 2006) with 100 bootstrap replicates using a single model across the data.

## Results

### DNA Amplification and Sequence Alignment

Amplifications were successful for all individuals with some exceptions for each DNA gene region (Table 1.2). Length for the aligned sequence and the aligned sequences with missing and ambiguous regions removed is in Table 1.2 for all regions. The 5.8S gene between ITS1 and ITS2 was identical across ingroup species and was excluded from the analyses and calculations. There were a total of 4,129 base pairs included in the phylogenetic analyses. Out of these, 2,898 were constant, and 716 were uninformative leaving 515 (12.5%) as phylogenetically informative. An inversion in *trnH-psbA* spacer was detected in individuals of *Columnnea lophophora* (J. L. Clark et al. 7888 and 8898), *C. moesta* (J. L. Clark 6690), *C. eburnea*, *C. picta*, and *C. schimpfii* (Appendix A). This region was reverse complemented for all individuals prior to analyses.

Maximum parsimony analyses to test the impact of single base and microsatellite repeats showed no major differences. The MP analysis including single base and microsatellite repeats resulted in reduced resolution and support across the tree including a loss of support (trees not shown) for the monophyly of Clade G (Figure 1.2). However, there were some areas that showed slightly better resolution (trees not shown), including resolving Clade A (Figure 1.2) as monophyletic. Overall, BS was approximately the same in both analyses, though there was a drop in the CI (Kluge and Farris 1969) from analyses with single base and microsatellite repeats included compared to the analysis with repeats excluded (single base and microsatellite repeats included: CI = 0.4533; excluded: CI = 0.4717). A lower CI is an indication of homoplasy among the included data. The reduced resolution and lower CI value in the analysis including single base and microsatellite repeats implies that the repeats are homoplastic, at least in part. Because the impact of including single base and microsatellite repeats resulted in lower resolution, support, and CI values, they were excluded from further analyses.

Analysis of the data set including scored indel events resulted in minimal topological differences (trees not shown). The MP analysis of the data set including indel event scores recovered Clade A (Figure 1.2) as monophyletic, which is the only difference between the MP results presented in Figure 1.2 and the MP results of the analysis with the indel event scores included (trees not shown). Bootstrap support was also similar between the two analyses with no changes in support resulting in BS > 75 in the BI indel analysis (trees not shown) that were not already present in the MP analysis without the indel event scores included (Figure 1.2).

### Test of Incongruence

The result of the partition homogeneity test ( $p = 0.01$ ) indicated significant differences between partitions. However, as has been reported on many occasions, this test often indicates incongruence when none exists (Reeves et al. 2001; Yoder et al. 2001), and as a result, comparing support for partitions may be a better indicator of incongruence (Seelanen et al. 1997). All regions for all accessions were in complete topological congruence or received BS < 50 for the individual analyses (trees not shown). Therefore, a combined analysis of DNA regions was performed and is the basis for all results and discussion, with the exception of the *C. xiphoidea* DNA sequences (see “DNA Extraction, Amplification, and Alignment”).

### Phylogenetic Analyses

Maximum parsimony analysis resulted in 232 trees of 2262 steps (CI = 0.4717, RI = 0.7318, RC = 0.4807) for the combined data set. Results for MP analyses of individual partitions are in Table 1.3 (individual MP trees not shown). The GTR +  $\Gamma$  + I model was chosen for both the cpDNA partition and the combined data. The GTR + I model was chosen for the ITS partition. Complete Modeltest 3.6 (Posada and Crandall 1998) results for individual partitions and combined data are in Table 1.4. I report the 50% majority-rule consensus tree sampled from the posterior probability (PP) distribution for each of the BI analyses separately (individual BI trees not shown). The AWTY (Nylander et al. 2008) output indicated that the separate chains approximated the same target distribution for both the BI one model analysis (Figure 1.3) and BI partition model analysis (Figure 1.4). The GTR +  $\Gamma$  + I model for the ML analysis resulted in one tree (-lnL = 21120.46019; individual ML tree not shown).

All analyses produced trees with congruent topologies that had varying amounts of resolution. The BI partition model produced the most resolved topology (Figure 1.2). The two BI analyses resulted in similar trees with minimal changes in PP between nodes. There were no nodes with PP > 95 in the BI one model consensus tree (tree not shown) that are not present in the BI partition model analysis (Figure 1.2). Therefore, a tree presenting the combined results of the MP, ML, and BI partition model is presented in Figure 1.2. Support for clades is represented by maximum parsimony bootstrap (MPBS), maximum likelihood bootstrap (MLBS), or Bayesian posterior probabilities from the partition model (PP) and is reported as MPBS/MLBS/PP hereafter in the text.

#### Phylogenetic Tree Topology

In all analyses, *Columnnea* is recovered as a well-supported monophyletic group (Figure 1.2; 96/95/100) with *Glossoloma* supported as sister (Figure 1.2; 85/87/100). Smith et al. (in review) identified seven clades (Figure 1.2: Clades A-G); however, support among the clades was not strong. This study shows support for the same seven clades within *Columnnea* (Figure 1.2). The present analyses show strong support based on all three analyses for the monophyly of Clade B (Figure 1.2; 84/81/100), Clade D (Figure 1.2; 76/81/99), and Clade E (Figure 1.2; 91/95/100). There is also moderate support, based on the BI partition model PP, for the monophyly of Clade C (Figure 1.2; 68/61/100), Clade F (Figure 1.2; -/-/97), and Clade G (Figure 1.2; 63/59/100). The seventh clade, Clade A, is not resolved as monophyletic (Figure 1.2), but is recovered in MP analyses of the data set including scores for the indel events (trees not shown).

There is little support for relationships within each of the clades, though species with multiple accessions are recovered as monophyletic with strong support, with the

exception of *C. moesta*. The *C. moesta* subclade (Figure 1.2, Clade B; 97/99/100) included all four accessions of *C. moesta*, but also included the only accession of *C. ultraviolacea* (Figure 1.2; 81/90/99). However, these species are not the focus of this study and, thus, will not be discussed further.

The monophyly of Clade G is maximally supported in BI partition model analysis and moderately supported in both MP and ML analyses (Figure 1.2; 63/59/100). The fifteen sampled species of section *Stygnanthe* sensu Smith (1994) are recovered in two separate clades. Twelve of the fifteen species are recovered as a monophyletic clade (Figure 1.2, Clade G; 63/59/100) that will herein be referred to as section *Angustiflorae* (Figure 1.2, Clade G; see “Taxonomic Treatment”). In addition, two species, *C. domingensis* and *C. ulei*, that had not been placed in section *Stygnanthe* (Smith 1994), were recovered as members of section *Angustiflorae* (Figure 1.2).

Most species of *Angustiflorae* represented by multiple accessions were recovered as monophyletic with the exception of *C. angustata*. Seven of the eight species with multiple accessions were recovered as monophyletic: *C. byrsina* (Figure 1.2; 100/100/100), *C. colombiana* (Figure 1.2; 80/75/100), *C. orientandina* (Figure 1.2; 100/100/100), *C. spathulata* (Figure 1.2; 82/73/100), *C. rileyi* (Figure 1.2; 99/100/100), *C. ovatifolia* (Figure 1.2; 71/69/99) and *C. tandapiana* (Figure 1.2; 100/100/100). The *C. angustata* clade (Figure 1.2; 98/87/100) included all the accessions of *C. angustata*, but also included the only accession of *C. ulei* (Figure 1.2; 100/87/70). Four species were sampled with only a single accession, and therefore their monophyly was not tested.

Within section *Angustiflorae* there was minimal resolution for relationships among species. There was strong support for *C. ambigua* as sister to *C. domingensis*

(Figure 1.2; 92/80/100). There was also evidence for a subclade grouping *C. crassicaulis*, *C. katzensteiniae*, and *C. rileyi* (Figure 1.2; 78/77/100). The final grouping within section *Angustiflorae* with strong support was *C. manabiana* as sister to *C. tandapiana* (Figure 1.2; 100/100/100).

All three of the remaining species sampled from the *Stygnanthe* sensu Smith (1994), *C. moesta*, *C. ultraviolacea*, and *C. xiphoidea* were supported in Clade B (Figure 1.2). In all analyses, *C. moesta* and *C. ultraviolacea* were strongly supported in Clade B (Figure 1.2; 84/81/100). In the separate two gene region MP analysis, *C. xiphoidea* was supported as sister to *C. moesta* (trees not shown; MPBS = 99) and thus, also belongs within Clade B (Figure 1.2; *C. xiphoidea* not shown).

*Columnnea moorei* and *C. grisebachiana* were thought to potentially belong in section *Angustiflorae* because they share a similar corolla morphology to species placed in *Stygnanthe* by Smith (1994). This study tested the phylogenetic placement of both species with molecular data, which had not been done previously. In the MP strict consensus tree of the ITS partition, *C. moorei* was resolved as sister to the Jamaican species *C. brevipila* and *C. repens* (Figure 1.2) in 94% of the trees (trees not shown). In the MP strict consensus tree of the cpDNA partition, *C. moorei* was resolved as part of Clade E (Figure 1.2) in 100% of the trees (trees not shown). The placement of *C. moorei* in two separate clades implies a hybrid origin; however, the placement of *C. moorei* in either of these clades receives MPBS < 50 (trees not shown). Regardless, *C. moorei* is not placed within section *Angustiflorae*. *Columnnea grisebachiana* was analyzed and found to be strongly supported in a monophyletic group (trees not shown, MPBS = 98)

with the other endemic Jamaican species *C. brevipila* and *C. repens* (Figure 1.2). Since neither species are within section *Angustiflorae*, they are not included in further analyses.

## Discussion

### Topology of Relationships among *Columnea* Species

Morphological characters have been the basis of classification systems, including that of *Columnea*, leading to problematic taxonomic histories due to convergence of morphological characters (Table 1.1). Characteristics such as the corolla, vegetation, and nectary can be used to circumscribe species boundaries; however, they are more troublesome to delimit higher taxa relationships. Most recently, the subgeneric classification within *Columnea* identified five sections based on morphology: *Columnea*, *Collandra*, *Ortholoma*, *Pentadenia*, and *Stygnanthe* (Smith 1994; Table 1.1).

Molecular analyses show evidence for seven clades within genus *Columnea* based on five cpDNA gene regions and one nuclear gene region. The phylogenetic tree presented here can identify where species belong at the subgeneric level (Figure 1.2). These seven clades were also identified in the study of Smith et al. (in review), which performed Shimodaira-Hasegawa (SH) tests (Shimodaira and Hasegawa 1999; Goldman et al. 2000) to determine whether the clades were significantly different from Wiehler's (1983) genera and the sections of Kvist and Skog (1993) and Smith (1994; Appendix A). Smith et al. (in review) rejected the monophyly of all genera and sections for *Columnea* based on their phylogenetic results. This study recovered a similar topology using the same sequences (Figure 1.2) with additional species. All the added species fell in section

*Angustiflorae*, which was already determined as monophyletic by Smith et al. (in review), so further SH tests were not conducted here.

### Monophyly of Species

Most species represented by more than one accession were recovered as monophyletic. Monophyletic species groups indicate that species have correctly been delimited based on morphological characters. The one exception where species were not recovered as a monophyletic species group was *C. angustata*. The presence of *C. ulei* among *C. angustata* species (Figure 1.2) is evidence for *C. ulei* having been misclassified as a separate species. The morphological characters of *C. ulei* (Smith unpublished results) fall within those of *C. angustata* (Smith 1994) and could thus be considered the same species.

### Section *Stygnanthe*

As classified by Smith (1994), section *Stygnanthe* included eighteen species of *Columnnea*. Here multiple accessions representing fifteen of the eighteen species of *Stygnanthe* sensu Smith (1994) were sampled for both partitions (cpDNA and ITS). Species were found to split into two separate clades showing that section *Stygnanthe* (Smith 1994) does not represent a monophyletic group based on molecular analyses.

The phylogenetic analyses show support for *Columnnea moesta* (Figure 1.2; 97/89/99), the type species for section *Stygnanthe*, and *C. ultraviolacea* (Figure 1.2; 81/90/100) in Clade B with at least three other species (Figure 1.2; 84/81/100): *C. atahualpae*, *C. lophophora*, and *C. isernii*. Maximum parsimony analysis of *C. xiphoidea* DNA sequences shows support for *C. xiphoidea* as sister to *C. moesta* (tree not

shown; MPBS = 99) providing evidence that it also belongs in Clade B. Although the clade contains only three of the species from *Stygnanthe* sensu Smith (1994), Clade B will be recognized as section *Stygnanthe* because it includes *C. moesta*, the type species for the section.

Morphological similarities can be found among the species of section *Stygnanthe* lending further support to the separation of this clade from section *Angustiflorae*. Both *C. lophophora* and *C. moesta* have leaves that cluster at the apex of the stem. *Columnnea moesta*, *C. ultraviolacea*, and *C. xiphoidea*, also have dark purple spots on the interior surface of the corolla lobe that distinguish them from the species of section *Angustiflorae*. Furthermore, all six species of section *Stygnanthe* as defined here (Clade B, Figure 1.3) - *C. moesta*, *C. ultraviolacea*, *C. xiphoidea*, *C. atahualpae*, *C. lophophora*, and *C. isernii* - are characterized by a sericeous or pilose pubescence that obscures the corolla (Smith 1994; Figure 1.1).

#### Section *Angustiflorae*

The remaining twelve species sampled from the *Stygnanthe* sensu Smith (1994) group together as a monophyletic clade (Figure 1.2; 63/59/100) that is recognized as section *Angustiflorae* (see “Taxonomic Treatment”). Species that had previously been unsampled were also included in these analyses. *Columnnea ulei* was sampled and well-supported as part of section *Angustiflorae* (Figure 1.2). However, as mentioned above, *C. ulei* was recovered among the *C. angustata* species, evidence that it belongs within section *Angustiflorae* but possibly should not be considered a separate species. *Columnnea domingensis* was previously classified as a species of *Trichantha* (Wiehler

1973) but was strongly supported as sister to *C. ambigua* in all analyses (Figure 1.2; 92/80/100).

The species of section *Angustiflorae* can also be characterized by similar morphological features. The species have similar leaf arrangements that are opposite, rarely dorsiventrally arranged, and isophyllous to anisophyllous. However, these traits are widely shared among other species of *Columnea* and cannot be diagnostic for this clade. The species in section *Angustiflorae* have corollas that are slightly ventricose and constricted at the base with a loosely clasping corolla (Figure 1.1). This combination of traits separates the species from most of the species in other clades in *Columnea*.

Species in section *Stygnanthe* (Figure 1.2, Clade B) and two Jamaican species, *C. grisebachiana* and *C. pubescens* share a similar corolla morphology to the species of *Angustiflorae*. Generally, the species of *Angustiflorae* have a shorter corolla length with proportionally longer and larger corolla lobes than the species in section *Stygnanthe* (Figure 1.1). The species in *Angustiflorae* can also be distinguished from *Stygnanthe* by the corolla pubescence. The species in *Stygnanthe* have a dense pubescence that obscures the corolla while species in *Angustiflorae* have a pilose pubescence where the corolla can still be seen (Figure 1.1). The species of *Angustiflorae* can be distinguished from *C. grisebachiana* and *C. pubescens* by their geographic distribution. *Columnea grisebachiana* and *C. pubescens* are endemic to the island of Jamaica; whereas the only species of *Angustiflorae* found in the Caribbean are restricted to the islands of Puerto Rico (*C. ambigua*) and Hispaniola (*C. domingensis*). Although no obvious morphological characters can be used to place either *C. grisebachiana* or *C. pubescens* outside of *Angustiflorae* besides geographic distribution, it is possible that a detailed

morphometric analysis or additional micromorphological characters may reveal states that unite these two species to the remaining Jamaican endemic species of *Columnnea*. Neither *C. grisebachiana* nor *C. pubescens* have been investigated morphologically in depth, and neither is known to be in cultivation where a more intensive study could be conducted. Nevertheless, the shared morphologies between these two endemic Jamaican species and members of *Angustiflorae* represent a remarkable case of convergent evolution (see “Morphological Homology”).

### Unsampled Species

Although this study includes increased taxon sampling, there are still some species of section *Stygnanthe* sensu Smith (1994) that need to be analyzed using molecular data to determine their placement within *Columnnea*. Smith (1994) had classified three other species, *C. antiocana*, *C. fritschii*, and *C. suffruticosa*, in section *Stygnanthe*. Due to the difficulties of obtaining DNA from herbarium specimens, I was unable to obtain leaf material for these three species. However, they can still be evaluated in a morphological context to determine where they belong in the subgeneric classification of *Columnnea*.

Based on morphological characteristics, both *C. antiocana* and *C. suffruticosa* should be considered part of section *Angustiflorae*. *Columnnea antiocana* has similar features to *C. katzensteiniae*, *C. rileyi*, *C. crassicaulis*, and *C. ovatifolia* including a similar ovate to lanceolate or elliptic lamina shape with an oblique base and the presence of darker colored lobe spots on the exterior surfaces of the lobes of the corolla (Smith 1994). The presence of dark spotting on the corolla lobes is a unique morphological characteristic that is not reported in other clades of *Columnnea*. *Columnnea suffruticosa*

also has darker lobe spots on the exterior surface of the corolla that suggest it is closely related to the same species as *C. antiocana*. However, Smith and Sytsma's (1994a) phylogenetic study placed *C. suffruticosa* with *C. colombiana* based on morphological characteristics, not taking into account the presence of exterior corolla lobe spots. In either case, *C. suffruticosa* groups with species belonging within section *Angustiflorae* based on morphology. In addition, both species have corollas that are only slightly pubescent, where the corolla can still be seen, (Smith 1994), which distinguishes them from the species of section *Stygnanthe* (Figure 1.1). All of these morphological characters are evidence that *C. antiocana* and *C. suffruticosa* belong in section *Angustiflorae*; however, this will need to be confirmed by molecular data in the future.

*Columnea fritschii* should not be classified with the species of section *Angustiflorae* based on morphology. The morphological characteristics of *C. fritschii* suggest that it belongs in section *Stygnanthe* as sister to *C. ultraviolacea*. *Columnea fritschii* and *C. ultraviolacea* are the only species of *Columnea* that have a whorl of four leaves (Smith 1994). Both species are also known only from a small area in Bolivia where they are found on opposite sides of the same mountain range. A cladistic analysis based on morphological characters (Smith and Sytsma 1994a) suggests the same relationship.

Another undescribed species of *Columnea* may be placed within section *Stygnanthe* based on morphological characteristics. *Columnea* sp. (*R. Ferreyra 351*) is only known from a single collection in Peru that is deposited at MO. This specimen is a sublignose, terrestrial herb with opposite, slightly anisophyllous leaves and limb spots on the interior surface of the corolla. This species also has a densely pilose corolla

distinguishing it from species of *Angustiflorae* and suggesting that it belongs in *Stygnanthe* with *C. moesta*, *C. ultravioleacea*, and *C. xiphoidea*.

### Jamaican Species

Two other previously unsampled species, *C. pubescens* and *C. grisebachiana*, are endemic to the island of Jamaica and have similar morphologies to the species of section *Angustiflorae* (Stearn 1968). I was unable to obtain leaf material for *C. pubescens*; however, its morphological characteristics are most similar to those of *C. grisebachiana* including a smaller corolla than the other endemic Jamaican species and a thin stem with a creeping habit. Using these morphological similarities, *C. grisebachiana* and *C. pubescens* could be considered sister species. *Columnnea grisebachiana*, along with eleven other Jamaican *Columnnea* species, were included in a MPBS analysis (tree not shown) along with all other accessions sampled here (Appendix A). The results indicated a well-supported monophyletic clade (tree not shown; MPBS = 98). This clade is separate from *Angustiflorae* and indicates that *C. grisebachiana* is not related to species of section *Angustiflorae* despite morphological similarities. It implies that *C. pubescens* is also not part of *Angustiflorae* due to its morphological similarities to *C. grisebachiana* and thus both have been excluded from section *Angustiflorae*.

### Morphological Homology

Morphological homology can be difficult to assess, leading to problems when used to classify species and higher taxa. Often morphological characters look similar but are the result of convergent evolution, making it difficult to determine which morphological characters to use to classify species. Within *Columnnea* systematists have

used floral, vegetative, and nectary characters to classify species (Table 1.1), but none reflect evolutionary lineages (Smith et al. in review; Figure 1.2). This study used molecular phylogenetic analyses to test the utility of corolla morphology in identifying a monophyletic clade within *Columnea*. Eighteen species with subradially to radially symmetric tubular corollas were analyzed using molecular phylogenetics and found to belong in three separate clades (Figure 1.2). These results are evidence for convergent evolution of subradially to radially symmetric tubular corollas within *Columnea*; however, upon closer examination, finer morphological characters identify a monophyletic clade.

Three species, *C. moesta*, *C. ultraviolacea*, and *C. xiphoidea*, were recovered in a single clade (Figure 1.2: Clade B). These three species all have subradially to radially symmetric tubular corollas, but are unique from the other fifteen species based on the relative size of their corolla lobes and the density of their corolla pubescence (Figure 1.1). Often molecular phylogenetic analyses can be used to identify monophyletic groups, and then morphological characters that are unique to the clade can be determined (Cunningham et al. 2001; Carlson et al. 2011; Clark et al. 2012). This approach allows for identification of species and higher taxa while in the field without the worry of confusing convergent characters.

However, sometimes this approach does not work due to complete convergence of morphological characters. In this study, one species, *C. grisebachiana*, was recovered in a separate clade from the remaining fourteen species with subradially to radially symmetric tubular corollas (Figure 1.2), but has no morphological differences that can be used to separate it from the other species. There may be other micromorphological

characters or (molecular pathways) that can separate *C. grisebachiana* from the remaining *Angustiflorae* species, but for all intents and purposes *C. grisebachiana* is a case of complete morphological convergence. In some cases, morphological characters are the only available data to classify species due to insufficient leaf material or the scarcity of species. However, morphological characters are not reliable for constructing evolutionary histories because of cases of complete morphological convergence (Cunningham et al. 2001).

Morphological convergence of floral form is often seen in plants due to pollinator selection (Schemske 1981; Armbruster 1993; Johnson 1996; Beardsley et al. 2003). Because many plants are dependent upon pollinators for gene flow, pollinator selection can have a large effect on the plant's morphological characters (Carson 1985) and can lead to morphological convergence in unrelated taxa (Cunningham et al. 2001; Carlson et al. 2011; Clark et al. 2012). Characters that are not the result of convergent evolution can be used to identify species after molecular analyses (Cunningham et al. 2001; Carlson et al. 2011; Clark et al. 2012), but complete morphological convergence can make identifying species and higher taxa in the field extremely difficult.

### **Taxonomic Treatment**

**Columnnea** section **Angustiflorae** L. J. Schulte and J. F. Smith – TYPE: *Pentadenia angustata* Wiehler

Small herbs, suffrutescent, epipetric, epiphytic, vining or terrestrial. Stems succulent to sublignose, frequently branching at base, ascending, creeping, spreading, or pendant to 3.0 m long, 1.5-15.0 mm in diameter, sometimes with a zigzag appearance, terete, green sometimes suffused with purple or tawny, or maroon to red-brown to tan,

squarish when dried, proximally smooth and glabrous to flaking, sometimes hirsute with a few multicellular transparent or red trichomes sometimes dark purple, distally glabrescent or glabrate to appressed pilose or pubescent to hirsute to sericeous sometimes lanate or villous with uniseriate to multicellular transparent or red trichomes with numerous adventitious, (sometimes conspicuous) roots; internodes 0.4-9.5 cm long, sometimes swollen; nodes flush with stem; leaf scars raised or flush with stem. Leaves opposite, isophyllous to strongly anisophyllous, sometimes dorsiventrally arranged; larger laminas 0.65-16.2 cm long, 0.4-6.0 cm wide, orbicular to oblong to ovate or elliptic to lanceolate, sometimes slightly falcate, obovate or oblanceolate, apex acute to long-acuminate, obtuse, sometimes blunt and rounded, base cuneate or rounded, oblique to strongly oblique, adaxially dull green to yellow-green to dark or deep green, sometimes purple, suffused with pink, or with violet spots, glabrous or strigillose to strigose, slightly appressed pilose to pilose or slightly hirsute to hirsute, sometimes pubescent or tomentose to villous with uniseriate or multicellular red or transparent trichomes, abaxially green or reddish, pale green sometimes suffused with red-purple mottling or entirely colored, rose-red, pink-purple, rarely with a red apex, glabrate to sparsely pilose, rarely appressed, to pilose, sericeous or long sericeous to lanate or strigose to hirsute, sometimes short tomentose with red or transparent unicellular transparent trichomes, veins glabrous to appressed pilose to lanate or strigose or appressed sericeous to sericeous or slightly hirsute to lanate, sometimes somewhat denser on veins with red or transparent uniseriate or multicellular trichomes, lateral veins 3-12, margin entire or subentire to crenulate or crenate to serrulate to slightly undulate or undulate to ciliate with red to violet or transparent uniseriate trichomes; smaller laminas 0.55-4.2 cm rarely

to 6.0 mm long, 0.2-2.4 cm wide, linear or lanceolate to ovate or elliptic, sometimes absent, otherwise like larger laminas; petioles 0.0-3.1 cm, green, sparsely pilose, sometimes appressed, sericeous to hirsute with red or transparent unicellular to multicellular trichomes. Inflorescence of 1-12 flowers per leaf axil, commonly in axil of larger leaf, rarely in both axils; floral bracts 1-3, 2-19 mm long, 0.4-9 mm wide, conspicuous, caducous, linear or lanceolate to ovate, apex acute to acuminate, green or pink-red, sometimes suffused with red or with red tips, villous or pilose to lanate, sericeous to sparsely hirsute or hirsute with red or transparent uniseriate to multicellular trichomes, margin entire. Pedicels 0.1-21 mm long, erect, maroon-red or green sometimes lavender, pilose to villous or hirsute to sericeous with red or transparent uniseriate to multicellular trichomes, eglandular or rarely with long round to oval purple glands near calyx 0.5-0.7 mm. Calyx loosely clasping corolla, rarely with slightly recurved tips; lobes equal to unequal 0.6-1.8 cm long, 0.1-0.6 mm wide, linear to lanceolate or oblanceolate sometimes subulate or spatulate to narrowly elliptic or ovate, apex acute to acuminate, rarely long acuminate or obtuse, green or purple or pink-red to maroon sometimes flushed with pink-rose or purple or with red or purple tips and teeth, exterior sparsely pilose, sometimes appressed, lanate to strigose or hirsute, villous to sericeous, rarely less densely sericeous toward apex with transparent uniseriate trichomes, interior glabrate or nearly glabrous to slightly pilose or sparsely hirsute to glandular-pubescent with multicellular transparent trichomes, margins entire or subentire to serrate or coarsely toothed to laciniate, rarely dissected at base of lobe to minutely denticulate in fruit. Corolla 1.0-5.2 cm long, 1.5-10.0 mm at widest point, 1.5-6.0 mm at constriction before limb, 1.0-3.0 mm wide at constriction before base, tubular, slightly

ventricose, rarely proximally and ventrally with two small invaginations of corolla tube, cream to lemon-yellow, orange, red or violet, exterior glabrate to puberulent or pubescent, sometimes appressed pilose or long-sericeous to long-hirsute or long-glandular, more densely pilose or villous towards limb with red or transparent sometimes lavender-purple uniseriate to multicellular trichomes with some trichomes, rarely trichomes on limb transparent with red base, interior glabrous to villous, slightly hirsute to slightly pilose or slightly pubescent at base with glandular trichomes dorsally and distally, limb 6.5-8.5 mm in diameter, pale yellow to green; lobes equal to subequal, sometimes inconspicuous, 1.0-3.0 mm long, 1.0-4.0 mm wide, lemon-yellow to green, semiorbicular, sometimes with darker red to orange-yellow or dark purple spots on interior surface or rarely with purple spots on exterior surface. Filaments connate at base 2.0-10.0 mm, adnate to base of corolla 1.0-5.0 mm, white-yellow or red, proximally pilose or slightly pubescent becoming glabrous distally; anthers 0.5-2.5 mm long, 0.5-2.5 mm wide, rectangular or quadrate to subquadrate, usually included in corolla tube, rarely exerted up to 9.0 mm beyond opening of corolla. Ovary 0.8-5.0 mm long, green, conical, nearly glabrous or glabrate becoming pilose or pubescent to sericeous at apex with uniseriate red or transparent trichomes; style white-yellow or red, proximally glabrous to sparsely pilose becoming minutely pilose to pilose or slightly pubescent distally with glandular, short multicellular trichomes distally; stigma stomatomorphic or bilobed, white-yellow, green or red, smooth, papillate, usually included in corolla tube, rarely exerted to 0.7 mm beyond opening of corolla. Nectary variable, with 5 free glands or with 2 dorsal glands connate and 3 free or ventrally connate glands. Berry 5.0-12.0 mm long, 3.5-7.0 mm wide, 1.0-12.0 mm in diameter, ovate or ovoid to globose,

nearly glabrous or glabrate to slightly pilose or pubescent, white to pink-red or pale lavender-purple to blue, sometimes dark in color when dried; seeds 0.8-1.6 mm long, 0.3 mm wide, fusiform to oblong or falcate, twisted, red-purple to light-brown or brown-yellow, striate.

Etymology. The name is derived from the narrow flowers.

## LITERATURE CITED

- Albach, D. C., H. M. Meudt, and B. Oxelman. 2005. Piecing together the “new” Plantaginaceae. *American Journal of Botany* 92: 297-315.
- Armbruster, W. S. 1993. Evolution of plant pollination systems: hypotheses and test with the Neotropical vine *Dalechampia*. *Evolution* 47: 1480-1505.
- Baldwin, B. G., M. J. Sanderson, J. M. Porter, M. F. Wojciechowski, C. S. Campbell, and M. J. Donoghue. 1995. The ITS region of nuclear ribosomal DNA: a valuable source of evidence on angiosperm phylogeny. *Annals of the Missouri Botanical Garden* 82: 247-277.
- Beardsley, P. M., A. Yen, and R. G. Olmstead. 2003. AFLP phylogeny of *Mimulus* section *Erythrhanthe* and the evolution of hummingbird pollination. *Evolution* 57: 1397-1410.
- Bentham, G. 1876. Gesneriaceae. Pp. 990-1025 in *Genera plantarum* Vol. 2, eds. G. Bentham and J. D. Hooker. London: L. Reeve and Co.
- Carlson, K. M., D. H. Mansfield, and J. F. Smith. 2011. A new species in the *Lomatium foeniculaceum* (Apiaceae) clade revealed through combined morphometric and phylogenetic analyses. *Systematic Botany* 36: 495-507.
- Carson, H. L. 1985. Unification of speciation theory in plants and animals. *Systematic Botany* 10: 380-390.

- Clark, J. L. and E. A. Zimmer. 2003. A preliminary phylogeny of *Alloplectus* (Gesneriaceae): implications for the evolution of flower resupination. *Systematic Botany* 28: 365-375.
- Clark, J. L., P. S. Herendeen, L. E. Skog, and E. A. Zimmer. 2006. Phylogenetic relationships and generic boundaries in the tribe Episcieae (Gesneriaceae) inferred from nuclear, chloroplast, and morphological data. *Taxon* 55: 313-336.
- Clark, J. L., M. M. Funke, A. M. Duffy, and J. F. Smith. 2012. Phylogeny of a Neotropical clade in the Gesneriaceae: more tales of convergent evolution. *International Journal of Plant Sciences* in press.
- Cunningham, C. O., T. A. Mo, C. M. Collins, K. Buchman, R. Thiery, G. Blanc, and A. Lauthraite. 2001. Redescription of *Gyrodactylus teuchis* Lauthraite, Blanc, Thiery, Daniel and Vigneulle, 1999 (Monogenea: Gyrodactylidae); a species identified by ribosomal RNA sequence. *Systematic Parasitology* 48: 141-150.
- Farris, J. S. 1989. The retention index and the rescaled consistency index. *Cladistics* 5: 417-419.
- Farris, J. S., M. Källersjö, A. G. Kluge, and C. Bult. 1994. Testing significance of incongruence. *Cladistics* 10: 315-319.
- Felsenstein, J. 1985. Confidence limits on phylogenies: an approach using the bootstrap. *Evolution* 39: 783-791.
- Fritsch, K. 1894. Gesneriaceae. Pp. 133-185 in *Die Natürlichen Pflanzenfamilien* Vol. 4 (3b), eds. A. Engler and K. Prantl. Leipzig, Germany: W. Engelmann.

- Goldman, N., J. P. Anderson, and A. G. Rodrigo. 2000. Likelihood-based tests of topologies in phylogenetics. *Systematic Biology* 49: 652-670.
- Hamilton, M. B. 1999. Four primer pairs for the amplification of chloroplast intergenic regions with intraspecific variation. *Molecular Ecology* 8: 521-523.
- Hanstein, J. 1854. Die Gesneriaceen des Königlichen Herbariums und der Gärten zu Berlin, nebst Beobachtungen über die Familie im Ganzen. I. Abschnitt. *Linnaea* 26: 145-216.
- Hanstein, J. 1865. Die Gesneriaceen des Königlichen Herbariums und der Gärten zu Berlin, nebst monographischer Uebersich der Familie im Ganzen, II. Abschnitt. *Linnaea* 34: 225-462.
- Huelsenbeck, J. P. and F. Ronquist. 2003. MRBAYES: Bayesian inference of phylogeny. *Bioinformatics* 17: 754-755.
- Johnson, S. D. 1996. Adaptation and speciation models in the Cape floral of South Africa. *Taxon* 45: 59-66.
- Kluge, A. G. and S. J. Farris. 1969. Quantitative phyletics and the evolution of anurans. *Systematic Zoology* 18: 1-32.
- Kvist, L. P. and L. E. Skog. 1993. The genus *Columnnea* (Gesneriaceae) in Ecuador. *Allertonia* 6: 327-400.
- Lewis, P. O. 2001. A likelihood approach to estimating phylogeny from discrete morphological character data. *Systematic Biology* 50: 913-925.

- Li, J.-M. and Y.-Z. Wang. 2007. Phylogenetic reconstruction among species of *Chiritopsis* and *Chirita* section *Gibbosaccus* (Gesneriaceae) based on nrDNA ITS and cpDNA *trnL-F* sequences. *Systematic Botany* 32: 888-898.
- Linnaeus, C. 1753. *Species Plantarum*. Stockholm: Impensis Laurentii Salvii.
- Mayer, V., M. Möller, M. Perret, and A. Weber. 2003. Phylogenetic position and generic differentiation of Epithemateae (Gesneriaceae) inferred from plastid DNA sequence data. *American Journal of Botany* 90: 321-329.
- Möller, M. and Q. C. B. Cronk. 1997. Phylogeny and disjunct distribution: evolution of *Saintpaulia* (Gesneriaceae) inferred from plastid DNA sequence data. *American Journal of Botany* 90: 321-329.
- Möller, M., M. Pfosser, C.-G. Jang, V. Mayer, A. Clark, M. L. Hollingsworth, M. H. J. Barfuss, Y.-Z. Wang, M. Kiehn, and A. Weber. 2009. A preliminary phylogeny of the 'didymocarpoid Gesneriaceae' based on three molecular data sets: incongruence with available tribal classifications. *American Journal of Botany* 96: 989-1010.
- Morley, B. D. 1974. Notes on some critical characters in *Columnea* classification. *Annals of the Missouri Botanical Garden* 61: 514-525.
- Morley, B. D. 1976. A key, typification and synonymy of the sections in the genus *Columnea* L. (Gesneriaceae). *Contributions of the National Botanical Garden of Glasnevin* 1:1-11.
- Morton, C. V. 1971. A reduction of *Trichantha* to *Columnea* (Gesneriaceae). *Phytologia* 22:223-224.

- Müller, K. 2004. PRAP – computation of Bremer support for large data sets. *Molecular Phylogenetics and Evolution* 31: 780-782.
- Nylander, J. A. A., J. C. Wilgenbusch, D. L. Warren, and D. L. Swofford. 2008. AWTY (are we there yet?): a system for graphical exploration of MCMC convergence in Bayesian phylogenetics. *Bioinformatics* 24: 581-583.
- Oersted, A. S. 1858. *Centralamericas Gesneraceer, et systematisk, Plantegeografisk Bidrad til centralamerikas Flora*. Copenhagen: F. S. Muhle.
- Olmstead, R. G., C. W. Depamphilis, A. D. Wolfe, N. D. Young, W. J. Elisons, and P. A. Reeves. 2001. Disintegration of the Scrophulariaceae. *American Journal of Botany* 88: 348-361.
- Oxelman, B., M. Lidén, and D. Berglund. 1997. Chloroplast *rps16* intron phylogeny of the tribe *Sileneae* (Caryophyllaceae). *Plant Systematics and Evolution* 206: 393-410.
- Oxelman, B., P. Kornhall, R. Olmstead, and B. Bremer. 2005. Further disintegration of Scrophulariaceae. *Taxon* 54: 411-425.
- Posada, D. and K. A. Crandall. 1998. MODELTEST: testing the model of DNA substitution. *Bioinformatics* 14: 817-818.
- Posada, D. and T. R. Buckley. 2004. Model selection and model averaging in phylogenetics: advantages of Akaike information criterion and Bayesian approaches over likelihood ratio tests. *Systematic Biology* 53: 793-808.
- Rambaut, A. and A. J. Drummond. 2005. Tracer v1.4, Available at <http://beast.bio.ed.ac.uk/Tracer>.

- Reeves, G., M. W. Chase, P. Goldblatt, M. F. Fay, A. V. Cox, B. Lejeune, and T. Suozachies. 2001. Molecular systematics of Iridaceae: evidence from four plastid DNA regions. *American Journal of Botany* 88: 2074-2087.
- Roalson, E. H., J. K. Boggan, and L. E. Skog. 2005a. Reorganization of tribal and generic boundaries in the Gloxinieae (Gesneriaceae: Gesnerioideae) and the description of a new tribe in the Gesnerioideae, Sphaerorrhizeae. *Selbyana* 25: 225-238.
- Roalson, E. H., J. K. Boggan, L. E. Skog, and E. A. Zimmer. 2005b. I. Phylogenetic patterns and generic boundaries inferred from nuclear, chloroplast, and morphological cladistic datasets. *Taxon* 54: 389-410.
- Roalson, E. H., L. E. Skog, and E. A. Zimmer. 2008. Untangling Gloxinieae (Gesneriaceae). II. Reconstructing biogeographic patterns and estimating divergence times among New World continental and island lineages. *Systematic Botany* 33: 159-175.
- Schemske, D. W. 1981. Floral convergence and pollinator sharing in two bee-pollinated tropical herbs. *Ecology* 62: 946-954.
- Seelanen, T., A. Schnabel, and J. F. Wendel. 1997. Congruence and consensus in the cotton tribe (Malvaceae). *Systematic Botany* 22: 275-288.
- Shaw, J., E. B. Lickey, E. E. Schilling, and R. L. Small. 2007. Comparison of whole chloroplast genome sequences to choose noncoding regions for phylogenetic studies in angiosperms: the tortoise and the hare III. *American Journal of Botany* 94: 275-288.

- Shimodaira, H. and M. Hasegawa. 1999. Multiple comparisons of log-likelihoods with applications to phylogenetic inference. *Molecular Biology and Evolution* 16: 1114-1116.
- Simmons, M. P., and H. Ochoterena. 2000. Gaps as characters in sequence-based phylogenetic analyses. *Systematic Biology* 49: 369-381.
- Smith, J. F. 1991. The evolution and systematics of *Columnea*. Ph. D. Dissertation, Madison: University of Wisconsin.
- Smith, J. F. 1994. Systematics of *Columnea* section *Pentadenia* and section *Stygnanthe* (Gesneriaceae). *Systematic Botany Monographs* 44: 1-89.
- Smith, J. F. 1996. Tribal relationships within the Gesneriaceae: a cladistic analysis of morphological data. *Systematic Botany* 21: 497-514.
- Smith, J. F. 2000. Phylogenetic resolution with the tribe Episcieae (Gesneriaceae): congruence of ITS and *ndhF* sequences from parsimony and maximum-likelihood analyses. *American Journal of Botany* 87: 883-897.
- Smith, J. F. and K. J. Sytsma. 1994a. Evolution in the Andean epiphytic genus *Columnea* (Gesneriaceae). Part I. Morphology. *Systematic Botany* 19: 220-235.
- Smith, J. F. and K. J. Sytsma. 1994b. Evolution in the Andean epiphytic genus *Columnea* (Gesneriaceae). Part II. Chloroplast DNA restriction site variation. *Systematic Botany* 19: 317-336.
- Smith, J. F. and K. J. Sytsma. 1994c. Molecular and morphology: Congruence of data in *Columnea* (Gesneriaceae). *Plant Systematics and Evolution* 193: 37-52.

- Smith, J. F. and C. L. Carroll. 1997. A cladistic analysis of the tribe Episcieae (Gesneriaceae) based on *ndhF* sequences: origin of morphological characters. *Systematic Botany* 22: 713-724.
- Smith, J. F., J. C. Wolfram, K. D. Brown, C. L. Carroll, and D. S. Denton. 1997. Tribal relationships in the Gesneriaceae: Evidence from DNA sequences of the chloroplast gene *ndhF*. *Annals of the Missouri Botanical Garden* 8: 50-66.
- Smith, J. F., M. Kresge, M. Møller, and Q. C. B. Cronk. 1998. The African violets (*Saintpaulia*) are members of *Streptocarpus* subgenus *Streptocarpella* (Gesneriaceae). *Edinburgh Journal of Botany* 31: 765-779.
- Smith, J. F., L. C. Hileman, M. P. Powell, and D. A. Baum. 2004. Evolution of GCYC, a Gesneriaceae homolog of *CYCLOIDEA*, within Gesnerioideae (Gesneriaceae). *Molecular Phylogenetics and Evolution* 31:765-779.
- Smith, J. F., M. Ooi, L. Schulte, M. Amaya M., and J. L. Clark. The disintegration of the subgeneric classification of *Columnnea* (Gesneriaceae). *Selbyana* in review.
- Stearn, W. T. 1968. Observations on a computer-aided survey of the Jamaican species of *Collandra* and *Alloplectus*. Pp. 219-244 in *Modern methods in Plant Taxonomy*. ed. V. H. Heywood. New York: Academic Press.
- Swofford, D. L. 2002. PAUP\*: phylogenetic analysis using parsimony (\*and other materials), version 4.0b10. Sunderland, Massachusetts: Sinauer.
- Wang, Y.-Z., R.-H. Liang, B.-H. Wang, J.-M. Li, Z.-J. Qiu, and Z.-Y. Li. 2010. Origin and phylogenetic relationship of the Old World Gesneriaceae with actinomorphic

flowers, inferred from nrDNA (ITS) and cpDNA (*trnL-F*) sequence data. *Taxon* 59: 1044-1052.

Wang, Y.-Z., R.-B. Mao, Y. Liu, J.-M. Li, Y. Dong, Z.-Y. Li, and J. F.

Smith. 2011. Phylogenetic reconstruction of *Chirita* and allies (Gesneriaceae) with taxonomic treatments. *Journal of Systematics and Evolution* 49: 50-64.

Weber, A. 2004. Gesneriaceae. Pp. 63–158 in *The families and genera of vascular plants*, vol. 7. eds. K. Kubitzki and J. Kadereit. Berlin: Springer-Verlag.

Wiehler, H. 1973. One hundred transfers from *Alloplectus* and *Columnnea* (Gesneriaceae). *Phytologia* 27: 309-328.

Wiehler, H. 1975. *Rufodorsia*, a new Central-American genus in the Gesneriaceae. *Selbyana* 1: 32-35.

Wiehler, H. 1977. New genera and species of Gesneriaceae from the Neotropics. *Selbyana* 2:67-132.

Wiehler, H. 1981. New species and name changes in Neotropical Gesneriaceae. *Selbyana* 5:378-384.

Wiehler, H. 1983. Synopsis of the Neotropical Gesneriaceae. *Selbyana* 6:1-219.

Woo, V. L., M. M. Funke, J. F. Smith, P. J. Lockhart, and P. J. Garnock-Jones. 2011.

New world origins of southwest Pacific Gesneriaceae: Multiple movements across and within the south Pacific. *International Journal of Plant Science* 172: 434-457.

- Xia, Z., Y.-Z. Wang, and J. F. Smith. 2009. Familial placement and relations of *Rehmannia* and *Triaenophora* (Scrophulariaceae s. l.) inferred from five gene regions. *American Journal of Botany* 96: 519-530.
- Yoder, A. D., J. A. Irwin, and B. A. Payseur. 2001. Failure of the ILD to determine data combinability for slow loris phylogeny. *Systematic Biology* 50: 408-424.
- Zimmer, E. A., E. H. Roalson, L. E. Skog, J. K. Boggan, and A. Idnurm. 2002. Phylogenetic relationships in the Gesnerioideae (Gesneriaceae) based on nrDNA and cpDNA *trnL-F* and *trnE-T* spacer region sequences. *Amer. J. Bot.* 89: 296-311.
- Zwickl, D. J. 2006. *Genetic algorithm approaches for the phylogenetic analysis of large biological sequence datasets under the maximum likelihood criterion*. Ph. D. dissertation. Austin: University of Texas.

**Table 1.1 – History of *Columnea* Species Classifications**

A history of the classification of the species of *Columnea* by various authors as adapted from Kvist and Skog (1993). The table includes the number of genera, sections, and subgenera classified by each author and the date of the classification system. Letters represent clades as referred to by Smith et al. (in review) and in Chapter One.

<b>Author</b>	<b>Year</b>	<b>No.</b>	<b>Genera Names</b>	<b>No.</b>	<b>Section Names</b>	<b>No.</b>	<b>Subgenera Names</b>
Hanstein	1854	7	<i>Columnea</i> <i>Ortholoma</i> <i>Collandra</i> <i>Pentadenia</i> <i>Pterygoloma</i> <i>Stenanthus</i> <i>Stygnanthe</i>		-		-
Oersted	1858	4	<i>Columnea</i> <i>Ortholoma</i> <i>Pentadenia</i> <i>Stenanthus</i>		-		-
Hanstein	1865	2	<i>Columnea</i> <i>Stygnanthe</i>		-	7	<i>Columnea</i> <i>Ortholoma</i> <i>Collandra</i> <i>Pentadenia</i> <i>Pterygoloma</i> <i>Stenanthus</i> <i>Cryptocolumnea</i>
Bentham	1876	2	<i>Columnea</i> <i>Trichantha</i>	7	<i>Columnea</i> <i>Ortholoma</i> <i>Collandra</i> <i>Pentadenia</i> <i>Cryptocolumnea</i> <i>Systolostoma</i> <i>Bucinellina</i>		-

Author	Year	Genera		Section		Subgenera	
		No.	Names	No.	Names	No.	Names
Fritsch	1894	2	<i>Columnnea</i> <i>Trichantha</i>	9	<i>Columnnea</i> <i>Ortholoma</i> <i>Collandra</i> <i>Pentadenia</i> <i>Pterygoloma</i> <i>Stenanthus</i> <i>Stygnanthe</i> <i>Cryptocolumnnea</i> <i>Systolostoma</i>	-	
Morton	1971	1	<i>Columnnea</i>	7	<i>Columnnea</i> <i>Ortholoma</i> <i>Collandra</i> <i>Pentadenia</i> <i>Stenanthus</i> <i>Stygnanthe</i> <i>Cryptocolumnnea</i>	-	
Wiehler	1973	4	<i>Columnnea</i> <i>Dalbergaria</i> <i>Ortholoma</i> <i>Pentadenia</i>	-		-	
Wiehler	1975	5	<i>Columnnea</i> <i>Dalbergaria</i> <i>Ortholoma</i> <i>Pentadenia</i> <i>Trichantha</i>	-		-	
Morley	1976	1	<i>Columnnea</i>	5	<i>Columnnea</i> <i>Ortholoma</i> <i>Collandra</i> <i>Pentadenia</i> <i>Pterygoloma</i>	-	

Author	Year	Genera		Section		Subgenera	
		No.	Names	No.	Names	No.	Names
Wiehler	1983	5	<i>Columnea</i> <i>Pentadenia</i> <i>Collandra</i> <i>Ortholoma</i> <i>Bucinellina</i>		-		-
Kvist & Skog	1993	1	<i>Columnea</i>	6	<i>Columnea</i> <i>Ortholoma</i> <i>Collandra</i> <i>Pentadenia</i> <i>Stygnanthe</i> <i>Bucinellina</i>		-
Smith	1994	1	<i>Columnea</i>	5	<i>Columnea</i> <i>Ortholoma</i> <i>Collandra</i> <i>Pentadenia</i> <i>Stygnanthe</i>		-
Smith et al.	In review	1	<i>Columnea</i>	7	Clade A - G		-
Schulte	Current work	1	<i>Columnea</i>	7	<i>Stygnanthe</i> <i>Angustiflorae</i> Clades A, C-F A = <i>Pentadenia</i> C = <i>Collandra</i> E = <i>Columnea</i>		-

**Table 1.2 – DNA Sequencing Results**

Nucleotide sequence characteristics of regions used for this study. Number of accessions sequenced is the number of accessions of 129 included that were successfully sequenced. PIC is the number of phylogenetically informative characters. Number of characters excluded is the number of ambiguities excluded from the data analysis including single base repeats, autapomorphies, or microsatellites. The phylogenetically informative and constant characters come from the data set used for analyses which excluded ambiguities. The \* indicates a mean length outside of the range due to multiple accessions that were not successfully sequenced.

<b>Gene Region</b>	<b>No. of Accessions Sequenced</b>	<b>Align Length</b>	<b>Mean Length</b>	<b>Range</b>	<b>PIC</b>	<b>Constant Characters</b>	<b>No. of Characters Excluded</b>
<i>trnQ-rps16</i> spacer	119	1,222	810	805-1,087	109	627	302
<i>rpl32-trnL<sub>UAG</sub></i> spacer	128	1,353	1003*	1,076-1,876	128	889	185
<i>rps16</i> intron	126	996	720	539-925	41	534	334
<i>trnS-G</i> spacer	121	1,038	568	534-838	47	448	416
<i>trnH-psbA</i> spacer	117	542	279	230-405	37	189	249
ITS	127	723	562*	600-696	153	211	299

**Table 1.3 – Maximum Parsimony Results**

The maximum parsimony results for both gene partitions (cpDNA and ITS) and results for combined partition data analysis from this study are presented. CI is the consistency index, RI is the retention index, and RC is the rescaled consistency index.

<b>Data Set</b>	<b>Number of Trees</b>	<b>Length</b>	<b>CI</b>	<b>RI</b>	<b>RC</b>
cpDNA partition	194	1,577	0.5580	0.7685	0.5829
ITS partition	340	647	0.3866	0.7320	0.3371
Combined gene partitions	232	2,262	0.4717	0.7318	0.4807

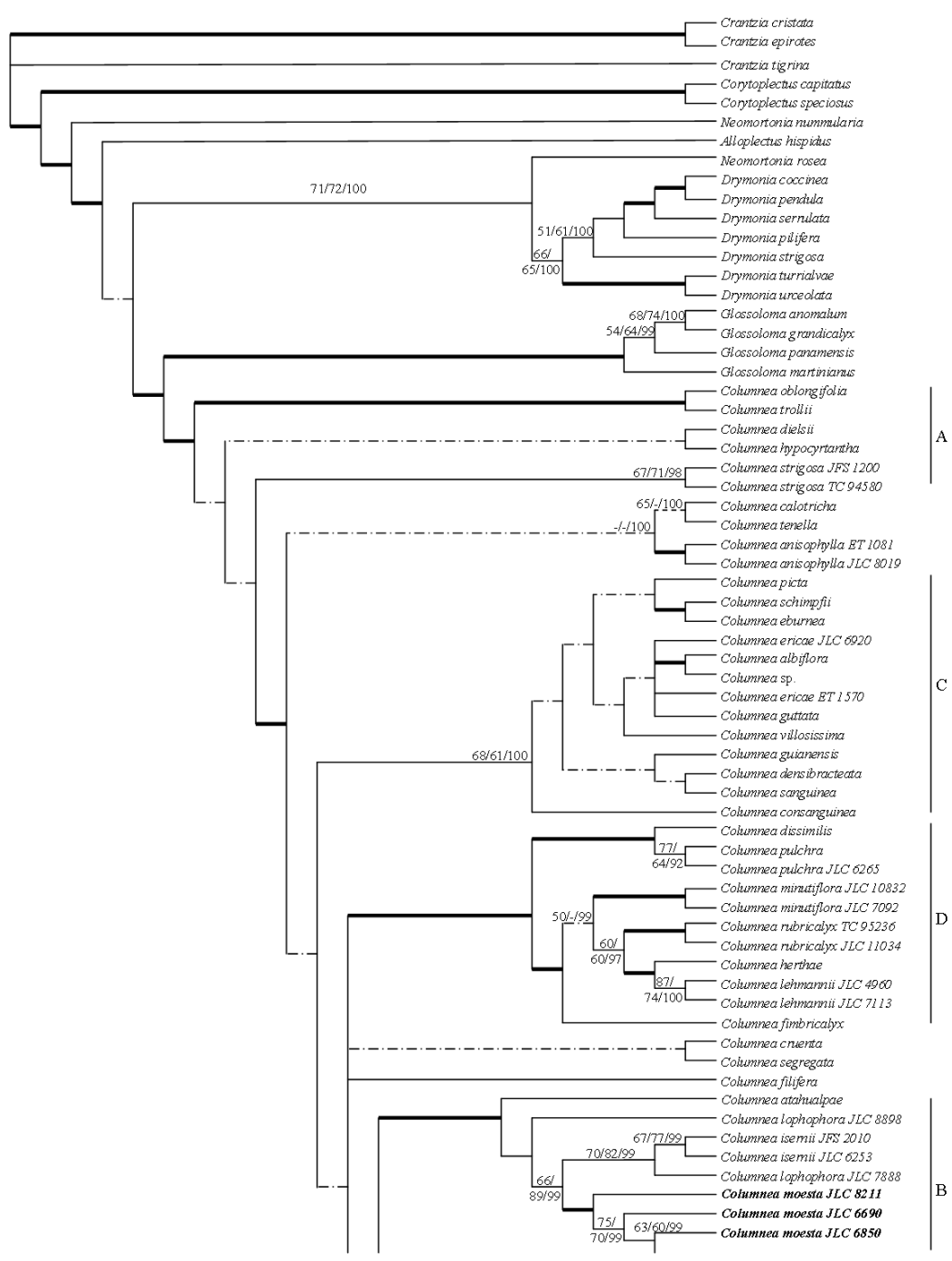
**Table 1.4 – Model Test Results**

The model test results for both gene partitions (cpDNA and ITS) and the combined partition data including the model values, frequency of each base, and the rate of change from one base to another.

<b>Data Set</b>	<b>cpDNA partition</b>	<b>ITS partition</b>	<b>Combined gene partitions</b>
<b>Model</b>	GTR + $\Gamma$ + I	GTR + $\Gamma$	GTR + $\Gamma$ + I
<b>I</b>	0.2518	-	0.3186
<b><math>\Gamma</math></b>	0.9672	0.5054	0.8125
<b>frequency A</b>	0.3328	0.1901	0.3225
<b>frequency C</b>	0.1499	0.2738	0.1583
<b>frequency G</b>	0.1563	0.2823	0.1659
<b>frequency T</b>	0.3610	0.2538	0.3534
<b>R(a) [A-C]</b>	0.9362	1.5960	0.9981
<b>R(b) [A-G]</b>	1.4955	3.7152	1.6106
<b>R(c) [A-T]</b>	0.3133	2.0740	0.3869
<b>R(d) [C-G]</b>	1.2088	0.5129	1.1364
<b>R(e) [C-T]</b>	1.1907	6.1466	2.0389
<b>R(f) [G-T]</b>	1.0000	1.0000	1.0000



**Figure 1.1 – *Columnnea katzensteiniae* (A), *C. tandapiana* (B), *C. isernii* (C), and *C. moesta* (D) demonstrating morphological characteristics. The arrow in plate A shows a ventricose corolla with slight swelling in the middle. Plates A and B are species in *Angustiflorae* that show the larger corolla lobes and less corolla pubescence compared to species in *Stygnanthe* pictured in plates C and D with smaller corolla lobes and more corolla pubescence.**



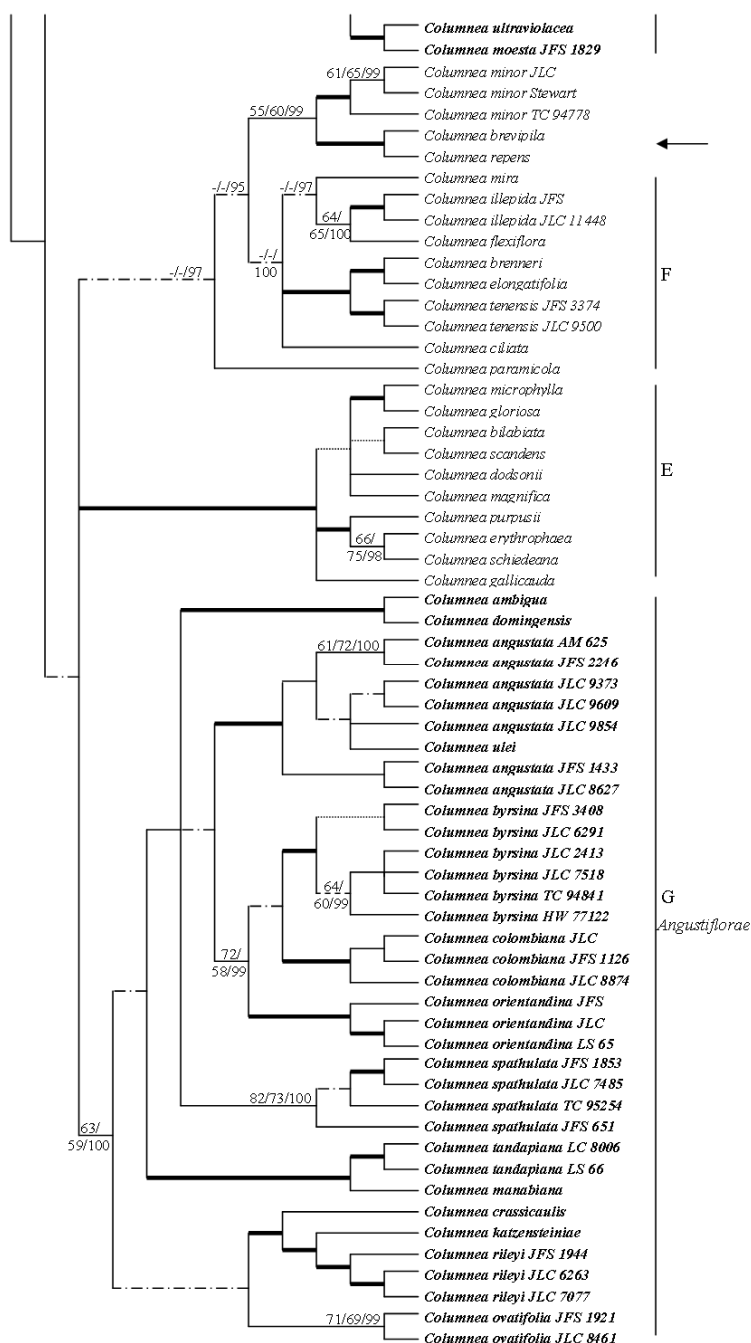


**Figure 1.2 – Summary of maximum parsimony (MP), maximum likelihood (ML), and Bayesian inference (BI) partition model analyses mapped on BI partition analysis tree topology. Numbers above branches represent MP bootstrap (BS)/MLBS/BI posterior probability (PP). Bold branches are strongly supported in all three analyses (MPBS/MLBS > 75; PP > 95). Letters represent clades identified by Smith et al. (in review). Lines with dash dot dash pattern represent branches that collapse in either MP or ML analyses. Accessions in bold represent species that have a similar corolla morphology (tubular corolla with radially to subradially**

symmetric limbs) to species of section *Stygnanthe* sensu Smith (1994). The arrow represents the clade where *C. grisebachiana* was recovered (tree not shown), the third clade of species with radially to subradially symmetric tubular corolla.

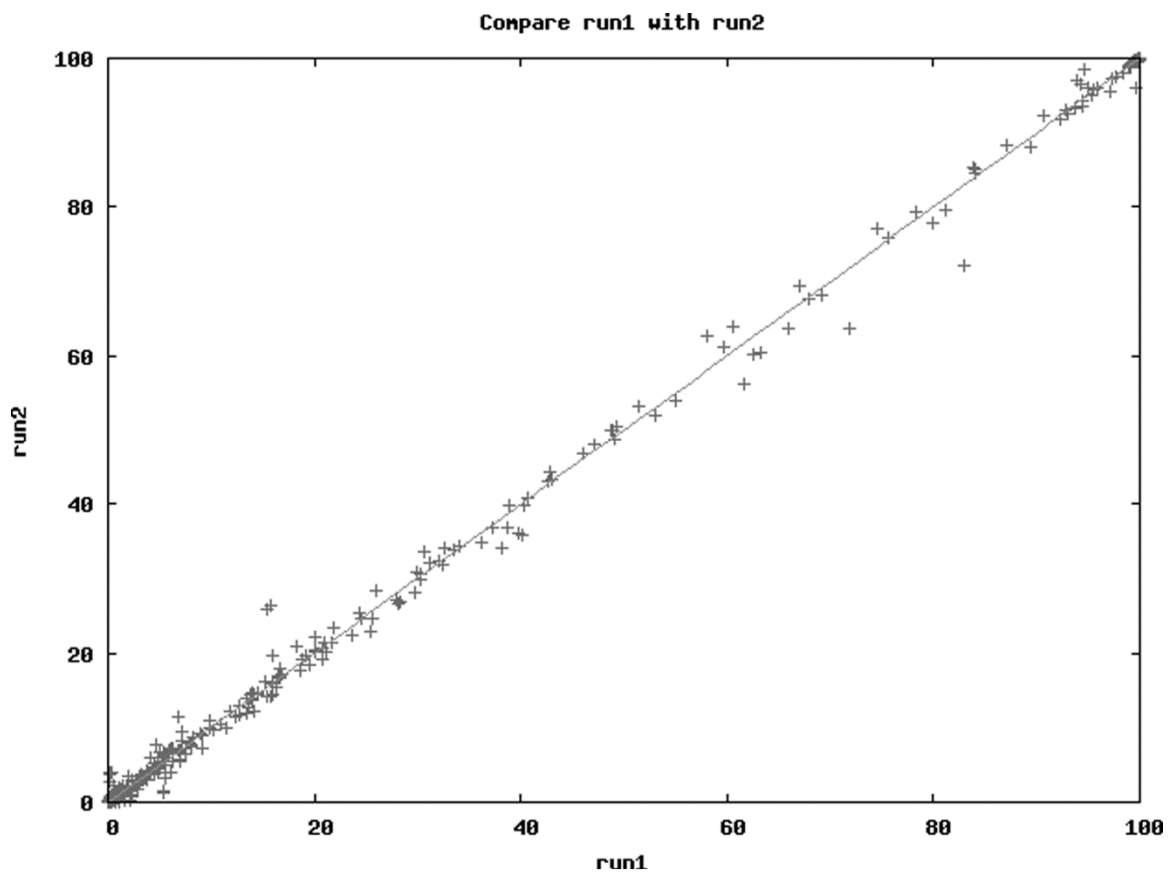
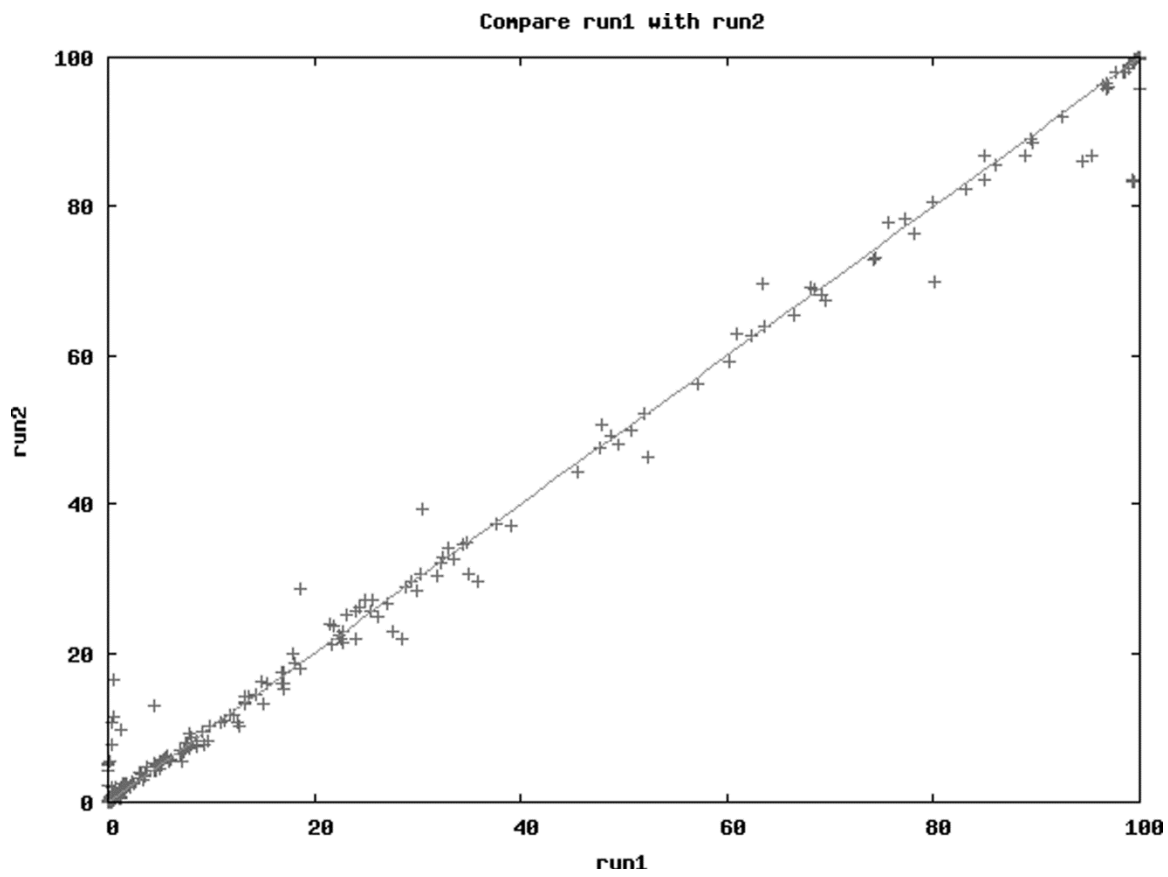


Figure 1.3 – The AWTY results from the comparison of the two Bayesian inference one model analysis runs.



**Figure 1.4 – The AWTY results from the comparison of the two Bayesian inference partition model analysis runs.**

CHAPTER TWO: SPECIES LEVEL PHYLOGENY OF SECTION *ANGUSTIFLORAE*  
IN *COLUMNEA* (GESNERIACEAE)

**Abstract**

Molecular phylogenetic analyses have provided systematists with an approach that allows for better systems of classification that more precisely reflect the common ancestry and evolutionary relationships of taxa. Molecular data also provide enough phylogenetically informative characters to generate trees at the species level with relatively less sequencing and more phylogenetic resolution. Building trees based on multiple independent gene regions generates a phylogenetic tree reflecting the ancestral history of the species rather than the history of an individual gene. In addition, species trees built with independent data can be used to study other aspects of evolutionary history, including patterns and processes of speciation. *Columnea* is the largest Neotropical genus in Gesneriaceae subfamily Gesnerioideae and has had a complex taxonomic history having been divided into various genera, subgenera, and sections over time. Most recent molecular data have divided *Columnea* into seven clades, including section *Angustiflorae*, but have failed to resolve species level relationships within the clades. The phylogenetic analyses presented here sampled 36 accessions representing thirteen of the fifteen species within *Angustiflorae* to provide a species level phylogenetic tree for the section. Five chloroplast DNA gene regions (*trnQ-rps16* spacer, *rpl32-trnL<sub>UAG</sub>* spacer, *rps16* intron, *trnS-G* spacer, and *trnH-psbA* spacer), nuclear ribosomal internal transcribed spacers (ITS1 and ITS2), and the external transcribed spacer (ETS)

were used to generate a well-resolved species level phylogeny of section *Angustiflorae*. In addition, two low-copy nuclear gene regions, glyceraldehyde 3-phosphate dehydrogenase (*G3pdh*) and NADP-dependent isocitrate dehydrogenase (*idh*), were included to boost phylogenetic support of the major branching events within section *Angustiflorae*.

### **Introduction**

Species-level phylogenies are valuable tools when asking various biological questions. Molecular phylogenies are used to delimit species boundaries and define new species when morphological characters are insufficient (Carlson et al. 2011). They can also be useful in identifying sister species and times of divergence. Ruvolo et al. (1993) provided evidence that humans are most closely related to chimpanzees, having diverged about 6.9 million years ago using a species level phylogeny. These phylogenies are also used to help better understand character evolution. Woo et al. (2011) used a species level phylogeny within Gesneriaceae to study bee versus bird pollinators and determine the number and direction of shifts between pollination types. Woo et al.'s (2011) study, along with others, has shown that species level phylogenies can also be used to study and understand the patterns and processes of speciation (Martén-Rodríguez et al. 2010; Meredith et al. 2011; Struwe et al. 2011). However, to accurately answer any of these biological questions, it is important to first build a well-supported species phylogeny (Ruvolo et al. 1993; Martén-Rodríguez et al. 2010; Carlson et al. 2011; Meredith et al. 2011; Struwe et al. 2011; Woo et al. 2011).

Advances in molecular phylogenetics have allowed systematists the opportunity to build species level trees that have the phylogenetic resolution and support required to

conduct further analyses (Carlson et al. 2011; Woo et al. 2011). However, researchers must be careful to build a species tree rather than a gene tree. Each individual gene has its own evolutionary history that can be phylogenetically reconstructed (Maddison 1997). Because of events such as lineage sorting and gene duplication or loss, a gene may have a different evolutionary history than the species (Page and Charleston 1997). This may lead to incongruencies in the branching order or timing of events between the gene tree and the species tree (Nichols 2001).

To build a species tree, it is important to include multiple unlinked gene regions in the phylogenetic analyses (Maddison 1997). If there are no incongruencies among the ancestral histories of the individual gene regions, then the species tree can be inferred from the gene region topologies. Though there is no guarantee that the species tree is being reconstructed, convergence from different data sources is the best means of producing a species tree from both a theoretical and practical perspective (Maddison 1997; Knowles and Carstens 2007).

This study aimed to estimate species trees with five unlinked gene regions to build a species level phylogeny for section *Angustiflorae* in genus *Columnea* L., the largest Neotropical genus in Gesneriaceae subfamily Gesnerioideae. Recent molecular phylogenetic analyses have shown that the 200 plus species of *Columnea* should be divided into seven clades, one of which is section *Angustiflorae* (Smith et al. in review; Chapter One). Species that belong in section *Angustiflorae* have been identified based on molecular analyses and morphological characters (Chapter One). However, previous molecular data have not resolved phylogenetic relationships among the species of

*Angustiflorae*. Therefore, it is the goal of this study to build a well-supported species-level phylogeny for *Angustiflorae*.

I sampled 36 accessions representing thirteen of the fifteen species of section *Angustiflorae* (Appendix B). Phylogenetic analyses were conducted using five chloroplast DNA (cpDNA) gene regions (*trnQ-rps16* and *rpl32-trnL<sub>UAG</sub>* spacers: both from Shaw et al. 2007; *rps16* intron: Oxelman et al. 1997; *trnS-G* spacer: Hamilton 1999; and *trnH-psbA* spacer: Clark et al. 2006), along with nuclear ribosomal internal transcribed spacers (ITS1 and ITS2, hereafter referred to as ITS; Baldwin et al. 1995), and the external transcribed spacer (ETS; Baldwin and Markos 1998). In addition, two low-copy nuclear genes, glyceraldehyde 3-phosphate dehydrogenase (*G3pdh*; Strand et al. 1997) and NADP-dependent isocitrate dehydrogenase (*idh*; Weese and Johnson 2005), were used to increase phylogenetic support for major branching events within *Angustiflorae*. All of these gene regions were chosen because previously they have successfully resolved species level relationships (Linder et al. 2000; Ingram and Doyle 2003; Levin et al. 2005; Johnson and Johnson 2006; Huertas et al. 2007; Smith et al. 2008; Ruiz-Sanchez and Sosa 2010; Steele et al. 2010).

## **Materials and Methods**

### DNA Extraction, Amplification, and Alignment

A complete list of samples and voucher specimens for the accessions used in all analyses is in Appendix B. Two separate data sets were used for all analyses, the first data set included sampling for all species for three gene partitions, and the second data set sampled a reduced set of taxa but with increased DNA sampling, herein referred to as the

full data set and reduced data set, respectively. The ingroup for phylogenetic analyses included 36 accessions for the full data set and a subset of 20 accessions for the reduced data set (Appendix B); accessions in both data sets represented thirteen of the fifteen species in section *Angustiflorae*. The outgroup for phylogenetic analyses included one accession each for eighteen species in the full data set and ten species in the reduced data set (Appendix B). Outgroup accessions for both data sets represented species within the remaining six clades of *Columnnea*, identified by Smith et al. (in review) and Chapter One, in addition to species of the sister genus *Glossoloma* Hanst. (Clark et al. 2012) in the full data set.

DNA was extracted from silica-dried leaf material of one individual plant using Qiagen DNeasy plant mini kits (Valencia, California, U.S.A.) according to manufacturer's instructions. Five cpDNA gene regions were chosen for amplification, including *trnQ-rps16* spacer (Shaw et al. 2007), *rpl32-trnL<sub>UAG</sub>* spacer (Shaw et al. 2007), *rps16* intron (Oxelman et al. 1997), *trnS-G* spacer (Hamilton 1999), and *trnH-psbA* spacer (Clark et al. 2006). The cpDNA gene regions were treated as a single partition in each of the data sets because they are inherited as a single non-recombining unit. The two nuclear DNA gene regions, ITS (Baldwin et al. 1995) and ETS (Baldwin and Markos 1998) were each treated as separate partitions for all analyses. These three gene partitions were amplified for all accessions and concatenated to form the full data set (cpDNA, ITS, and ETS) for analyses.

Five additional gene regions were tested to identify which were the most phylogenetically informative at the species level. The most phylogenetically informative regions were then added to the phylogenetic analyses of *Angustiflorae* to boost

phylogenetic support for relationships among the species within the section. Three separate portions of the chloroplast gene region *trnK-matK* (*trnK1F-matKR*, *matK1F-1R*, *matK2F-2R*; Johnson and Soltis 1994), and two low-copy nuclear genes, *G3pdh* (Strand et al. 1997) and *idh* (Weese and Johnson 2005), were amplified via polymerase chain reaction (PCR) for nine species (Appendix B) of *Columnnea* to test the ability of each gene region to resolve species level relationships within the genus. When *G3pdh* (Strand et al. 1997) and *idh* (Weese and Johnson 2005) were amplified and separated using electrophoresis, they both produced two distinct bands, an indication of two separate loci for each gene region. Each locus was separated by gel cutting, based on its relative size, with the larger loci referred to as A and the smaller loci referred to as B for both low-copy nuclear gene regions (*G3pdhA*, *G3pdhB*, *idhA*, and *idhB*). The separate loci were then gel purified using a Millipore kit (Billerica, Massachusetts, U.S.A.) and used as the template for a second round of PCR. The separation of the two low-copy nuclear genes into two distinct loci each resulted in a comparison of seven separate gene regions: *trnK1F-matKR*, *matK1F-1R*, *matK2F-2R*, *G3pdhA*, *G3pdhB*, *idhA*, and *idhB*. Once all seven gene regions were amplified for each of the nine species (Appendix B), the percent phylogenetically informative characters, number of parsimony informative characters, and consistency index (CI; Kluge and Farris 1969) were determined for each gene region using PAUP\* v4.0 b10 (Swofford 2002). These three values were compared to the same values for ITS and *rpl32-trnL<sub>UAG</sub>* spacer (Table 2.1) that had been determined to be useful for identifying relationships at the species level within *Angustiflorae* (see “Phylogenetic Tree Topology: Full Data Set”). The gene regions with the highest values for all three parameters identified the most rapidly evolving gene regions. When the parameters were

compared, *G3pdhA*, *G3pdhB*, and *idhA* had the highest values of the seven tested gene regions (Table 2.1) and were chosen for further analyses.

Both loci of *G3pdh* (*G3pdhA* and *G3pdhB*) and *idhA* were then amplified for a subset of species from the full data set (Appendix B). In previous phylogenetic analyses of *Columnea*, all of the species of *Angustiflorae* were well-supported as monophyletic species groups when more than one accession was sampled for a species (Chapter One; “Phylogenetic Tree Topology: Full Data Set), with the exception of *C. angustata*. *Columnea angustata* accessions were resolved in a clade with the single accession of *C. ulei*. In full phylogenetic analyses of *Columnea*, seven monophyletic clades were resolved and well-supported (Smith et al. in review; Chapter One). Because species groups and clades were well-supported as monophyletic in previous phylogenetic analyses (Smith et al. in review; Chapter One; “Phylogenetic Tree Topology: Full Data Set”), I am concerned with species level relationships within *Angustiflorae* rather than intraspecific species relationships, and because low-copy nuclear genes are more labor intensive to amplify than cpDNA or nuclear transcribed regions (ITS and ETS), I chose to use a single accession representing each species within *Angustiflorae*, including both *C. angustata* and *C. ulei*, and one to two representatives from each of the six monophyletic clades of *Columnea* (Smith et al. in review; Chapter One) to minimize sequencing. I amplified the low-copy nuclear gene regions for 30 accessions (Appendix B) referred to as the reduced data set.

Though *G3pdhA*, *G3pdhB*, and *idhA* had the highest parameter values and were chosen for further analyses of the reduced data set (Table 2.1), *idhB* was also analyzed for the 30 taxa (Appendix B) because *idhA* and *idhB* were amplified together in the first

round of PCR. Again PAUP\* v4.0 b10 (Swofford 2002) was used to compare the percent phylogenetically informative characters, number of parsimony informative characters, and CI (Kluge and Farris 1969) for each of the four gene regions to the same values of ITS and *rpl32-trnL<sub>UAG</sub>* spacer (Table 2.2). When analyzed for 30 accessions, all four gene regions (*G3pdhA*, *G3pdhB*, *idhA*, and *idhB*) were determined to be phylogenetically informative at the species level based on higher numbers of phylogenetically informative characters, higher percentages of phylogenetically informative characters, and approximately equal CI (Kluge and Farris 1969) values compared to ITS and *rpl32-trnL<sub>UAG</sub>* (Table 2.2).

Maximum parsimony (MP) analyses were performed on each gene region separately to generate individual MP bootstrap (BS) trees. To check for congruence among gene regions, topologies of each of the individual MPBS trees (*G3pdhA*, *G3pdhB*, *idhA*, and *idhB*; trees not shown) were compared to one another and to the topology from the full data set analyses. Both *G3pdhB* and *idhA* partitions were incongruent with *G3pdhA*, *idhB*, and the three partition data set topologies (trees not shown). The *G3pdhB* partition MPBS tree recovered *C. domingensis* as sister to the species of Clade E (Smith et al. in review; Chapter One) with strong support (MPBS = 84; trees not shown). The *idhA* MP strict consensus tree recovered *C. domingensis* as sister to *C. minor*; however, this relationship was not recovered in the MPBS analysis (trees not shown). Another round of MP analyses was conducted to further test the congruence of the four low-copy nuclear regions (*G3pdhA*, *G3pdhB*, *idhA*, and *idhB*). Concatenated data sets were created by combining sequences from cpDNA, ITS, ETS, and one of each of the low-copy nuclear gene regions for all 30 accessions (Appendix B), generating four data

sets with four partitions each (full + *G3pdhA*, full + *G3pdhB*, full + *idhA*, and full + *idhB* data sets). Maximum parsimony BS analyses were run on each of these four data sets. To check for congruence, topologies of each of the MPBS trees (trees not shown) were compared to one another and the topology from the full data set analyses. The topologies from the MPBS analysis of the full + *G3pdhB* and full + *idhA* data sets were incongruent with the MPBS tree topologies of the full + *G3pdhA*, full + *idhB* data sets, and the full data set topology. In the MPBS tree topology of the full + *G3pdhB* data set, the species of Clade E (Smith et al. in review; Chapter One) were sister to *C. ambigua* and *C. domingensis* with MPBS = 54 (trees not shown). In the MPBS tree topology of the full + *idhA* data set, *C. moorei* was recovered as sister to *C. crassicaulis* with MPBS = 96 (trees not shown), and *C. moesta* was recovered as belonging to section *Angustiflorae* (MPBS = 54; trees not shown). The incongruent topologies were most likely due to paralogs, and thus *G3pdhB* and *idhA* were completely removed from further analyses. Of the original seven gene regions, only two low-copy nuclear gene regions, *G3pdhA* and *idhB*, were included in further analyses. The two low-copy nuclear gene regions were amplified for the 30 accessions (Appendix B) and were each treated as individual partitions. The sequences from cpDNA, ITS, and ETS for each of the 30 accessions (Appendix B) were added to the sequences from *G3pdhA* and *idhB* to create the reduced data set with a smaller taxon sampling but increased DNA sampling.

Double-stranded DNA was amplified via PCR, following the methods of Smith et al. (1997). Sequences were obtained either through the methods of Smith et al. (2004) or through Genewiz (Plainfield, New Jersey, U.S.A.); chromatograms were viewed and sequences edited and aligned by hand in PhyDE (<http://www.phyde.de/>).

Nearly each gene region had missing data at the beginning and end in the full alignments, due to different sequencing methods. Additionally, the alignment produced regions of ambiguity due to single base or microsatellite repeats. Areas of missing data and ambiguous alignments were excluded from phylogenetic analyses. Single base and microsatellite repeats can be unambiguously aligned; however, the homology of these repeats is uncertain. To assess the utility of including single base and microsatellite repeats, the resolution and support within the tree can be compared with and without the repeats included. Thus, two additional MP analyses were performed for both the full and reduced data sets. The first analysis of each data set included the single base and microsatellite repeats, and the second analysis for each data set excluded these repeats. If characters were homoplastic, they would lead to less resolution and support within the tree, due to increased homoplasy in the data, which would be reflected in reduced CI (Kluge and Farris 1969) values for the MP analyses with the single base and microsatellite repeats included.

The alignments also resulted in gaps to account for insertion or deletion (indel) events. The inclusion of indel events can often be of phylogenetic significance (Simmons and Ochoterena 2000). Each indel event for both the full and reduced data sets was scored as present or absent for all accessions. An additional partition was added to the end of each concatenated data set representing the indel event scores (Simmons and Ochoterena 2000). The data sets that included the indel event scores were analyzed using MP in PAUP\* v4.0 b10 (Swofford 2002) and BI with the Mk1 model (Lewis 2001) in MrBayes 3.1.1 (Huelsenbeck and Ronquist 2003).

### Test of Incongruence

The partition homogeneity test (Farris et al. 1994) was performed as implemented in PAUP\* v4.0 b10 (Swofford 2002) with 10,000 bootstrap replicates (using a heuristic search, simple addition, and no branch swapping). For each data set, the partitions were treated separately for the analysis. As an additional measure of congruence among partitions, bootstrap analyses were performed for both concatenated data sets (full and reduced) and on each partition separately (full data set: cpDNA, ITS, and ETS; reduced data set: cpDNA, ITS, ETS, *G3pdhA*, and *idhB*) to assess areas of conflict and to determine if any conflict was strongly supported (Seelanen et al. 1997). Sequences that were incongruent with other partitions were removed. Analyses were then repeated to verify that deleted regions were the source of incongruence based on increased resolution and branch support in combined analyses (Mason-Gamer and Kellogg 1996; Smith 2000).

### Phylogenetic Analyses

Phylogenetic trees were estimated using MP, maximum likelihood (ML), and Bayesian inference (BI) for both data sets. Maximum parsimony analyses were performed using PRAP2 (Müller 2004) in conjunction with PAUP\* v4.0 b10 (Swofford 2002). Bootstrap support (BS) for nodes (Felsenstein 1985) was estimated with 1000 heuristic replicates using PRAP2 (Müller 2004). Descriptive statistics reflecting the amount of phylogenetic signal in the parsimony analysis were given by the CI (Kluge and Farris 1969), retention index (RI; Farris 1989), and the resulting rescaled consistency index (RC; Farris 1989).

Maximum likelihood and BI analyses were performed using optimal substitution models suggested by Modeltest 3.6 (Posada and Crandall 1998). The Akaike information criterion (AIC), which allows non-nested models to be evaluated, was used as a selection criterion (Posada and Buckley 2004) for all partition regions separately (full data set: cpDNA, ITS, and ETS; reduced data set: cpDNA, ITS, ETS, *G3pdhA*, and *idhB*) and as combined data sets (full and reduced).

Substitution models were determined for individual partitions separately because three BI analyses were completed using MrBayes 3.1.1 (Huelsenbeck and Ronquist 2003). All three BI analyses were run for the full and reduced data sets separately. The first BI analyses, referred to as the one model analyses, were performed using a single model for all data in each set. The second BI analyses, referred to as the partition model analyses, were performed using individual models for each partition (full data set: cpDNA, ITS, and ETS; reduced data set: cpDNA, ITS, ETS, *G3pdhA*, and *idhB*). The third BI analyses, referred to as the indel analyses, used a single model for all partitions and included the additional partition in each data set, representing the indel event scores.

All analyses were run with 4 to 1 heated chains, for ten million generations. Convergence was determined by viewing in Tracer v1.3 (Rambaut and Drummond 2005), and a burnin of 50,000 generations was discarded prior to sampling the posterior distribution for all BI analyses. All of the BI analyses were repeated twice to ensure that parameter estimates converged to similar values. The separate runs were compared using the online version of Are We There Yet (AWTY; Nylander et al. 2008) as a means of determining if the separate chains approximated the same target distribution. The ML

analyses were completed using GARLI v0.96 (Zwickl 2006) with 100 bootstrap replicates using a single model for both the full and reduced data sets.

## **Results**

### DNA Amplification and Sequence Alignment

Amplifications were successful for all regions for all individuals with some exceptions for each DNA region (Table 2.3). Length for the aligned sequence and the aligned sequences with missing and ambiguous regions removed are in Table 2.3 for all gene regions. In the phylogenetic analyses there were a total of 4,282 base pairs included for the full data set and a total of 6,281 base pairs included for the reduced data set. The 5.8S gene between ITS1 and ITS2 was identical across ingroup species for both data sets and was excluded from the analyses and calculations. Of the 4,282 base pairs of the full data set, 3,604 were constant and 410 were uninformative leaving 268 (6.3%) as phylogenetically informative. Of the 6,281 base pairs of the reduced data set, 5,340 were constant, and 612 were uninformative leaving 276 (4.4%) as phylogenetically informative.

Additional MP analyses to test the impact of single base and microsatellite repeats showed a loss of resolution and support when these characters were included in analyses for both data sets (trees not shown). There was also a drop in the CI (Kluge and Farris 1969) between the analyses with and without single base and microsatellite repeats for both the full data set (included: CI = 0.5448; excluded: CI = 0.5572) and the reduced data set (included: CI = 0.4625; excluded: CI = 0.7905). A lower CI (Kluge and Farris 1969) is an indication of homoplasy among the included data. The reduced resolution and

lower CI (Kluge and Farris 1969) values in the analyses including single base and microsatellite repeats implies that the repeats are homoplastic, at least in part. Because the inclusion of single base and microsatellite repeats resulted in lower resolution, support, and CI values (Kluge and Farris 1969), I excluded them from further analyses for both the full and reduced data sets.

The data sets with the indel event scores included were identical to the combined data sets for the number of base pairs included, constant base pairs, uninformative base pairs, and phylogenetically informative characters (Table 2.3). The full data set included 55 indel events that were scored as present or absent, ranging in length from 2 to 66 base pairs. The reduced data set included 27 indel events that were scored as present or absent, also ranging in length from 2 to 66 base pairs. Analyses of data sets including indel event scores will herein be referred to as the full indel data set and reduced indel data set. Number and range of lengths for indel events in each gene region are in Table 2.4.

#### Test of Incongruence

The result of the partition homogeneity test ( $p = 0.01$ ) indicated significant differences between partitions. However, as has been reported on many occasions, this test often indicates incongruence when none exists (Reeves et al. 2001; Yoder et al. 2001), and as a result, comparing MPBS support for individual partitions may be a better indicator of incongruence (Seelanen et al. 1997). The comparison of the full data set partitions resulted in incongruencies between the MPBS tree topology for the ETS partition and the topologies of the MPBS trees of the other two partitions (cpDNA and

ITS; trees not shown). The ETS partition MP tree had a BS > 50 for a subclade containing *C. microphylla*, *C. minor*, *C. moorei*, and *C. purpusii* (trees not shown). In the other two partitions' MPBS trees (cpDNA and ITS; trees not shown), these four species were in four different clades (trees not shown; Clades B, D, E, and F of Smith et al. in review; Chapter One). As a result, the ETS sequences for these four species (*C. microphylla*, *C. minor*, *C. moorei*, and *C. purpusii*) were removed from further analyses. Removing these sequences was confirmed by a second MPBS analysis of the ETS partition that increased the support of a congruent topology for the placement of the four species (trees not shown). The comparison of the MPBS tree topologies of the five individual partitions of the reduced data set also resulted in incongruencies. The individual *G3pdhA* partition MPBS analysis showed support for *C. katzensteiniae* as sister to *C. ovatifolia* (trees not shown). In the other four partitions' (cpDNA, ITS, ETS, and *idhB*) MPBS analyses, *C. katzensteiniae* was supported as sister to *C. rileyi* (trees not shown). Because of the incongruence between the *G3pdhA* partition topology and the topologies of the other four partitions, the *C. katzensteiniae G3pdhA* sequence was removed from all further analyses. There was also a difference between the *idhB* partition topology and the other four partition MPBS topologies. In the *idhB* MPBS tree, *C. crassicaulis* was resolved as sister to *C. ovatifolia* (trees not shown). In the other four partitions' (cpDNA, ITS, ETS, and *G3pdhA*) MPBS trees, *C. crassicaulis* was resolved as sister to *C. katzensteiniae* and *C. rileyi* (trees not shown). Because of this incongruence, the *C. crassicaulis idhB* sequence was removed from all further analyses. Removing the *G3pdhA* and *idhB* sequences for *C. katzensteiniae* and *C. crassicaulis* respectively was confirmed by performing MPBS analyses of each partition that resulted

in congruent topologies among the MPBS trees of the other three partitions of the reduced data set (trees not shown). The differences between the partition MPBS tree topologies including the *C. katzensteiniae* *G3pdhA* sequence and the *C. crassicaulis* *idhB* sequence may have been the result of paralogs between the two low-copy nuclear gene regions (see “Discrepancies among Data Partitions”).

All other regions of the final analyses were in complete topological congruence or received BS < 50 for the individual analyses, which is an indication that the ancestral history of the species is being reconstructed rather than individual gene region ancestral histories. Therefore, a combined analysis of DNA regions for each data set was performed and is the basis for all results and discussion.

### Phylogenetic Analyses

Maximum parsimony analysis resulted in 175 trees of 1045 steps (CI = 0.5572, RI = 0.7764, RC = 0.5810) for the full data set and four trees of 1160 steps (CI = 0.7905, RI = 0.6421, RC = 0.5076) for the reduced data set. Results from MP analyses of individual partitions for both data sets are in Table 2.5 (individual MP trees not shown). The TVM + I +  $\Gamma$  model was chosen for both the combined full reduced data sets for the BI one model analyses. Complete Modeltest 3.6 (Posada and Crandall 1998) results for individual partitions used for both data sets in the BI partition model analyses are in Table 2.6. The Mk1 model was used for both data sets in the BI indel analyses (Lewis 2001). I report the 50% majority-rule consensus tree sampled from the posterior probability (PP) distribution for all of the BI analyses separately (individual BI trees not shown). The AWTY (Nylander et al. 2008) output indicated that the separate chains

approximated the same target distribution for both data sets in the one model analyses (Figures 2.1 and 2.2), the partition model analyses (Figures 2.3 and 2.4), and the indel model analyses (results not shown). The TVM + I +  $\Gamma$  model for both the full and reduced data sets for the ML analyses produced one tree each. The results were  $-\ln L = 13484.81077$  for the full data set and  $-\ln L = 15833.2151$  for the reduced data set (individual ML trees not shown).

All analyses produced trees with congruent topologies with varying amounts of resolution for both the full and reduced data sets. The BI partition model produced the most resolved topology for both data sets. The BI partition model tree with the combined results from the MP, ML, BI one model, and BI partition model analyses are in Figures 2.5 for the full data set and 2.6 for the reduced data set. Support for clades is represented by MPBS, maximum likelihood BS (MLBS), BI one model PP (OBPP), and BI partition model PP (PBPP) and is reported as MPBS/MLBS/OBPP/PBPP hereafter in the text.

#### Phylogenetic Tree Topology: Full Data Set

In the full data set, BI analyses section *Angustiflorae* was recovered as monophyletic (Figure 2.5; -/-/100/100). There was no resolution to support which clade is sister to section *Angustiflorae*; however, there was support for the monophyly of each of the other six clades (Figure 2.5; Clade A: 88/90/100/100; Clade B: 67/54/99/99; Clade C: 90/86/96/97; Clade D: 97/95/100/100; Clade E: 58/72/100/100; Clade F: -/-/93/91) of *Columnea* identified by Smith et al. (in review) and Chapter One.

Despite the lack of BS support for the monophyly of *Angustiflorae*, there was phylogenetic support for subclades and relationships among species (Figure 2.5) within the section. The first subclade, referred to as subclade A<sub>s</sub>, relationship showed strong

support for *C. ambigua* and *C. domingensis* as sister (Figure 2.5; 98/99/100/100; Figure 2.6: 98/88/100/100) and are supported as sister to all other species of *Angustiflorae* (Figure 2.5: -/-/100/100; Figure 2.6: -/55/99/99).

The next subclade within *Angustiflorae*, subclade B<sub>s</sub>, was supported as the next monophyletic group sister to the remaining species of *Angustiflorae* (Figure 2.5: -/-/98/98; Figure 2.6: -/-/93/89) and included three species: *C. spathulata*, *C. manabiana*, and *C. tandapiana* (Figure 2.5; 87/93/100/100). Within subclade B<sub>s</sub>, *C. manabiana* was recovered as sister to *C. tandapiana* (Figure 2.5: 99/100/100/100; Figure 2.6: 99/100/100/100). *Columnnea spathulata* was supported as sister to these two species (Figure 2.5: 87/93/100/100; Figure 2.6: -/-/100/100).

The next subclade, subclade C<sub>s</sub>, had moderate support and included four species: *C. crassicaulis*, *C. katzensteiniae*, *C. rileyi*, and *C. ovatifolia* (Figure 2.5; 61/65/100/100). It was recovered as sister to the five species of *Angustiflorae* (Figure 2.5: -/-/100/100; Figure 2.6: -/-/96/91). The full data set analyses recovered *C. ovatifolia* as the sister to the remaining three species within subclade C<sub>s</sub> (Figure 2.5; 61/65/100/100). This relationship was also recovered by the reduced data set analyses (Figure 2.6; 73/82/100/100). *Columnnea crassicaulis* was recovered as sister to the remaining two species (Figure 2.5; 71/69/95/97; Figure 2.6; -/-/55/60). Finally, within subclade C<sub>s</sub>, *C. katzensteiniae* and *C. rileyi* were well-supported as sister to one another in both the full and reduced data set analyses (Figure 2.5: 93/95/100/100; Figure 2.6: 50/53/90/97). The loss of support for the sister relationship between *C. katzensteiniae* and *C. rileyi* in the reduced data set analyses compared to the full data set analyses may have been the result of paralogs or incomplete lineage sorting (see “Discrepancies among Data Partitions”).

The final subclade in section *Angustiflorae*, subclade D<sub>s</sub>, had low support, but was recovered by all analyses and included five species: *C. angustata*, *C. ulei*, *C. colombiana*, *C. byrsina*, and *C. orientandina* (Figure 2.5; 62/55/56/85). In all analyses, *C. ulei* fell within the grouping of *C. angustata* accessions (Figure 2.5: 76/75/97/97; Figure 2.6: 94/90/100/100). In both the full and reduced data set analyses, *C. byrsina* and *C. orientandina* were recovered as sister to one another (Figure 2.5: 53/54/69/-; Figure 2.6: 81/74/87/95). In the analyses of the full data set, *C. colombiana* was recovered as sister to *C. angustata* with moderate support (Figure 2.5; 53/55/98/99). This relationship was also recovered by the reduced data set analyses but with less support than the full data set analyses (Figure 2.6; -/82/59). The loss of support for *C. angustata* and *C. colombiana* as sister may be the result of paralogs or incomplete lineage sorting (see “Discrepancies among Data Partitions”).

#### Phylogenetic Tree Topology: Reduced Data Set

Overall, the reduced data set recovered the same topology (Figure 2.6) as the full data set (Figure 2.5). In the reduced data set BI analyses, section *Angustiflorae* was recovered as monophyletic (Figure 2.6; -/55/100/99). The other clades (Smith et al. in review; Chapter One) of *Columnnea* were strongly supported as monophyletic by all analyses when more than one species from the clade was included in the reduced data set analyses (Figure 2.6; Clade C: 90/96/100/100; Clade E: 94/96/100/100; Clade F: 100/100/100/100).

The reduced data set also recovered the same four subclades within section *Angustiflorae*. The subclades are subclade A<sub>s</sub>: *C. ambigua* and *C. domingensis* (Figure 2.6; 98/88/100/100); subclade B<sub>s</sub>: *C. spathulata*, *C. manabiana*, and *C. tandapiana*

(Figure 2.6; -/-/100/100); subclade C<sub>s</sub>: *C. ovatifolia*, *C. crassicaulis*, *C. katzensteiniae*, and *C. rileyi* (Figure 2.6; 73/82/100/100); and subclade D<sub>s</sub>: *C. angustata*, *C. ulei*, *C. colombiana*, *C. byrsina*, and *C. orientandina* (Figure 2.6; 72/82/100/100). The same species level relationships as the full data set analyses were recovered with the same or greater phylogenetic support, except in the cases of *C. katzensteiniae/C. rileyi* and *C. angustata/C. colombiana* as sister species pairs (see “Discrepancies among Data Partitions”).

#### Analyses of Data Sets Including Indel Event Scores

Results for the full indel data set were similar to the results from the full data set for MP and BI analyses. For the full data set, the MPBS tree with the indel event scores included (trees not shown) recovered the same topology as the MPBS tree without the indel event scores included (Figure 2.5) with two exceptions. The first difference between the two analyses was that the MPBS tree from the full indel data set lacked resolution for subclade D<sub>s</sub> (trees not shown) and instead had support for the five species of subclade D<sub>s</sub> in two separate subclades, grouping *C. angustata*, *C. ulei*, and *C. colombiana* together and *C. byrsina* and *C. orientandina* together (trees not shown). The analyses of the full data set resolved subclade D<sub>s</sub> as monophyletic (Figure 2.5; 62/55/56/85). The other difference between the two MP analyses was in the MPBS tree of the full indel data set there was support (trees not shown; MPBS = 66) for clades C and D of *Columnea* (Figure 2.5) as sister to one another. The MPBS tree of the full data set had no support for this relationship (Figure 2.5). The BI indel analysis (trees not shown) had the same topology as the BI partition model analysis of the full data set with only one exception. Similar to the MP analysis of the full indel data set (trees not

shown), the BI indel analysis lost resolution of subclade D<sub>s</sub> (trees not shown). In Figure 2.5, the BI partition model analysis of the full data set showed resolution for *C. colombiana* as sister to *C. angustata/C. ulei* (Figure 2.5; 53/55/98/99) and *C. byrsina* as sister to *C. orientandina* (Figure 2.5; 53/54/69/-). These sister relationships were lost in the BI indel analysis; instead *C. angustata/C. ulei*, *C. colombiana*, *C. byrsina*, and *C. orientandina* were recovered as a single polytomy with no resolution of relationships among the species (trees not shown).

The results from both the MP and BI analyses of the reduced indel data set (trees not shown) were similar to the results from the reduced data set analyses (Figure 2.6) with two exceptions in each the MP and BI analyses. Though there is little support, in the MP, ML and BI analyses of the reduced data set, *C. colombiana* was recovered as sister to *C. angustata* (Figure 2.6; -/-/75/59). In both the MP and BI analyses of the reduced data set, *C. colombiana* was recovered as sister to *C. byrsina* and *C. orientandina* (trees not shown; MPBS = 51; BI Indel PP = 54). The second difference between the reduced data set analyses with and without the indel event scores included was the resolution of *C. katzensteiniae* as sister to *C. rileyi*. In the BI analyses of the reduced data set, *C. katzensteiniae* was supported as sister to *C. rileyi* (Figure 2.6; 50/53/97/97). In both the MP and BI analyses of the reduced indel data set, this relationship was not recovered; instead the MP and BI analyses of the reduced indel data set recovered *C. katzensteiniae* as sister to *C. crassicaulis* (trees not shown; MPBS = 51; BI indel PP = 53). The differences between the sister relationships of both *C. colombiana* and *C. katzensteiniae* in the MP and BI analyses of the reduced indel data set compared to the reduced data set without the indel event scores included were most likely due to paralogs

among the two-low copy nuclear genes *G3pdhA* and *idhB* (see “Discrepancies among Data Partitions”).

## Discussion

### Data Partitions

All phylogenetic analyses were run for both the full and reduced data sets. The full data set analyses showed support for the same seven clades as Smith et al. (in review) and Chapter One within *Columnnea* (Figure 2.5). The full data set analyses also showed support for four subclades (Figure 2.5; subclades A<sub>s</sub>-D<sub>s</sub>) among the species of section *Angustiflorae*. However, the branching events among the subclades within *Angustiflorae* were not well-supported (Figure 2.5). The reduced data set was thus created to boost support among the major branching events within *Angustiflorae* (Figure 2.6). The full data set analyses showed minimal support for subclade D<sub>s</sub> (Figure 2.5; 62/55/56/85). The ML and BI analyses of the reduced data set the boosted support for the monophyly of subclade D<sub>s</sub> (Figure 2.6; 72/82/100/100). In the full data set analyses, *C. byrsina* was recovered as sister to *C. orientandina* but with minimal support (Figure 2.5; 53/54/69/-). The reduced data set analyses increased support for *C. byrsina* as sister to *C. orientandina* in all analyses (Figure 2.6; 81/74/87/95). The reduced data set was able to better resolve the relationships among species within section *Angustiflorae* because of the inclusion of the two low-copy nuclear genes. Because both *G3pdhA* and *idhB* are rapidly evolving gene regions, they provided additional phylogenetic information (Table 2.2) and increased support and resolution among species (Figure 2.6).

### Monophyly of Section *Angustiflorae*

The species specifically belonging within section *Angustiflorae* have previously been circumscribed within the section (Chapter One) and remain monophyletic in these analyses (Figures 2.5 and 2.6). The thirteen sampled species of fifteen morphologically defined species in section *Angustiflorae* were recovered as monophyletic by both the full and reduced data sets' BI analyses (Figure 2.5: -/-/100/100; Figure 2.6: -/55/100/99). The lack of support for the monophyly of section *Angustiflorae* in the MP and ML analyses may be because these phylogenetic models are less likely than BI to recover monophyletic groups (Fitch 1971). If a clade is monophyletic because of a few character state changes that are rare, the MP analyses will often not recover this relationship. The MP analysis is based on the fewest number of changes rather than the likelihood of changes. Character state changes that are more likely under a probabilistic model are all considered equal in the MP analysis (Tuffley and Steel 1997). In a BI analysis, character state changes that are less likely can have a larger impact on the resulting topology, but would be equally weighted in the MP analysis, potentially resulting in a loss of resolution (Fitch 1971). Though character state changes are not equally likely in ML analyses, section *Angustiflorae* was not recovered as monophyletic in the MLBS tree (Figure 2.6). Similar to BI, ML analyses use a probabilistic model for character state changes. However, in the ML analysis, the BS tree was based on resampling the data with replacement (Tuffley and Steel 1997). Rare character state changes that support monophyletic clades are less likely to be sampled over 50% of the time. My data was not rich in phylogenetically informative characters (three partition data set: 6.3%; five partition data set: 4.4%) implying that support for any one clade is the result of a few

characters. Those few characters may not have been sampled in BS analyses (either MP or ML), resulting in less resolution. The simplified model of MP amplifies this effect.

#### Subclades within *Angustiflorae*

Though the monophyly of section *Angustiflorae* was only recovered by the BI analyses for both the full and reduced data sets, four subclades within section *Angustiflorae* were recovered by all analyses. These subclades were mostly well-supported and represented groups of species with similarities in either geographic distribution or morphology.

The first subclade, subclade A<sub>s</sub> included two species: *C. ambigua* and *C. domingensis*, which are similar in both their geographic distribution and morphology. Geographically, both species are endemic to the Caribbean, *C. ambigua* to Puerto Rico and *C. domingensis* to the island of Hispaniola. Morphologically, both species share the standard morphological features of *Angustiflorae*, with small tubular corollas that are radially to subradially symmetric, sparsely hirsute or pilose corollas, and opposite, anisophyllous leaves. *Columnea ambigua* and *C. domingensis* can be distinguished from each other and other species of *Angustiflorae* by distinct calyx lobes. *Columnea ambigua* has coarsely toothed calyx lobes (Smith 1994), and *C. domingensis* has lacinate calyx lobes (see “Taxonomic Treatment”).

Subclade B<sub>s</sub> included *C. spathulata*, *C. manabiana*, and *C. tandapiana* (Figure 2.5: 87/93/100/100; Figure 2.6: -/-/100/100). The three species within this subclade share morphological similarities. Both *C. manabiana* and *C. tandapiana* have long, narrow, lanceolate to slightly falcate leaves and small yellow corollas (Smith 1994). *Columnea*

*spathulata* is a widespread species with various morphological characteristics, though it usually has lanceolate-oblong leaves and a small yellow corolla (Smith 1994).

*Columnnea crassicaulis*, *C. katzensteiniae*, *C. rileyi*, and *C. ovatifolia* comprised the next subclade within section *Angustiflorae*, subclade C<sub>s</sub>. Despite the difference in support between the two data sets (see “Phylogenetic Tree Topology: Full Data Set), there are still morphological similarities among the four species. All four species have opposite leaves that are similar in size and with entire calyx margins. The most unifying morphological characteristic for the four species of subclade C<sub>s</sub> is the presence of darker colored spots on the lobes of the corolla. This morphological trait is unique to these four species of the 90 species sampled within genus *Columnnea* (Smith 1994; Chapter One).

Subclade D<sub>s</sub>, the final subclade within section *Angustiflorae*, included five species. Morphologically, there are similarities among all five of these species, even if the relationships among them are not well-supported. All five species of subclade D<sub>s</sub> have inflorescences with two to eight flowers per axil, anisophyllous leaves with pilose to hirsute pubescence and entire margins, and lanceolate calyx lobes that are green with pink to red coloration (Smith 1994). The five species also have morphologies that are similar among sister species. The morphological variation of *C. ulei* falls completely within the morphological variation of *C. angustata* and implies that *C. ulei* had been misclassified as a separate species and should be considered a synonym of *C. angustata* (see “Taxonomic Treatment”). Within *Angustiflorae*, *C. byrsina* and *C. orientandina* are the only two species that have dorsiventrally arranged leaves (Smith 1994). Both species also have corollas with a different coloration on the limb and lobe. This morphological

characteristic is shared with *C. colombiana*, which usually has a red-purple corolla with a green-yellow limb and lobes (Smith 1994).

#### Discrepancies among Data Partitions

There were two differences in the resolution of the resulting topologies from the MP and BI analyses of the reduced indel data set compared to the resulting topologies from the analyses of the reduced data set without the indel event scores included. In the reduced indel data set topology in subclade D<sub>s</sub>, *C. colombiana* was recovered as sister to *C. byrsina* and *C. orientandina* (trees not shown; MPBS = 51, BI indel PP = 54). This was different from the topology of the reduced data set, with *C. colombiana* recovered as sister to *C. angustata/C. ulei* (Figure 2.6; -/-/75/59). There was also a difference in subclade C<sub>s</sub> between the reduced data set analyses with and without the indel event scores. In the reduced indel data set analyses, *C. katzensteiniae* was recovered as sister to *C. crassicaulis* (trees not shown; MPBS = 51; BI indel PP = 53). However, in the reduced data set analyses without the indel event scores included, *C. katzensteiniae* was recovered as sister to *C. rileyi* (Figure 2.6; 50/53/97/97). In both subclades C<sub>s</sub> and D<sub>s</sub>, there was a loss of resolution in the reduced indel data set analyses compared to the reduced data set analyses without the indel event scores included. Including scores for the indel events amplifies the effect of indel events in the overall MP and BI analyses. Because there were differences in resolution between the reduced data set with and without indel event scores included, but not in the full data set with and without indel event scores included (see “Analyses of Data Sets Including Indel Event Scores”), it is possible that there was a duplication event or lineage sorting in either *G3pdhA* or *idhB*.

There were also two differences in support between the full and reduced data sets. The first difference was in subclade C<sub>s</sub> where support of *C. katzensteiniae* as sister to *C. crassicaulis* was lost in the reduced data set analyses (Figure 2.6; 50/53/90/97) compared to the full data set analyses (Figure 2.5; 93/95/100/100). The second difference was in subclade D<sub>s</sub>, where there was a loss of support for *C. colombiana* as sister to *C. angustata* in the reduced data set analyses (Figure 2.6; -/-/82/59) compared to the full data set analyses (Figure 2.5; 53/55/9/99). In both subclades C<sub>s</sub> and D<sub>s</sub>, support for sister species pairs was lost with the addition of the two low-copy gene regions (*G3pdhA* and *idhB*). Because *G3pdhA* and *idhB* are providing additional phylogenetically informative characters (Table 2.2), sister species pairs are expected to have higher support values in the reduced data set analyses compared to the full data set analyses; instead there is a loss of support between sister species pairs in both subclades C<sub>s</sub> and D<sub>s</sub>.

The loss of support in the reduced data set analyses compared to the full data set analyses may be the result of paralogs or incomplete lineage sorting in the history of either *G3pdhA* or *idhB*. In both subclades C<sub>s</sub> and D<sub>s</sub>, the support for the monophyly of both subclades increased in the reduced data set analyses (subclade C<sub>s</sub> – Figure 2.5: 61/65/100/100, Figure 2.6: 73/82/100/100; subclade D<sub>s</sub> – Figure 2.5: 62/55/56/85, Figure 2.6: 72/82/100/100). However, the support for sister species pairs within both subclades C<sub>s</sub> and D<sub>s</sub> decreased (sisters *C. katzensteiniae*/*C. rileyi* – Figure 2.5: 93/95/100/100, Figure 2.6: 50/53/-/97; sisters *C. angustata*/*C. colombiana* – Figure 2.5: 53/55/98/99, Figure 2.6: -/-/75/59). Therefore, it is possible that a duplication event has occurred in either *G3pdhA* or *idhB* just below the node of each subclade, creating an undetected paralog. If a duplication event has occurred within each subclade, and different paralogs

were sampled in the molecular analyses, then relationships among the species within both subclades would have decreased support or may be lost completely, while the monophyly of each of the subclades in their entirety would be increased. The same results would occur if there had been incomplete lineage sorting at the node of each of the subclades. Because there is increased monophyly of each of the subclades and decreased resolution within each of the subclades, either gene duplication or lineage sorting may have occurred, though further analyses would need to be performed to determine what has occurred within section *Angustiflorae*.

Maximum parsimony analyses of individual gene partitions of the reduced data set and comparison of resulting topologies indicated that within subclade C<sub>s</sub> the *G3pdhA* sequence for *C. katzensteiniae* and the *idhB* sequence for *C. crassicaulis* (see “Results: Test of Incongruence”) should be removed from the concatenated reduced data set for all analyses presented here. After the reduced data set analyses were completed (Figure 2.6), there was still evidence for paralogs present in subclade C<sub>s</sub>. To test which species were contributing paralogs to the molecular analyses, additional MP analyses were run, excluding sequences for *G3pdhA* and *idhB* for species within subclade C<sub>s</sub>. There was not an increase in MPBS support for species relationships within the subclade after removing individual *G3pdhA* sequences for *C. crassicaulis* and *C. rileyi*, individual *idhB* sequences for *C. katzensteiniae*, *C. rileyi*, and *C. ovatifolia*, and combinations with either *G3pdhA* or *idhB* removed for different groupings of species. Because there was no difference in MPBS support within subclade C<sub>s</sub>, there must still be at least one paralog present in either *G3pdhA* or *idhB*. However, without exhausting all possible combinations of accessions

with either *G3pdhA*, *idhB*, or both gene regions removed, there is no guarantee that the paralog contributing to the loss of support within subclade C<sub>s</sub> can be detected.

### Unsampled Species

Within section *Angustiflorae*, fifteen species have been included based on morphology, but DNA material for molecular phylogenetic analyses was only available for thirteen species. The two unsampled species, *C. antiocana* and *C. suffruticosa*, have been placed within section *Angustiflorae* based on their morphology (Chapter One). These characteristics can also be used to place the species within one of the identified subclades of the section. Both *C. antiocana* and *C. suffruticosa* have morphological characteristics that would place them in the subclade C<sub>s</sub> with *C. crassicaulis*, *C. katzensteiniae*, *C. rileyi*, and *C. ovatifolia* (Figure 2.5 and 2.6).

*Columnnea antiocana* has a similar leaf shape, ovate to lanceolate or elliptic with an oblique base, to *C. crassicaulis*, *C. katzensteiniae*, and *C. ovatifolia* (Smith 1994). However, the most telling morphological feature for placing *C. antiocana* in subclade C<sub>s</sub> is the presence of darker colored spots on the lobe of the corolla that are also present for *C. ovatifolia*, *C. crassicaulis*, *C. katzensteiniae*, and *C. rileyi* (Smith 1994). More exact placement of *C. antiocana* within the subclade is difficult until further molecular analyses can be conducted including DNA material from *C. antiocana*.

*Columnnea suffruticosa* should also be placed in subclade C<sub>s</sub> based on morphological characteristics. Similar to *C. antiocana*, *C. suffruticosa* has darker colored lobe spots on the lobe of the corolla (Smith 1994). The presence of darker colored lobe spots is unique to these six species in the entire genus *Columnnea*. The lobe spots on *C. suffruticosa* are on the interior surface and are orange in color. The only other species

with orange lobe spots on the interior surface of the corolla is *C. crassicaulis* (Smith 1994). This similarity in color and placement of the lobe spots may imply that these two species are sister to one another. However, the placement of *C. suffruticosa* within subclade C<sub>s</sub> as sister to *C. crassicaulis* remains uncertain until further molecular analyses can be conducted with *C. suffruticosa* DNA material.

### **Taxonomic Treatment**

In *Columnnea*, section *Angustiflorae* includes 15 species based on morphology, 13 of which have been tested using molecular analyses. The species of *Angustiflorae* can be distinguished by their small corollas that range in size from 1.0 to 5.2 cm in length and from 0.15 to 1.0 cm in width at the widest point. A few other species within Clade D (Smith et al. in review; Chapter One; Figures 2.5 and 2.6) of *Columnnea* also have small corollas including *C. minutiflorae* and *C. parviflorae*. However, the species of Clade D can be distinguished from the species of *Angustiflorae* by broad calyx lobes. *Columnnea grisebachiana* and *C. pubescens* also have small corollas similar to those of section *Angustiflorae*; however, they have a different geographic distribution. These two species, *C. grisebachiana* and *C. pubescens*, are endemic to the island of Jamaica, while the species of *Angustiflorae* range from Mexico in the north to Bolivia in the south and east into Brazil. They are also found on the islands of Puerto Rico and Hispaniola in the Caribbean but do not spread further west into Jamaica (Figures 2.7-2.11). Other species with similar corolla morphologies, *C. moesta*, *C. ultraviolacea*, and *C. xiphoidea*, belong to section *Stygnanthe* (Chapter One). The species of *Angustiflorae* can be separated from the species of *Stygnanthe* by a comparatively shorter corolla length with longer and larger corolla lobes. The species of *Stygnanthe* also have a denser pubescence that obscures the

corolla. Finally, six species within *Angustiflorae* have colored lobe spots that are not found on any other species within *Columnnea*.

**Columnnea** section *Angustiflorae* L. J. Schulte and J. F. Smith

Note: Specimens examined to compose distribution maps (Figures 2.7-2.11) and collect climate analyses data (Chapter Three) include all specimens examined by Smith (1994) and additional specimens listed below for each species. Also note that morphological descriptions are not updated except for species not included previously.

**1. *Columnnea ambigua*** (Urban) Morley, Proc. Roy. Irish Acad. 74B(24): 423. 1974.

*Alloplectus ambiguus* Urban, Symb. Antill. 1: 408. 1899. *Alloplectus ambiguus* var. *chlorosepalus* Urban, Symb. Antill. 1: 408. 1899, nom. superfl. *Crantzia ambigua* (Urban) Britton, Britton and Wilson, Sci. Surv. P. R. and V. I. 6: 204. 1925. *Ortholoma ambiguum* (Urban) Wiehler, Phytologia 27: 320. 1973. *Trichantha ambigua* (Urban) Wiehler, Selbyana 1(1): 34. 1975. – TYPE: PUERTO RICO. Eggers 1303 (lectotype, designated by Smith, 1994: US).

*Alloplectus ambiguus* var. *erythrosepalus* Urban, Symb. Antill. 1: 408. 1899. – TYPE: PUERTO RICO. Eggers 1302 (lectotype, designated by Smith, 1994: US).

*Columnnea ambigua* is endemic to Puerto Rico and most closely related to *C. domingensis* (Figures 2.5 and 2.6). *Columnnea ambigua* can be readily distinguished from

*C. domingensis* by relatively larger laminas and more flowers per inflorescence and its coarsely toothed calyx lobes (Smith 1994).

Phenology. Flowering from March to October.

Distribution (Figure 2.7). Puerto Rico; 350-1075 m.

ADDITIONAL SPECIMENS EXAMINED. **Puerto Rico.** Sierra Naguabo, *Sintenis 1301* (MO); Reserva Forestal Carite, *Boom 9861* (US); Eastern Slope of the Luquillo Mountains, *Heller 4617* (US); Caribbean National Forest, Pico del Este Road, *Boom 7972* (US); Pico del Este, Caribbean National Forest, along highway 930, *Boom 6925* (US); Trail to Cerro La Santa, Carite Forest, *Howard 16828* (US); El Yunque, Caribbean National Forest, along El Toro Park trail, *Acevedo-Rodriguez 7108* (US); Monte Jayuya, Reserva Forestal Toro Negro, 6 km west of Divisoria, *Thompson 9995* (US); Carite Forest Reserve: Cerro La Santa, along secondary road off of road 184, *Acevedo-Rodriguez 7923* (US); Sierra de Naguabo, Quebrada Grande to Chuchilla Firme, *Shafer 3594* (US); Alto de La Bandera, near Adjuntas, *Britton & Shafer 20016* (US); Mt. Mandios, near Jayuya, *Britton & Cowell 931* (US); Mt. Britton, Luquillo Insular Forest, along trail, *Schubert & Winters 393* (US); Mt. Jayuya, forest, *Sargent 3170* (US, MO); Rt 191, km 18, *D'Arcy 1859* (MO); El Yunque, *Sargent 8137* (MO); Rt 187, Jct 195, *D'Arcy 1860* (MO); Pico del Oeste, Luquillo Mtns., *Wagner 1750* (MO); Municipio Rio Grande, El Verde Research Station, route 186 at the Rio Sonadora, wet montane forest, *Taylor & Gereau 11857* (MO); Municipio Rio Grande, El Verde Research Station, route 186 at the Rio Sonadora, wet montane forest, *Taylor 11679* (MO); Naguabo, Bo. Rio Blanco, Caribbean National Forest, along closed portion of Rt. 191 from gate at Rio Caboy to landslide area, wet mountain forest, *Axelrod & Chavez 2958* (MO); Villalba, Toro Negro Forest, road 149 close to Maravilla, *Acevedo Rodriguez & Alvarez 002987* (MO).

## 2. *Columnea angustata* (Wiehler) L. E. Skog, Ann. Missouri Bot. Gard. 65: 85. 1979

["1978"]. *Pentadenia angustata* Wiehler, Selbyana 2: 118. 1977. – TYPE:

COLOMBIA. Valle del Cauca: 8 km past La Elsa, old rd from Cali to

Buenaventura, *Wiehler et al. 7276* (holotype: SEL).

*Columnea sericea* Mansfield, Biblioth. Bot. 116: 145. 1937, non *Columnea sericea*

(Hanstein) Kuntze, 1891. *Pentadenia sericea* (Mansfield) Wiehler, Phytologia 27:

315. 1973. – TYPE: ECUADOR. Tungurahua: Rio Negro, *Diels 878* (holotype:

B, destroyed). – ECUADOR. Chimborazo: Naranjapata, Rio Chanchan, 1933,

*Schimpff 523* (neotype, designated by Kvist and Skog, 1993: M; isoneotypes: MO,

TRT, GH).

*Pentadenia ecuadorana* Wiehler, Selbyana 2: 82. 1977. *Columnea ecuadorana* (Wiehler)

L. E. Skog, Taxon 33: 126. 1984. – TYPE: ECUADOR. Pastaza: Puyo, *Wiehler et al.* 7163 (holotype: SEL).

*Columnea ulei* Mansf., syn. nov. Fedde Repert. 38: 26. 1935. *Trichantha ulei* (Mansf.)

Wiehler, Selbyana 1:35. 1975. – TYPE: BRASIL. Ceará Oct. 1910, *E. Ule* 9109 (isotypes: G, K, L, US).

*Columnea angustata* is widely distributed across most of the range of section *Angustiflorae*. It is morphologically variable, but can be readily distinguished from other species by a relatively small, yellow, orange, or red corolla in combination with leaves that are slightly but not strongly anisophyllous (Smith 1994).

Phenology. Flowering from March to October in Central America, December to June (one collection in August) in Colombia, and continuously in Ecuador.

Distribution (Figure 2.7). Costa Rica to Ecuador; wet montane forests; 0-1950 m.

ADDITIONAL SPECIMENS EXAMINED: **Colombia.** Municipio de Mistrato, en la via San Antonio de Chami y Mistrato, *F. Alonso* 10235 (US); Dpto. Choco, Mpio de Nuqui. Corregimiento de Coqui. *M. Amaya & L. P. Kvist* 412 (US); Antioquia, In wet and dense forest between Guapa River and Leon River *E. R. Landa et al.* 123 (US, COL); Choco, Municipio de Novita, en peccion de Curundo, right margin of Ingard River *S. Diaz* 3419 (COL); Choco, on the Panamericana road (in construction) between the San Pablo River and the Pato River *E. Forero et al.* 5528 (COL, MO); Choco, Nuqui-Pangui. Playa la Olimpica. *A. Gomez et al.* 499 (SEL); Choco, Lloro 50 km south of Quibdo at junction of Rio Atrata and Rio Andagueda *W. A. Archer* 2053 (SEL); Choco, Mpio de Nuqui. Corregimiento de Coqui. Por el bosque que rodea la quebrada Trapiche. *M. Amaya & L. P. Kvist* 402 (US); Choco, Carretera Quibda-Medellin *M. Amaya & L. P. Kvist* 434 (US); Choco, Near hwy 5-8 km E of Playa de Oro (E of Tado), disturbed forest above pasture *A. Juncosa* 2504 (US); Choco, Rio Atrato; Yuto, rocky margins of the river above Yuto *J. Cuatrecasas & M. Llano* 24150 (US); Choco, Bicordo River, tributary of the San Juan River *E. Forero et al.* 4646 (US, MO, COL); Putumayo, Municipio Mocoa, corregimiento de San Antonio, vereda Alto Campucana, finca La Mariposa *J. B. Dataneur et al.* 5183 (US); Risaralda, Santuario. Borde de carretera de Santuario a Pueblo Rico *M. Amaya & J. F. Smith* 534 (US); Risaralda, Mun. Pueblo Rico; Corr. Santa Cecilia *F. Gonzalez* 2331 (US); Valle, Rio Maya upriver from Puerto Merizalda *A. Gentry & A. Juncosa*

40668 (COL, MO); Valle, Bajo Calima, road to Juanchaco Palmeras A. *Gentry et al.* 48327 (MO); Valle, Municipio Buenaventura, forest exploitation in the concession of Carton de Colombia *J. van Rooden* 540 (US, COL); Valle del Cauca, Old road to Buena-ventura from Cali, 65 km from inception, 83 km from Cali *J. P. Folsom & L. Escobar* 10477 (US); **Costa Rica.** Jungles near Cariblanco *M. H. Stone* 1168 (US); Alajuela, Biologica Monteverde Rio Penas Blancas. *W. Haber & E. Bello* 6878 (MO); Alajuela, Reserva Biologica Monteverde Rio Penas Blancas. Finca de Jesus Rojas. *E. Bello* 1548 (MO); Alajuela, Reserva Biologica Monteverde Valle del Rio Penas Blancas, Quebrada Celeste. *W. Haber & E. Bello* 7069 (MO); **Ecuador.** Road from Quito to Puerto Quito, km 104, then nw on side road toward Pachical. *M. Whitten et al.* 91276 (SEL); Bolivar, Along road from Guaranda to Balsapamba. *H. Wiehler* 34 (SEL); Bolivar, along road from Guaranda to Balsapamba. *H. Wiehler* 95145 (US); Bolivar, Hcda. Changuil, en potrero. Bosque muy humido Tropical, nubiado. Suelos fertiles. *X. Cornejo & C. Bonifaz* 4533 (US); Carchi, 5 km above Lita (Colonia) along open road & by small creeks. *H. Wiehler & GRF Study Group* 9050 (SEL); Cotopaxi, Km 5 to km 15 above La Mana. *H. Wiehler & GRF Study Group* 9751 (SEL); El Oro, 10 km W of Pinas along new road from Pinas-Machala *C. H. Dodson et al.* 8448 (SEL); El Oro, 10 km W of Pinas along new road from Pinas-Machala *C. H. Dodson et al.* 8447 (SEL); El Oro, Road from Pinas to Sta. Rosa km 19 *C. H. Dodson & A. Gentry* 8916 (SEL); El Oro, Hcda. Daucay. Bosque humedo premontano. Bosque nublado estacional. *X. Cornejo & C. Bonifaz* 323 (US); Esmeraldas, Quininde. Noreste de Las Golondrinas. Cooperativa 3 de Septiembre en sect San Isidro, cerca a Rio Jordan. *W. Palacios* 11501 (SEL); Esmeraldas, Quininde. Noreste de Las Golondrinas. Cooperativa 3 de Septiembre en sect San Isidro, cerca a Rio Jordan. *W. Palacios* 11496 (SEL); Esmeraldas, Km 5-18 on road Lita to Alto Tambo. *C. H. Dodson et al.* 16856 (SEL); Esmeraldas, Between Lita & Alto Tambo, 5 km from Lita, Rio Chuchubi. *H. Wiehler* 29 (SEL); Esmeraldas, 35 km W of Quininde *J. L. Clark et al.* 8776 (US); Esmeraldas, Quininde. Bilsa Biological Reserve. Montanas de Mache, 35 km W of Quininde, 5 km W of Santa Isabella. Premontane wet forest. Primary and disturbed forest on recently logged property of Sr. Rios, along old road to Mono. *N. Pitman & M. Bass* 874 (US); Esmeraldas, Quininde Canton. Reserva Ecologica Mache-Chindul. Bilsa Biological Station, 35 km W of Quininde. Permanent plot #3. *J. L. Clark* 4747 (US); Esmeraldas, Quininde Canton. Reserva Ecologica Mache-Chindul. Comunidad Cana Bravel. Cabaceras del Rio Viche, estero Sabaleta. Tropical wet forest. Sunny clearing near rice plantation. *J. L. Clark* 4689 (US); Esmeraldas, Between Lita & Alto Tambo, 5 km from Lita, Rio Chuchubi. *H. Wiehler* 9024 (US); Esmeraldas, Reserva Cotacachi-Cayapas, al pie de rio Bravo, en lugar abierto. Bosque muy humedo tropical. Primario. *X. Cornejo & C. Bonifaz* 6234 (US); Esmeraldas, 1 km W of Santa Isabel, toward Bilsa Biological Station, along logging road. In Pouteria tree in cacao plantation. *P. Mendoza-T. et al.* 599 (US); Esmeraldas, Area of Rio Barbosa (near Lita). *H. Wiehler* 9567 (US); Esmeraldas, San Lorenzo Canton. Carretera Lita-Alto Tambo-La Punta. Bosque muy humedo tropical. Bosque primario. *E. Gudino & R. Moran* 1294 (US); Esmeraldas, Lita-San Lorenzo road, 10-20 km NW of Lita *A. Gentry et al.* 70070 (US); Esmeraldas, Bilsa Biological Station, Rana Roja Trail. We primary and secondary forest; roadside. *P. Mendoza-T. et al.* 555 (US, MO); Esmeraldas, Eloy Alfaro. Reserva Ecologica Cotacachi Cayapas. Rio Santiago. Angostura. Bosque muy humedo tropical. Bosque primario, sobre colina. *M. Tirado et al.* 1131 (US, MO); Esmeraldas, Quininde. Reserva Ecologica Mache-Chindul, 35 km W of Quininde. The Bilsa Biological Station. Cordillera Mache-Chindul. Collections made along main road between Sta. Isabel and Station. *J. L. Clark* 9609 (US, SEL); Esmeraldas: Eloy Alfaro, Reserva Ecologica Cotacachi-Cayapas. Charco Vicente. Rio San Miguel. Bosque humedo Tropical. Bosque primario. *M. Tirado et al.* 482 (US, SEL); Esmeraldas: Quininde, Bilsa Biological Reserve. Montanas de Mache, 35 km W of Quininde, 5 km W of Sanata Isabela. Premontane Wet Forest. Primary and disturbed forest along Dogala trail. *N. Pitman & M. Bass* 998 (US); Esmeraldas: Quininde, Community Chorrera Grande, 15 km SW of Cube (via pircuta). Premontane wet forest. *J. L. Clark et al.* 2835 (US); Esmeraldas: Quininde, Bilsa Biological Station. Mache Mountains. 35 km W of Quininde, 5 km W of Santa Isabel. Premontane wet forest. Monkey Bone trail. *J. L. Clark & B. Adnepos* 50 (US, SEL); Imbabura, Ibarra *J. L. Clark et al.* 7484 (US); Imbabura, Cotacachi *J. L. Clark et al.* 7380 (US); Los Rios, Rio Waija, on second hill beyond Rio Palenque past bridge by Dodson's house, on bank by river. *H. Wiehler* 7129 (SEL); Los Rios, Rio Palenque Science Center. Km 56 on the Quevedo-St. Domingo Rd. *J. B. Watson* 331 (SEL); Manabi, Just below entering cloud forest on Mt. Montecriste *C. H. Dodson & L. B. Thien* 1736 (SEL); Manabi, Jama Canton. Cordillera de Jama (costal range). Cerro Nueve, 15 km E of Jama, N of Rio Jama. Remnant wet forest with frequent fog, below microwave tower. *D. Neill* 11579 (US); Manabi, Canton: Pedernales. Cerro Pata de Pajaro, 10 km E of Pedernales. Finca of the family Aroyo. Fog/Cloud forest, wet forest. *J. L. Clark et al.* 2635 (US); Manabi, Canton: Jipijapa. Parroquia: Jipijapa. Cerro Montecristi (ca. 1 km W of the town of Montecristi). *J. L. Clark et al.* 6193 (US); Morona Santiago,

Along road from Milagro & Limon - then toward Mendez. *H. Wiehler & GRF Study Group 97137* (SEL); Morona Santiago, Macas. Along new road, west into the Andes, first 17 km westward, then ca. 12 km south on side road. *H. Wiehler & GRF Study Group 8801* (SEL); Morona Santiago, Sucua. Along road to Los Tanques de Aguas, ca. 12 km out of town. *H. Wiehler & GRF Study Group 8885* (SEL); Morona Santiago, San Juan Bosco. Road between San Juan Bosco and El Pangui; 27 km S of San Juan Bosco. *J. L. Clark 9915* (US); Morona Santiago, Canton: Limon Indanza. Parroquia: Chiviaza. Road from Limon (Gral Leonidas Plaza Gutierrez) to Santa Susana de Chiviaza. *J. L. Clark et al. 5982* (US); Morona Santiago, San Juan Bosco. Road between San Juan Bosco and the village of Santiago de Panantza (following Rio Panantza) *J. L. Clark 9854* (US, SEL); Morona-Santiago: Palora, Parroquia San Vicente de Tarqui, vegetacion alterada camino al rio Yushin. *J. Caranqui et al. 821* (US); Napo, Tena; road Baeza-Rio Hollin. *A. Hirtz & X. Hirtz 4468* (SEL); Napo, Rio Jatunyacu (Shandia). *A. Hirtz 9609* (SEL); Napo, Tena to Baeza. *H. Wiehler & GRF Study Group 86224* (SEL); Napo, Along road from Napo to Puyo on way to Hacienda Dos Rios below Evangelical Mission, Tena. *H. Wiehler 71124* (SEL); Napo, Tena to Rio Pano. *H. Wiehler & GRF Study Group 93219* (SEL); Napo, Tena to Rio Pano. *H. Wiehler & GRF Study Group 93220* (SEL); Napo, Tena to Pano and Rio Janinyacu, on tree in field in front of Hotel Auca. *H. Wiehler & GRF Study Group 93203* (SEL); Napo, 25km from Baeza *H. Wiehler 3351* (SEL); Napo, Hollin to Loreto, past km 45. *H. Wiehler 95118* (SEL); Napo, Along road from Hollin to Loreto, past km 45. *H. Wiehler 9594* (SEL); Napo, Archidona *J. L. Clark et al. 7220* (US); Napo, archidona *J. L. Clark & N. Harris 7232* (US); Napo, Baeza to Lago Agrio, about 25 km from Baeza. *H. Wiehler & GRF Study Group 86169* (US, SEL); Napo, Archidona Canton. Reserva Ecologica Antisana. Comunidad Shamato. Entrada por km 21-Shamato. Camino Sardinias-Shamato. Premontane/montane wet forest. *J. L. Clark et al. 5233* (US); Pastaza, Puyo-Puerto Napo road, 14-18 kms N of Puyo, heavily cut-over forest, now pasture with remnant trees *J. L. Luteyn & M. Lebron-Luteyn 5820* (NY, SEL); Pastaza, Shell-Mara rainforest, 2 km N of Shell-Mara *L. Holm-Nielsen & S. Jeppesen 469* (OV, S); Pastaza, "Gesneriad woods," 2 km NE outside Puyo at Rio Pi...Grande. *H. Wiehler & D. Masterson 79208* (SEL); Pastaza, South of Mera *J. L. Clark et al. 7797* (US); Pastaza, Puyo, Veracruz *J. L. Clark & J. Katzenstein 9302* (US); Pastaza, Puyo, Puyo-Tena road *J. L. Clark et al. 9373* (US); Pastaza, Simon Bolivar *J. L. Clark & J. Katzenstein 8322* (US); Pastaza, Hacienda San Antonio de Baron von Humboldt, 2 km to the NE of Mara *D. Neill et al. 5790* (US); Pastaza, Hotel Germania, Mera *J. L. Clark & M. Mailloux 7834* (US); Pastaza, Pastaza Canton. Puyo. Sector Tarqui. Bosque pluvial premontano. *G. Tipaz et al. 408* (US); Pastaza, Puyo, epiphyte on trees surrounding Hotel Turingia. *H. Wiehler 1176* (US); Pastaza, Shell. Bosque muy humedo subtropical. *X. Cornejo & C. Bonifaz 1408* (US); Pastaza, 3 km S of Puyo close to the Pastaza river and the border to the province of Morona-Santiago, slopes close to the village Madre Tierra, farmland and forest remnants mixed with banana plantations *L. P. Kvist 60325* (US); Pastaza, Along rock road to Tarabita and the portage over the Rio Pastaza, ca. 3 km from the turnoff from main Puyo-Mera Road *T. B. Croat 49680* (US); Pastaza, Canton: Puyo. Parroquia: Fatima. Secondary forest along border of Escobar Finca (ca., 2 km N of Puyo near turn off toward Ahuano) *J. L. Clark et al. 9368* (US); Pastaza, Veracruz (Indillama) *H. Lugo S. 34* (US); Pastaza, Teresa Mama on the Rio Bobonaza c. 35 km SE of Sarayacu *H. Lugo S. 5702* (US, GB); Pichincha, Road off road to Puerto Quito at Maldonado, km 116 to Cecilia. *A. Hirtz 4473* (SEL); Pichincha, Montanas de Ila; sub-cloud forest, exposure toward the Pacific *H. Wiehler & GRF Study Group 9098* (SEL); Pichincha, Golf course and pastures of Hotel Tinalandia. *H. Wiehler 7997* (SEL); Pichincha, Quito, Rio Guaycuyacu *J. L. Clark 8270* (US); Pichincha, Trek from Lloa to Mindo, forest between Hacienda Pacay and main bridge to Mindo (south side of Rio Cinto). *J. L. Clark 4520* (US); Pichincha, Quito Canton. Reserva Rio Guaycuyacu. Near confluence of Rio Guaycuyacu and Rio Guayabamba. *J. L. Clark et al. 4959* (US); Pichincha, Between km 104 on Quito-Esmeraldas Road and Pachijal. Along wet roadside banks. Terrestrial. *P. Mendoza-T. et al. 515* (US); Pichincha, Between Reserva Rio Guaycuyacu and Guayabillas. Wet montane forest; on trees at forest edge. *P. Mendoza-T. et al. 546* (US); Pichincha, Between Puerto Quito and Pedro Vincente Maldonado, in creek area. *H. Wiehler 90111* (US); Pichincha, Sto. Domingo de los Colorados. Bosque humedo Premontano. *X. Cornejo & S. Laegaard 2038* (US); Pichincha, Santo Domingo de los Colorados. Tinalandia resort. *R. W. Dunn 95-04-136* (US); Pichincha, Montanas de Ila *H. Wiehler & GRF Study Group 9081* (US, SEL); Pichincha, Cloud forest along ridge near La Centinella at km 12, road from Patricia Pilar to Flor de Mayo *G. L. Webster 22927* (US); Tungurahua, Road Banos to Puyo; 5 km past Banos near Rio Blanco. *H. Wiehler & GRF Study Group 8665* (SEL); Tungurahua, Banos *J. L. Clark & J. Katzenstein 8397* (US); Tungurahua/Pastaza, Along road from Banos to Puyo; 2 km below Rio Topo. *H. Wiehler 79140* (SEL); Tungurahua, Valley of Pastaza River, between Banos and Cashurco, 8 hours east of Banos *A. S. Hitchcock 21769* (MO); Tungurahua, Canton: Banos.

Parroquia: Rio Negro. Locality near Rio Topo. Wet montane forest. *J. L. Clark & V. Duran 6024* (US); Zamora, Chinchipe. In the vicinity of the mining camp at the Rio Tundaime. Pastures along Rio Quimi with small patches of disturbed forest. *H. Van der Werff et al. 19260* (US, MO); **Panama.** Cocle, Near Aserradero El Cope, ca 8 km N of El Cope, Atlantic slope *R. L. Dressler 5642* (SEL); Cocle, La Pintada, Corregimiento, El Arino, Omar Torrijos National Park, 6-10 km NNW from El Cope, main trail from abandoned sawmill to the Comunidad La Rice *J. L. Clark 8627* (US); Darien, South of Cerro Pirre *J. A. Duke 15614* (US); Distrito de Santa Fe, Alrededores del Rio Primer brazo de Ulaha *C. Galames et al. 3171* (US); **Venezuela.** Distrito Petit, Falcon, Falcon *W. Meier & G. Forbes 12856* (US).

**3. *Columnnea antiocana*** (Wiehler) J. F. Smith, *Pentadenia antiocana* Wiehler, Selbyana

7: 335. pl. 2D. 1984. – TYPE: COLOMBIA. Antioquia: *Jewise s.n.* (holotype: K).

*Columnnea antiocana* is most likely related to the species of subclade C<sub>s</sub> (Figure 2.5 and 2.6). These species share a similar lamina shape and vesture. They are also the only species, along with *C. suffruticosa*, of *Columnnea* with darker colored spots on the lobes of the corollas. *Columnnea antiocana* can be distinguished by the entire margins of its calyx lobes and its more ovate, acute to acuminate laminas (Smith 1994).

Phenology. Unknown. Single collection from February.

Distribution (Figure 2.8). Colombia (Antioquia, Valle del Cauca); ca. 2000 m.

**4. *Columnnea byrsina*** (Wiehler) L. P. Kvist and L. E. Skog, *Allertonia* 6: 384. 1993.

*Pentadenia byrsina* Wiehler, Selbyana 2: 119. 1977. – TYPE: [ECUADOR.]

Cultivated material grown from seeds collected near Baeza, Napo, *Wiehler 77122*

(holotype: SEL).

*Columnea byrsina* is most closely related to *Columnea orientandina* both molecularly and morphologically (Figure 2.5 and 2.6; Smith 1994). Both *C. byrsina* and *C. orientandina* have dorsiventrally arranged leaves and share corolla movements. The flowers are located beneath the larger leaf of a pair. In full sun the flowers are in the open; in low light or shade they are covered by the larger leaf (Smith and Sytsma 1994a, b, c). *Columnea byrsina* is readily distinguished from other species by its anisophyllous, acute to acuminate leaves, and bright red corollas with exserted stamens and styles. It is also the only species of *Columnea* known to have a variable fruit shape. The berries are generally globose, but several collections from near Baeza, Napo, Ecuador, have ovoid berries (Smith 1994).

Phenology. Flowering continuously.

Distribution (Figure 2.9). Central Colombia to Ecuador; wet forests; 650-4000 m.

ADDITIONAL SPECIMENS EXAMINED: **Colombia.** Reserva Natural La Planada, municipio de Ricaurte, departamento de Narino. *C. Restrepo & G. Ramirez 563* (US); Antioquia, Mpio. de Frontino; km 14 of road Nutibara-Murri. Disturbed wet/very wet montane vegetation; roadside. *J. L. Zarucchi et al. 5670* (US); La Planada, Salazar Pinca 7 km above Ricaurte A. *Gentry 34996* (COL, US, MO); Narino, Pinca La Planada, near Chucunes *S. Libenson et al. 30577* (MO); Narino, Ricaurte *K. von Sneidern 10.IV.1941* (OV); Narino, Ricaurte, Chucunes, The Planada Natural Reserve, the bank towards the way that you see the Administration of the Mirador X. *Londono 240* (US); Narino, La Planada Reserve, 7 km from Chucunes. *A. Gentry et al. 60328* (US); Narino, La Planada Biological Reserve, ca. 7 km S of Chucunéz, along trail to Pialapi to Quebrada La Calledita. Disturbed premontane forest and open potreros. *J. L. Luteyn et al. 13912* (US); Narino, trail from El Mirador up to open field, *J. F. Smith & M. Galeano 1457* (WIS); Valle, Queremal, on tree near river *P. J. M. Maas & T. Plowman 1838* (OV); **Ecuador.** Carchi, Tulcan Canton. Reserva Indigena Awa. Comunidad El Baboso, 12 km al norte de Lita. Bosque pluvial Premontano. Bosque primario *D. Rubio et al. 2203* (MO); Carchi, Tulcan Canton. Reserva Indigena Awa. Comunidad Gualpi Alto, parroquia Chical. Bosque pluvial Montano Bajo. *D. Rubio et al. 1692* (MO); Carchi, Trail from Rafael Quindi's Finca back toward Untal to stream, approx. 0.5 km from finca. *W. S. Hoover & S. Wormley 1577* (MO); Carchi, Vic of Chical *L. Besse et al. 887* (SEL); Carchi, environs of Maldonado *M. T. Madison et al. 4419* (SEL); Carchi, vicinity of Maldonado *M. T. Madison 3873* (SEL); Carchi, environs of Chical, 12 km below Maldonado on the Rio San Juan *M. T. Madison et al. 4451* (SEL, F); Carchi, Vicinity of Chical, west of Maldonado on trail to Penas Blancas *A. Gentry & G. Shupp 26406* (SEL, MO); Carchi, Tulcan Canton. Parroquia Tobar Donoso. Reserva Indigena Awa. Centro El Baboso. Bosque primario. Bosque muy humedo premontano. *G. Tipaz et al. 1914* (SEL, MO); Carchi, Canton: Tulcan. Parroquia: Chical. Collection made along path from the village of Chical towards an area known locally as "Crystal." Walked along Rio Blanca via the Cordillera Guilchan (ca. 6-8 km SW of Chical) *J. L. Clark et al. 6343*

(SEL, US); Carchi, From Maldonado to Chical and return. *H. Wiehler 93110* (SEL, US, MO); Carchi, Canton: Tulcan. Parroquia: Chical. Collection made along path from the village of Quinyal toward an area known locally as "Gualpi" (near the boarder of the Reserva Awa). *J. L. Clark & O. Mejia 6291* (SEL, US, MO); Carchi, Canton: Espejo. Parroquia: Guatal. Mirador de las Golondrinas (Fundacion Golondrinas). Trail from El Corazon toward La Cortader (2 km NE of refugio) *J. L. Clark et al. 8460* (US); Carchi, Chical, pasture and edge of pasture *S. A. Thompson & J. A. Rawlins 719* (US); Carchi, Canton: Mira. Parroquia: Jijon Y Camano. Unfinished road from El Carmen toward Chical. Agua Amarilla. *J. L. Clark & E. Folleco 8539* (US); Carchi, Mira. El Carmen. Cerro Golondrinas. Bosque Montano. Bosque primario en colinas. *M. Tirado et al. 1230* (US, MO); Carchi, Espejo. Bosque Protector Mirador de Golondrinas. Collections made between the village, Las Juntas, and la Cabana del Corazon. Lower montane wet forest. *J. L. Clark et al. 2413* (US, MO); Cotopaxi, Canton Pujili. Reserva Ecologica Los Ilinizas, Sector II (Sector Sur), sector Chuspitambo, al occidente de Choasilli, Cordillera Occidental, vertiente occidental. *P. Silverstone-Sopkin et al. 9967* (MO); Esmeraldas, Alto Tambo A. *Hirtz & J. Kent 4556* (SEL); Esmeraldas, Canton: San Lorenzo. Parroquia: Alto Tambo. Comunidad El Cristal; 8-10 km S of San Lorenzo-Ibarra highway. *J. L. Clark et al. 7539* (US); Esmeraldas, Km 12. Cristal, Lita-(La Merced de) Buenos Aires. Edge of Cotacachi Cayapas Reserva Ecologica. *C. H. Dodson 17604* (US, MO); Imbabura, Canton: Ibarra. Parroquia: Lita. Comunidad San Francisco; next to Rio Verde (13 air-km S of Lita). *J. L. Clark et al. 7518* (US); Manabi, Montecristi. Cerro Monecristi. Carretera Manta-Jipijapa, entrada por Montecristi o El Chorrillo. Bosque seco Pre-Montano. *T. Nunez et al. 356* (MO); Morona-Santiago, Canton: Limon-Indanza. Cordillera del Condor. Trail from camp #1 to camp #2 towards crest of Cordillera del Condor (ca. 10-15 km S/SE of the Comunidad Warints). *J. L. Clark & L. Jost 6992* (US); Morona-Santiago, Canton: Limon Indanza. Parroquia: Chiviaza. Road from Limon (Gral Leonidas Plaza Gutierrez) to Santa Susana de Chiviaza. *J. L. Clark et al. 5969* (US); Napo, road Baeza-Lago Agrio, 18 km from Baeza *H. Balslev & E. Madsen 10575* (MO, OV, COL, SEL, F); Napo, Along road from Baeza to Lago Agria about 42 km from Baeza *H. Wiehler 79298* (SEL); Napo, Forest north of Baeza A. *Hirtz 4496* (SEL); Napo, cloud forest north of Baeza *C. Luer et al. 3177* (SEL); Napo, cloud forest north of Baeza *C. Luer et al. 4496* (SEL); Napo, km 20 Baeza-Tena *L. Besse et al. 2329* (SEL); Napo, Canton El Chaco. Margen derecha del Rio Quijos. Finca "La Ave Brava" de Segundo Pacheco. Bosque pluvial Premontano. Bosque primario, sobre suelos saturados. *W. Palacios 5410* (SEL, MO); Napo, Cloud forest 44-45 km by road N of Tena. *G. L. Webster 23237* (US); Napo, Road Baeza-Lago Agrio, km 14. Road, pasture. *B. B. Klitgaard et al. 606* (US); Pichincha, Montanas de Ila; sub-cloud forest, exposure towards the Pacific. *H. Wiehler 9095* (SEL, US); Pichincha, Quito Canton. Trek from Lloa to Mindo, following south side of Rio Cinto. Disturbed, sunny roadside with remnant forest of steep/veritcal sections. Growing along stream. *J. L. Clark 4502* (US); Sucumbios, Cosanga area-10 km to rio aliso; between Rio Aliso and Rio Cosanga 6 km; then south of Cosanga about 5 km. *H. Wiehler 98156* (SEL, US).

**5. *Columnnea colombiana*** (Wiehler) L. P. Kvist and L. E. Skog, *Allertonia* 6: 385. 1993.

*Pentadenia colombiana* Wiehler, *Selbyana* 2: 120. 1977. –TYPE: COLOMBIA.

Valle del Cauca: along Rio Dagua, old rd Cali-Buenaventura, near Buenaventura,

1 May 1972, *Wiehler et al. 72130* (holotype: SEL).

*Columnnea colombiana* is clearly within subclade D<sub>s</sub> of section *Angustiflorae*

based on molecular analyses (Figure 2.5 and 2.6); however, the exact placement is

unknown. Cladistic analysis of morphology allied *C. colombiana* with *C. rileyi* and *C. suffruticosa* (Smith and Sytsma 1994a). Chloroplast restriction site DNA analysis placed it as a sister to *C. brycina* and *C. orientandina* (Smith and Sytsma 1994b, c), while the molecular phylogenetic analyses presented here placed *C. colombiana* as sister to *C. angustata* (Figure 2.5). The slightly anisophyllous, ovate to orbicular leaves, thin pendent stems, red corollas with green limb, and dissected calyx lobes distinguish *C. colombiana* from other species (Smith 1994).

Phenology. Flowering from May to August, possibly longer.

Distribution (Figure 2.9). Colombia and northern Ecuador; wet forests; sea level to 800 m.

ADDITIONAL SPECIMENS EXAMINED: **Colombia**. Boca Pepe, Pacific coast of Choco, downstream of Porto Maluk Rio Baudo, tree growing on edge of riverbank *J. W. White & R. H. Warner 74* (COL, MO); El Valle: Sabaletas, km. 29 of highway from Buenaventura to Cali. *E. P. Killip & J. Cuatrecasas 38847* (US).

**6. *Columnnea crassicaulis*** (Wiehler) L. P. Kvist and L. E. Skog, *Allertonia* 6: 385. 1993.

*Pentadenia crassicaulis* Wiehler, *Selbyana* 2: 122. 1977. – TYPE: COLOMBIA.

Narino: *Wiehler and Williams 72185* (holotype: SEL).

*Columnnea crassicaulis* is most closely related to *C. katzensteiniae*, *C. rileyi*, and *C. ovatifolia* based on molecular analyses (Figure 2.5 and 2.6). These species are also all morphologically similar based on the presence of darker colored spots on the lobe of the corolla. A thickened stem, ovate to orbicular leaves, and long yellow corollas with a long

constriction at the base distinguishes *C. crassicaulis* from other species of *Columnea* (Smith 1994).

Phenology. Flowering continuously.

Distribution (Figure 2.8). Southern Colombia to northern Ecuador; wet forests; 1200-2300 m.

ADDITIONAL SPECIMENS EXAMINED: **Bolivia.** La Paz, Prov. Sud Yungas, Huancane 6.5 km hacia el sud sobre camino nuevo 30-35 degrees SW. *St. G. Beck 3043* (SEL); **Colombia.** Narino, Dpto. de Narino: Mpio. de Mallama. Piedrancha. Orilla izquierda del Rio Guisa. *B. R. Ramirez P. & A. L. Jojoa B. 5.718* (US); **Ecuador.** Carchi, Road to Chical: back to Maldonado and toward Tulcan and return to Maldonado, along Rio San Juan. *H. Wiehler 93128* (SEL, US); Cotopaxi, Nanegalito *H. Wiehler & GRF Study Group 97172* (SEL); Imbabura, Selva Alegre *A. Hirtz 4500* (SEL); Imbabura, Road from Guallupe to Buenos Aires off road from Ibarra to Lita at km 32 *C. H. Dodson et al. 16779* (SEL); Imbabura, Otavalo via Quiroga, Apuela, Vacas Galindo to the mines of Selva Alegre and back to Otavalo, total of 139 km *H. Wiehler & GRF Study Group 93164* (SEL); Pichincha, Along road near Nanegal, in pasture land or small forest remnants. *H. Van der Werff et al. 12307* (SEL, US).

**7. *Columnea domingensis*** (Urban) B. Morley. Proc. Royal Irish Acad. 74: 424. 1974.

*Alloplectus domingensis* Urban Symb. Antill. 2: 357. 1901. *Trichantha*

*domingensis* (Urban) Wiehler. TYPE: SANTO DOMINGO. Rio Jimenes May 1887 *Eggers 2314* (K, HBG, isotypes).

*Alloplectus domingensis* Urban var. *microphylla* Morton. Contr. U. S. Natn. Herb. 29: 19.

1944. TYPE: HAITI. Summit of Morne Delcour, Montagnes de la Hotte Aug.

1927 *W. J. Eyerdam 351* (holotype: US; isotypes: GH, NY).

Epiphytic vining herb, stems to 50 cm long, to 3.5 mm diameter, red-brown to tan, proximally nearly glabrous with a few multicellular transparent trichomes, distally appressed pilose with multicellular red or transparent trichomes; internodes 0.9-4.0 cm

long; leaf scars raised or flush with the surface. Leaves opposite, subequal to anisophyllous, larger lamina of a pair 6.5-60.0 mm long, 4.0-28.0 mm wide, ovate to oblanceolate, apex acute to blunt and rounded, base oblique or cuneate, lateral veins 2-3 per side, adaxially green, sparsely appressed pilose with multicellular and unicellular transparent trichomes, adaxially pale green to reddish, sparsely appressed pilose with unicellular transparent trichomes, veins glabrous to appressed pilose with multicellular red trichomes; margin crenate to crenulate; petioles 0.0-22.0 mm long, sparsely pilose with appressed multicellular transparent trichomes. Smaller lamina of a pair 5.5-22.0 mm long, 2.0-13.0 mm wide, ovate, apex acute to blunt and rounded, base oblique or cuneate, lateral veins 2-3 per side, adaxially green, sparsely appressed pilose with multicellular and unicellular transparent trichomes, adaxially pale green to reddish, sparsely appressed pilose with unicellular transparent trichomes, veins glabrous to appressed pilose with multicellular red trichomes; margin crenate to crenulate; petioles 0.0-4.0 mm long, sparsely pilose with appressed multicellular transparent trichomes. Inflorescences of 1 flower per leaf axil; bracts 2.0-5.5 mm long, 0.4-1.0 mm wide, linear, apex acute, red, pilose with multicellular red trichomes. Pedicels 8.0-21.0 mm long, red, pilose with multicellular red trichomes. Calyx clasping corolla, lobes 7.5-17.0 mm long, 1.5-3.0 mm wide without lobes, lanceolate without lobes, apex acute, interior nearly glabrous, exterior sparsely pilose with multicellular transparent trichomes, red, margins lacinate. Corolla 1.7-2.6 cm long, 5.5-7.0 mm at widest point, 3.0-5.0 mm at constriction before limb, 2.0 mm wide at constriction before gibbous base, tubular, slightly ventricose, yellow, exterior sparsely pilose with long multicellular transparent trichomes, interior glabrous; limb 6.5-8.5 mm in diameter, lobes semi-orbicular, 2.0-2.5

mm long, 2.0-3.0 mm wide, yellow. Filaments connate 3.5 mm, adnate to corolla 2.0 mm, glabrous; anthers 1.0 mm long, 1.4 mm wide, rectangular, included in corolla tube. Ovary 2.5-3.0 mm long, conical, nearly glabrous; style yellow, pilose with short multicellular trichomes distally, glabrous proximally; stigma bilobed, papillate, included in corolla tube. Nectary two dorsal glands. Fruit an ovate to globose berry 5.0-7.0 mm long, 3.5-7.0 mm wide, nearly glabrous, red to purple. Seeds 1.0 mm long, red-brown, twisted striate.

Phenology. Flowering all year. Fruiting specimens known from February, June, August, and November, presumably all year.

Distribution (Figure 2.7). Endemic to Hispaniola; 0-1725 m.

ADDITIONAL SPECIMENS EXAMINED: **Dominican Republic.** Puerto Plata Prov., In elfin forest, Cordillera de Yaroa, on limestone ridge, facing the Yaroa valley A. H. Liogier 11206 (NY, GH); Constanza, on old track in wet woods La Descubierta A. H. Liogier 18055 (NY, F); Santo Domingo, Pep. Dominicana T. Zanoní & R. García 30462 (NY); Near Jarabacoa. De JS. Jiménez 3033 (US); Los Cacaos, Colonia Ranfis, San Cristobal. Ravines among coffee plantations. B. A. H. Liogier 11624 (US); Barahona, Monteada Nueva, near Polo W. S. Judd et al. 1078 (AAH, AAU); Barahona, Mt. Laho, trail from La Cueva to Plaza Bonita. R. A. Howard 12291 (US); Barahona, Monteada Nueva, forested hillslopes SE of Polo. R. A. Howard & E. S. Howard 8556 (US); Barahona, Vicinity of Paradis W. L. Abbott 1610 (US); Barahona, Vicinity of Paradis W. L. Abbott 1583 (US); Independencia, Plants collected above Aguacate toward Los Arroyos T. E. Talpey 73 (BH); Jarabacoa, Ciénaga de Manabao, along Tablones river, mostly second growth forest. B. A. H. Liogier 12066 (US); La Vega, Los Tablones, ca. 2 miles W of La Ciénaga. G. J. Gastony et al. 244 (US); Pedernales, 4 km NE of Los Arroyos. Edges of remnant cloud forest. S. A. Thompson et al. 7592 (US); Santo Domingo, in dark forest of Sierra de Neiba A. H. Liogier & P. Liogier 22699 (NY); Santo Domingo, in sylvia ad Río Jimenoa Eggers 2314 (KEW); Santo Domingo, Barahona. Monteada Nueva, 6.3 km from Cruce de El Puerto-Monteado-Nueva, 3.4 km E of Cortico. A. Gentry & M. Mejía 50693 (MO); Santo Domingo, Constanza H. von Turckhelm 3375 (NY); Santo Domingo, Cordillera Central, Santiago Rodríguez, National Park, between Monte Llano & Los Descansaderos T. Zanoní & R. García 41853 (NY); Santo Domingo, Sierra de Baoruco, Independencia 38km Sur de Duverge T. Zanoní & J. Pimentel 26542 (NY); Santo Domingo, Santiago, SW spur of Monte Pallo, in forest. E. L. Ekman 12898 (US); Santo Domingo, Vicinity of Constanza W. L. Abbott 6 (US); Santo Domingo, Sierra de Neiba: Prov. Estrella: en la ladera del Norte de la Loma El Hoyazo, entre el Puesto Militar Aniseto Martínez y el Puesto Militar "Km. 204" en la Carretera Internacional: bosque latifoliado, en su límite bajo donde cambia a bosque de Pinus. T. Zanoní et al. 39798 (US); Santo Domingo, Sierra de Bahoruco (extremo oriental): Prov. Barahona: mas arriba de la Finca Habib, Loma Pie de Pol (Pie Pol), al final de la carretera de La Guasara (de Barahona): bosque latifoliado, humedo sobre el firme de la loma, muchas plantas epifíticas. T. Zanoní et al. 41040 (US); Santo Domingo, Barahona. Paradis. P. Fuertes 329 (US, MO); Santo Domingo, Sierra de Baoruco: Prov. Barahona: 4 km. arriba el pueblecito rural de "Entrada de

Corico" en el camino a El Gajo (sitio tradicional de Botánicos, bajo el nombre "Monteada Nueve"; un bosque latifoliado y nublado con *Maganolia pallescens* y *M. hamori*) *T. Zanoni et al.* 18876 (US, MO); Santo Domingo, Cordillera Central: Prov. La Vega: en las orillas del Arroyo La Sal, approx 1 km arriba (este) del poblado rural de La Sal: bosque latifoliado y secundario, con cafetales, entre Loma La Sal Y Loma La Golondrina. *T. Zanoni et al.* 19975 (US, MO); Santo Domingo, Cordillera Central: Parque Nacional J. A. Bermudez. Prov. La Vega: en el sendero entre la caseta de parques Nacionales en lost Tablones (de La Ciénaga de Manabao y Loma Alto de La Cotorra: bosque latifoliado y humedo, a veces con *Pinus occidentalis*. *T. Zanoni et al.* 39209 (US, MO); Santo Domingo, Sierra de Baoruco: Prov. Barahona: Loma "Pie Pol" (Pie de Palo en el mapa) de La Guasara de Barahona; bosque latifoliado y humedo, con *Magnolia hamori*, *Obolanga zanonii*. *T. Zanoni et al.* 38670 (US, MO); **Haiti**. Collected along path 3/4 of way from Furcy toward M. La Visite *T. E. Talpey* 46 (BH); Summit of Mount Dilcorer, Montagnos de la Hotte *W. J. Everdam* 351 (NY, US, GH); Vicinity of Furcy *E. C. Leonard* 4630 (US); Vicinity of Marmelade, Department du Nord; thicket on mountain slope east of road. *E. C. Leonard* 8359 (US); Vicinity of Bassin Bleu; *E. C. Leonard & G. M. Leonard* 15058 (US); De L'ouest, Massif de la Selle, Parc National Morne la Visite, vicinity of lower cascade of Riviere Blanche about 2km SW of Park Headquarters, S of Morne la Visite *W. S. Judd & J. D. Skeeve Jr* 4436 (GH); Dep du Sud, Morne de la Hotte in dechiv. Sept-orient in sylvis moutanis *E. L. Ekman* 79 (S, AAH); Massif de La Selle, Sud'Est 8 km north of Seguin in the carretera Furcy and Petionville *T. Zanoni & M. Mejia* 24559 (NY); Riviere Glace, Cloud forest *J. T. Curtis & E. C. Leonard* 45 (WIS); Talpey no. 46. Seed collected long path from Furcy to Morne La Viste. Grown in the Hortorium Conservatory, Cornell Univ. *M. H. Stone* 1136 (US); Massif de la Selle *L. H. Bailey* 199 (US); Near Petite Source, Morves des Commissaires. *L. R. Holdridge* 955 (US); Camp No. 2, Mt. Maleuvre *G. V. Nash & N. Taylor* 1154 (US); Gonave Island *W. J. Everdam* 280 (US); Vicinity of Mission, Fonds Varettes *E. C. Leonard* 3802 (US); Peli on Ville *E. L. Ekman* 1129 (US).

**8. *Columnnea katzensteiniae*** (Wiehler) L. E. Skog and L. P. Kvist, *Novon* 7 (4): 413.

1997 [1998]. *Pentadenia katzensteiniae* Wiehler, *Phytologia* 73(3): 235. 1992. –

TYPE: ECUADOR. Morona-Santiago: Cordillera del Boliche, ca 60 km from Limón, *Wiehler & GRF Expedition 88128* (holotype: GES; isotype: F, K, MO, NY, QCA, US).

*Columnnea lavandulacea* L. P. Kvist and L. E. Skog, *Allertonia* 6: 387. 1993. – TYPE:

ECUADOR. Pichincha: Quito-Santo Domingo rd, 11 Dec 1983, *Kvist and Barfod* 49066 (holotype: AAU; photo: AAU).

*Columnnea katzensteiniae* is most closely related to *C. rileyi* based on molecular phylogenetic analyses (Figure 2.5 and 2.6). Both species, along with *C. crassicaulis* and *C. ovatifolia*, have similar corollas with darker colored lobe spots. However, the

lavender corollas with purple spots, lavender pubescence, and anisophyllous leaves distinguish *C. katzensteiniae* from other species of *Columnnea* (Smith 1994).

Phenology. Flowering continuously.

Distribution (Figure 2.10). Northern Ecuador into northern Peru; wet forests; 1400-2430 m.

ADDITIONAL SPECIMENS EXAMINED: **Ecuador.** Cotopaxi, Canton: Sigchos. Parroquia: San Francisco de las Pampas. Bosque Integral Otonga *J. L. Clark & A. Munoz 6129* (SEL, US, MO); Manabi, Old road from Santo Domingo to Quito *R. W. Dunn 57* (US); Morona-Santiago, Cordillera del Boliche; about 60km from Limon south to Gualaquiza *H. Wiehler & GRF Expedition 88128* (SEL); Morona-Santiago, Plan del Milagro at cross-road between Limon and Indanza *G. Harling & L. Andersson 24524* (US); Pastaza, Mera near Rio Pastaza. *G. C. G. Argent & R. B. Burbidge 423* (MO); Pichincha, Route Tandayapa - Nanegalito. *F. Billiet & B. Jadin 6690* (MO); Pichincha, Along road from Los Bancos to Mindo; 4 km from western road to Mindo *H. Wiehler et al. 90145* (SEL, US); Pichincha, Canton: Quito. Reserva Floristica-Ecologica "Rio Guajalito," km 59 de la cerretera antigua Quito-Sto. Domingo de los Colorados, a 3.5 km al NE de la carretera. *J. L. Clark et al. 7625* (US); Pichincha, Road Aloag-Santo Domingo, San Ignacio *B. Sparre 14693* (US); Zamora-Chinchiipe, Area of the Estacion Cientifica San Fransico. Road Loja-Zamora, ca. 35 km from Loja. *J. Homeier 1527* (MO); Zamora-Chinchiipe, Area of the Estacion Cientifica San Fransico. Road Loja-Zamora, ca. 35 km from Loja. *J. Homeier & E. Brandes 1218* (MO); Zamora-Chinchiipe, Canton: Chinchiipe. Parroquia: Zumba. Finca de Sandy Leon. Forest near Rio Tarrangami. *J. L. Clark et al. 8915* (US); Zamora-Chinchiipe, Area of Estacion Cientifica San Francisco, road Loja-Zamora, ca. 35 km from Loja *F. A. Werner 876* (US); **Peru.** Cajamarca, San Ignacio. Distrito Huarango. Poblado Selva Andina, trocha camino a Paquisha. *J. Perea & J. Mateo 3038* (MO).

**9. *Columnnea manabiana*** (Wiehler) J. F. Smith and L. E. Skog, Novon 3: 189. 1993.

*Pentadenia manabiana* Wiehler, Phytologia 73: 236. 1992. - TYPE: cultivated plants from living material (Dodson and Dodson 6791), collected in Manabi, Ecuador, Km 67 on rd Chone-Santo Domingo, 500 m, 31 Jul 1977, *Wiehler 87102* (holotype: GES; isotypes: B, F, HBG, K, MO, NY, QCA, SEL, U, US).

*Columnnea manabiana* is most closely related to *C. tandpaiana* with which it shares similar morphological characteristics (Figures 2.5 and 2.6). Both *C. manabiana*

and *C. tandapiana* have long, narrow, lanceolate to slightly falcate leaves and small yellow corollas. The two species can be distinguished from one another by the presence of large, conspicuous, ovate floral bracts, which partly obscure the inflorescence on *C. manabiana* (Smith 1994).

Phenology. Flowering from October to April.

Distribution (Figure 2.10). Ecuador (Manabí, El Oro); 50-1700 m.

ADDITIONAL SPECIMENS EXAMINED: **Ecuador.** Azuay, Cuenca. Bosque Protector Molleturo Mullopungo. Collections made along main road near the village, Mantareal and forest ca. 2 km East *J. L. Clark et al. 2487* (US); Bolivar, Hcda. Changuil, Nuevo Mundo. Bosque muy humedo Tropical, hublado. *X. Cornejo & C. Bonifaz 4591* (US); Canar, La Troncal. Manta Real. Tropical wet forest. Mixture of mature forest, cocoa plantation, and cow pasture. *J. L. Clark et al. 1588* (US, MO); Manabi, Manta. Bosque seco Tropical, area de bosque comunal. *C. Espinoza 58* (MO); Manabi, San Sebastian, Machalilla National Park, ridgetop moist forest. *A. Gentry et al. 72571* (MO); Manabi, San Sebastian, Machalilla National Park, ridgetop moist forest. *A. Gentry et al. 72578* (MO); Pichincha, Ca. 35 km N of Santo Domingo de los Colorados, vicinity of bridge over Rio Blanco. *A. Gentry 9625* (MO).

**10. *Columnea orientandina*** (Wiehler) L. P. Kvist and L. E. Skog. Allertonia 6: 392.

1993. *Pentadenia orientandina* Wiehler, Selbyana 2: 123. 1977. - TYPE:

cultivated material, grown from cuttings (Madison and Coleman 2532) collected in the Cordillera de Cutucu, Morona-Santiago, Ecuador, *Wiehler 77123* (holotype: SEL; isotype: US).

A relatively compact habit, laminas with a blunt red apex and a dorsiventral arrangement, and yellow corollas distinguish *C. orientandina* from other species of *Columnea*. *Columnea orientandina* is most closely related to *C. byrsina* (Figures 2.5 and 2.6), both of which have bright red corollas and dorsiventrally arranged leaves. The

exserted anthers and stigma can also be a distinguishing characteristic of *C. orientandina*, but they are not always seen in specimens (Smith 1994).

Phenology. Flowering continuously.

Distribution (Figure 2.8). Ecuador (Morona-Santiago) and Peru (Pasco); 1000-1500 m.

ADDITIONAL SPECIMENS EXAMINED: **Ecuador**. Morona-Santiago, Gualaquiza. Cordillera del Condor. Vertiente occidental de la Cordillera del Condor, arriba del valle del rio Quimi. *G. Pabon & J. Caranqui 309* (MO); Morona-Santiago, San Juan Bosco. Road between San Juan Bosco and El Pangui; 27 km S of San Juan Bosco. *J. L. Clark 9924* (US); Morona-Santiago, San Juan Bosco. Road between San Juan Bosco and El Pangui; 2-3 km S of San Juan Bosco. *J. L. Clark 9885* (US); Morona-Santiago, Collected outside city limits of General Leonidas Plaza Gutierrez (Limo) *J. L. Clark 6264* (US); Morona-Santiago, Macas, garden around Hotel el Valle *L. P. Kvist 60424* (US, MO); Morona-Santiago, N of Macas, on border to Sangai National Park *L. P. Kvist 60439* (US, MO); Pastaza, Pastaza Canton. Km 17 del propuesto oleoducto ARCO-Villano-El Triunfo. *W. Palacios 12088* (MO); Pastaza, Canton: Puyo. Parroquia: Veracruz. La Esperanza (Siguin); Finca Salina (de Hilda Perez). Km 14 on the Puyo-Macas road. *J. L. Clark & J. Katzenstein 8294* (US); Tungurahua, Canton: Banos. Small path of forest on north side of main highway between Banos and Puyo; 3-5 km east of El Topo. *J. L. Clark & J. Katzenstein 8282* (US, MO); Zamora-Chinchipe, El Pangui. Cordillera del Condor. Valle del Rio Quimi. Bosque alterado y potreros, en suelo aluvial del val. *T. Montenegro 142* (MO); Zamora-Chinchipe, Los Encuentros. Estacion Experimental El Padmi (Universidad de Loja). Located on the northern outskirts of the town El Padmi. *J. L. Clark 9949* (US); Zamora-Chinchipe, Zamora Canton. Jamboe Bajo. Eastern border of Podocarpus National Park. Mature forest near cow pasture. *J. L. Clark et al. 3203* (US); **Peru**. Cusco, Quispicanhis. Hills around Rio Araza between Pande Azucar and Quince Mil Airport. Forests 292 km from Cusco. *P. Nunez V. 14090* (MO); San Martin, Prov. Rioja. Dist. Pardo Miguel, El Afluente y la Marginal. *I. Sanchez Vega & M. Dillon 9023* (US).

**11. *Columnea ovatifolia*** L. P. Kvist and L. E. Skog, *Allertonia* 6: 393. 1993. - TYPE:

ECUADOR. Carchi: rd Tulcan-Maldonado, 10 km SE of Maldonado,

Campamente Machinrs, 28 Nov 1974, *Harling and Andersson 12316* (holotype:

GB; isotype: SEL).

*Columnea ovatifolia* is most closely related to *C. crassicaulis*, *C. katzensteiniae*, and *C. rileyi* (Figures 2.5 and 2.6). All four of these species, along with *C. antiocana* and

*C. suffruticosa*, have darker colored lobe spots. *Columnnea ovatifolia* can be distinguished from these species and other species of *Columnnea* by its smaller leaves, pink-purple corolla, and thinner stem (Smith 1994).

Phenology. Flowering from January to May.

Distribution (Figure 2.10). Northern Ecuador; cloud forests; 1900-2800 m.

ADDITIONAL SPECIMENS EXAMINED: **Ecuador**. Carchi, Canton: Espejo. Parroquia: Guatal. Mirador de las Golondrinas (Fundacion Golondrinas). Trail from El Corazon toward La Cortadera (2 km NE of refugio). *J. L. Clark & E. Folleco 8461* (US); Cotopaxi, Canton Sigchos. Orillas del Rio Los Illinizas, dentro del bosque *J. Ramos et al. 6025* (US); Cotopaxi, Canton: Sigchos. Parroquia: San Francisco de las Pampas. Bosque Integral Otonga *J. L. Clark & A. Munoz 6129* (US); Cotopaxi, Canton Sigchos, bosque al lado izquierdo de via Sigchos-Las Pampas *J. Ramos et al. 7188* (US, MO); Cotopaxi, Canton Sigchos, Triunfo Grande, bosque al N de carretera, ca. 2 horas de casa de Galo Roballo, loma La Delicia *J. Ramos et al. 7003* (US, MO); Pichincha, Route Tandayapa-Nanegalito. *F. Billiet & B. Jadin 6687* (MO).

**12. *Columnnea rileyi*** (Wiehler) J. F. Smith, *Pentadenia rileyi* Wiehler, *Phytologia* 73:

236. 1992. - TYPE: ECUADOR. Napo: 37 km from Baeza on rd to Lago Agrio, 24 Apr 1986, *Wiehler and GRF Expedition 86243* (holotype: GES; isotypes: F, K, MO, NY, QCA, SEL, U, US).

*Columnnea leucerinea* L. P. Kvist and L. E. Skog, *Allertonia* 6: 389. 1993. - TYPE:

ECUADOR. Napo: Lago Agrio-Baeza rd, km 145, Rio Aya Cachi, 8 Jan 1987, *Kvist et al. 60377* (holotype: AAU; isotypes: COL, MO, NY, QCA, QCNE, US).

Phylogenetic analyses placed *C. rileyi* as sister to *C. katzensteiniae* (Figures 2.5 and 2.6). *Columnnea rileyi* has a dense white pubescence covering the entire plant body that distinguishes it from other species of *Columnnea*. *Columnnea lophophora* has a similar

pubescence; however, the small orange-yellow corolla of *C. rileyi* easily separates these two species (Smith 1994).

Phenology. Flowering continuously.

Distribution (Figure 2.10). Northern and western Ecuador; wet forests; 1200-2000 m.

ADDITIONAL SPECIMENS EXAMINED: **Ecuador**. Cotopaxi, Nanegalito area *H. Wiehler 97176* (US); Cotopaxi, Canton: Sigchos. Parroquia: San Francisco de las Pampas. Propiedad de Cesar Tapia. *J. L. Clark et al. 6180* (US); Cotopaxi, Canton: Sigchos. Parroquia: San Francisco de las Pampas. Collections made along trail near entrance of Bosque Integral Otonga. *J. L. Clark & A. Munoz 6099* (US, MO); Napo, Along road from Baeza to El Chaco, vic. Rio Sardinas Grande, along Rio Quijos, disturbed area along swampy pasture; 6 km NNE of San Francisco Borja. *T. B. Croat et al. 87690* (US); Napo, Along road between main Baeza-Lago Agrio Hwy. and village of Gonzalo Diaz de Pineda on road to Parque Nacional Sumaco Napo Galeras, Sector Gonzales Diaz de Pineda, 0.6 km from main highway, between main highway and bridge over Rio Quijos *T. B. Croat & L. Hannon 93495* (US); Napo, Rio Panteor SW of Borja. Montane forest and rocky outcrops *L. Holm-Nielsen et al. 26744* (US); Napo, Union of Rio Borja and Rio Quijos, E bank. Wet riverside forest, never inundated. *L. Holm-Nielsen et al. 26229* (US); Pichincha, Canton: Quito. Parroquia: Nanegalito. Finca Kayalami; south of Cartegena; 2-3 air-km SE of Nanegalito *J. L. Clark et al. 7077* (US, MO).

**13. *Columnea spathulata*** Mansfeld, Notizbl. Gard. Berlin-Dahlem 14(121): 37. 1938.

*Pentadenia spathulata* (Mansfeld) Wiehler, Phytologia 27: 315. 1973. - TYPE:

ECUADOR. Pinchincha: Santo Domingo de los Colorados, *Schultze-Rhonhof*

1876 (holotype: B, destroyed) - ECUADOR. Pinchincha: Santo Domingo de los

Colorados, Centinella, Montanas de Ila, 12 km from Patricia Pilar, 575 m, 10 Jul

1979. *Lojtnant and Molau 15811* (neotype, designated by Kvist and Skog, 1993:

AAU; isoneotype: US).

*Alloplectus microsepalus* C. Morton, Fieldiana, Bot. 28: 523. 1953. *Pentadenia*

*microsepala* (C. Morton) Wiehler, Phytologia 27: 375. 1973. *Columnea*

*microsepala* (C. Morton) L. P. Kvist and L. E. Skog, Allertonia 6: 391. 1993. -

TYPE: VENEZUELA. Monagas: Cerro de la Cueva de Dona Anita, S of and bordering valley of Caripe, 1100-1200 m, 7 Apr 1945, *Steyermark 61905* (holotype: F; isotype: US).

*Pentadenia zapotalana* Wiehler, *Selbyana* 2: 85, pl 26B. 1977. *Columnnea zapotalana* (Wiehler) L. E. Skog, *Taxon* 33: 126. 1984 - TYPE: ECUADOR. Los Rios: 20 km S of Quevedo, *Wiehler et al. 71312* (holotype: SEL; isotype: US).

Similar to *C. angustata*, *C. spathulata* is a widely distributed species covering most of the range of section *Angustiflorae*. To survive in a wide range, the species of *C. spathulata* have highly variable morphological characteristics including leaf coloration, corolla color, and the number of flowers per axil. *Columnnea spathulata* can be distinguished by strongly anisophyllous leaves in combination with crenate laminar margin and a dense inflorescence (Smith 1994).

Phenology. Flowering and fruiting continuously throughout most of its range, restricted to July to April in Venezuela.

Distribution (Figure 2.11). Venezuela to Bolivia; cloud forest, wet forest, also in disturbed areas, such as *Citrus* plantations; 40-2800 m.

ADDITIONAL SPECIMENS EXAMINED: **Bolivia**. La Paz, Nor Yungas, Coroico, valle del rio Huarinilla, +/- 3 km abajo de Chairo, Yucupi. *L. S. G. Beck 21427* (US); **Ecuador**. Azuay, Cuenca, road from Cuenca to Guayaquil (via Molleturo/El Cajas), San Jose de Molleturo, trail from road leading South through small patch of primary forest *J. L. Clark 9823* (US); Azuay, Rio Patul. Collection made along path from El Cajas to Manta Real following Rio Patul (2-3 day Trek). *J. L. Clark et al. 6256* (US); Bolivar, Hcda. Changuil, en potrero. Bosque muy humedo Tropical, nublado. *X. Cornejo & C. Bonifaz 4532* (US); Carchi, 5 km above Lita (Colonia) along open road & by small creeks *H. Wiehler 9042* (SEL, US); Carchi, Espejo. Bosque Protector Mirador de Golondrinas. Collections made between the village, Las Juntas, and la Cabana del Corazon. Lower Montane Wet Forest. *J. L. Clark et al. 2420* (US); Chiguango, about 70km

west of Loja *R. Espinosa 1216* (SEL); Cotopaxi, 3 km E of El Palmar on road Quevedo-Latacunga *C. H. Dodson & A. Gentry 10242* (SEL); Cotopaxi, Km 5 to km 15 above La Mana. *H. Wiehler 9775* (SEL, US); Cotopaxi, foothills above Valencia near cane mill *M. E. Mathias & D. Taylor 5180* (US); El Oro, Along the new road west of Pinas *C. Luer et al. 5555* (SEL); El Oro, Road Loja-Santa Rosa, ca. 20 km past Pinas *H. Wiehler & GRF Expedition 8648* (SEL); El Oro, 10 km west of Pinas along new road from Pinas - Machala *C. H. Dodson et al. 8463* (SEL); El Oro, Along road from Loja to Santa Rosa ca. 20 km past Pinas; below cloud forest; at edge of road cut. *H. Wiehler 8649* (SEL, US); El Oro, Canton: Pinas. Parroquia: Moromoro. Reserva Ecologica Buenaventura. Remnant patch of forest S of "Entrada la Virgin." *J. L. Clark et al. 7958* (SEL, US); El Oro, Canton: Pinas. Parroquia: Moromoro. Reserva Ecologica Buenaventura. Remnant patch of forest S of "Entrada la Virgin." *J. L. Clark et al. 7957* (SEL, US); El Oro, Zaruma, Cerro El Calvario. Bosque tra si io al seco-humedo montano. *C. Bonifaz & X. Cornejo 3678* (US); Esmeraldas, environs of Lita, on the Ibarra-San Lorenzo *M. T. Madison et al. 4991* (SEL); Esmeraldas, Canton: San Lorenzo. Parroquia: Alto Tambo. Small patch of forest between Lita and Alto Tambo. *J. L. Clark et al. 7482* (SEL, US); Esmeraldas, Along road from Lita *H. Wiehler 9074* (SEL, US); Esmeraldas, Canton: Quininde. Bilsa Biological Reserve. Reserva Ecologica Mache-Chindul, 35 km W of Quininde. *J. L. Clark et al. 8777* (US); Esmeraldas, Quininde. Reserva Ecologica Mache-Chindul, 35 km W of Quininde. The Bilsa Biological Station. Cordillera Mache-Chindul. Sendero Café to Rio Cube and then to Rio Piscina to vivero near man Bilsa cabin. *J. L. Clark 9768* (US); Esmeraldas, Quininde Canton. Bilsa Biological Station. Reserva Ecologica Mache-Chindul, 35 km W of Quininde. Permanen Plot #3. *J. L. Clark 4644* (US); Esmeraldas, Quininde Canton. Reserva Ecologica Mache-Chindul. Comunidad Cana Bravel. Cabaceras del Rio Viche, estero Sabaleta. *J. L. Clark 4711* (US); Esmeraldas, Quininde. Community Piedrita, 10 km SW of Cube (via pircuta). *J. L. Clark et al. 2823* (US); Esmeraldas, Canton: Quininde. Bilsa Biological Reserve. Reserva Ecologica Mache-Chindul, 35 km W of Quininde. Trail from SW border of reserve to Don Bolivar's home (trail connecting the road toward Piedrita and the road toward Mono) *J. L. Clark et al. 8827* (US); Esmeraldas, Canton: San Lorenzo. Parroquia: Alto Tambo. Comunidad El Cristal; 8-10 km S of San Lorenzo-Ibarra highway. *J. L. Clark et al. 7532* (US); Esmeraldas, Quininde. Fundacion Paraiso de Papagayos. Centro de Rescate de Aves y Mamiferos. Km 2 via Esmeraldas. *J. L. Clark et al. 2793* (US); Esmeraldas, Bilsa Biological Station, N and NE border cut in NE part, then to Cube River tributary, then Invader Trail to Dogala Trail. *P. Mendoza-T. et al. 591* (US); Esmeraldas, 1 km W of Santa Isabel, toward Bilsa Biological Station, along logging road. *P. Mendoza-T. et al. 598* (US); Guayas, Cord. Chongon-Colonche. Bosque Protector Loma Alta. *X. Cornejo & C. Bonifaz 5716* (US); Guayas, La Crucita, Cuenca Rio Ayampe. Bosque transicional seco-humedo tropical *X. Cornejo & C. Bonifaz 939* (US); Guayas, Cord. Chongon-Colonche. Bosque Protector Loma Alta. *X. Cornejo & C. Bonifaz 6650* (US); Imbabura, Canton: Ibarra. Parroquia: Lita. Comunidad San Francisco; next to Rio Verde (13 air-km S of Lita). *J. L. Clark et al. 7530* (SEL, US); Imbabura, Along road from Ibarra to Lita. 5 km W of Lita. *H. Wiehler 9503* (SEL, US); Imbabura, Canton: Ibarra. Parroquia: Lita. Comunidad San Francisco; near Rio Verde (13 air-km S of Lita). *J. L. Clark et al. 7485* (SEL, US); Imbabura, Canton: Cotacachi. Parroquia: Garcia Moreno. Cordillera de Toisan. Cerro de la Plata. Bosque Protector Los Cedros. Main trail from the comunidad El Chontal to Los Cedros. *J. L. Clark et al. 7368* (SEL, US); Los Rios, mature forest across Rio Palenque from biological Station following road along river after crossing Rio Bimbo and Rio Waija A. *Gentry & C. H. Dodson 18027* (MO); Los Rios, Centinela Ridge area, 12.5 km E of Patricia Pilar *B. Hansen et al. 7774* (SEL); Los Rios, Centinela ridge, ca. 20 km E of Patricio Pilar. Cultivated land with scattered thickets. *H. Van der Werff et al. 12386* (US); Los Rios, 9 km E of (11 km by road from) Patricia Pilar (1 km to the E of Escuela Centrinelas, a minute settlement) 58 km ENE of Quevedo, on Pan-Am highway to Santo Domingo de los Colorados *H. H. Iltis & M. G. Iltis 59* (WIS); Manabi, Barbasmonte. Cuenca Rio Ayampe. Bosque transicional-humedo. *X. Cornejo & C. Bonifaz 1011* (US); Manabi, Canton: Pedernales. Cerro Pata de Pajaro, 10 km E of Pedernales. Finca of the family Aroyo. *J. L. Clark et al. 2700* (US); Manabi, Manta. Bosque seco Tropical, area de bosque comunal *C. Espinoza 58* (US); Manabi, Naranja, north of Pajan O. *Huaght 3408* (US); Manabi, Pedernales Canton. Reserva Ecologica Mache-Chindul. Comunidad Ambache (via marginal de la costa-Chindul) *J. L. Clark et al. 4143* (US); Manabi, Jama. 28 km S of Pedernales (as the crow flies); 3.5 km SW of the town Camarones; remnant tropical fog forest; off trail NW of Pertextaxto Gutierrez's house. *T. Delinks 504* (US); Morona-Santiago, Canton: Tiwintza. Parroquia: Santiago. Cordillera Winchinkiaim Naint #19. South of Centro Shuar Kusumas. Ridge and border between Ecuador and Peru *J. L. Clark et al. 9268* (US); Pichincha, Santo Domingo de los Colorados *F. Fagerlind & G. Wibom 1657* (OV, S); Pichincha, 5 km S of Santo Domingo at Hacienda San Fernando *B. Hansen et al. 7850* (SEL); Pichincha, bridge over Rio Chiguilpe near junction with Rio Baba, 7 km from Junction of

entrance and road from Sto Domingo to Quevedo at km 7 *C. H. Dodson 5944* (SEL); Pichincha, Along Rio Toachi, below Tinalandia, on both sides of river. *H. Wiehler 7972* (SEL, US); Pichincha, Montanas de Ila; sub-cloud forest, exposure toward the Pacific. *H. Wiehler 9082* (SEL, US); Pichincha, Along road from Quevedo to Latacunga; along western slope. *H. Wiehler 79133* (SEL, US); Pichincha, 7 km S of Santo Domingo, along Rio Chiguilpe *H. Wiehler 79365* (SEL, US); Pichincha, Between Puerto Quito and Pedro Vincente Maldonado, in creek area. *H. Wiehler 90112* (SEL, US); Pichincha, Santo Domingo de los Colorados. Tinalandia resort. *R. W. Dunn 95-04-135* (US); Pichincha, 35 km N of Santo Domingo de los Colorados, vicinity of bridge over Rio Blanco *A. Gentry 9625* (US); Pichincha, Between km 104 on Quito-Esmeraldas Road and Pachijal. *P. Mendoza-T. et al. 530* (US); Pichincha, Along old road between new Santo Domingo-Quito road and Chiriboga. *P. Mendoza-T. et al. 615* (US); Pichincha, Along trail between Guayabillas and Pachijal; ca. 1 km from Pachijal. *P. Mendoza-T. et al. 549* (US); Pichincha, Canton: Santo Domingo. Parroquia: Allurquin. La Union del Toachi. Cow pasture with remnant patches of primary forest. *J. L. Clark & A. Munoz 6098* (US); Pichincha, Santo Domingo de los Colorados *A. Gilli 116* (W);

**Venezuela.** Aragua, Rancho Grande; Paraiso trail *H. Wiehler 72378* (SEL, US); Estado, Monagas: Distrito Caripe. Cordillera de la Costa: 10 km al este de Caripe (distancia aerea): Quebrada Grande: propiedad de Rolf Struppek: bosque nublado. *W. Meier & R. Struppek 13461* (US); Estado, Yaracuy: Distrito Nirgua/Distrito San Felipe Serrania Santa Maria: al norte de Nirgua: Cerro La Chapa: bosque nublado en la cumbre con Dictyocaryum fuscum como palma emergente y areas intervenidas *W. Meier et al. 8467* (US); Estado, Sucre: Limite Distritos Arismendi/Bermudez/Benitez Peninsula de Paria: al sureste de Carupano, al noreste de Maturincito: Cerro Cerbatana: bosque nublado perturbado. *W. Meier & P. Molina 6790* (US); Estado, Sucre: Limite Distritos Bermudez/Benitez. Peninsula de Paria: al sureste de Carupano: Cerro La Cerbatana: carretera Maturincito-refugio: montana al este de Maturincito con estacion sismica de FUNVISIS: remanente de bosque nublado: al sur de carretera *W. Meier & C. Mentel 11860* (US); Estado, Monagas: Municipio Caripe, parroquia Teresen, sector Quebrada Grande. Cordillera de la Costa: 10 km al este de Caripe (distancia aerea): parte oriental de la propiedad de Rolf Struppek: zona de cultivos. *W. Meier & R. Stuppek 10868* (US); Estado, Yaracuy: Limites Distrito Nirgua-Distrito San Felipe Cerro La Chapa: ca. 5 km al norte de Nirgua: fila de la montana al este de la pica Nirgua-Las Maria: pastos de ganado. *W. Meier et al. 7790* (US); Estado Miranda, Limite Municipio Baruta/Municipio El Hatillo. Cerro El Volcan: sureste de Caracas: entre Baruta y El Hatillo: a lo largo de la carretera que sigue hacia las antenas: arbustales y herbazales secundarios. *W. Meier 12912* (US); Estado Miranda, Distrito Urdaneta. Cordillera de la Costa: Serrania del Interior: Macizo del Golfo Triste: subida al macizo entre la Quebrada La Providencia y la Fila Las Yaguas: bosque. *W. Meier & S. Nehlin 10188* (US); Monagas, Bosque Siempre Verde. Quebrada Pajal, 3 km al E de Escuela Rural El Aguacate, 11.2 km al E del puente sobre el Rio Colorado. Cuenca del Rio Caripe, al E de Caripe, via Las Margaritas, Edo. Monagas. *F. A. Michelangeli & M. Alfor 613* (US); Monagas, Distrito Caripe. Parque Nacional Guacharo: Cordillera de la Costa: 12.5 km al nornoreste de Caripe (distancia aerea): Alto El Silencio: vertiente norte: conucos alternado con remanentes de bosque. *W. Meier & R. Struppek 10464* (US); Estado Sucre, Distrito Benitez. Peninsula de Paria: al sureste de Carupano: Cerro La Cerbatana: antiguo camino desde carretera Maturincito-refugio hacia el caserio San Juan: bosque nublado. *W. Meier et al. 14354* (US); Estado Yaracuy, Distrito Nirgua y Distrito San Felipe: Serrania Sant Maria-Cerro La Chapa: en la cumbre: al este de la pica Nirgua-Las Marias; en selva nublado con Iriarte fusca. *W. Meier 3231* (US); Estado Yaracuy, Distrito Nirgua: Serrania Santa Maria-Cerro La Chapa: 6 km al norte de Nirgua: en selva nublada on Iriarte fusca. *W. Meier & M. Roesser 1006* (US); Yaracuy, Cumbre Gamelatal, 4.3-11 km N. of Salom on road from Salom to Candelaria. *S. Mori et al. 14658* (US).

#### **14. *Columnnea suffruticosa* J. F. Smith and L. E. Skog, Novon 3: 190. 1993. - TYPE:**

COLOMBIA. Choco: Mpio. San Jose del Palmar, Cerro del Torra, 7 Jan 1984,

*Silverstone-Sopkin et al. 1594* (holotype: CUVC; isotypes: MO, US).

The presence of lobes with darker colored spots places *C. suffruticosa* with the species of *C. ovatifolia*, *C. crassicaulis*, *C. katzensteiniae*, and *C. rileyi* (Figure 2.5 and 2.6). However, previous cladistic analyses of morphology placed *C. suffruticosa* with *C. colombiana* (Smith and Sytsma 1994a) but did not score the presence of dark colored lobe spots. *Columnea suffruticosa* can be distinguished from other *Columnea* species by a shrubby woody habit (Smith 1994).

Phenology. Flowering in August. One collection from January and one collection from February. Presumably from August to February.

Distribution (Figure 2.9). Colombia (Chocó, Valle del Cauca); 1870-2770 m.

ADDITIONAL SPECIMENS EXAMINED: **Colombia.** Valle, Municipio El Cairo. Cerro del Ingles (Cordillera Occidental, Serrania de los Paraguas, al hora en jeep de El Cairo, Valle). *F. A. Silverstone-Sopkin et al. 2764* (MO); Choco, San Jose del Palmar *F. A. Silverstone-Sopkin et al. 4246* (US); Choco, San Jose del Palmar *J. E. Ramos et al. 1670* (US); Choco, San Jose del Palmar *F. A. Silverstone-Sopkin et al. 4570* (US).

**15. *Columnea tandapiana*** (Wiehler) L. E. Skog and L. P. Kvist, *Novon* 7(4): 414.

1997[1998]. *Pentadenia tandapiana* Wiehler, *Phytologia* 73(3): 238. 1992. –

TYPE: ECUADOR. Pichincha: 7 km from San Miguel de los Bancos on road to Mindo, *Wiehler & GRF Expedition 90133* (holotype: GES, isotypes: QCA, US).

*Columnea inconspicua* L. P. Kvist and L. E. Skog, *Allertonia* 6: 385. 1993. - TYPE:

ECUADOR. Pichincha: Tandapi, confluence between Rio Tandapi with Rio Pilaton, 1500 m, 27 Jul 1967, *Sparre 17761* (holotype: S).

*Columnnea tandapiana* is most closely related to *C. manabiana* (Figures 2.5 and 2.6). The two species share similar lanceolate to slightly falcate leaves, small inconspicuous pale yellow corollas, and narrow calyx lobes. However, *C. tandapiana* can be distinguished from *C. manabiana* by caducous floral bracts (Smith 1994).

Phenology. Flowering continuously.

Distribution (Figure 2.10). Ecuador; wet forests; 1200-1950 m.

ADDITIONAL SPECIMENS EXAMINED: **Ecuador.** Azuay, Dense, rich jungle between Rio Blanco and Rio Norcay on road between Chacanceo and Molleturo *J. A. Steyermark* 52825 (US); Cotopaxi, Nanegalito area. *H. Wiehler* 97171 (SEL, US); Cotopaxi, Canton: Sigchos. Parroquia: San Francisco de las Pampas. Bosque Integral Otonga. *J. L. Clark & A. Munoz* 6106 (SEL, US); Cotopaxi, Canton: Sigchos. Parroquia: San Francisco de las Pampas. Propiedad de Cesar Tapia. *J. L. Clark et al.* 6181 (US); Cotopaxi, Trail from El Corazon to Facundo Vela, 1-3 km S of El Corazon, remnants of montane rain forest and secondary scrub *G. Harling & L. Andersson* 19225 (US); Cotopaxi, Canton: Sigchos. Parroquia: San Francisco de las Pampas. Bosque Integral Otonga. *J. L. Clark et al.* 6168 (US); Cotopaxi, Canton Pujili. Reserva Ecologica Los Ilinizas, Sector II (Sector Sur), sector Chuspitambo, al occidente de Choasilli, Cordillera Occidental, vertiente occidental, bosque nublado primario y arboles aislados en potrero. *P. Silverstone-Sopkin et al.* 9967 (US); El Oro, Canton: Pinas. Buffer zone/border region of Reserva Ecologica Buenaventura; 11 km (air-km) north of the "Entrada la Virgin" on road toward Viron. *J. L. Clark* 8006 (SEL, US); Morona-Santiago, Cordillera de Cutucu, western slopes, along a trail from Logrono to Yaupi *M. Madison et al.* 3370 (SEL); Pichincha, 7 km from San Miguel de los Bancos on road to Mindo; on tree in meadow along roadside *H. Wiehler & GRF Expedition* 90133 (SEL); Pichincha, Tandapi forest, on south side of Rio Pilaton, after crossing bridge. *H. Wiehler & D. Masterson* 7954 (SEL, US); Pichincha, Canton: Quito. Parroquia: Nanegalito. Finca Kayalami; south of Cartegena; 2-3 air-km SE of Nanegalito. *J. L. Clark et al.* 7076 (US, MO); Pichincha, Along road near Nanegal, in pasture land or small forest remnants. *H. Van der Werff et al.* 12298 (US, MO).

## LITERATURE CITED

- Baldwin, B. G., M. J. Sanderson, J. M. Porter, M. F. Wojciechowski, C. S. Campbell, and M. J. Donoghue. 1995. The ITS region of nuclear ribosomal DNA: a valuable source of evidence on angiosperm phylogeny. *Annals of the Missouri Botanical Garden* 82: 247-277.
- Baldwin, B. G. and S. Markos. 1998. Phylogenetic utility of the external transcribed spacer (ETS) of 18S-26S rDNA: congruence of ETS and ITS trees of *Calycadenia* 10: 449-463.
- Carlson, K. M., D. H. Mansfield, and J. F. Smith. 2011. A new species in the *Lomatium foeniculaceum* (Apiaceae) clade revealed through combined morphometric and phylogenetic analyses. *Systematic Botany* 36: 495-507.
- Clark, J. L., P. S. Herendeen, L. E. Skog, and E. A. Zimmer. 2006. Phylogenetic relationships and generic boundaries in the tribe Episcieae (Gesneriaceae) inferred from nuclear, chloroplast, and morphological data. *Taxon* 55: 313-336.
- Clark, J. L., M. M. Funke, A. M. Duffy, and J. F. Smith. 2012. Phylogeny of a Neotropical clade in the Gesneriaceae: more tales of convergent evolution. *International Journal of Plant Sciences*. In press.
- Farris, J. S. 1989. The retention index and the rescaled consistency index. *Cladistics* 5: 417-419.

- Farris, J. S., M. Källersjö, A. G. Kluge, and C. Bult. 1994. Testing significance of incongruence. *Cladistics* 10: 315-319.
- Felsenstein, J. 1985. Confidence limits on phylogenies: an approach using the bootstrap. *Evolution* 39: 783-791.
- Fitch, W. M. 1971. Defining the course of evolution: minimum change for a specific tree topology. *Systematic Zoology* 20: 406-416.
- Hamilton, M. B. 1999. Four primer pairs for the amplification of chloroplast intergenic regions with intraspecific variation. *Molecular Ecology* 8: 521-523.
- Huelsenbeck, J. P. and F. Ronquist. 2003. MRBAYES: Bayesian inference of phylogeny. *Bioinformatics* 17: 754-755.
- Huertas, M. L., J. V. Schneider, and G. Zizka. 2007. Phylogenetic analysis of *Palaua* (Malveae, Malvaceae) based on plastid and nuclear sequences. *Systematic Botany* 32: 157-165.
- Ingram, A. L. and J. J. Doyle. 2003. The origin and evolution of *Eragrostis tef* (Poaceae) and related polyploids: evidence from nuclear *waxy* and plastid *rps16*. *American Journal of Botany* 90: 116-122.
- Johnson, L. A. and R. L. Johnson. 2006. Morphological delimitation and molecular evidence for allopolyploidy in *Collomia vilkenii* (Polemoniaceae), a new species from northern Nevada. *Systematic Botany* 31: 349-360.
- Johnson, L. A. and D. E. Soltis. 1994. *matK* DNA sequences and phylogenetic reconstruction in Saxifragaceae s. str. *Systematic Botany* 19: 143-156.

- Kluge, A. G. and S. J. Farris. 1969. Quantitative phyletics and the evolution of anurans. *Systematic Zoology* 18: 1-32.
- Knowles, L. L. and B. C. Carstens. 2007. Delimiting species without monophyletic gene trees. *Systematic Biology* 56: 887-895.
- Kvist, L. P. and L. E. Skog. 1993. The genus *Columnnea* (Gesneriaceae) in Ecuador. *Allertonia* 6: 327-400.
- Levin, R. A., K. Watson, and L. Bohs. 2005. A four-gene study of evolutionary relationships in *Solanum* section *Acanthophora*. *American Journal of Botany* 92: 603-612.
- Lewis, P. O. 2001. A likelihood approach to estimating phylogeny from discrete morphological character data. *Systematic Biology* 50: 913-925.
- Linder, C. R., L. R. Goertzen, B. V. Heuvel, J. Francisco-Ortega, R. K. Jansen. 2000. The complete external transcribed spacer of 18S-26S rDNA: amplification and phylogenetic utility at low taxonomic levels in Asteraceae and closely allied families. *Molecular Phylogenetics and Evolution* 14: 285-303.
- Maddison, W. P. 1997. Gene trees in species trees. *Systematic Biology* 46: 523-536.
- Martén-Rodríguez, S., C. B. Fenster, I. Agnarsson, L. E. Skog, and E. A. Zimmer. 2010. Evolutionary breakdown of pollination specialization in a Caribbean plant radiation. *New Phytologist* 188: 403-417.
- Mason-Gamer, R. J. and E. A. Kellogg. 1996. Chloroplast DNA analysis of the monogenomic Triticeae: phylogenetic implications and genome-specific markers

- of special interest. Pp. 301-325 in *Methods of Genome Analysis in Plants* ed. P. Jauhar Boca Raton: CRC Press.
- Meredith, R. W., M. N. Pires, D. N. Reznick, and M. S. Springer. 2011. Molecular phylogenetic relationships and the coevolution of placentotrophy and superfetation in *Poecilia* (Poeciliidae: Cyprinodontiformes). *Molecular Phylogenetics and Evolution* 59: 148-157.
- Müller, K. 2004. PRAP – computation of Bremer support for large data sets. *Molecular Phylogenetics and Evolution* 31: 780-782.
- Nichols, R. 2001. Gene trees and species trees are not the same. *Trends in Ecology and Evolution* 16: 358-364.
- Nylander, J. A. A., J. C. Wilgenbusch, D. L. Warren, and D. L. Swofford. 2008. AWTY (are we there yet?): a system for graphical exploration of MCMC convergence in Bayesian phylogenetics. *Bioinformatics* 24: 581-583.
- Oxelman, B., M. Lidén, and D. Berglund. 1997. Chloroplast *rps16* intron phylogeny of the tribe *Sileneae* (Caryophyllaceae). *Plant Systematics and Evolution* 206: 393-410.
- Page, R. D. M. and M. A. Charleston. 1997. From gene to organismal phylogeny: reconciled tree and the gene tree/species tree problem. *Molecular Phylogenetics and Evolution* 7: 231-240.
- Posada, D. and K. A. Crandall. 1998. MODELTEST: testing the model of DNA substitution. *Bioinformatics* 14: 817-818.

- Posada, D. and T. R. Buckley. 2004. Model selection and model averaging in phylogenetics: advantages of Akaike information criterion and Bayesian approaches over likelihood ratio tests. *Systematic Biology* 53: 793-808.
- Rambaut, A. and A. J. Drummond. 2005. Tracer v1.4, Available at <http://beast.bio.ed.ac.uk/Tracer>.
- Reeves, G., M. W. Chase, P. Goldblatt, M. F. Fay, A. V. Cox, B. Lejeune, and T. Suozachies. 2001. Molecular systematics of Iridaceae: evidence from four plastid DNA regions. *American Journal of Botany* 88: 2074-2087.
- Ruiz-Sanchez, E. and V. Sosa. 2010. Delimiting species boundaries within the Neotropical bamboo *Otatea* (Poaceae: Bambusoideae) using molecular, morphological, and ecological data. *Molecular Phylogenetics and Evolution* 54: 344-356.
- Ruvolo, M., S. Zehr, M. von Dornum, D. Pan, B. Change, et al. 1993. Mitochondrial COII sequences and modern human origins. *Molecular Biology and Evolution* 10: 1115-35.
- Seelanen, T., A. Schnabel, and J. F. Wendel. 1997. Congruence and consensus in the cotton tribe (Malvaceae). *Systematic Botany* 22: 275-288.
- Shaw, J., E. B. Lickey, E. E. Schilling, and R. L. Small. 2007. Comparison of whole chloroplast genome sequences to choose noncoding regions for phylogenetic studies in angiosperms: the tortoise and the hare III. *American Journal of Botany* 94: 275-288.

- Simmons, M. P. and H. Ochoterena. 2000. Gaps as characters in sequence-based phylogenetic analyses. *Systematic Biology* 49: 369-381.
- Smith, J. F. 2000. Phylogenetic signal common to three data sets: combining data which initially appear heterogeneous. *Plant Systematics and Evolution* 221: 179-198.
- Smith, J. F. and K. J. Sytsma. 1994a. Evolution in the Andean epiphytic genus *Columnnea* (Gesneriaceae). Part I. Morphology. *Systematic Botany* 19: 220-235.
- Smith, J. F. and K. J. Sytsma. 1994b. Evolution in the Andean epiphytic genus *Columnnea* (Gesneriaceae). Part II. Chloroplast DNA restriction site variation. *Systematic Botany* 19: 317-336.
- Smith, J. F. and K. J. Sytsma. 1994c. Molecular and morphology: Congruence of data in *Columnnea* (Gesneriaceae). *Plant Systematics and Evolution* 193: 37-52.
- Smith, J. F., J. C. Wolfram, K. D. Brown, C. L. Carroll, and D. S. Denton. 1997. Tribal relationships in the Gesneriaceae: Evidence from DNA sequences of the chloroplast gene *ndhF*. *Annals of the Missouri Botanical Garden* 8: 50-66.
- Smith, J. F., L. C. Hileman, M. P. Powell, and D. A. Baum. 2004. Evolution of *GCYC*, a Gesneriaceae homolog of *CYCLOIDEA*, within Gesnerioideae (Gesneriaceae). *Molecular Phylogenetics and Evolution* 31:765-779.
- Smith, J. F., A. C. Stevens, E. J. Tepe, and C. Davidson. 2008. Placing the origin of two species-rich genera in the late Cretaceous with later species divergence in the tertiary: a phylogenetic, biogeographic and molecular dating analysis of *Piper* and *Peperomia* (Piperaceae). *Plant Systematics and Evolution* 275:9-30.

- Smith, J. F., M. Ooi, L. Schulte, M. Amaya M., and J. L. Clark. The disintegration of the subgeneric classification of *Columnnea* (Gesneriaceae). *Selbyana* in review.
- Steele, P. R., L. M. Friar, L. E. Gilbert, and R. K. Jansen. 2010. Molecular systematics of the Neotropical genus *Psiguria* (Cucurbitaceae): Implications for phylogeny and species identification. *American Journal of Botany* 97: 156-173.
- Strand, A. E., J. Leebens-Mack, and B. G. Milligan. 1997. Nuclear DNA-based markers for plant evolutionary biology. *Molecular Ecology* 6: 113-118.
- Struwe, L., P. E. Smouse, E. Heiberg, S. Haag, and R. C. Lathrop. 2011. Spatial evolutionary and ecological vicariance analysis (SEEVA), a novel approach to biogeography and speciation research, with an example from Brazilian Gentianaceae. *Journal of Biogeography* 38: 1841-1854.
- Swofford, D. L. 2002. PAUP\*: phylogenetic analysis using parsimony (\*and other materials), version 4.0b10. Sunderland, Massachusetts: Sinauer.
- Tuffley, C. and M. Steel. 1997. Links between maximum likelihood and maximum parsimony under a simple model of site substitution. *Bulletin of Mathematical Biology* 59: 581-607.
- Weese, T. L. and L. A. Johnson. 2005. Utility of NADP-dependent isocitrate dehydrogenase for species-level evolutionary inference in angiosperm phylogeny: A case study in *Saltugilia*. *Molecular Phylogenetics and Evolution* 36: 24-41.
- Woo, V. L., M. M. Funke, J. F. Smith, P. J. Lockhart, and P. J. Garnock-Jones. 2011. New world origins of southwest Pacific Gesneriaceae: Multiple movements

across and within the south Pacific. *International Journal of Plant Science* 172: 434-457.

Yoder, A. D., J. A. Irwin, and B. A. Payseur. 2001. Failure of the ILD to determine data combinability for slow loris phylogeny. *Systematic Biology* 50: 408-424.

Zwickl, D. J. 2006. *Genetic algorithm approaches for the phylogenetic analysis of large biological sequence datasets under the maximum likelihood criterion*. Ph. D. dissertation. Austin: University of Texas.

**Table 2.1 – Results from Testing Seven Gene Regions to Determine the Ability to Resolve Species-level Relationships**

Results for each of the seven gene regions amplified for nine species of *Columnnea* (Appendix B) to test the ability of seven gene regions (*trnK1F-matKR*, *matK1F-1R*, *matK2F-2R*, *G3pdhA*, *G3pdhB*, *idhA*, and *idhB*) to identify species level relationships within section *Angustiflorae*. No. of constant characters is the number of base pairs that remained constant across all nine taxa. Uninformative characters are the number of phylogenetically uninformative characters. Informative characters are the number of phylogenetically informative characters. PIC (%) is the percent of phylogenetically informative characters (informative characters/base pairs compared). CI is the consistency index (Kluge and Farris 1969) and RI is the retention index (Kluge and Farris 1969). The informative characters, PIC, and CI were compared to the values of ITS and *rpl32-trnL<sub>UAG</sub>* spacer that had already been determined to resolve species level relationships within section *Angustiflorae* (see “Phylogenetic Tree Topology: Full Data Set”). Bold numbers indicate the gene regions with the highest values for all three parameters, informative characters, PIC, and CI, indicating the most rapidly evolving gene regions.

Gene region	Base pairs compared	No. of constant characters	Uninformative characters	Informative characters	PIC (%)	CI	RI
ITS	699	627	48	24	3.40	0.85	0.62
<i>rpl32-trnL<sub>UAG</sub></i> spacer	1,100	1,045	53	2	0.18	0.98	0.67
<i>G3pdhA</i>	1,140	986	136	<b>18</b>	<b>1.60</b>	<b>0.96</b>	0.67
<i>G3pdhB</i>	839	718	110	<b>11</b>	<b>1.30</b>	<b>0.97</b>	0.71
<i>idhA</i>	992	837	136	<b>19</b>	<b>1.90</b>	<b>0.97</b>	0.70
<i>idhB</i>	718	667	48	3	0.42	0.98	0.83
<i>trnK1F-matKR</i>	795	785	8	2	0.25	0.91	0.50
<i>matK1F-1R</i>	713	704	6	3	0.42	1.00	0.00
<i>matK2F-2R</i>	708	691	13	4	0.56	0.94	0.83

**Table 2.2 – Results for Ability of Two Low-copy Nuclear Gene Regions to Resolve Species-level Relationships within Section *Angustiflorae***

Results for all loci of the two low-copy nuclear gene regions amplified for 30 accessions (Appendix B) to test the ability of gene regions to resolve species level relationships within *Angustiflorae*. No. of constant characters is the number of base pairs that remained constant across all taxa. Uninformative characters are the number of phylogenetically uninformative characters. Informative characters are the number of phylogenetically informative characters. PIC (%) is the percent of phylogenetically informative characters (informative characters/base pairs compared). CI is the consistency index (Kluge and Farris 1969) and RI is the retention index (Farris 1989). The informative characters, PIC, and CI were compared to the values of ITS and *rpl32-trnL<sub>UAG</sub>* spacer that had already been determined to resolve species level relationships within section *Angustiflorae* (see “Phylogenetic Tree Topology: Full Data Set”). Bold numbers indicate gene regions with the highest values for all three parameters, informative characters, PIC, and CI, indicating the most rapidly evolving gene regions.

<b>Gene Region</b>	<b>Base Pairs Compared</b>	<b>No. of Constant</b>	<b>Uninformative Characters</b>	<b>Informative Characters</b>	<b>PIC (%)</b>	<b>CI</b>	<b>RI</b>
ITS	699	627	48	24	3.40	0.85	0.62
<i>rpl32-trnL<sub>UAG</sub></i> spacer	1,100	1,045	53	2	0.18	0.98	0.67
<i>G3pdhA</i>	1226	891	231	<b>104</b>	<b>8.50</b>	<b>0.80</b>	0.76
<i>G3pdhB</i>	885	722	134	<b>29</b>	<b>3.30</b>	<b>0.89</b>	0.76
<i>idhA</i>	1214	904	214	<b>96</b>	<b>7.90</b>	<b>0.82</b>	0.54
<i>idhB</i>	731	627	66	<b>38</b>	<b>5.20</b>	<b>0.83</b>	0.75

**Table 2.3 – DNA Sequencing Results**

Nucleotide sequence characteristics of gene regions amplified for accessions of the full and reduced data sets (Appendix B). Number of accessions sequenced is the number of accessions successfully sequenced out of 54 accessions for the full data set and 30 accessions for the reduced data set. PIC is the number of phylogenetically informative characters. Number of characters excluded is the number of ambiguities excluded from the data analyses including single base pair repeats, autapomorphies, and microsatellite repeats. The phylogenetically informative characters, number of constant characters, and number of uninformative characters are from the full and reduced data sets excluding areas of ambiguity.

<b>Data Set</b>	<b>Gene Region</b>	<b>No. of Accessions Sequenced</b>	<b>Align Length</b>	<b>Mean Length</b>	<b>Range</b>	<b>PIC</b>	<b>Constant Characters</b>	<b>Uninformative Characters</b>	<b>No. Characters Excluded</b>
<b>Full</b>	<i>trnQ-rps16</i> spacer	54	1,240	917	812-1,086	33	704	99	404
	<i>rpl32-trnL<sub>UAG</sub></i> spacer	54	1,228	1,019	966-1,070	41	938	75	174
	<i>rps16</i> intron	53	992	764	618-913	9	571	44	368
	<i>trnS-G</i> spacer	54	1,059	687	534-842	12	518	57	472
	<i>trnH-psbA</i> spacer	49	525	298	262-372	19	311	10	185
	ITS	54	726	595	389-694	80	280	65	301
	ETS	49	546	487	447-520	74	282	60	130
<b>Reduced</b>	<i>trnQ-rps16</i> spacer	31	1,208	877	812-1,072	28	719	89	372
	<i>rpl32-trnL<sub>UAG</sub></i> spacer	31	1,228	1,027	968-1,065	30	963	61	174
	<i>rps16</i> intron	31	992	754	625-913	6	597	22	367
	<i>trnS-G</i> spacer	31	1,058	679	542-842	9	745	34	270
	<i>trnH-psbA</i> spacer	30	525	296	262-372	13	313	14	185

ITS	31	724	595	418-694	50	303	72	299
ETS	28	546	493	463-520	35	324	57	130
<i>G3pdhA</i>	26	1,224	1,084	981-1,137	78	790	220	136
<i>idhB</i>	27	736	683	634-719	27	586	43	27

---

**Table 2.4 – Results of Scoring Indel Events**

Results from scoring the indel events in the full and reduced data sets including the number of indel events per gene region and the range of the length of the indel events for each gene region.

<b>Data Set</b>	<b>Gene Region</b>	<b>No. Indels Included</b>	<b>Range of Indel Lengths</b>
<b>Full</b>	<i>trnQ-rps16</i> spacer	6	6-9
	<i>rpl32-trnL<sub>UAG</sub></i> spacer	4	6-66
	<i>rps16</i> intron	0	-
	<i>trnS-G</i> spacer	31	2-19
	<i>trnH-psbA</i> spacer	11	3-11
	ITS	1	4
	ETS	2	2
<b>Reduced</b>	<i>trnQ-rps16</i> spacer	4	6-8
	<i>rpl32-trnL<sub>UAG</sub></i> spacer	3	8-66
	<i>rps16</i> intron	0	-
	<i>trnS-G</i> spacer	5	3-19
	<i>trnH-psbA</i> spacer	7	3-11
	ITS	0	-
	ETS	0	-
	<i>G3pdhA</i>	6	2-7
	<i>idhB</i>	2	2-5

**Table 2.5 – Maximum Parsimony Results**

Results from MP analyses for each partition in both the full and reduced data sets and the concatenated data sets. CI is the consistency index (Kluge and Farris 1969), RI is the retention index (Farris 1989), and RC is the rescaled consistency index (Farris 1989).

<b>Data Set</b>	<b>Partition</b>	<b>Number of Trees</b>	<b>Length</b>	<b>CI</b>	<b>RI</b>	<b>RC</b>
<b>Full</b>	cpDNA	44	517	0.6214	0.8351	0.7091
	ITS	165	286	0.5421	0.7322	0.4813
	ETS	278	268	0.5738	0.8207	0.5818
	Concatenated	175	1,045	0.5572	0.7764	0.5810
<b>Reduced</b>	cpDNA	8	416	0.6818	0.7832	0.6909
	ITS	99	231	0.5753	0.6543	0.4702
	ETS	48	190	0.5738	0.7570	0.5498
	<i>G3pdhA</i>	14	111	0.6226	0.7590	0.6223
	<i>idhB</i>	5	452	0.5751	0.5684	0.4653
	Concatenated	4	1,160	0.7905	0.6421	0.5076

**Table 2.6 – Model Test Results**

Results from Modeltest 3.6 (Posada and Crandall 1998) for partitions of both the full and reduced data sets and the concatenated data sets including the chosen model based on Akaike information criterion (Posada and Buckley 2004), the model values for I and  $\Gamma$ , the frequency of each base, and the rate of change from one base to another.

Full Data Set					Reduced Data Set					
Partition	cpDNA	ITS	ETS	Concatenated	cpDNA	ITS	ETS	<i>G3pdhA</i>	<i>idhB</i>	Concatenated
<b>Model</b>	TVM + I + $\Gamma$	GTR + $\Gamma$	TVM + $\Gamma$	TVM + I + $\Gamma$	TVM + I + $\Gamma$	TVM + $\Gamma$	TVM + $\Gamma$	K81uf + I + $\Gamma$	TrN + I	TVM + I + $\Gamma$
<b>Value of I</b>	0.5267	-	-	0.5396	0.5393	-	-	0.2729	0.7803	0.5819
<b>Value of <math>\Gamma</math></b>	1.1372	0.3912	0.5117	0.8766	1.0205	0.4442	0.2627	0.8396	-	0.8137
<b>Freq of A</b>	0.3522	0.1869	0.3486	0.3399	0.3531	0.1835	0.3377	0.2684	0.2720	0.3164
<b>Freq of C</b>	0.1448	0.2890	0.2400	0.1641	0.1420	0.2961	0.2473	0.1646	0.1868	0.1672
<b>Freq of G</b>	0.1514	0.2912	0.2309	0.1648	0.1453	0.2967	0.2391	0.2062	0.2065	0.1772
<b>Freq of T</b>	0.3516	0.2329	0.1805	0.3312	0.3596	0.2237	0.1759	0.3609	0.3347	0.3392
<b>R(a) [A-C]</b>	0.7991	1.0727	0.5905	0.8703	0.8908	1.6294	0.4627	1.0000	1.0000	0.9264
<b>R(b) [A-G]</b>	1.1881	3.5225	2.4182	2.1096	1.2404	4.1093	3.6327	1.5540	2.8505	1.9904
<b>R(c) [A-T]</b>	0.2067	1.9130	1.1584	0.3898	0.2408	2.1521	1.4575	0.7673	1.0000	0.5078
<b>R(d) [C-G]</b>	0.9087	0.6332	0.3989	0.9887	0.8521	0.7284	0.3308	0.7673	1.0000	0.9548
<b>R(e) [C-T]</b>	1.1881	4.9395	2.4182	2.1096	1.2404	6.3814	3.6327	1.5540	1.5131	1.9904
<b>R(f) [G-T]</b>	1.0000	1.0000	1.0000	1.0000	1.0000	1.0000	1.0000	1.0000	1.0000	1.0000

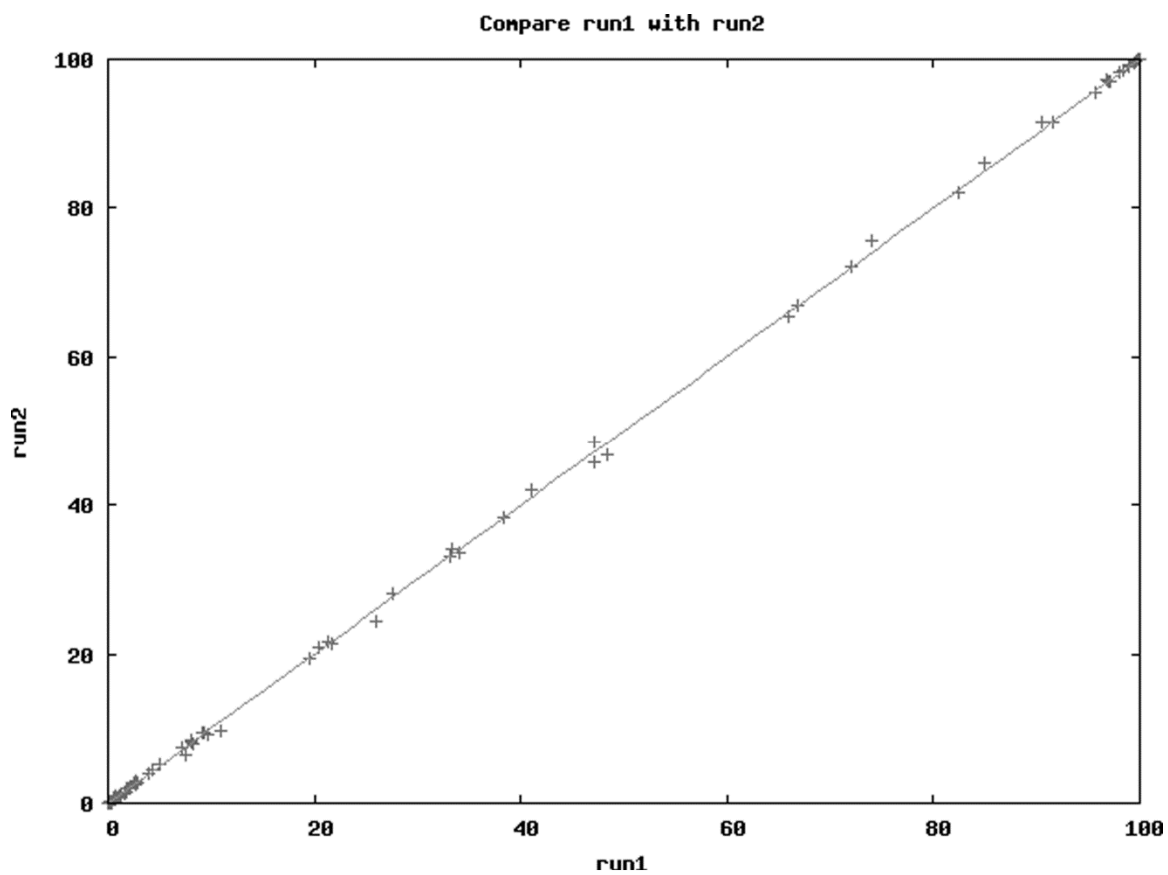


**Figure 2.1 – The Are We There Yet results from the comparison of the two Bayesian inference one model analyses of the full data set.**

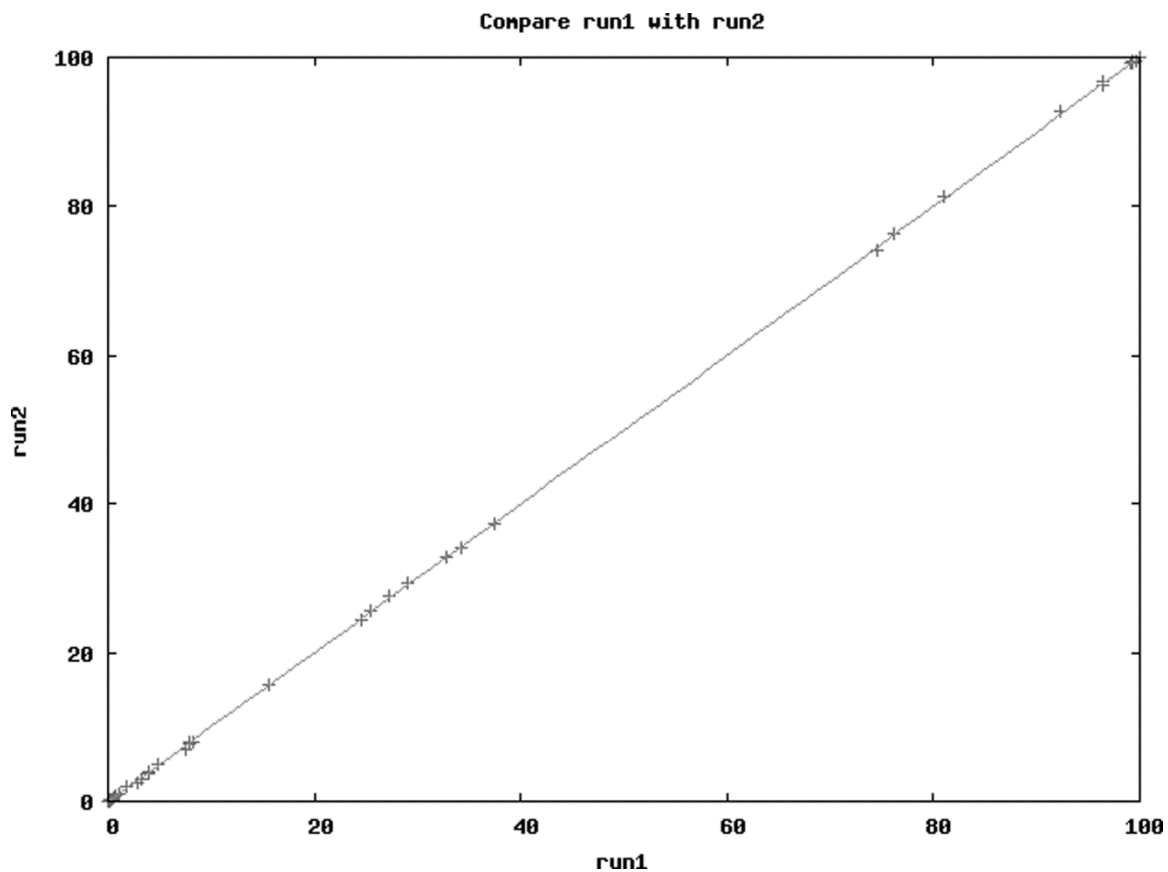


**Figure 2.2 – The Are We There Yet results from the comparison of the two Bayesian inference one model analyses of the reduced data set.**

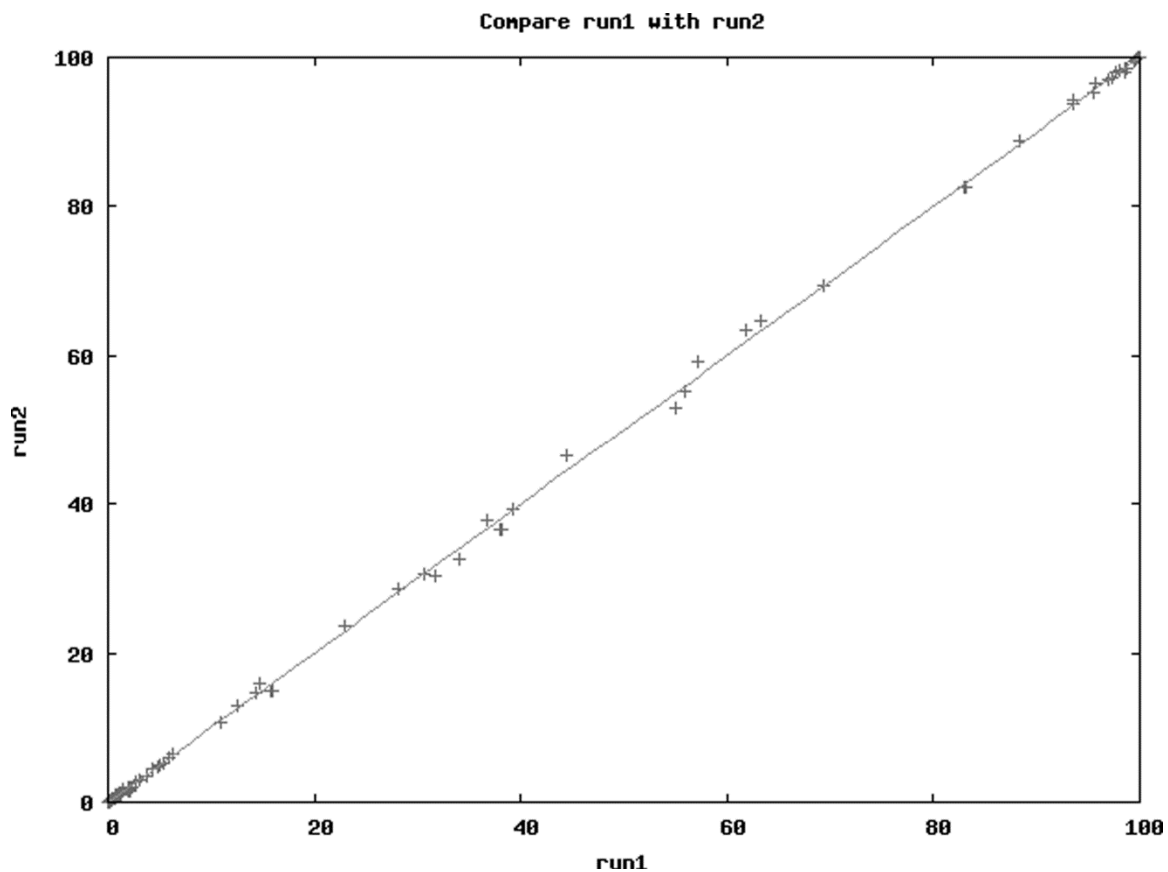


**Figure 2.3 – The Are We There Yet results from the comparison of the two Bayesian inference partition model analyses of the full data set.**

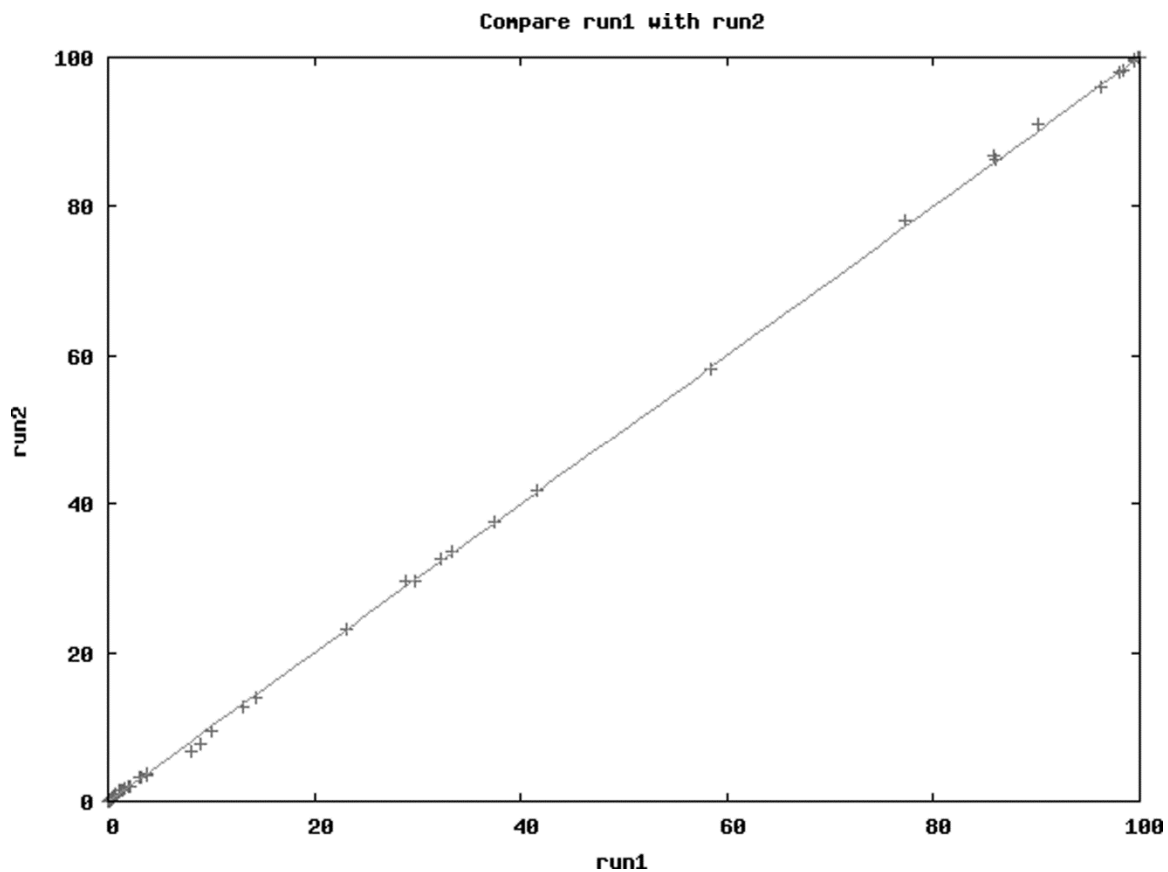


**Figure 2.4 – The Are We There Yet results from the comparison of the two Bayesian inference partition model analyses of the reduced data set.**

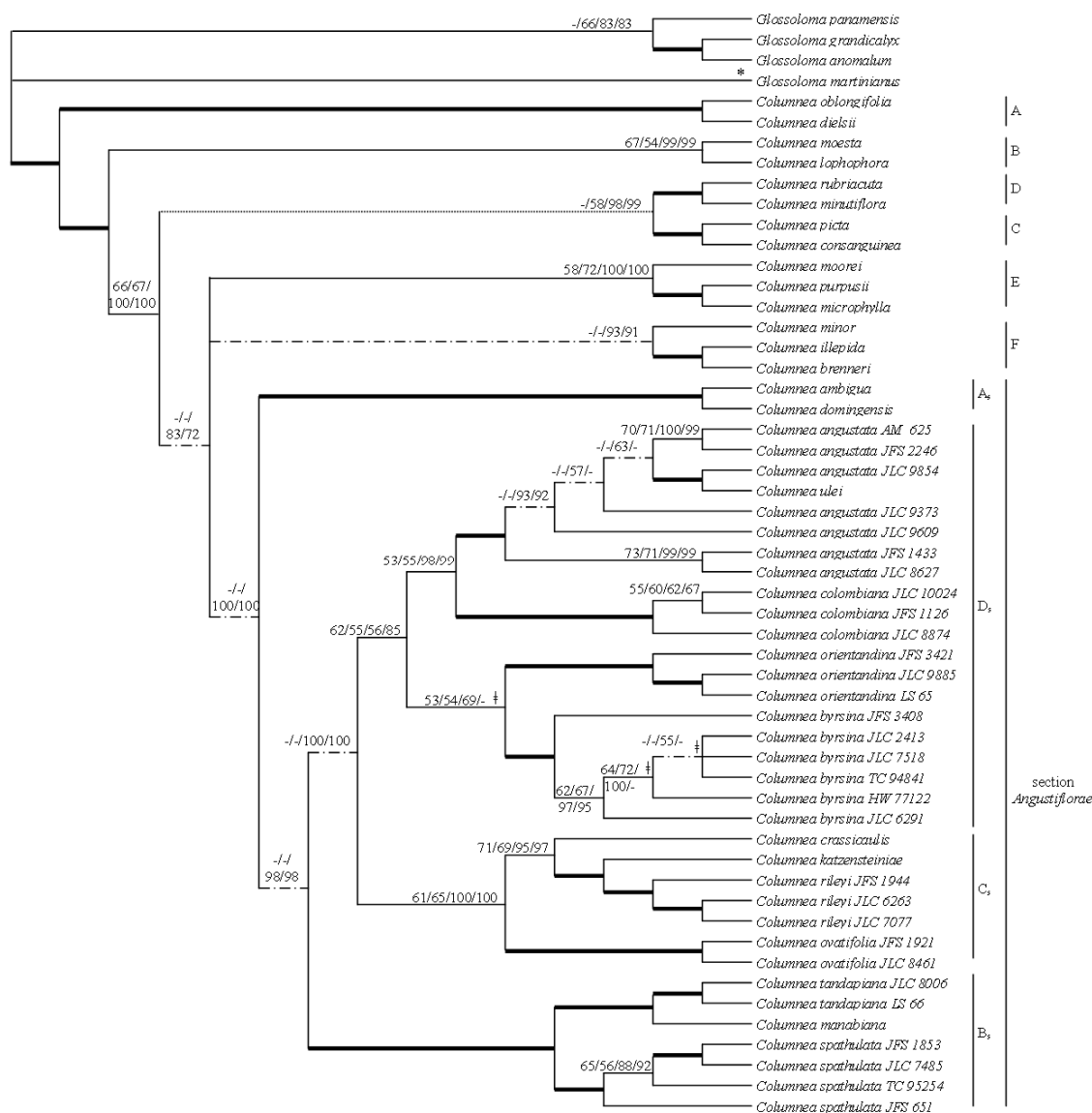


**Figure 2.5 – Summary of maximum parsimony (MP), maximum likelihood (ML), Bayesian inference (BI) one model, and BI partition model analyses mapped onto the BI partition analysis tree topology for the full data set. Numbers above branches represent MP bootstrap (BS)/MLBS/BI one model posterior probability (PP)/BI partition model PP. Bold branches are strongly supported in all four analyses (BS > 75; PP > 95). Letters on the left of the tree represent the subclades within section *Angustiflorae* (A<sub>s</sub>, B<sub>s</sub>, C<sub>s</sub>, and D<sub>s</sub>). Letters on the far right represent clades identified by Smith et al. (in review) and Chapter One. Dotted lines represent branches that collapse in the MP analysis. Dashed and dotted lines represent branches that collapse in the MP and ML analyses. Asterisk indicates that the branch was not present in the MP analysis. Line with double strike through indicates that the branch was not present in the ML analysis.**

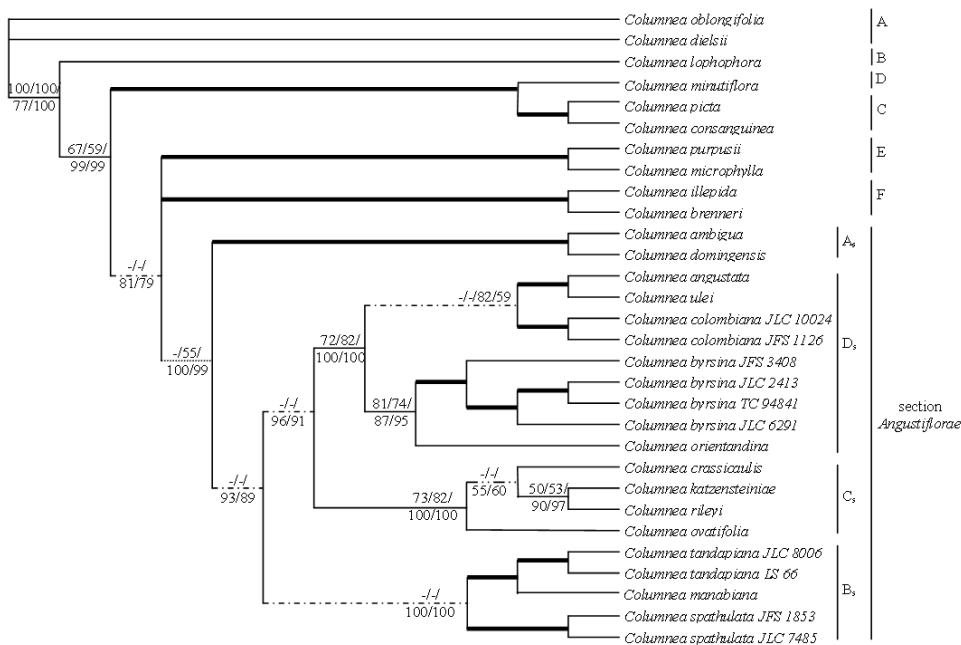


**Figure 2.6 – Summary of maximum parsimony (MP), maximum likelihood (ML), Bayesian inference (BI) partition model analyses model mapped on the BI partition analysis tree topology for the reduced data set. Numbers on branches represent MP bootstrap (BS)/MLBS/BI one model posterior probability (PP)/BI partition model PP. Bold branches are strongly supported in all four analyses (BS > 75; PP > 95). Letters on the left represent subclades in section *Angustiflorae* (A<sub>s</sub>, B<sub>s</sub>, C<sub>s</sub>, and D<sub>s</sub>). Letters on the far right represent clades identified by Smith et al. (in review) and Chapter One. Dashed and dotted lines represent branches that collapse in both MP and ML analyses.**

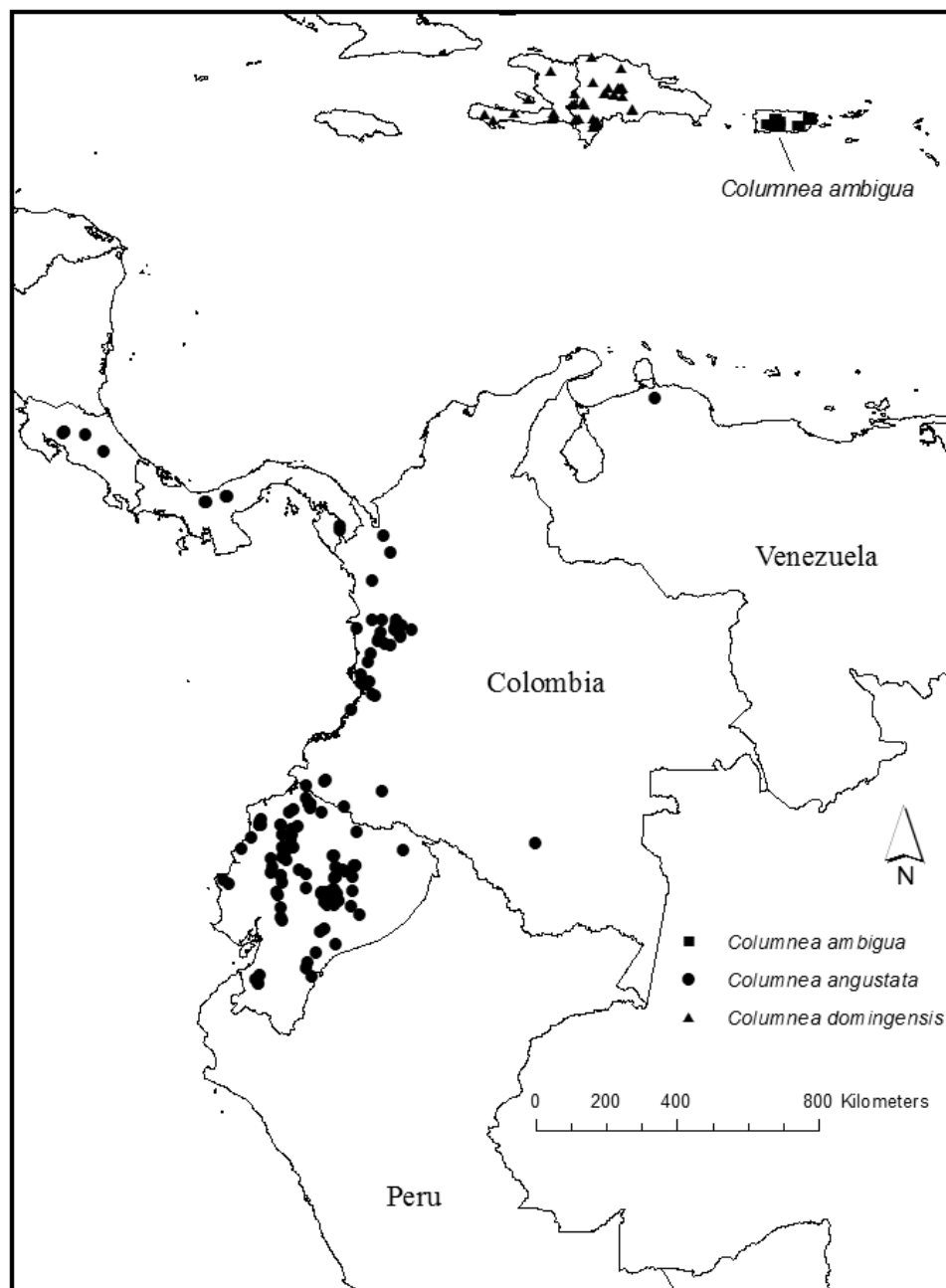


Figure 2.7 – Distribution of *Columnnea ambigua*, *C. angustata*, and *C. domingensis*.

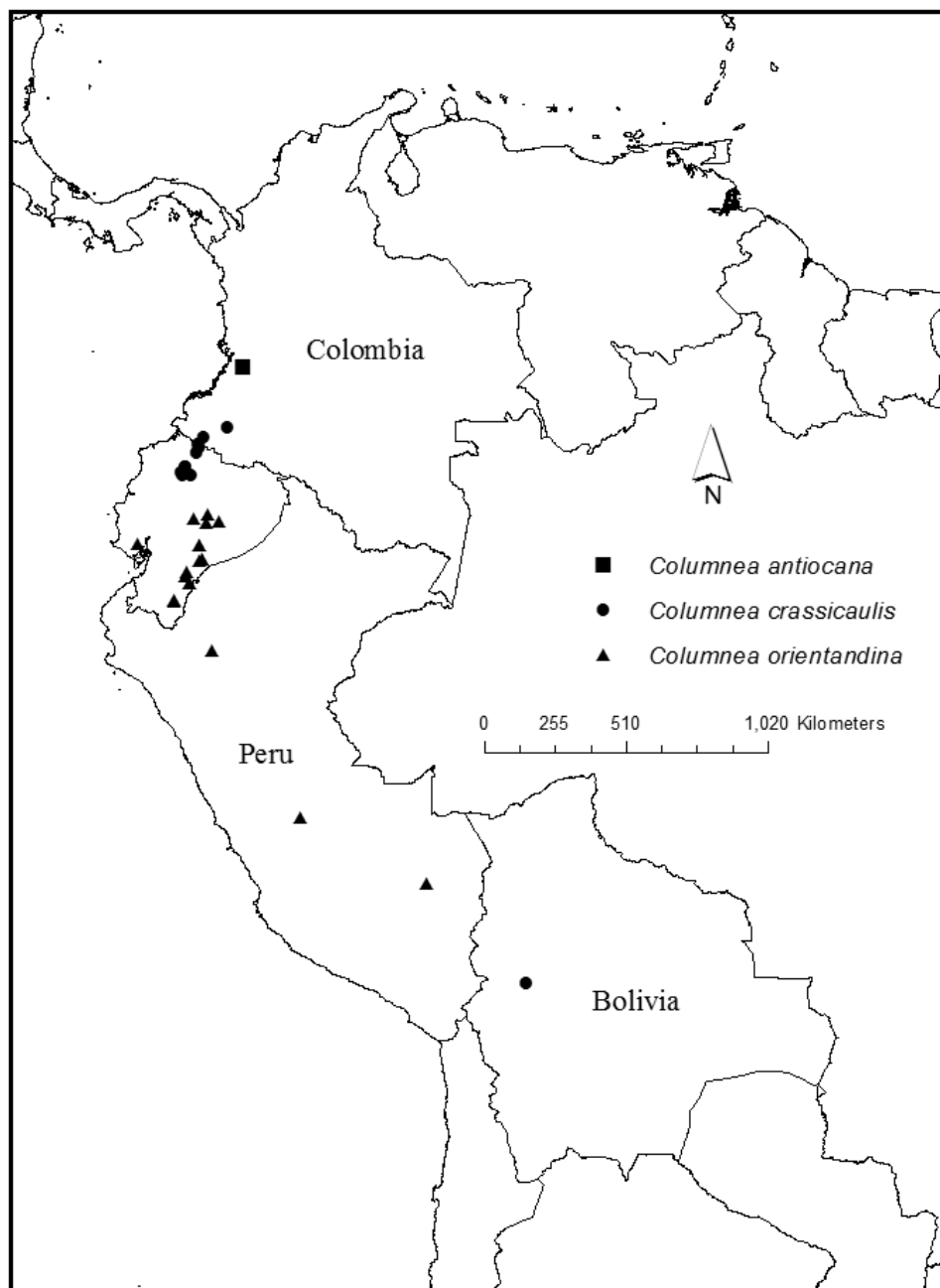
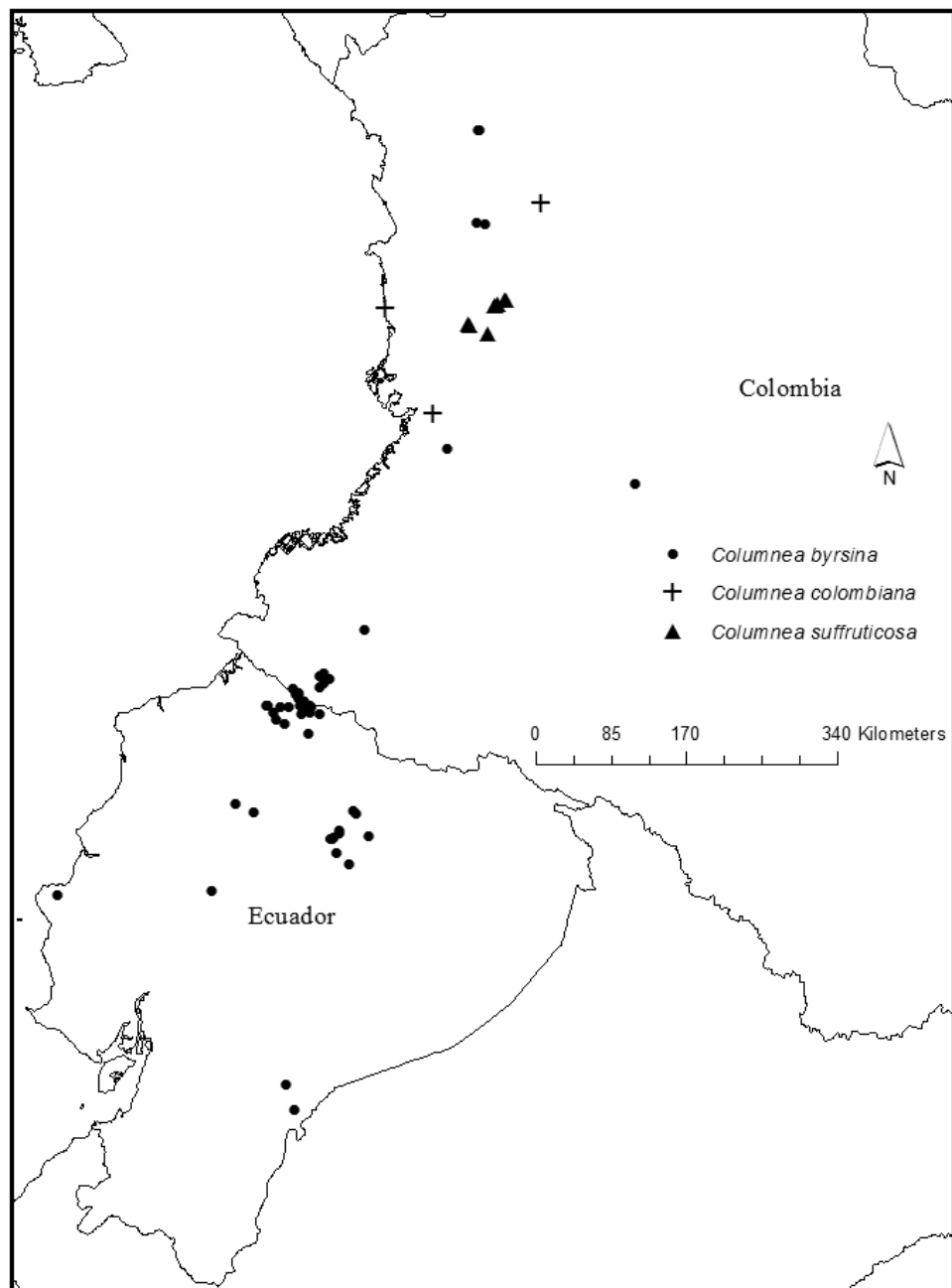
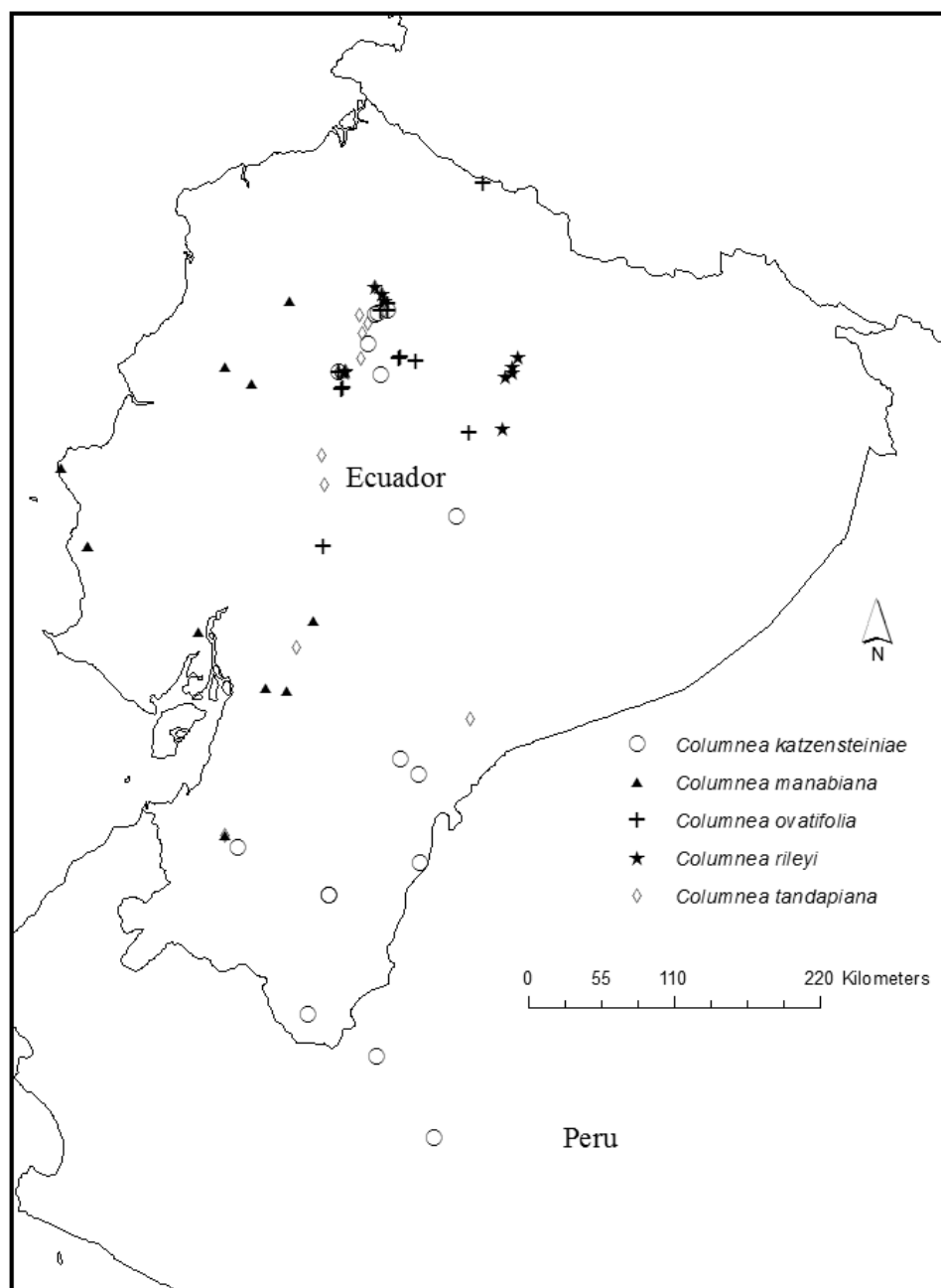


Figure 2.8 – Distribution of *Columnea antiocana*, *C. crassicaulis*, and *C. orientandina*.



**Figure 2.9 – Distribution of *Columnnea byrsina*, *C. colombiana*, and *C. suffruticosa*.**



**Figure 2.10 – Distribution of *Columnnea katzensteiniae*, *C. manabiana*, *C. rileyi*, *C. ovatifolia*, and *C. tandapiana*.**

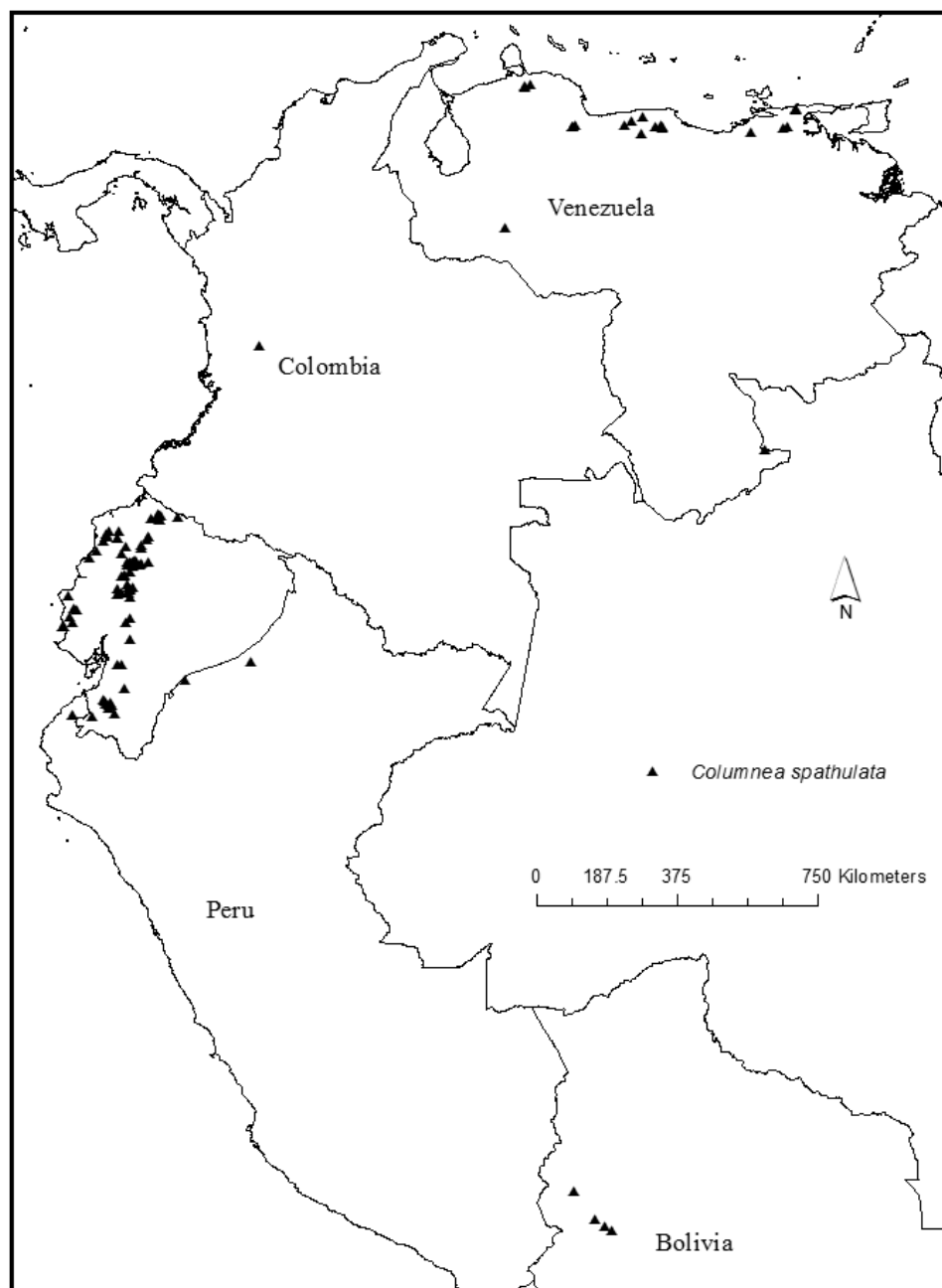


Figure 2.11 – Distribution of *Columnea spathulata*.

CHAPTER THREE: DRIVING FORCES OF SPECIATION WITHIN SECTION  
*ANGUSTIFLORAE*: MORPHOLOGICAL AND CLIMATE VARIABLES

**Abstract**

Speciation studies have previously been intractable because of the extensive amount of resources they required. Yet identifying the forces that drive evolutionary divergence is important to gain a full understanding of species. Studying the patterns of evolutionary and ecological parameters approaches speciation from a new angle. Molecular phylogenetic analyses both identify evolutionary patterns and provide an independent phylogeny on which ecological parameters can be mapped. Using these evolutionary and ecological patterns, correlation analyses identify relationships between parameters, such as morphological characters and climatic variables. Highlighting morphological and climatic character state shifts at the same node in the phylogenetic tree provides insight into possible forces driving speciation, such as a niche shift or pollinator shift. In the tropical plant family Gesneriaceae, there is both morphological and climatic variation among closely related species. This study used section *Angustiflorae* in *Columnnea* (Gesneriaceae subfamily Gesnerioideae) to analyze fourteen morphological characters, phenology, and nineteen climate variables and determined possible forces that drove speciation within the section. In section *Angustiflorae*, correlations were identified between leaf size and precipitation, corolla color and temperature, and phenology with both temperature and precipitation variables. There were also character state shifts that suggest evolutionary divergence resulted from

allopatric speciation, photosynthetic shifts, nectar robbing, pollinator shifts, and niche shifts in both precipitation and temperature.

### **Introduction**

It has been over 150 years since Darwin published *On the Origin of Species* (1859) explaining that Earth's biodiversity is a product of natural selection, yet understanding which forces drive evolutionary divergence still present challenges today. Determining the specific factors that played a role in speciation previously took extensive resources that made such studies nearly intractable. Despite the difficulties presented by speciation studies, we are still interested in determining what forces drive the process of evolution to gain a better understanding of divergence among the species. Advances in technology allow for a new approach that determines the driving forces of speciation by identifying patterns among phylogenetic studies, morphological characters, and ecological variables. Correlations between the various parameters shed light on possible forces that drive divergence by identifying relationships between morphological and climatic character state shifts (Harvey and Pagel 1991; Hardy and Linder 2005; Bollback 2006; Struwe et al. 2011). Once specific factors have been identified, field studies of extant species can test specific factors driving speciation.

Species distributions are a first factor to determine potential gene flow and, more importantly, whether gene flow has been disrupted, causing genetic and evolutionary divergence. Extant species distributions are used to identify sister species pairs as allopatric, parapatric, or sympatric and to better understand potential gene flow between species. Allopatric speciation occurs via vicariance or dispersal, when ancestral populations are geographically divided into two isolated subpopulations, resulting in

reduced gene flow. There may be no genetic divergence between the two subpopulations; however, they are subject to separate evolutionary forces including mutation, selection, and genetic drift, increasing the likelihood of genetic divergence between the subpopulations (Wiley and Lieberman 2011). Allopatric speciation is the most widely recognized means by which speciation occurs in sexually reproducing animals (Bush 1975). Both parapatric and sympatric speciation have been more controversial as a means of speciation (Slabbekoorn and Smith 2002; Barluenga et al. 2006). Parapatric speciation occurs when a small portion of the ancestral population becomes separated on the outer edge of the ancestor's range again resulting in two subpopulations that are subject to separate evolutionary forces. The subpopulations are immediately adjacent to one another but not physically separated, though there may be a niche shift and, as a result, disruption in gene flow between the subpopulations (Wiley and Lieberman 2011). This can lead to speciation due to disruptive selection (Slabbekoorn and Smith 2002), selection against hybrids between subpopulations (Wiley and Lieberman 2011), or karyotype rearrangement (Bush 1975). Sympatric speciation occurs with no clear barrier to gene flow and may result in a niche shift as the result of polyploidy (Bush 1975; Wiley and Lieberman 2011) or disruptive selection possibly due to divergence among pollination syndromes (Levin and Kerster 1967).

Once species distributions have been plotted, the patterns of divergence and important evolutionary and ecological forces must be identified. Evolutionary patterns are identified using molecular phylogenetics to construct a well-resolved species level phylogeny of the study taxa (Harvey and Pagel 1991). Molecular characters provide an independent source of data to identify patterns by mapping parameters, such as

morphological characters or climatic variables, onto the species level phylogenetic tree (Felsenstein 1985; Harvey and Pagel 1991; Hardy and Linder 2005). Correlation analyses between the chosen parameters elucidate possible forces that drove speciation by highlighting character state shifts that co-occurred in the phylogenetic tree (Bollback 2006).

Tropical forests provide numerous opportunities to study the forces driving speciation (Martén-Rodríguez et al. 2010; Viljanen et al. 2010; Tolley et al. 2011). Over half the world's plant and animal species are found in tropical forests, which cover only a small portion of the Earth's surface, resulting in a high concentration of biodiversity (Wills et al. 2006; Mittelbach et al. 2007). The tropical Andes, western Ecuador, Mesoamerica, and the Caribbean are among the world's top biodiversity hotspots with approximately 90,000 plant species and 9,000 vertebrate species (Myers et al. 2000). Although tropical forests have less striking seasonal temperature variation compared to temperate regions, the climate varies depending upon latitude, elevation, and physiogeographic features, creating a broad array of both biotic and abiotic factors that may contribute to speciation (Struwe et al. 2011).

Gesneriaceae is a tropical plant family whose evolutionary history offers insight into the speciation process (Perret et al. 2007; Martén-Rodríguez et al. 2010; Woo et al. 2011). Although pantropically distributed, Gesneriaceae is divided into two subfamilies, the almost exclusively Paleotropical *Crytandroideae* and nearly exclusively Neotropical *Gesnerioideae* (Weber 2004). The species of *Gesnerioideae* are distributed throughout the Neotropics in many of the top biodiversity hotspots (Myers et al. 2000), making them ideal candidates for speciation studies. Using species from the Antilles in the tribe

Gesnerieae (Gesneriaceae subfamily Gesnerioideae), Martén-Rodríguez et al. (2010) studied correlations between pollination systems (hummingbird, bat, generalist, bee) and other floral characteristics (corolla shape, timing of anther dehiscence and nectar production, quantity of nectar production, corolla color, and dichogamy state). They found that there were correlations between the pollinator systems and the other floral characters, suggesting that speciation within the tribe Gesnerieae is a result of pollinator mediated selection (Martén-Rodríguez et al. 2010).

The study of Martén-Rodríguez et al. (2010) demonstrated the utility of Gesneriaceae as a model to study forces driving speciation; however, their study only sampled allopatric species from the Antilles. To expand our understanding of speciation within Gesneriaceae subfamily Gesnerioideae, it is important to sample species with parapatric and sympatric distributions across continental South America. Within Gesnerioideae, *Columnea* L. is the largest genus and has a similar Neotropical distribution to other genera within Gesneriaceae subfamily Gesnerioideae. The 200 plus species of *Columnea* are distributed in the Caribbean and throughout the Andes, from Mexico to Bolivia and eastward into northern Brazil (Smith 1994).

Recent phylogenetic analyses have recovered seven monophyletic clades within *Columnea* (Chapter One; Smith et al. in review) including section *Angustiflorae* L. J. Schulte and J. F. Smith (Chapter One). Section *Angustiflorae* has been recovered as a monophyletic group in molecular phylogenetic analyses, and a species level phylogeny has been determined (Chapter Two). Species of *Angustiflorae* are characterized by small tubular corollas that are radially to subradially symmetric, narrow calyx lobes loosely clasping the corolla, and sparse pubescence on the corolla (Chapter Two). The species

also have variable morphological characteristics with opposite leaves that range from isophyllous to strongly anisophyllous, with a dorsiventral arrangement in *Columnea byrsina* and *C. orientandina*; leaf coloration that is dull green to yellow-green or dark green, sometimes purple, suffused with pink, or with violet spots; and corollas ranging from cream to lemon-yellow, orange, red or violet, that have darker colored lobe spots in *C. ovatifolia*, *C. crassicaulis*, *C. rileyi*, *C. katzensteiniae*, *C. antiocana*, and *C. suffruticosa*. The species of section *Angustiflorae* cover nearly the full geographic and climatic range of *Columnea*, ranging from sea level to 4000 meters in elevation. The species range from narrow endemics, such as *C. ambigua* and *C. domingensis* (Chapter Two: Figure 2.7) on Caribbean islands, and *C. tandapiana*, *C. manabiana*, *C. ovatifolia*, *C. rileyi*, and *C. katzensteiniae* (Chapter Two: Figure 2.10) that are all found in various parts of Ecuador, to species that are widespread, such as *C. angustata* (Chapter Two: Figure 2.7), ranging from Costa Rica to Ecuador and into Brazil, and *C. spathulata* (Chapter Two: Figure 2.11), which is distributed along the Andes from Venezuela to Bolivia. A wide range of morphological variation and distributions covering nearly the full geographic and climatic range of species in *Columnea* makes section *Angustiflorae* an interesting group for speciation studies. I mapped fourteen morphological characters, phenology, and nineteen climatic variables on the species-level phylogeny (Chapter Two) to identify morphological and ecological patterns. I then conducted correlation analyses among the morphological (including phenology) and climatic parameters and identified possible forces that drove speciation within section *Angustiflorae*.

## Materials and Methods

### Phylogenetic Analyses

Previous molecular phylogenetic analyses produced a species-level phylogeny for thirteen of the fifteen species within section *Angustiflorae* (Chapter Two). The phylogenetic analyses used five chloroplast DNA (cpDNA) gene regions (*rpl32-trnLUAG* spacer, *rps16-trnQ* spacer, *rps16* intron, *trnS-G* spacer, and *trnH-psbA* spacer), two nuclear transcribed spacers (ITS1 and ITS2), external transcribed spacer (ETS), and two low-copy nuclear gene region loci (*G3pdhA* and *idhB*) to identify species level relationships within section *Angustiflorae* (Chapter Two). Branch lengths were determined using the topology of the Bayesian inference (BI) partition model analysis of the reduced data set (Chapter Two) in PAUP\* v4.0 b10 (Swofford 2002) using parsimony criterion based on the number of character state changes and are included in Figure 3.1. Because I am concerned with past speciation rather than speciation of extant species, species with multiple accessions (Chapter Two: Figure 2.6) were collapsed into a single representative. In previous analyses, thirteen of the fifteen species in section *Angustiflorae* were included in molecular phylogenetic analyses because DNA material was unavailable for two species (Chapter Two). I used this topology because it was the most strongly supported in maximum parsimony (MP), maximum likelihood (ML), and BI analyses, and is the most current species level phylogeny within genus *Columnnea* based solely on molecular data (Chapter Two).

## Species Distributions

A total of 493 herbarium collection records of the thirteen species of *Angustiflorae* were included in the analyses (Appendix C). All species were represented by more than one specimen ranging from three specimens of *C. colombiana* to 155 specimens of *C. angustata*. Each herbarium collection locality was georeferenced using Google Earth. Only specimens with recorded locations known to the nearest minute were included in analyses. Latitude and longitude coordinates for each specimen can be found in Appendix C. Once all herbarium collections were georeferenced, they were converted from latitude and longitude coordinates to decimal degrees. Coordinates were then converted to a point shapefile in ArcMap version 10.0 (ESRI, Redlands, CA, USA), and distribution maps of each species were produced (Chapter Two: Figures 2.7-2.11).

To determine if species were allopatric, parapatric, or sympatric, only geographic distributions and climate ranges of sister species pairs were compared because ancestor species distributions are not known based on a combination of extant data. If sister species did not overlap at all in their geographic distribution, they were classified as allopatric sister species. If sister species pairs had overlapping geographic distributions, then climatic variables were compared. Using the output from SEEVA version 1.00 (Heiberg 2012; see “Materials and Methods: Climate Variables”) sister species pairs that had at least one significant difference in a bioclim variable were determined to be parapatric sister species. Sympatric sister species were those that had overlapping geographic distributions and no significant differences in bioclim variables.

## Morphological Characters

Fourteen morphological characters and phenology were examined to determine their importance in the process of speciation. These characters were chosen for further analyses because they are floral and vegetative characters that vary among the species of section *Angustiflorae*. All fourteen morphological characters and phenology were scored based on a recent monograph of the species in section *Angustiflorae* (Smith 1994) with the exception of *C. domingensis* (Chapter Two). Habit, leaf isophylly, adaxial pubescence of leaves, abaxial pubescence of leaves, abaxial coloration of leaves, calyx margin, corolla color, and corolla lobe color were all scored based on the variation of each variable present within individual species (Smith 1994; Chapter Two). Petiole length, number of flowers per inflorescence, floral bract length, and corolla length were scored based on the maximum value of variation observed within individual species (Smith 1994; Chapter Two). Lamina surface area was determined using the observed maximum value of the larger lamina (in anisophyllous species; Smith 1994; Chapter Two) and calculated by multiplying the length by the width at the widest point for each species. The corolla to calyx ratio was determined using the maximum observed values for the corolla and calyx lengths (Smith 1994; Chapter Two) and calculated by dividing the corolla length by the calyx length. Phenology of flowering was determined by looking at collection dates for all herbarium collection specimens for each species (Appendix C) that had not previously been determined by Smith (1994) and scored as continuous if there were collections from every month of the year or within a limited range if there were not collections year round for a species.

Character state categories were determined by plotting raw values for each morphological character for all thirteen species and dividing categories based on clear divisions within the data. The morphological characters were habit, scored as upright (stems growing from 45° to perpendicular with the ground), horizontal (stems growing from 45° to parallel to the ground), or pendent (stems growing downward); leaf isophylly, scored as anisophyllous (opposite leaves of different sizes) or isophyllous (opposite leaves of approximately the same size); lamina surface area, scored as  $< 30 \text{ cm}^2$  (smaller leaf surface area) or  $> 30 \text{ cm}^2$  (larger leaf surface area); adaxial pubescence, scored as few to no trichomes or dense trichomes; abaxial pubescence, scored as few to no trichomes or dense trichomes; abaxial coloration, scored as green, green with purple apices, entirely purple, or variable (multiple coloration patterns seen); petiole length, scored as 0.0-5.0 mm (small petiole), 5.0-20.0 mm (medium petiole), or  $> 20.0 \text{ mm}$  (large petiole); number of flowers per inflorescence, scored as one flower per axil or more than one flower per axil; floral bract size, scored as 0.0-6.0 mm (small floral bract), 6.0-13.0 mm (medium floral bract), or  $> 13.0 \text{ mm}$  (large floral bract); corolla to calyx ratio, scored as  $< 2.5$  (small corolla to calyx ratio) or  $> 2.5$  (large corolla to calyx ratio); calyx margin, scored as entire or serrate; corolla length, scored as 10.0-40.0 mm or greater than 40.0 mm; corolla color, scored as yellow, red, purple, or variable (multiple corolla colors seen); corolla lobe color, scored as the same as the corolla color or different than the corolla color; and phenology, scored as flowering continuously (herbarium collection specimens collected year round), flowering from January to March (herbarium collection specimens collected only from January to March), or flowering from March to October

(herbarium collection specimens collected only from March to October). A complete list of scores for each species can be found in Table 3.1.

Ancestral state reconstructions for each of the fourteen morphological characters and phenology were conducted with a single topology for species relationships using a ML approach in Mesquite version 2.75 (Maddison and Maddison 2011) and Bayesian stochastic character mapping (Huelsenbeck et al. 2003) in Simmap version 1.5 (Bollback 2006). In Mesquite v. 2.75, ML ancestral state reconstructions used the Mk1 model (Lewis 2001) with all character state changes equally probable. Ancestral state reconstructions were given as ML probabilities (MLP). Simmap 1.5 used Bayesian stochastic character mapping to perform the ancestral state reconstructions. The bias parameter was set to the empirical prior, and the rate parameter was set to the branch length prior with the character state changes unordered for all fourteen morphological characters and phenology. The Bayesian stochastic character mapping analyses conducted by Simmap 1.5 will hereafter be referred to as the branch length model (BL model). Ancestral character state reconstructions using the BL model in Simmap 1.5 were given as Bayesian posterior probabilities (BPP). Both Mesquite v. 2.75 and Simmap 1.5 were used for ancestral state reconstructions of the fourteen morphological characters and phenology to determine if the model had an effect on interpreting ancestral character states.

### Climate Variables

Climate data for each georeferenced herbarium collection (Appendix C) were extracted using the nineteen available bioclim layers (Hijmans et al. 2005) at 30s Arc (~1

km) accuracy. Bioclimatic variables were derived from the monthly temperature and rainfall values (Hijmans et al. 2005). Eleven variables were related to the temperature and reported in degrees Celsius, with the exception of isothermality and temperature seasonality. Isothermality was calculated by dividing the mean diurnal range (mean monthly maximum temperature – mean monthly minimum temperature) by the temperature annual range then multiplying by 100, resulting in a possible range from 0-100. A higher value for isothermality indicates that the temperature does not vary throughout the year, and a lower value indicates that the temperature has more variation throughout the year. Temperature seasonality was calculated by multiplying the standard deviation by 100. The remaining seven variables were related to the amount of precipitation and reported in millimeters of rainfall with the exception of precipitation seasonality. Precipitation seasonality was the coefficient of variation. A quarter (for temperature and precipitation variables) was considered a period of three months (Hijmans et al. 2005). The number of individuals in each of the four SEEVA v. 1.00 categories for all species is in Appendix D. ArcMap v.10.0 was used to combine each of the bioclim layers with a 500 m buffer zone around all data points, and climate information was collected for all herbarium collection records (Appendix C).

Extracted environmental data were analyzed in SEEVA v. 1.00. The topology of the species level molecular phylogeny was used to map environmental data. SEEVA v. 1.00 divided each of the nineteen bioclim qualitative variables into four arbitrary categories, spanning the variation of each variable (Table 3.1; Heiberg and Struwe 2012). At each node below the species level, significance of SEEVA v. 1.00 analyses was determined by comparing the two sister clades at the node. To obtain environmental data

for each sister clade, extracted environmental data from species within the clade were pooled together. All variables were analyzed independently according to Heiberg and Struwe (2012). For each of the nineteen bioclim variables,  $P$ -values were calculated at each node using a chi-squared test and Fisher's exact test ( $H_0$ : data distribution at the node is not different between the two sister clades). The Fisher's exact test results were used for all analyses because they provide a more accurate  $P$ -value when analyzing smaller sample sizes (e.g. *C. colombiana* specimens = 3; Appendix C). A Bonferroni correction was used to account for multiple comparisons for each climatic variable based on the number of nodes in the phylogenetic tree ( $n = 12$ ), and significance was established at  $P < 0.00417$  for all SEEVA v. 1.00 analyses. SEEVA v. 1.00 also calculated the divergence index ( $D_i$ ) at all nodes for each climate variable independently (Heiberg and Struwe 2012). The  $D_i$  value ranges from 0.0 (no difference between sister clades) to 1.0 (maximum possible difference between sister clades). Significant  $D_i$  values were determined as  $D_i > 0.75$  according to Struwe et al. (2011).

Ancestral state reconstructions of the nineteen bioclim variables were conducted using Bayesian stochastic character mapping in Simmap 1.5. Simmap 1.5 cannot use multiple data points for each species (493 herbarium collections); environmental data extracted from ArcMap v. 10.0 for SEEVA v. 1.00 analyses were converted to scores prior to Simmap 1.5 analyses because each of the thirteen species were represented by more than one specimen (Appendix C). SEEVA v. 1.00 divided each of the nineteen qualitative bioclim variables into four arbitrary categories spanning the range of the variation within each variable and classified specimens into one of the four categories (Heiberg and Struwe 2012). Because potentially important speciation data would be lost

by averaging climate variables or using only the maximum or minimum range for each species, the entire range for each species was taken into account when they were scored. Data were combined for individual species to determine the range of variation for each of the nineteen bioclim variables separately. Species that fell within one of the four categories determined by SEEVA v. 1.00 were scored as being only in that range (e.g. category A = character state 0). Species that fell within two sequential categories (category A and B; category B and C; category C and D) were scored separately for each of the three possible combinations (e.g. category A and B = character state 1; category B and C = character state 2). Species that fell within two of the four categories that were not sequential (e.g. category A and C) were assumed to occupy the entire climatic range (e.g. categories A, B, and C) but were lacking collections representing the entire variation within the species. The specimens occupying two non-sequential categories were scored as spanning either three or four categories based on which two non-sequential categories they fell into (e.g. categories A and C = A, B, and C; categories A and D = A, B, C, and D). Species that had variation within any three of the four categories or all four categories were scored as polymorphic (e.g. categories A, B, and C = character state 4; categories A, B, C, and D = character state 4). If there was at least one species that fell into only one category (e.g. species X = category A) and at least one species that fell into two categories (e.g. species Y = categories A and B), species were scored as separate character states even though they are overlapping in the tolerance at the lower end of the climatic variable's range. By scoring species X and Y in separate categories, the upper tolerance of the climatic variable is represented, which may have been important in speciation. This was also done for species that had overlapping climatic variables at the

upper end of a climatic variable's range but differences in tolerance at the lower end of the climatic variable's range (e.g. species X = category D; species Y = categories C and D). When all nineteen bioclim variables had been scored for Simmap 1.5 analyses, two variables, annual precipitation and precipitation of the wettest month, had no variation among species (Table 3.1). Because there was no variation, I did not include these two variables in any further analyses. A complete list of character states and scores for each species is in Table 3.1.

Bayesian stochastic character mapping was performed to reconstruct ancestral character states for the remaining seventeen climate variables. Analyses were conducted with the bias parameter set to the empirical prior and the rate parameter set to the branch length prior with the character state changes unordered for all seventeen characters.

Though re-scoring extracted climate data is not ideal for comparing results from SEEVA v. 1.00 analyses to Simmap 1.5 analyses, I could not determine a better approach to score climate variables while maintaining the range of variability within each species. SEEVA v. 1.00 analyses pool the climate data at each node below the species level, which may not be a reflection of the ancestral history. To avoid this error, I conducted Simmap 1.5 analyses that used a model to account for the probability of each character state over the ancestral history. However, the re-scored bioclim variables may be a poor reflection of the actual variability within each species, potentially losing important climate boundaries.

### Correlation Analyses

Correlated character evolution was evaluated with Bayesian stochastic character mapping in Simmap 1.5, which estimates the associations among character states over the phylogenetic tree. The probability of each character state is proportional to the amount of time the character was in the given state over the history of the phylogenetic tree.

Expected character associations were calculated by multiplying the frequency of individual character states for each combination of two character states (Huelsenbeck et al. 2003; Bollback 2006). This method allows for detection of associations if character states co-occur, even if evolutionary transitions are rare.

Correlation analyses were conducted with the bias parameter set to the empirical prior and the rate parameter set to the branch length prior with all character state changes unordered. The analyses were conducted with thirty-two characters included (fourteen morphological, phenology, and seventeen climatic variables), the number of samples was set to 2000, the number of prior draws was set to 1, and the number of predictive samples was set to 1000. Values were chosen to generate an observed sample size  $\geq 2000$  and a predictive sample size  $\geq 1000$  (Meredith et al. 2011).

Correlation analyses generate two separate test statistics,  $D_c$  and  $M_c$  that are calculated for the state-by-state associations between two characters. The  $D_c$  statistic measures the overall association between individual states of each character. The  $M_c$  statistic measures the overall association along the phylogeny between states of each character. Simmap 1.5 reported significant results at  $P \leq 0.05$ ; however, due to the high number of relationships tested,  $P$ -values were corrected using the false discovery rate test (FDR; Benjamini and Hochberg 1995) in SAS software version 9.2 (SAS Institute, Cary,

NC, USA). Prior to performing the FDR test, morphological characters that were unchanging in the ancestral state reconstructions (see “Results: Morphological Characters”), polymorphic climate variable character states (Table 3.1), and correlations between two morphological characters (including phenology; e.g. habit to leaf isophylly), or two climatic characters (annual mean temperature to mean diurnal range) were removed from correlation analyses. Polymorphic bioclim characters were excluded because ancestral character state shifts to or from a polymorphic character state are not informative. Correlations between two morphological characters or two climatic characters were not included because I am only interested in relationships between morphological characters and climatic characters. The FDR test was run for the  $D_c$  and  $M_c$  statistic  $P$ -values separately, because the two statistics represented separate tests in Simmap 1.5. The FDR test minimized the number of false positives given the total number of positive tests and reported an adjusted  $P$ -value. The adjusted  $P$ -values from the FDR test were reported as significant at  $P \leq 0.05$ .

Once correlations were determined using Simmap 1.5 correlation analyses and the  $P$ -values were adjusted, ancestral state reconstructions of morphological characters were compared to output from SEEVA v. 1.00 analyses to determine when character states had co-occurred on the phylogenetic tree. For morphological characters, nodes below extant taxa were scored as a character state if the BPP of the ancestral state reconstructions from Simmap 1.5 analyses was  $> 50$ . Only Simmap 1.5 ancestral state reconstructions were used for Simmap 1.5 correlation analyses. For seventeen bioclim variables, species and nodes were scored based on extracted environmental data as categorized by SEEVA v. 1.00. If a species or node had more than half of the herbarium specimens in the category

(or categories) that corresponded to the character state, the species or node was scored as that character state. Character states of morphological characters (including phenology) and bioclim characters were compared to extant species and all nodes to determine when correlated character states co-occurred on the phylogenetic tree.

## Results

### Species Distributions

When using distributions to determine if species were allopatric, parapatric, or sympatric, only sister species pairs were considered. Within section *Angustiflorae* there were five sister species pairs (Chapter Two, Figure 2.6). *Columnea ambigua* and *C. domingensis* are the first sister species pair. Both species are endemic to Caribbean islands, *C. ambigua* to Puerto Rico and *C. domingensis* to Hispaniola. Because the two species do not overlap in their distribution, they were considered allopatric species (Chapter Two: Figure 2.7).

The four other sister species pairs had overlapping geographic distributions (Chapter Two: Figures 2.7-2.10). The results from the SEEVA v. 1.00 analyses for each species in a pair were then compared to determine if sister species pairs were parapatric or sympatric. *Columnea byrsina*/*C. orientandina* and *C. manabiana*/*C. tandapiana* did not have the same climatic range for all nineteen bioclim variables. *Columnea byrsina* and *C. orientandina* had significant differences in eleven climatic variables (annual mean temperature; isothermality; temperature seasonality; maximum temperature of the warmest month; minimum temperature of the coldest month; mean temperatures of the wettest, driest, warmest, and coldest quarters; precipitation of the driest month; and

precipitation seasonality) with a significant  $D_i$  value for temperature seasonality. *Columnnea manabiana* and *C. tandapiana* also had significant differences in eleven climatic variables (annual mean temperature; temperature seasonality; maximum temperature of the warmest month; minimum temperature of the coldest month; mean temperatures of the wettest, driest, warmest, and coldest quarters; precipitation seasonality; and precipitation of the driest and coldest quarters) with significant  $D_i$  values for nine variables (annual mean temperature; temperature seasonality; maximum temperature of the warmest month; minimum temperature of the coldest month; mean temperatures of the wettest, driest, warmest, and coldest quarters; and precipitation of the coldest quarter). Because both sister species pairs had significant differences in climatic variables, they were classified as parapatric sister species pairs. The remaining two sister species pairs, *C. angustata/C. colombiana* and *C. katzensteiniae/C. rileyi*, had overlapping geographic distributions and no significant shifts in the nineteen bioclim variables and were thus classified as sympatric sister species pairs.

### Morphological Characters

Ancestral character state reconstructions of the fourteen morphological characters and phenology resulted in five morphological characters that were autapomorphic in both Mesquite v. 2.75 and Simmap 1.5 analyses (adaxial pubescence, abaxial pubescence, abaxial coloration, number of flowers per inflorescence, and corolla length). Thus these five characters were removed from further analyses (trees not shown). These five morphological characters' ancestral state reconstructions can be found in Table 3.2 with MLP and BPP values for each node for all characters in Appendix E.

The Mesquite v. 2.75 and Simmap 1.5 analyses resulted in similar ancestral state reconstructions for the nine remaining morphological characters (habit, leaf isophylly, lamina surface area, petiole length, floral bract size, corolla to calyx ratio, calyx margin, corolla color, and corolla lobe color) and phenology. The results from the ancestral state reconstructions of nine morphological characters and phenology were mapped onto the phylogenetic tree using both the Mk1 model and BL model in Figures 3.1-3.10. Maximum likelihood probabilities and BPP for each node for all variables are in Appendix E. Ancestral state reconstructions had MLP and BPP within 0.01 probability of each other for habit (Figure 3.1; Appendix E) and within 0.03 probability for phenology (Figure 3.10; Appendix E), with one exception in the ancestral state reconstruction of phenology at node 12 (Figure 3.10; Appendix E). The ancestral state reconstructions of the other eight morphological characters had differences between MLP and BPP ranging from 0.01 to 0.74 (Figures 3.2-3.9; Appendix 3).

### Climate Variables

Results from SEEVA v. 1.00 analyses for  $P$ -values and  $D_i$  values at all nodes for each climate variable are presented in Table 3.3. All nodes except nodes 6 and 10 (Figures 3.11-3.14) had at least one climate variable with a significant  $P$ -value (Table 3.3). Only nodes 1, 2, 7, and 12 (Figures 3.11-3.14) had climate variables with significant  $D_i$  values (Table 3.3).

Ancestral state reconstructions of the seventeen bioclim variables resulted in ten variables that were unchanging throughout the ancestral history and thus, are not presented for these ten climatic variables (Table 3.2; mean diurnal range; isothermality;

maximum temperature of the warmest month; minimum temperature of the coldest month; temperature annual range; precipitation of the driest month; precipitation seasonality; and precipitation of the wettest, driest, and warmest quarters). The ancestral state reconstructions for the remaining seven bioclim variables are presented in Figures 3.11-3.14 with BPP values in Appendix F. Ancestral state reconstructions for the precipitation of the wettest, driest, warmest, and coldest quarters resulted in the exact same BPP (Appendix F) even though each of the character states represented different values and are therefore presented in a single figure (Figure 3.13). All shifts in the ancestral state reconstructions of the seven bioclim variables (Figures 3.11-3.14) were from a polymorphic character state and therefore do not provide valuable information for correlation analyses.

### Correlations

Simmap 1.5 analyzed 5,597 correlations each for the  $D_c$  and  $M_c$  statistic. The FDR test using SAS software v. 9.2 compared 1,204 correlations each for the  $D_c$  and  $M_c$  statistic after removing five morphological characters (Table 3.2), polymorphic character states for bioclim variables (Table 3.1), and correlations between two morphological characters (including phenology; e.g. habit to leaf isophylly) or two bioclim characters (e.g. annual mean temperature to mean diurnal range). Correlations with an adjusted  $P < 0.10$  from the FDR test are presented in Table 3.4. Of these 1,204 correlations, six  $D_c$  statistic correlations and seven  $M_c$  statistic correlations were statistically significant (adjusted  $P$ -value  $< 0.05$ ; Table 3.4). Because the six significant  $D_c$  statistic correlations were the same as six of the seven significant  $M_c$  statistics, only significant  $M_c$  statistics

are further discussed. Significant correlations of morphological characters to climatic variables were as follows: a pendent habit was correlated to a mean diurnal range  $> 9.7$  °C; a smaller lamina surface area was correlated with precipitation of the driest quarter  $< 198.43$  mm; a larger lamina surface area was correlated with precipitation of the driest quarter  $< 198.43$  mm; a yellow corolla color was correlated with temperature of the coldest quarter  $< 18.133$  °C; flowering continuously was correlated with temperature annual range  $> 11.45$  °C; flowering continuously was correlated with precipitation of the driest month  $< 53$  mm; and flowering from March to October was correlated with precipitation of the driest quarter  $< 198.43$  mm (Table 3.4).

### Discussion

The species within family Gesneriaceae have a widespread tropical distribution and morphological variation that make speciation studies both interesting and possible. With over 200 species, *Columnea* represents nearly the full geographic range found within Gesneriaceae subfamily Gesnerioideae. Distributed throughout the Caribbean, Central America, and northern South America, from sea-level to 4,000 meters in elevation, the species have a wide array of ecological niches. The species of *Columnea* are morphologically united by tubular corollas that are gibbous at the base with superior ovaries and berry fruits but have an array of variation and divergence in vegetative, nectary, and floral characteristics including corolla shape, size, and corolla color pattern (Kvist and Skog 1993; Smith 1994; Smith and Sytsma 1994). *Columnea* had previously been classified based solely on morphological characters, most predominantly floral form (Fritsch 1894); however, molecular phylogenetic analyses have deconstructed these previous classification systems (Chapter One). Species level phylogenetic analyses allow

for specific questions on the forces that drive speciation to be addressed by determining correlations between various parameters (Harvey and Pagel 1991; Hardy and Linder 2005).

#### Distribution and Speciation of Sister Species Pairs

Allopatric speciation is one of the most widely recognized means through which speciation occurs (Bush 1975), but within *Angustiflorae* it seems to have less of an effect on speciation. Within the section there is one allopatric, two parapatric, and two sympatric sister species pairs. *Columnnea ambigua* and *C. domingensis* are on separate Caribbean islands from one another, suggesting that geographic isolation caused speciation. However, geographic isolation may have only increased the potential for divergence via other evolutionary processes, including selection, mutation, or genetic drift.

Speciation within section *Angustiflorae* seems to have occurred in parapatric or sympatric sister species pairs, rather than allopatric speciation. The frequency of parapatric and sympatric speciation occurring has often been questioned because of the lack of empirical evidence (Barluenga et al. 2006) compared to evidence of allopatric speciation (Bush 1975). Sister species pairs in *Angustiflorae* provide evidence of both parapatric and sympatric speciation. Because species are not geographically isolated from one another in either case, a disruption in gene flow must be due to other factors such as climatic variables or disruptive selection. Within *Angustiflorae* the latter seems to be having a large effect on speciation due to pollinator selection (see “Forces Driving Speciation”).

### Ancestral State Reconstructions of Climate using SEEVA and Simmap

Both SEEVA v. 1.00 and Simmap 1.5 were used to reconstruct ancestral character states of climatic variables because the two analyses each have limitations. SEEVA v. 1.00 gathers environmental data from multiple individuals of each species and uses the data to statistically analyze differences between sister clades (Heiberg and Struwe 2012). This approach analyzes ecological differences between both sympatric and allopatric species, which is unique to the program. One caveat of SEEVA v. 1.00 is that it does not account for the probability of each character state below extant nodes on the phylogenetic tree. At each node below the species level, significance was determined by comparing the two sister clades at the node. To obtain environmental data for each sister clade, extracted environmental data from species within the clade were pooled together. This approach may not reflect the actual ancestral history of individual climate variables. Movement into a new ecological niche may have been important in the speciation process but lost in SEEVA v. 1.00 analyses due to pooling of environmental data.

Simmap 1.5 analyses account for the probability of character states at each node on the phylogenetic tree throughout the ancestral history using stochastic character mapping. However, Simmap 1.5 does not allow an individual species to be coded for more than one character state or to use continuously variable characters. When the extracted environmental data was divided into categories by SEEVA v. 1.00, many species fell into more than one category because environmental data was extracted for multiple specimens of each species. The four categories created by SEEVA v. 1.00 then had to be converted into categorical data for Simmap 1.5 analyses. Converting categorical data from SEEVA v. 1.00 into single character states for Simmap 1.5 proved

difficult because of the inability of Simmap 1.5 to analyze multiple character states for each species. Instead of coding a species as truly polymorphic for multiple categories for each climatic variable (e.g. categories A and B = character states 1 and 2), additional character states had to be created for Simmap 1.5 (e. g. categories A and B = character state 4) analyses. These additional character states were treated as unique states and are not a real reflection of shared character state history. This polymorphic state referred to species that had specimens in all four SEEVA v. 1.00 categories; however, this masks any major climatic shifts in the ancestral history, because a switch from a polymorphic character state to a more specific character state may not always indicate a real shift.

Both SEEVA v. 1.00 and Simmap 1.5 have benefits and drawbacks for reconstructing ancestral character states and analyzing character state shifts in the phylogenetic history. In the analyses presented here, Simmap 1.5 did not identify the same ancestral character state shifts as SEEVA v. 1.00. The loss of information in the Simmap 1.5 analyses was most likely due to characters scored as polymorphic. Two climatic variables (annual precipitation and precipitation of the wettest month) were not analyzed at all because all species were scored as polymorphic. Ten of the climatic variables (Table 3.2; mean diurnal range; isothermality; maximum temperature of the warmest month; minimum temperature of the coldest month; temperature annual range; precipitation of the driest month; precipitation seasonality; and precipitation of the wettest, driest, and warmest quarters) had no ancestral character state shifts because almost all species were scored as polymorphic. The remaining seven climatic variables (Figures 3.11-3.14; annual mean temperature; temperature seasonality; mean temperatures of the wettest, driest, warmest, and coldest quarters; and precipitation of the

coldest quarter) only had character states shifts from a polymorphic character state to a more specific character state, which does not give any information about ancestral trends. Therefore, only shifts in climate variables identified by SEEVA v. 1.00 analyses were considered significant character state shifts.

## Correlation Analyses

### Eliminated Correlations

Mapping morphological and climatic character states over the molecular phylogenetic history of *Angustiflorae* elucidated shifts in ecological factors. Correlation analyses comparing morphological characters and phenology to climatic variables showed where significant shifts had co-occurred. By studying these correlations, we gain a better understanding of forces that drove speciation within section *Angustiflorae*. Simmap 1.5 correlation analyses resulted in six statistically significant  $D_c$  correlations that were encompassed by the seven statistically significant  $M_c$  correlations between a morphological character or phenology and a climatic variable (Table 3.4). However, three of these correlations seemed to be artifacts of the analyses.

When correlations are statistically significant, they should have co-occurred at multiple nodes throughout the phylogenetic tree. Three of the correlations that were statistically significant only co-occurred at one extant species each. A pendent habit was correlated with a mean diurnal range of  $> 9.7$  °C. These two character states only co-occurred at *C. ovatifolia* (Figure 3.3 and Table 3.1). A smaller lamina surface area (Table 3.1: [0] 0.0-30.0 cm<sup>2</sup>) was correlated with a low precipitation for the driest quarter (Table 3.1: [1]  $< 198.43$  mm). These two character states only co-occurred at *C.*

*tandapiana* (Figure 3.3 and Table 3.1). Flowering from March to October (Figure 3.10; Table 3.1 [2]) was correlated with a lower precipitation in the driest quarter (Table 3.1: [1] < 198.43 mm). These two character states only co-occurred at *C. manabiana* (Figure 3.10 and Table 3.1). Because character states of all correlations were rare, the significant correlation between them may have been an artifact of the Simmap 1.5 correlation analyses. It may also be a type II error due to the less conservative FDR test that was used to adjust the *P*-values for Simmap 1.5 correlation analyses. If these three character state correlations were truly significant, all sets of correlated character states would be expected to appear together at other nodes in the phylogenetic tree. Because this does not occur for any of these correlations, I will not consider these three character state correlations as forces driving evolution within section *Angustiflorae* but will focus on the four remaining correlations.

#### Leaf Surface Area and Precipitation

Leaves are essential for performing photosynthesis; thus plants would benefit from leaves with a larger surface area that increases the amount of light absorbed for photosynthesis. However, as with most biological traits, there are tradeoffs that limit the size of leaf surface area including nitrogen content (Roderick et al. 1999), leaf life span (Bonser 2006), and water loss (Givnish 1987). This study did not measure either nitrogen content or leaf life span so their effect on leaf surface area will not be considered further. The amount of water a leaf loses is related to various morphological and climatic factors, such as cuticle thickness (Ristic and Jenks 2002), leaf pubescence (Meinzer and Goldstein 1985), stomatal size, shape, and distribution (Parkhurst and Loucks 1972), and humidity (Givnish 1987) among other characters.

Studies have demonstrated that an increase in the amount of rainfall increases the percentage of species with larger leaves (Parkhurst and Loucks 1972; Dilcher 1973; Dolph and Dilcher 1980; Givnish 1987). The results from the correlation analyses of morphological characters and climatic variables in section *Angustiflorae* showed evidence for the opposite relationship between lamina surface area and precipitation. In section *Angustiflorae*, a larger lamina surface area (Figure 3.3; Table 3.1: [1] > 30.0 cm<sup>2</sup>) was correlated with lower precipitation during the driest quarter (Table 3.1: [1] < 198.43 mm). This study also did not measure other morphological characters that could have contributed to a larger leaf surface area. One or more of these other characters, such as cuticle thickness, leaf pubescence, or stomatal size, shape, and distribution, may have a larger impact on water retention efficiency than the amount of precipitation contributing to a larger lamina surface area within section *Angustiflorae*, which resulted in a counterintuitive correlation between a larger leaf size and lower amount of precipitation.

A larger lamina surface area co-occurred with a lower precipitation during the driest quarter at three nodes on the phylogenetic tree (Figure 2.2; nodes 1, 11, and 12). Because these two character states did not co-occur in any of the extant species, the correlation may have been important for past speciation within section *Angustiflorae*. A larger lamina surface area and lower precipitation during the driest quarter separated the common ancestor of *C. ambigua* and *C. domingensis* from the ancestor of the entire section (Figure 3.3: node 1). It is likely that the ancestor to *C. ambigua* and *C. domingensis* (Figure 3.3: node 1) moved to the Caribbean from the mainland because the majority of *Columnea* species, including the remaining species in *Angustiflorae*, are found on the mainland. It is the most parsimonious option to have a single introduction

into the Caribbean rather than multiple introductions to the mainland from the Caribbean. The presence of a larger lamina surface area with tolerance of less precipitation during the driest quarter may have been important in allowing the common ancestor of *C. ambigua* and *C. domingensis* to move from the mainland to the Caribbean (Figure 3.15). These two character states also separated the common ancestor of *C. spathulata*, *C. manabiana*, and *C. tandapiana* (subclade B<sub>s</sub>; Figure 3.1) from the remaining species of section *Angustiflorae* (Figure 3.3: node 11). These two character states then persisted within subclade B<sub>s</sub> (Figure 3.1) to the common ancestor of *C. manabiana* and *C. tandapiana* (Figure 3.3: node 12). Because a larger lamina surface area does not co-occur with a lower precipitation in the driest quarter for any of the three extant species within subclade B<sub>s</sub> (Figure 3.1), a shift away from either one or both of these character states may have been important in recent speciation of *C. spathulata*, *C. manabiana*, or *C. tandapiana*.

#### Corolla Color and Temperature

Plant-pollinator interactions are often important in driving speciation (Bawa 1990; Roalson et al. 2003; Perret et al. 2007; Muchhala et al. 2008) because the efficiency of pollination systems is directly related to the fitness of the plant (Proctor et al. 1996). Tropical habitats have a diverse array of potential pollinators including hummingbirds, bats, and insects ranging from bees and beetles to butterflies and moths (Bawa 1990). The number and type of pollinators that visit a specific plant species depend upon the corolla shape, color, and size, the pollen or nectar reward, or scent among other characters (Proctor et al. 1996; Muchhala et al. 2008); however, within Gesneriaceae, the corolla color and shape are usually indicative of whether the flower is a generalist, visited

by a variety of pollinators, or visited by a specific pollinator (Roalson et al. 2003; Perret et al. 2007; Martén-Rodríguez et al. 2010).

Within Gesneriaceae subfamily Gesnerioideae, plant-pollinator interactions have been studied and have identified relationships between the pollinator syndrome and morphological characters: red, tubular, diurnal flowers are associated with hummingbird pollinators; campanulate or tubular corollas with purple, blue, or yellow colors are associated with bee pollinators; and long tubular white or yellow flowers are associated with moth pollinators (Roalson et al. 2003; Perret et al. 2007; Martén-Rodríguez et al. 2010). These same plant-pollinator interactions are likely the same among the species of section *Angustiflorae* because they are found in the same tropical habitats and have similar floral morphologies, though there have not been extensive studies examining plant-pollinator interactions within the section.

This study showed a correlation between a yellow corolla color (Figure 3.8; Table 3.1: [0]) and a lower temperature during the coldest quarter (Table 3.1: [0] < 18.133 °C). The correlation between corolla color and temperature may also be an indication that there was a pollinator shift. In the phylogenetic tree (Figure 3.8), each time there was a shift to a yellow corolla, it occurred from an ancestor that had a variable corolla color. A species with a variable corolla color may be an indication that the ancestor species was a generalist and visited by a variety of pollinators (Martén-Rodríguez et al. 2010). A colder temperature may not have been tolerated by all the pollinators of the ancestor species year round, eliminating them as potential pollinators. Normally hummingbirds would be expected to tolerate colder temperatures than insects, which are more temperature sensitive (Kendeigh 1969). A shift to hummingbird pollinators would have

been indicated by a shift to red corollas with a colder temperature during the coldest quarter. However, in section *Angustiflorae*, there is a correlation between yellow corollas and a colder temperature. This may be an indication that there are a few insects which can tolerate the colder temperatures and selected for a yellow colored corolla.

A yellow colored corolla co-occurred with a colder temperature during the coldest quarter at four nodes on the phylogenetic tree (Figure 3.8: nodes 1, 7, 9, and 12). Of the four nodes where these character states co-occurred, three are common ancestors to extant species (Figure 3.8; node 7: *C. byrsina* and *C. orientandina*; node 9: *C. crassicaulis*; node 12: *C. manabiana* and *C. tandapiana*). Because these three nodes are the common ancestors to extant species, these character states may have been an important driving force in more recent speciation within section *Angustiflorae*. The other node where a yellow corolla co-occurred with a colder temperature, node 1 (Figure 3.8), is the common ancestor to *C. ambigua* and *C. domingensis*. The common ancestor to these two species likely migrated from the mainland to the Caribbean (see “Leaf Surface Area and Precipitation”); therefore, these character states may not have been important in recent speciation but were likely important in allowing the ancestor of *C. ambigua* and *C. domingensis* to move into the Caribbean.

### Phenology and Climate

In the tropics, an aseasonal climate allows for the potential for plants to flower year round (Bawa et al. 2003). However, the flowering phenology of each species is limited by both biotic and abiotic factors, such as pollinators (Bawa et al. 2003) and seasonal changes in precipitation (Gentry 1974). Pollinator selection may cause directional or divergent selection in the timing of flowering to eliminate competition and

select for the most optimal time of year for a specialized pollinator (Gentry 1974). Seasonal changes can limit a plant's resources also leading to a limited flowering time (Reich and Borchert 1984). Often tropical trees will flower during the dry season with a lack of leaves making flowers more visible to pollinators (Bawa et al. 2003) and allocate resources during the wet season to shoot elongation and growth (Reich and Borchert 1984).

In section *Angustiflorae*, there is variation in the timing of flowering among species (Table 3.1). Some of the species have only been found flowering from January to March, while other species have been found flowering from March to October; still other species have been found flowering continuously (Table 3.1). We would expect species that are flowering continuously to be found in regions with little temperature variation and a consistent amount of rainfall (Gentry 1974; Reich and Borchert 1984; Bawa et al. 2003). However, correlation analyses within section *Angustiflorae* showed a significant correlation between a continuous flowering phenology (Figure 3.10; Table 3.1: [0]) with both a larger temperature annual range (Table 3.1: [2] > 11.45 °C) and lower precipitation during the driest month (Table 3.1: [1] < 53 mm) compared to other species in the section. However, ancestral state reconstructions indicated that a continuous flowering phenology was the most likely ancestral character state to the entire section (Figure 3.10: node 2). Therefore, correlations between phenology and climate variables are not a reflection of character state shifts in both variables at the same nodes. Correlation analyses determine significance based on the frequency of character states co-occurring, not when character state shifts co-occur. Because the phenology did not shift at any of these nodes, speciation is likely to have occurred due to changes in the

climate alone. These correlations likely indicate that species with a continuously flowering phenology and larger temperature annual range or lower precipitation during the driest month are hardier species because they are found in the less hospitable environments but are still able to flower while setting fruit and producing seeds year round. The larger temperature range and lower precipitation would preclude some species from surviving and adapting in these conditions.

A phenology of flowering continuously and a larger temperature annual range co-occurred at four nodes in the phylogenetic tree (Figure 3.10: nodes 1, 8, 9, and 10) while a phenology of flowering continuously co-occurred with lower precipitation during the driest month at three nodes (Figure 3.10: nodes 1, 11, and 12). None of these character states co-occurred in extant species of section *Angustiflorae* indicating that they may have been important in past speciation. Both correlations (Figure 3.10) are present at node 1, which is the common ancestor to *C. ambigua* and *C. domingensis* and may have been important characters in allowing the common ancestor to move into the Caribbean (see “Leaf Surface Area and Precipitation”) because the common ancestor was able to tolerate more variable climatic conditions. Because a phenology of flowering continuously and a larger temperature annual range co-occurred at node 8 (Figure 3.10), the common ancestor to subclade C<sub>s</sub> (Figure 3.1), a larger temperature annual range is likely to have been important in separating the common ancestor of subclade C<sub>s</sub> from the common ancestor of subclade D<sub>s</sub> (Figure 3.1) in the past. These two character states then persisted throughout the common ancestors within subclade C<sub>s</sub> at nodes 9 and 10 (Figure 3.10). Speciation of extant taxa may have been caused by specialization of species within subclade C<sub>s</sub> as they moved into different climatic ranges. A phenology of flowering

continuously co-occurred with lower precipitation during the driest month at node 11, the common ancestor to subclade B<sub>s</sub> (Figure 3.1). Tolerating less precipitation is likely to have been important for separating subclade B<sub>s</sub> from the remaining species of subclades C<sub>s</sub> and D<sub>s</sub>. This trait then persisted at node 12, the common ancestor of *C. manabiana* and *C. tandapiana*, which may indicate again that specialization into a climatic region with more rainfall year round or the inability to flower continuously was important in speciation of these two species in the past.

### Forces Driving Speciation

Correlations between morphological characters (including phenology) and climatic variables shed light on possible forces driving speciation; however, patterns among all morphological characters and climatic variables also elucidated possible forces that contributed to evolutionary divergence. Within section *Angustiflorae*, ancestral character state reconstructions of morphological characters, including phenology, SEEVA v. 1.00 analyses of climatic variables, and correlation analyses illuminated all individual character state shifts at each node in phylogenetic tree. By taking into account each of the character state shifts at all nodes; I identified biotic and abiotic forces that may have driven speciation.

One force driving evolutionary divergence within section *Angustiflorae* was allopatric speciation. Allopatric speciation is one of the most widely recognized forces driving speciation among sexually reproducing animals and plants (Bush 1975). Because both *C. ambigua* and *C. domingensis* are found on Caribbean islands (Chapter Two: Figure 2.7) and all other species of *Angustiflorae* are found on the mainland of Central

and South America (Chapter Two: Figures 2.7-2.11), it is likely that a subpopulation of the common ancestor to section *Angustiflorae* (Figure 3.15: node 2) was dispersed into the Caribbean (see “Leaf Surface Area and Precipitation”) where a physical barrier to gene flow between the two populations resulted in subsequent speciation of the common ancestor to *C. ambigua* and *C. domingensis* (Figure 3.15: node 1). The separation of populations on the islands of Puerto Rico and Hispaniola also caused a disruption in gene flow and resulted in subsequent speciation of the two separate species, *C. ambigua* and *C. domingensis* (Figure 3.15).

Changes in photosynthetic ability may have also driven speciation within section *Angustiflorae*. Leaf traits are under extreme selection pressure in plants, because they are responsible for the capture and utilization of light energy (Carson 1985; Hopkins et al. 2008). Adaptations in vegetative characters to better capture light are likely to increase a plant’s fitness because it will be able to grow larger, possibly attracting more pollinators, withstand climate variation, and produce more fruit and seeds (Carson 1985; Hopkins et al. 2008). Over time, differences in vegetative characters and the ability to perform photosynthesis are likely to result in speciation. Character state shifts in vegetative characters including stem habit, lamina surface area, leaf isophylly, and petiole length, were used to indicate a shift in photosynthetic ability within *Angustiflorae*. Character state shifts in one or more of these vegetative characters occurred at nodes 1, 4, 6, 7, 11, and in *C. angustata*, *C. crassicaulis*, *C. katzensteiniae*, and *C. ovatifolia* (Figure 3.15).

Another force driving speciation may have been nectar robbing or the adaptations to decrease nectar robbing. Some insects can push aside the calyx margins and chew through the corolla to eat the nectar but do not collect and spread pollen (Inouye 1983).

Because most plants depend upon pollinators for reproduction, and nectar robbers are not performing pollinator, there is likely to be a decrease in the fitness of plants that are being nectar robbed (Inouye 1983). To counter the detrimental effect of nectar robbers, plants have adapted morphological and physiological characters to deter nectar robbing (Inouye 1983). One morphological adaptation is reinforcement of the calyx (Inouye 1983). Within section *Angustiflorae*, character state shifts in the calyx margin (from entire to serrate) and the corolla to calyx ratio (from a larger ratio to a smaller ratio) are likely to be adaptations reinforcing the calyx and deterring nectar robbing leading to speciation. Character state shifts in one or both of these characters occurred at nodes 5 and 10 (Figure 3.15).

One of the most likely forces driving speciation within section *Angustiflorae* is a pollinator shift. Pollinator selection has been shown to drive character state changes in many plant groups (Schemske 1981; Whitten et al. 1986; Galen 1989; Johnson 1996; Ree 2005; Irwin 2006; Martén-Rodríguez et al. 2010; van der Niet and Johnson 2012). Because pollinators directly affect gene flow, they can have a large impact on floral characters (Carson 1985). Within section *Angustiflorae*, speciation due to pollinator shifts was indicated by character state shifts in corolla color, corolla lobe color, floral bract size, and flowering phenology. Pollinator selection seemed to have a large impact on speciation in *Angustiflorae* with character shifts likely related to a pollinator shift occurring at nodes 1, 2, 4, 7, 8, 9, 10, 12, and in *C. angustata*, *C. colombiana*, *C. byrsina*, *C. rileyi*, *C. ovatifolia*, *C. manabiana*, *C. tandapiana*, and *C. spathulata* (Figure 3.15).

Changes in climate characters, both temperature and precipitation, may have also driven evolutionary divergence within *Angustiflorae*. As sessile organisms, plants are

more sensitive to environmental conditions (Hopkins et al. 2008). Changes in temperature or precipitation variables are likely to drive speciation because plants must adapt to climatic conditions to survive (Hancock et al. 2011). Significant *P*-values and *Di* values from SEEVA v. 1.00 analyses indicated significant shifts in temperature at *C. manabiana* and *C. tandapiana* (Figure 3.15) and significant shifts in precipitation at nodes 1 and 11 (Figure 3.15).

This study has identified possible forces that drove speciation within section *Angustiflorae*; however, at node 3 (Figure 3.15) there are no major character state shifts that indicated a force driving speciation. Speciation at node 3 (Figure 3.15) may have been the result of morphological character shifts that were not scored, microclimate variables that were not measured, or other evolutionary forces that were not possible to measure such as mutations or genetic drift.

These forces possibly drove evolution and speciation within section *Angustiflorae*; however, to identify causation field studies focused on specific morphological and climatic variables must be conducted.

#### Speciation in Section *Angustiflorae*

Ancestral state reconstructions and correlations analyses identified six possible forces driving speciation within section *Angustiflorae*. Correlation analyses have identified shifts between a larger lamina surface area and less precipitation during the coldest quarter (Table 3.4 and Figure 3.3), a yellow corolla and a lower temperature during the coldest quarter (Table 3.4 and Figure 3.8), and a continuously flowering phenology with both a larger temperature annual range and lower precipitation during the driest month (Table 3.4 and Figure 3.10). Identifying patterns among morphological

characters also illuminated allopatric speciation, changes in photosynthetic ability, nectar robbing adaptations, pollinator shifts, and climate changes in temperature or precipitation as possible forces driving evolutionary divergence. Of these forces, pollinator shifts are likely to have had the largest effect on speciation within *Angustiflorae* (Figure 3.15).

Molecular phylogenetics and correlation analyses have identified pollinators as a major force driving angiosperms divergence (Armbruster 1993; Johnson et al. 1998; Beardsley et al. 2003; Perret et al. 2007; Martén-Rodríguez et al. 2010; van der Niet and Johnson 2012). Pollinators can have a large effect on a plant's morphological and physiological characters (Carson 1985). Many studies provide phylogenetic support for pollinator selection driving speciation but lack empirical evidence (van der Niet and Johnson 2012). Many studies assume a plant's pollinator based on floral characters (Armbruster 1993; Johnson et al. 1998; Martén-Rodríguez et al. 2010), but this data may not be accurate. Therefore, it is important to conduct field studies focused on pollinator systems to determine the effect of pollinator selection on speciation.

## LITERATURE CITED

- Armbruster, W. S. 1993. Evolution of plant pollination systems: hypotheses and test with the Neotropical vine *Dalechampia*. *Evolution* 47: 1480-1505.
- Barluenga, M., K. N. Stölting, W. Salzburger, M. Muschick, and A. Meyer. 2006. Sympatric speciation in Nicaraguan crater lake cichlid fish. *Nature* 439: 719-723.
- Bawa, K. S. 1990. Plant-pollinator interactions in tropical rain forests. *Annual Review of Ecology and Systematics* 21: 399-422.
- Bawa, K. S., H. Kang, and M. H. Grayum. 2003. Relationships among time, frequency, and duration of flowering in tropical rain forests. *American Journal of Botany* 90: 877-887.
- Beardsley, P. M., A. Yen, and R. G. Olmstead. 2003. AFLP phylogeny of *Mimulus* section *Erythrhanthe* and the evolution of hummingbird pollination. *Evolution* 57: 1397-1410.
- Benjamani, Y. and Y. Hochberg. 1995. Controlling the false discovery rate: a practical and powerful approach to multiple testing. *Journal of the Royal Statistical Society B* 57: 289-300.
- Bollback, J. P. 2006. SIMMAP: stochastic character mapping of discrete traits on phylogenies. *BMC Bioinformatics* 7: 88.
- Bonser, S. P. 2006. Form defining function: interpreting leaf functional variability in integrated plant phenotypes. *Oikos* 114: 187-190.

- Bush, G. L. 1975. Modes of animal speciation. *Annual Review of Ecology and Systematics* 6: 339-364.
- Carson, H. L. 1985. Unification of speciation theory in plants and animals. *Systematic Botany* 10: 380-390.
- Darwin, C. 1859. *On the Origin of Species*. New York: Signet Classics.
- Dilcher, D. L. 1973. The Eocene floras of southeastern North America. Pp. 39-59 in *Vegetation and Vegetational History of Northern Latin America* ed. A. Graham. New York: Elsevier.
- Dolph, G. E. and D. L. Dilcher. 1980. Variation in leaf size with respect to climate in the tropics of the western hemisphere. *Bulletin of the Torrey Botanical Club* 107: 154-162.
- ESRI (Environmental Systems Resource Institute). 2012. ArcMap 10.0. ESRI, Redlands, CA.
- Felsenstein, J. 1985. Phylogenies and the comparative method. *The American Naturalist* 125:1-15.
- Fritsch, K. 1894. Gesneriaceae. Pp. 133-185 in *Die Natürlichen Pflanzenfamilien* Vol. 4 (3b), eds. A. Engler and K. Prantl. Leipzig, Germany: W. Engelmann.
- Galen, C. 1989. Measuring pollinator-mediated selection on morphometric floral traits: bumblebees and the alpine sky pilot, *Polemonium viscosum*. *Evolution* 43: 882-890.
- Gentry, A. H. 1974. Flowering phenology and diversity in tropical Bignoniaceae. *Biotropica* 6: 64-68.

- Givnish, T. J. 1987. Comparative studies of leaf form: assessing the relative roles of selective pressures and phylogenetic constraints. *New Phytologist* 106: 131-160.
- Hancock, A. M., B. Brachi, N. Faure, M. W. Horton, L. B. Jarymowycz, F. G. Sperone, C. Toomajian, F. Roux, and J. Bergelson. 2011. Adaptation to climate across the *Arabidopsis thaliana* genome. *Science* 334: 83-86.
- Hardy, C. R. and H. P. Linder. 2005. Intraspecific variability and timing in ancestral ecology reconstruction: a test case from the Cape flora. *Systematic Biology* 54: 299-316.
- Harvey, P. H. and M. D. Pagel. 1991. *The comparative method in evolutionary biology*. Oxford: Oxford University Press.
- Heiberg, E. 2012. SEEVA ver. 1.00. Software for Spatial Evolutionary and Ecological Vicariance Analysis. Available from the author at <http://seeva.heiberg.se>
- Heiberg, E. and L. Struwe. 2012. SEEVA manual, ver. 1.00. On-line publication, Rutgers University. Available from the authors at <http://www.rci.rutgers.edu/~struwe/seeva>
- Hijmans, R. J., S. E. Cameron, J. L. Parra, P. G. Jones, and A. Jarvis. 2005. Very high resolution interpolated climate surfaces for global land areas. *International Journal of Climatology* 25: 1965-1978.
- Hopkins, R., J. Schmitt, and J. R. Stinchcombe. 2008. A latitudinal cline and response to vernalization in leaf angle and morphology in *Arabidopsis thaliana* (Brassicaceae). *New Phytologist* 179: 155-164.
- Huelsenbeck, J. P., R. Nielsen, and J. P. Bollback. 2003. Stochastic mapping of morphological characters. *Systematic Biology* 52: 131-158.

- Inouye, D. W. 1983. The ecology of nectar robbing. Pp. 153-173 in *Biology of nectarines* eds. B. Bentley and T. S. Elias. New York: Colombia University Press.
- Irwin, R. E. 2006. The consequences of direct versus indirect species interactions to selection on traits: pollination and nectar robbing in *Ipomopsis aggregate*. *The American Naturalist* 137: 315-328.
- Johnson, S. D. 1996. Adaptation and speciation models in the Cape floral of South Africa. *Taxon* 45: 59-66.
- Johnson, S. D., H. P. Linder, and K. E. Steiner. 1998. Phylogeny and radiation of pollination systems in *Disa* (Orchidaceae). *American Journal of Botany* 85: 402-411.
- Kendeigh, S. C. 1969. Tolerance of cold and Bergmann's rule. *The Auk* 86: 13-25.
- Kvist, L. P. and L. E. Skog. 1993. The genus *Columnnea* (Gesneriaceae) in Ecuador. *Allertonia* 6: 327-400.
- Levin, D. A. and H. W. Kerster. 1967. Natural selection for reproductive isolation in *Phlox*. *Evolution* 21: 679-687.
- Lewis, P. O. 2001. A likelihood approach to estimating phylogeny from discrete morphological character data. *Systematic Biology* 50: 913-925.
- Maddison, W. P. and D. R. Maddison. 2011. Mesquite: a modular system for evolutionary analysis. Version 2.75 <http://www.mesquiteproject.org>
- Martén-Rodríguez, S., C. B. Fenster, I. Agnarsson, L. E. Skog, and E. A. Zimmer. 2010. Evolutionary breakdown of pollination specialization in a Caribbean plant radiation. *New Phytologist* 188: 403-417.

- Meinzer, F. and G. Goldstein. 1985. Some consequences of leaf pubescence in the Andean giant rosette plant *Espeletia timotensis*. *Ecology* 66: 512-520.
- Meredith, R. W., M. N. Pires, D. N. Reznick, and M. S. Springer. 2011. Molecular phylogenetic relationships and the coevolution of placentotrophy and superfetation in *Poecilia* (Poeciliidae: Cyprinodontiformes). *Molecular Phylogenetics and Evolution* 59: 148-157.
- Mittelbach, G. G., D. W. Schemske, H. V. Cornell, A. P. Allen, J. M. Brown, M. B. Bush, S. P. Harrison, A. H. Hurlbert, N. Knowlton, H. A. Lessios, C. M. McCain, A. R. McCune, M. A. McPeck, T. J. Near, T. D. Price, R. E. Ricklefs, K. Roy, D. F. Sax, D. Schluter, J. M. Sobel, and M. Turelli. 2007. Evolution and the latitudinal diversity gradient: speciation, extinction and biogeography. *Ecology Letters* 10: 315-331.
- Muchhala, N., A. Caiza, J. C. Vizquete, and J. D. Thomson. 2008. A generalized pollination system in the tropics: bats, birds, and *Aphelandra acanthus*. *Annals of Botany* 103: 1481-1487.
- Myers, N., R. A. Mittermeier, C. G. Mittermeier, G. A. B. da Fonseca, and J. Kent. 2000. Biodiversity hotspots for conservation priorities. *Nature* 403: 853-858.
- Parkhurst, D. F. and O. L. Loucks. 1972. Optimal leaf size in relation to environment. *Journal of Ecology* 60: 505-537.
- Perret, M., A. Chautems, R. Spichiger, T. G. Barraclough, and V. Savolainen. 2007. The geographical pattern of speciation and floral diversification in the Neotropics: the tribe Sinningieae (Gesneriaceae) as a case study. *Evolution* 61: 1641-1660.

- Proctor, M., P. Yeo, and A. Lack. 1996. *The Natural History of Pollination*. Portland, OR: Timber Press.
- Ree, R. H. 2005. Phylogeny and the evolution of floral diversity in *Pedicularis* (Orobanchaceae). *International Journal of Plant Science* 166: 595-613.
- Reich, P. B. and R. Borchert. 1984. Water stress and tree phenology in a tropical dry forest in the lowlands of Cost Rica. *Journal of Ecology* 72: 61-74.
- Ristic, Z. and M. A. Jenks. 2002. Leaf cuticle and water loss in maize lines differing in dehydration avoidance. *Journal of Plant Physiology* 156: 645-651.
- Roalson, E. H., L. E. Skog, and E. A. Zimmer. 2003. Phylogenetic relationships and the diversification of floral form in *Achimenes* (Gesneriaceae). *Systematic Botany* 28: 593-608.
- Roderick, M. L., S. L. Berry, I. R. Noble, and G. D. Farquhar. 1999. A theoretical approach to linking the composition and morphology with the function of leaves. *Functional Ecology* 13: 683-695.
- Schemske, D. W. 1981. Floral convergence and pollinator sharing in two bee-pollinated tropical herbs. *Ecology* 62: 946-954.
- Slabbekoorn, H. and T. B. Smith. 2002. Habitat-dependent song divergence in the little greenbul: an analysis of environmental selection pressures on acoustic signals. *Evolution* 56: 1849-1858.
- Smith, J. F. 1994. Systematics of *Columnea* section *Pentadenia* and section *Stygnanthe* (Gesneriaceae). *Systematic Botany Monographs* 44: 1-89.
- Smith, J. F. and K. J. Sytsma. 1994. Evolution in the Andean epiphytic genus *Columnea* (Gesneriaceae). Part I. Morphology. *Systematic Botany* 19: 220-235.

- Smith, J. F., M. Ooi, L. Schulte, M. Amaya M., and J. L. Clark. The disintegration of the subgeneric classification of *Columnnea* (Gesneriaceae). *Selbyana* in review.
- Struwe, L., P. E. Smouse, E. Heiberg, S. Haag, and R. G. Lathrop. 2011. Spatial evolutionary and ecological vicariance analysis (SEEVA), a novel approach to biogeography and speciation research, with an example from Brazilian Gentianaceae. *Journal of Biogeography* 38: 1841-1854.
- Swofford, D. L. 2002. PAUP\*: phylogenetic analysis using parsimony (\*and other materials), version 4.0b10. Sunderland, Massachusetts: Sinauer.
- Tolley, K. A., C. R. Tilbury, G. J. Measey, M. Menegon, W. R. Branch, and C. A. Matthee. 2011. Ancient forest fragmentation or recent radiation? Testing refugial speciation models in chameleons within an African biodiversity hotspot. *Journal of Biogeography* 38: 1748-1760.
- van der Niet, T. and S. D. Johnson. 2012. Phylogenetic evidence for pollinator-driven diversification of angiosperms. *Trends in Ecology and Evolution* 27: 353-361.
- Viljanen, H., F. Escobar, and I. Hanski. 2010. Low local but high beta diversity of tropical forest dung beetles in Madagascar. *Global Ecology and Biogeography* 19: 886-894.
- Weber, A. 2004. Gesneriaceae. Pp. 63–158 in *The families and genera of vascular plants*, vol. 7. eds. K. Kubitzki and J. Kadereit. Berlin: Springer-Verlag.
- Whitten, W. M., N. H. Williams, W. S. Armbruster, M. A. Battiste, L. Strekowski, and N. Lindquist. 1986. Carvone oxide: an example of convergent evolution in euglossine pollinated plants. *Systematic Botany* 11: 222-228.

- Wiley, E. O. and B. S. Lieberman. 2011. *Phylogenetics: theory and practice of phylogenetics systematics*. Hoboken, N. J.: Wiley-Blackwell.
- Wills, C., K. E. Harms, R. Condit, D. King, J. Thompson, F. He, H. C. Muller-Landau, P. Ashton, E. Losos, L. Comita, S. Hubbell, J. LaFrankie, S. Bunyavejchewin, H. S. Dattaraja, S. Davies, S. Esufali, R. Foster, N. Gunatilleke, S. Gunatilleke, P. Hall, A. Itoh, R. John, S. Kiratiprayoon, S. Loo de Lao, M. Massa, C. Nath, M. N. S. Noor, A. R. Kassim, R. Sukumar, H. S. Suresh, I. Sun, S. Tan, T. Yamakura, and J. Zimmerman. 2006. Nonrandom processes maintain diversity in tropical forests. *Science* 311: 527-531.
- Woo, V. L., M. M. Funke, J. F. Smith, P. J. Lockhart, and P. J. Garnock-Jones. 2011. New world origins of southwest Pacific Gesneriaceae: Multiple movements across and within the south Pacific. *International Journal of Plant Science* 172: 434-457.

**Table 3.1 – Character State Definitions and Scores**

Definition of character states for fourteen morphological characters, phenology, and nineteen climatic variables and scores for the thirteen species in section *Angustiflorae* included in this study.

Character	0	1	2	3	<i>C. ambigua</i>	<i>C. angustata</i>	<i>C. byrsina</i>	<i>C. colombiana</i>	<i>C. crassicaulis</i>	<i>C. domingensis</i>	<i>C. katzensteiniae</i>	<i>C. manabiana</i>	<i>C. orientandina</i>	<i>C. ovatifolia</i>	<i>C. rileyi</i>	<i>C. spathulata</i>	<i>C. tandapiana</i>
<b>Habit</b>	upright	horizontal	pendent	-	0	0	1	2	1	1	0	0	1	2	0	0	0
<b>Leaf Isophylly</b>	anisophyllous	isophyllous	-	-	0	1	0	1	1	1	0	0	0	1	1	0	0
<b>Lamina Surface Area</b>	0.0-30.0 cm <sup>2</sup>	> 30.0 cm <sup>2</sup>	-	-	1	1	0	0	0	0	0	1	0	0	0	1	0
<b>Adaxial Pubescence</b>	few to no trichomes	dense trichomes	-	-	0	0	0	0	0	0	0	0	0	0	1	1	0
<b>Abaxial Pubescence</b>	few to no trichomes	dense trichomes	-	-	0	1	1	1	0	1	1	1	1	1	1	1	1
<b>Abaxial Coloration</b>	green	purple apices	entirely purple	variable	0	0	0	0	0	0	0	2	1	0	0	3	1
<b>Petiole Length</b>	0.0-5.0 mm	5.0-20.0 mm	> 20.0 mm	-	1	2	0	1	1	1	0	0	0	0	1	1	0
<b>Number of Flowers per Inflorescence</b>	1 flower per axil	> 1 flower per axil	-	-	1	1	1	1	0	0	1	1	1	0	1	1	1
<b>Floral Bract Size</b>	0.0-6.0 mm	6.0-13 mm	> 13 mm	-	1	2	0	0	1	0	1	2	0	0	1	1	0
<b>Corolla to Calyx Ratio</b>	0.0 to 2.5	> 2.5	-	-	0	0	0	0	1	0	0	1	1	1	0	0	0
<b>Calyx Margin</b>	entire	serrate	-	-	1	1	0	1	0	1	0	0	1	0	0	0	0
<b>Corolla</b>	> 40 mm	10.0 to 40.0	-	-	1	1	1	1	0	1	1	1	1	0	1	1	1

Character	0	1	2	3	<i>C. ambigua</i>	<i>C. angustata</i>	<i>C. byrsina</i>	<i>C. colombiana</i>	<i>C. crassicaulis</i>	<i>C. domingensis</i>	<i>C. katzensteiniae</i>	<i>C. manabiana</i>	<i>C. orientandina</i>	<i>C. ovatifolia</i>	<i>C. rileyi</i>	<i>C. spathulata</i>	<i>C. tandapiana</i>
<b>Length</b>		mm															
<b>Corolla Color</b>	yellow	red	purple	variable	0	3	1	3	0	0	2	0	0	3	1	3	0
<b>Corolla Lobe Color</b>	same color as corolla	different color than corolla	-	-	0	0	1	1	1	0	1	0	0	1	0	0	0
<b>Phenology</b>	flowering continuously	flowering January to March	flowering March to October	-	2	0	0	1	0	0	0	2	0	1	0	0	0
<b>Annual Mean Temperature</b>	< 18.667 °C	21.225 to 23.0 °C	polymorphic	< 21 °C	2	2	2	1	3	2	2	2	2	0	3	2	2
<b>Mean Diurnal Range (Monthly Max Temp - Monthly Min Temp)</b>	polymorphic	> 9.7 °C	-	-	0	0	0	0	0	0	0	0	0	1	0	0	0
<b>Isothermality (Mean Diurnal Range / Temperature Annual Range * 100)</b>	< 77.75	polymorphic	> 84	< 84	0	1	1	2	1	3	1	1	1	1	1	1	1
<b>Temperature Seasonality (Standard Deviation * 100)</b>	polymorphic	265.75 to 439.5 °C	< 439.5 °C	> 703.33 °C	3	0	0	1	0	3	0	0	0	0	2	0	0

Character	0	1	2	3	<i>C. ambigua</i>	<i>C. angustata</i>	<i>C. byrsina</i>	<i>C. colombiana</i>	<i>C. crassicaulis</i>	<i>C. domingensis</i>	<i>C. katzensteiniae</i>	<i>C. manabiana</i>	<i>C. orientandina</i>	<i>C. ovatifolia</i>	<i>C. rileyi</i>	<i>C. spathulata</i>	<i>C. tandapiana</i>
Maximum Temperature of Warmest Month	< 24.925 °C	polymorphic	< 27 °C	> 29.133 °C	1	1	1	3	1	1	1	1	1	0	2	1	1
Minimum Temperature of Coldest Month	< 12.533 °C	polymorphic	< 15.4 °C	> 17.933 °C	1	1	1	3	1	1	1	1	1	0	2	1	1
Temperature Annual Range	polymorphic	> 12.84 °C	> 11.45 °C	-	2	0	0	0	0	1	0	0	0	0	0	0	0
Mean Temperature of Wettest Quarter	< 18.85 °C	polymorphic	< 21.5 °C	> 23.667 °C	1	1	1	3	2	1	1	1	1	0	2	1	1
Mean Temperature of Driest Quarter	< 18.3 °C	polymorphic	< 20.98 °C	> 22.633 °C	1	1	1	3	2	1	1	1	1	0	2	1	1
Mean Temperature of Warmest Quarter	< 19.375 °C	polymorphic	< 21.85 °C	> 23.9 °C	1	1	1	3	2	1	1	1	1	0	2	1	1
Mean Temperature of Coldest Quarter	< 18.133 °C	polymorphic	< 20.5 °C	> 22.433 °C	1	1	1	3	2	1	1	1	1	0	2	1	1
Annual Precipitation	polymorphic	-	-	-	0	0	0	0	0	0	0	0	0	0	0	0	0

<b>Character</b>	<b>0</b>	<b>1</b>	<b>2</b>	<b>3</b>	<i>C. ambigua</i>	<i>C. angustata</i>	<i>C. byrsina</i>	<i>C. colombiana</i>	<i>C. crassicaulis</i>	<i>C. domingensis</i>	<i>C. katzensteiniae</i>	<i>C. manabiana</i>	<i>C. orientandina</i>	<i>C. ovatifolia</i>	<i>C. rileyi</i>	<i>C. spathulata</i>	<i>C. tandapiana</i>
<b>Precipitation of Wettest Month</b>	polymorphic	-	-	-	0	0	0	0	0	0	0	0	0	0	0	0	0
<b>Precipitation of Driest Month</b>	polymorphic	< 53 mm	> 53 mm	-	2	0	0	2	0	0	0	1	0	0	0	0	0
<b>Precipitation Seasonality (Coefficient of Variation)</b>	polymorphic	< 44	> 44	> 70.5	0	0	0	2	1	0	0	3	0	0	0	0	0
<b>Precipitation of Wettest Quarter</b>	polymorphic	< 921.67 mm	-	-	0	0	0	0	0	1	0	0	0	0	0	0	0
<b>Precipitation of Driest Quarter</b>	polymorphic	< 198.43 mm	> 198.43 mm	-	0	0	0	2	0	0	0	1	0	0	0	0	0
<b>Precipitation of Warmest Quarter</b>	polymorphic	< 698.3 mm	486.0 to 1022.0 mm	-	2	0	0	0	0	1	0	0	0	0	0	0	0
<b>Precipitation of Coldest Quarter</b>	polymorphic	< 382.0 mm	> 382.0 mm	158.0 to 829.0 mm	3	0	0	2	0	1	0	0	0	1	0	0	0

**Table 3.2 – Morphological and Climatic Variables not Used in Analyses**

Morphological and climatic variables that were removed from analyses because ancestral state reconstructions were unchanging across the tree. “Ancestral State” is the ancestral character state with the Bayesian posterior probability (BPP) and maximum likelihood probability (MLP) values for morphological characters and BPP for climatic variables. “Character State Shifts” are the nodes or species where there was a shift from the ancestral character state with the new character state listed after the node or species with BPP and MLP included for shifts at node. If only the BPP or MLP was included, then only the Simmap 1.5 or Mesquite v. 2.75 analyses recovered a character state shift, respectively.

<b>Variable</b>	<b>Ancestral State</b>	<b>Character State Shifts</b>
<b>Adaxial Pubescence</b>	0 - BPP 0.99766 MLP 0.99006834	<i>Columnea rileyi</i> (1) <i>C. spathulata</i> (1)
<b>Abaxial Pubescence</b>	1 - BPP 0.985151 MLP 0.98845547	<i>C. ambigua</i> (0) <i>C. crassicaulis</i> (0)
<b>Abaxial Coloration</b>	0 - BPP 0.998129 MLP 0.98808357	Node 11 (3 - MLP 0.53056534) Node 12 (1 - BPP 0.755186; MLP 0.31952160) <i>C. manabiana</i> (2) <i>C. orientandina</i> (1) <i>C. spathulata</i> (3)
<b>Number of Flowers per Inflorescence</b>	1 - BPP 0.986947 MLP 0.70958736	Node 1 (0 - MLP 0.54493802) Node 8 (1 - BPP 0.682411) Node 9 (1 - BPP 0.659907) <i>C. crassicaulis</i> (0) <i>C. domingensis</i> (0) <i>C. ovatifolia</i> (0)
<b>Corolla Length</b>	1 - BPP 0.997769	Node 8 (1 - BPP 0.627045)

<b>Variable</b>	<b>Ancestral State</b>	<b>Character State Shifts</b>
	MLP 0.99307017	Node 9 (1 - BPP 0.513779)  <i>C. crassicaulis</i> (0) <i>C. ovatifolia</i> (0)
<b>Mean Diurnal Range</b>	0 - BPP 0.999984	<i>C. ovatifolia</i> (1)
<b>Isothermality</b>	1 - BPP 0.999994	<i>C. ambigua</i> (0)  <i>C. colombiana</i> (2) <i>C. domingensis</i> (3)
<b>Maximum Temperature of Warmest Month</b>	1 - BPP 0.999999	<i>C. colombiana</i> (3)  <i>C. ovatifolia</i> (0) <i>C. rileyi</i> (2)
<b>Minimum Temperature of Coldest Month</b>	1 - BPP 0.999999	<i>C. colombiana</i> (3)  <i>C. ovatifolia</i> (0) <i>C. rileyi</i> (2)
<b>Temperature Annual Range</b>	0 - BPP 0.999988	<i>C. ambigua</i> (2)  <i>C. domingensis</i> (1)
<b>Precipitation of Driest Month</b>	0 - BPP 0.999984	<i>C. ambigua</i> (2)  <i>C. colombiana</i> (2) <i>C. manabiana</i> (1)
<b>Precipitation Seasonality</b>	0 - BPP 0.999999	<i>C. colombiana</i> (2)  <i>C. crassicaulis</i> (1) <i>C. manabiana</i> (3)
<b>Precipitation of Wettest Quarter</b>	0 - BPP 0.999994	<i>C. domingensis</i> (1)
<b>Precipitation of Driest Quarter</b>	0 - BPP 0.999998	<i>C. colombiana</i> (2)  <i>C. manabiana</i> (1)
<b>Precipitation of Warmest Quarter</b>	0 - BPP 0.999988	<i>C. ambigua</i> (2)  <i>C. domingensis</i> (1)

**Table 3.3 – SEEVA Results**

SEEVA v. 1.00 results for  $P$ -value and  $D_i$  value results for all nineteen climatic variables at each node (Figure 3.1). Numbers in bold represent significant  $P$ -values ( $P \geq 0.05$ ) and significant  $D_i$  values ( $D_i \geq 0.75$ ).

	Node 1		Node 2		Node 3		Node 4		Node 5		Node 6	
	D value	p-value	D value	p-value	D value	p-value	D value	p-value	D value	p-value	D value	p-value
Annual Mean Temperature	0.532413	<b>0.000006</b>	0.077719	0.015909	0.081647	<b>0.000556</b>	0.569443	<b>0</b>	0.415032	<b>0</b>	0.326935	0.448353
Mean Diurnal Range	<b>0.882633</b>	<b>0</b>	0.268263	<b>0</b>	0.122125	<b>0.000027</b>	0.301325	<b>0</b>	0.314791	<b>0</b>	0.403255	0.085883
Isothermality	0.002063	0.534161	<b>0.761602</b>	<b>0</b>	0.254957	<b>0</b>	0.048442	0.107844	0.069867	0.057564	0.283918	0.648725
Temperature Seasonality	0	1	<b>0.790549</b>	<b>0</b>	0.20081	<b>0</b>	0.277741	<b>0.000001</b>	0.184778	<b>0.000031</b>	0.396319	0.37112
Maximum Temperature of Warmest Month	0.236966	0.006073	0.056172	0.084022	0.070927	<b>0.002392</b>	0.509041	<b>0</b>	0.340399	<b>0</b>	0.462738	0.248758
Minimum Temperature of Coldest Month	0.62504	<b>0</b>	0.292491	<b>0</b>	0.048239	0.015831	0.642852	<b>0</b>	0.402092	<b>0</b>	0.344609	0.401908
Temperature Annual Range	0.416136	<b>0</b>	0.601985	<b>0</b>	0.007221	0.661439	0.326248	<b>0</b>	0.248879	<b>0</b>	0.415606	0.068864
Mean Temperature of Wettest Quarter	0.456978	<b>0.000067</b>	0.014994	0.609926	0.110607	<b>0.000048</b>	0.571876	<b>0</b>	0.372421	<b>0</b>	0.434632	0.273569
Mean Temperature of Driest Quarter	0.402716	<b>0.000251</b>	0.251994	<b>0</b>	0.044728	0.022463	0.602524	<b>0</b>	0.369459	<b>0</b>	0.343507	0.40466
Mean Temperature of Warmest Quarter	0.377304	<b>0.00031</b>	0.025721	0.383179	0.088731	<b>0.000358</b>	0.599818	<b>0</b>	0.369939	<b>0</b>	0.398613	0.380051

	Node 1		Node 2		Node 3		Node 4		Node 5		Node 6	
	D value	p-value	D value	p-value	D value	p-value	D value	p-value	D value	p-value	D value	p-value
Mean Temperature of Coldest Quarter	0.586696	<b>0.000001</b>	0.180916	<b>0.000011</b>	0.064809	<b>0.00219</b>	0.608225	<b>0</b>	0.384666	<b>0</b>	0.302805	0.53334
Annual Precipitation	0.680629	<b>0</b>	0.151859	<b>0.00008</b>	0.281886	<b>0</b>	0.348779	<b>0</b>	0.175425	<b>0.000232</b>	0.119906	0.642976
Precipitation of Wettest Month	0.573293	<b>0</b>	0.28824	<b>0</b>	0.018372	0.325243	0.401396	<b>0</b>	0.473611	<b>0</b>	0.22679	0.294586
Precipitation of Driest Month	<b>0.911308</b>	<b>0</b>	0.231674	<b>0</b>	0.384456	<b>0</b>	0.231645	<b>0.000087</b>	0.14766	<b>0.00059</b>	0.126348	1
Precipitation Seasonality	0.444444	<b>0.000004</b>	0.42571	<b>0</b>	0.519882	<b>0</b>	0.37766	<b>0</b>	0.165428	<b>0.000003</b>	0.393305	0.196702
Precipitation of Wettest Quarter	<b>0.77214</b>	<b>0</b>	0.268805	<b>0</b>	0.021707	0.239888	0.387005	<b>0</b>	0.447902	<b>0</b>	0.204993	0.310403
Precipitation of Driest Quarter	<b>0.904393</b>	<b>0</b>	0.174873	<b>0</b>	0.399351	<b>0</b>	0.245978	<b>0.000043</b>	0.19741	<b>0.000055</b>	0.127229	0.717004
Precipitation of Warmest Quarter	0.617361	<b>0</b>	0.276223	<b>0</b>	0.078212	<b>0.000488</b>	0.250452	<b>0</b>	0.323318	<b>0</b>	0.109273	0.845734
Precipitation of Coldest Quarter	0.671828	<b>0</b>	0.246863	<b>0</b>	0.36326	<b>0</b>	0.290296	<b>0.000001</b>	0.331688	<b>0</b>	0.111323	0.706327

	Node 7		Node 8		Node 9		Node 10		Node 11		Node 12	
	D value	p-value	D value	p-value	D value	p-value	D value	p-value	D value	p-value	D value	p-value
<b>Annual Mean Temperature</b>	0.423858	<b>0.000151</b>	0.12692	0.059532	0.197788	0.062681	0.040747	0.584586	0.29269	<b>0.000318</b>	<b>0.893073</b>	<b>0.000012</b>
<b>Mean Diurnal Range</b>	0.035449	0.531605	0.081779	0.245493	0.125309	0.276743	0.104611	0.310533	0.154718	0.046006	0.459485	0.031131
<b>Isothermality</b>	0.707627	<b>0</b>	0.00466	1	0.283256	0.013904	0.21009	0.115497	0.217005	<b>0.001604</b>	0.461596	0.030818
<b>Temperature Seasonality</b>	<b>0.782528</b>	<b>0</b>	0.201521	0.040413	0.464293	<b>0.000251</b>	0.055847	0.547216	0.18447	0.028553	<b>0.830809</b>	<b>0.000152</b>
<b>Maximum Temperature of Warmest Month</b>	0.7	<b>0</b>	0.141914	0.065037	0.004295	1	0.005785	1	0.310775	<b>0.000223</b>	<b>0.869948</b>	<b>0.000082</b>
<b>Minimum Temperature of Coldest Month</b>	0.3183	<b>0.00317</b>	0.094584	0.101411	0.08192	0.2365	0.004048	1	0.194443	0.010939	<b>0.835998</b>	<b>0.000059</b>
<b>Temperature Annual Range</b>	0.159647	0.045177	0.139145	0.373639	0.27173	0.016262	0.338058	0.057051	0.136103	0.105073	0.074982	0.80267
<b>Mean Temperature of Wettest Quarter</b>	0.442247	<b>0.000185</b>	0.087333	0.115257	0.147837	0.051958	0.019184	1	0.278689	<b>0.000405</b>	<b>0.886699</b>	<b>0.00001</b>
<b>Mean Temperature of Driest Quarter</b>	0.606946	<b>0.000002</b>	0.200666	0.01307	0.025813	0.668139	0.109656	0.39455	0.264112	<b>0.000888</b>	<b>0.873476</b>	<b>0.000014</b>
<b>Mean Temperature of Warmest Quarter</b>	0.508958	<b>0.000025</b>	0.070488	0.161162	0.07996	0.222575	0.019184	1	0.335539	<b>0.000049</b>	<b>0.905124</b>	<b>0.00001</b>
<b>Mean Temperature of Coldest Quarter</b>	0.491071	<b>0.000108</b>	0.12692	0.059532	0.090312	0.25832	0.019099	0.776021	0.246391	<b>0.000883</b>	<b>0.884129</b>	<b>0.000019</b>
<b>Annual Precipitation</b>	0.118812	0.344315	0.105532	0.436045	0.243794	0.097658	0.44106	0.038234	0.036842	0.670018	0.418151	0.037227

	Node 7		Node 8		Node 9		Node 10		Node 11		Node 12	
	D value	p-value	D value	p-value	D value	p-value	D value	p-value	D value	p-value	D value	p-value
<b>Precipitation of Wettest Month</b>	0.05871	0.463893	0.020929	0.862865	0.055081	0.731578	0.465193	0.013523	0.176478	0.060582	0.374348	0.051104
<b>Precipitation of Driest Month</b>	0.444595	<b>0.000315</b>	0.28244	0.04824	0.293926	0.027244	0.239915	0.328381	0.019897	0.520659	0.4715	0.017664
<b>Precipitation Seasonality</b>	0.385606	<b>0.000783</b>	0.094624	0.257953	0.365669	<b>0.000881</b>	0.043506	0.549148	0.044643	0.201898	0.649123	<b>0.000334</b>
<b>Precipitation of Wettest Quarter</b>	0.110904	0.253162	0.032258	0.811693	0.019619	0.938229	0.367612	0.028144	0.094992	0.279567	0.310762	0.090561
<b>Precipitation of Driest Quarter</b>	0.167602	0.037164	0.180606	0.125233	0.245322	0.027946	0.039364	0.919908	0.088285	0.091777	0.553774	<b>0.003616</b>
<b>Precipitation of Warmest Quarter</b>	0.05174	0.752634	0.01816	0.841773	0.04272	0.693352	0.387339	0.029628	0.092529	0.203892	0.247295	0.219814
<b>Precipitation of Coldest Quarter</b>	0.014831	0.874264	0.398675	<b>0.002454</b>	0.087208	0.657263	0.129366	0.526609	0.003723	0.984038	<b>0.763163</b>	<b>0.000667</b>

**Table 3.4 – Results from the False Discovery Rate Test**

Results from the false discovery rate (FDR) test using SAS software v. 9.2. “Morphological Variable” and “Climate Variable” are the two characters that were compared for each correlation. “Stat” represents the two character states that are being compared for either the  $D_c$  or  $M_c$  statistic. “Value” is the raw value for the  $D_c$  or  $M_c$  statistic test. “Raw  $P$ -value” is the  $P$ -value as given by Simmap 1.5 correlation analyses. “FDR Adjusted  $P$ -value” is the adjusted  $P$ -value from FDR test that was used to determine significance of correlations with  $P < 0.05$  as significant; only FDR  $P$ -values  $< 0.01$  are presented in table. Bold values indicate significant  $P$ -values from the FDR test ( $P < 0.05$ ).

<b>Morphological Variable</b>	<b>Climate Variable</b>	<b>Stat</b>	<b>Value</b>	<b>Raw <math>P</math>-value</b>	<b>FDR Adjusted <math>P</math>-value</b>
<b>Habit</b>	<b>Mean Diurnal Range</b>	<b>d (2,1)</b>	<b>0.002201</b>	<b>0.000</b>	<b>0.000</b>
<b>Lamina Surface Area</b>	<b>Precipitation of Driest Quarter</b>	<b>d (0,1)</b>	<b>-0.002165</b>	<b>0.000</b>	<b>0.000</b>
<b>Lamina Surface Area</b>	<b>Precipitation of Driest Quarter</b>	<b>d (1,1)</b>	<b>0.002066</b>	<b>0.000</b>	<b>0.000</b>
<b>Corolla Color</b>	<b>Mean Temperature of Coldest Quarter</b>	<b>d (0,0)</b>	<b>-0.001453</b>	<b>0.000</b>	<b>0.000</b>
<b>Phenology</b>	<b>Temperature Annual Range</b>	<b>d (0, 2)</b>	<b>-0.002196</b>	<b>0.000</b>	<b>0.000</b>
<b>Phenology</b>	<b>Precipitation of Driest Month</b>	<b>d (0,1)</b>	<b>-0.002697</b>	<b>0.000</b>	<b>0.000</b>
Habit	Precipitation of Wettest Quarter	d (0,1)	-0.002550	0.001	0.080267
Adaxial Pubescence	Maximum Temperature of Warmest Month	d (0,2)	-0.002221	0.001	0.080267
Adaxial Pubescence	Maximum Temperature of Warmest Month	d (1,2)	0.002160	0.001	0.080267
Calyx Margin	Temperature Annual Range	d (0,1)	-0.001358	0.001	0.080267
Calyx Margin	Temperature Annual Range	d (1,1)	0.001265	0.001	0.080267

<b>Morphological Variable</b>	<b>Climate Variable</b>	<b>Stat</b>	<b>Value</b>	<b>Raw <i>P</i>-value</b>	<b>FDR Adjusted <i>P</i>-value</b>
Corolla Color	Mean Diurnal Range	d (0,1)	-0.002308	0.001	0.080267
Phenology	Precipitation of Driest Month	d (2,1)	0.002289	0.001	0.080267
Phenology	Precipitation of Driest Quarter	d (0,1)	-0.002867	0.001	0.080267
Phenology	Precipitation of Driest Quarter	d (2,1)	0.002919	0.001	0.080267
<b>Habit</b>	<b>Mean Diurnal Range</b>	<b>m (2,1)</b>	<b>0.002585</b>	<b>0.000</b>	<b>0.000</b>
<b>Lamina Surface Area</b>	<b>Precipitation of Driest Quarter</b>	<b>m (0,1)</b>	<b>-0.001805</b>	<b>0.000</b>	<b>0.000</b>
<b>Lamina Surface Area</b>	<b>Precipitation of Driest Quarter</b>	<b>m (1,1)</b>	<b>0.002419</b>	<b>0.000</b>	<b>0.000</b>
<b>Corolla Color</b>	<b>Mean Temperature of Coldest Quarter</b>	<b>m (0,0)</b>	<b>-0.000641</b>	<b>0.000</b>	<b>0.000</b>
<b>Phenology</b>	<b>Temperature Annual Range</b>	<b>m (0,2)</b>	<b>-0.001634</b>	<b>0.000</b>	<b>0.000</b>
<b>Phenology</b>	<b>Precipitation of Driest Month</b>	<b>m (0,1)</b>	<b>-0.002097</b>	<b>0.000</b>	<b>0.000</b>
<b>Phenology</b>	<b>Precipitation of Driest Quarter</b>	<b>m (2,1)</b>	<b>0.003513</b>	<b>0.000</b>	<b>0.000</b>
Habit	Precipitation of Wettest Quarter	m (0,1)	-0.002189	0.001	0.086
Adaxial Pubescence	Maximum Temperature of Warmest Month	m (0,2)	-0.001773	0.001	0.086
Adaxial Pubescence	Maximum Temperature of Warmest Month	m (1,2)	0.002605	0.001	0.086
Calyx Margin	Temperature Annual Range	m (1,1)	0.001639	0.001	0.086
Corolla Color	Mean Diurnal Range	m (0,1)	-0.001888	0.001	0.086
Phenology	Precipitation of Driest Month	m (2,1)	0.002859	0.001	0.086
Phenology	Precipitation of Driest Quarter	m (0,1)	-0.002315	0.001	0.086
Habit	Annual Mean Temperature	m (0,0)	-0.001220	0.002	0.09632
Habit	Annual Mean Temperature	m (2,0)	0.002677	0.002	0.09632
Habit	Mean Diurnal Range	m (0,1)	-0.001913	0.002	0.09632

<b>Morphological Variable</b>	<b>Climate Variable</b>	<b>Stat</b>	<b>Value</b>	<b>Raw <i>P</i>-value</b>	<b>FDR Adjusted <i>P</i>-value</b>
Habit	Minimum Temperature of Coldest Month	m (0,3)	-0.000784	0.002	0.09632
Habit	Mean Temperature of Coldest Quarter	m (2,3)	0.002291	0.002	0.09632
Habit	Precipitation of Coldest Quarter	m (0,1)	-0.001482	0.002	0.09632
Leaf Isophylly	Precipitation of Coldest Quarter	m (0,1)	-0.000985	0.002	0.09632
Leaf Isophylly	Precipitation of Coldest Quarter	m (1,1)	0.001746	0.002	0.09632
Calyx Margin	Temperature Annual Range	m (0,1)	-0.000981	0.002	0.09632
Phenology	Mean Diurnal Range	m (1,1)	0.002344	0.002	0.09632
Phenology	Mean Temperature of Coldest Quarter	m (1,0)	0.002523	0.002	0.09632

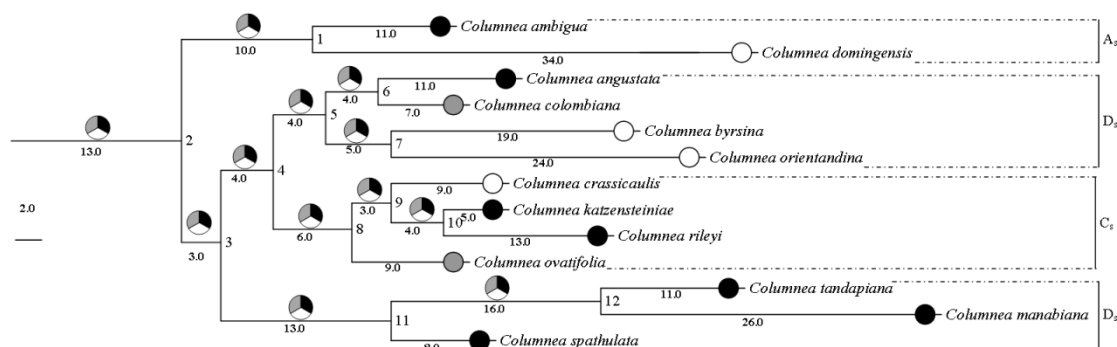


**Figure 3.1 – Ancestral State Reconstruction of Habit: Ancestral state reconstructions from Mk1 model and branch length reconstruction mapped onto a species level phylogenetic tree of section *Angustiflorae*. Character states are upright [0] – black, pendent [1] – white, and horizontal [2] – gray. Circles at extant taxa represent character state for species (Table 3.1). Pie charts at nodes represent the Bayesian posterior probabilities (BPP) and maximum likelihood probabilities (MLP) from ancestral state reconstructions. Nodes with only one pie chart have equal BPP and MLP values. Exact BPP and MLP values are available in Appendix E. Numbers below branches represent branch lengths with size corresponding to branch length. Letters to right represent subclades within section *Angustiflorae* (Chapter Two).**

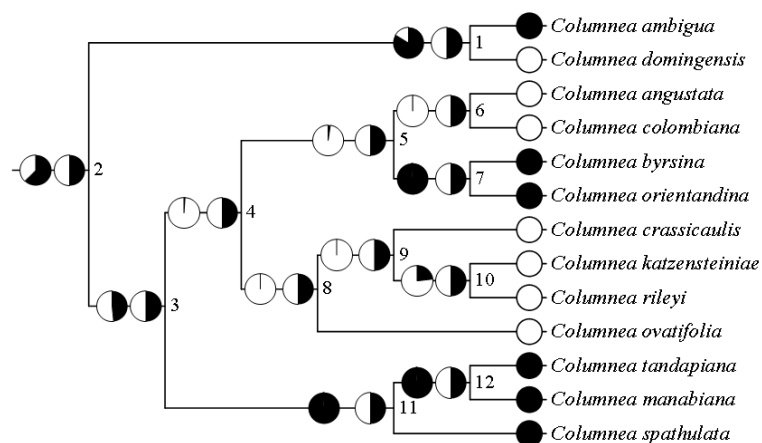


**Figure 3.2 – Ancestral State Reconstruction of Leaf Isophylly: Ancestral state reconstructions from Mk1 model and branch length reconstruction mapped onto a species level phylogenetic tree of section *Angustiflorae*. Character states are anisophyllous [0] – black and isophyllous [1] – white. Circles at extant taxa represent character state for species (Table 3.1). Pie charts at each node on the left**

are the Bayesian posterior probabilities and pie charts on the right are the maximum likelihood probabilities from ancestral state reconstructions. Exact probabilities are available in Appendix E.

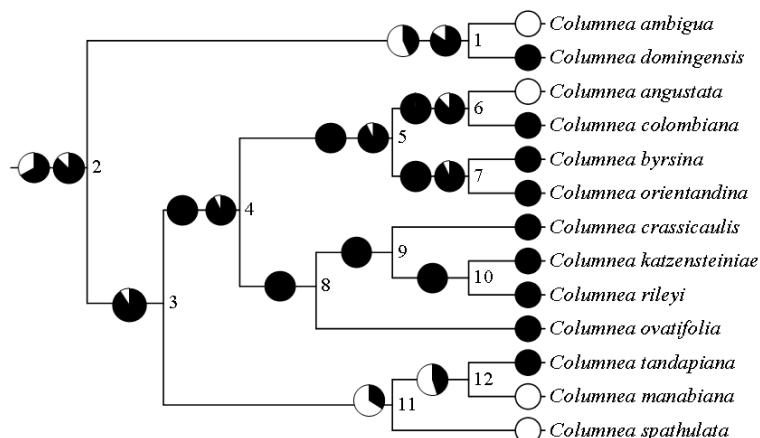


**Figure 3.3 – Ancestral State Reconstruction of Lamina Surface Area: Ancestral state reconstructions from Mk1 model and branch length reconstruction mapped onto a species level phylogenetic tree of section *Angustiflorae*. Character states are 0.0-30.0 cm<sup>2</sup> [0] – black and > 30.0 cm<sup>2</sup> [1] – white. Circles at extant taxa represent character state for species (Table 3.1). Pie charts at each node on the left are the Bayesian posterior probabilities (BPP) and pie charts on the right are the maximum likelihood probabilities (MLP) from ancestral state reconstructions. Nodes with only one pie chart have equal BPP and MLP values. Exact probabilities are available in Appendix E.**

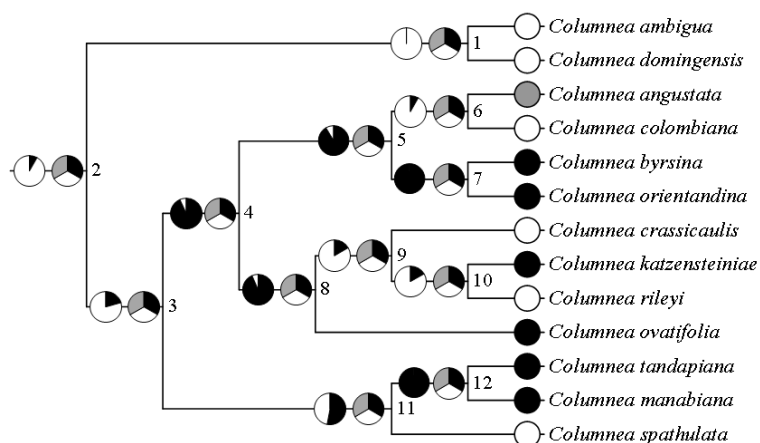


**Figure 3.4 – Ancestral State Reconstruction of Petiole Length: Ancestral state reconstructions from Mk1 model and branch length reconstruction mapped onto a species level phylogenetic tree of section *Angustiflorae*. Character states are 0.0-5.0 mm [0] – black, 5.0-20.0 mm [1] – white, and > 20.0 mm [2] – gray. Circles at extant taxa represent character state for species (Table 3.1). Pie charts at each node on the left are the Bayesian posterior probabilities and pie charts on the right are the maximum likelihood probabilities from ancestral state reconstructions. Exact probabilities are available in Appendix E.**

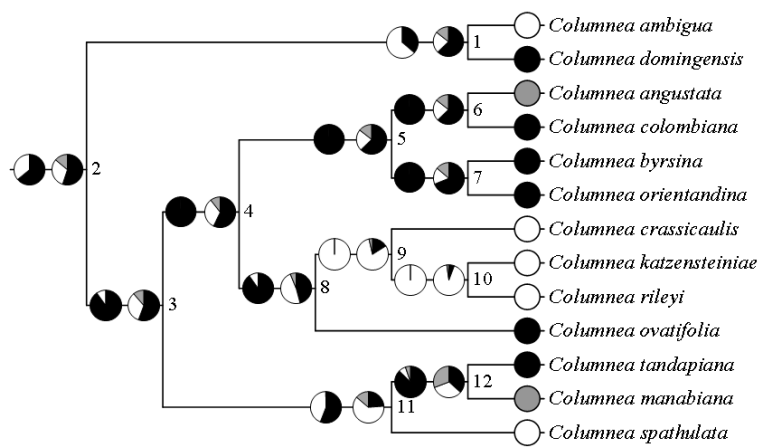


**Figure 3.5 – Ancestral State Reconstruction of Floral Bract Size: Ancestral state reconstructions from Mk1 model and branch length reconstruction mapped onto a species level phylogenetic tree of section *Angustiflorae*. Character states are 0.0-6.0 mm [0] – black, 6.0-13.0 mm [1] – white, and > 13.0 mm [2] – gray. Circles at extant taxa represent character state for species (Table 3.1). Pie charts at each node on the left are the Bayesian posterior probabilities and pie charts on the right are the maximum likelihood probabilities from ancestral state reconstructions. Exact probabilities are available in Appendix E.**

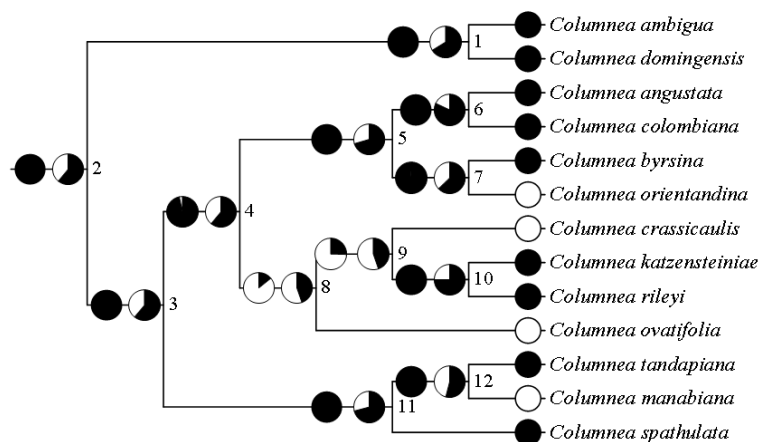


**Figure 3.6 – Ancestral State Reconstruction of Corolla to Calyx Ratio:** Ancestral state reconstructions from Mk1 model and branch length reconstruction mapped onto a species level phylogenetic tree of section *Angustiflorae*. Character states are 0.0-2.5 [0] – black and > 2.5 [1] – white. Circles at extant taxa represent character state for species (Table 3.1). Pie charts at each node on the left are the Bayesian posterior probabilities and pie charts on the right are the maximum likelihood probabilities from ancestral state reconstructions. Exact probabilities are available in Appendix E.

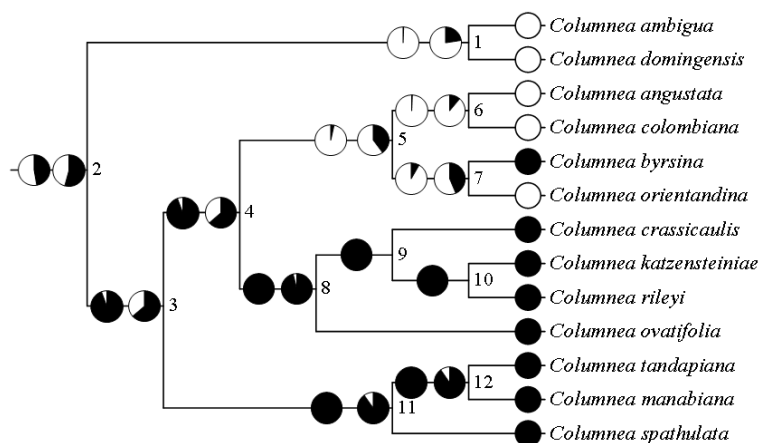


**Figure 3.7 – Ancestral State Reconstruction of Calyx Margin:** Ancestral state reconstructions from Mk1 model and branch length reconstruction mapped onto a species level phylogenetic tree of section *Angustiflorae*. Character states are entire [0] – black and serrate [1] – white. Circles at extant taxa represent character state for species (Table 3.1). Pie charts at each node on the left are the Bayesian posterior probabilities and pie charts on the right are the maximum likelihood probabilities

from ancestral state reconstructions. Exact probabilities are available in Appendix E.

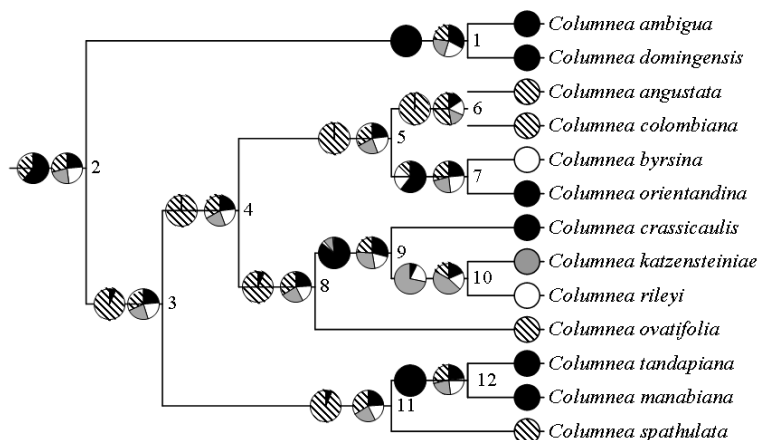


**Figure 3.8 – Ancestral State Reconstruction of Corolla Color:** Ancestral state reconstructions from Mk1 model and branch length reconstruction mapped onto a species level phylogenetic tree of section *Angustiflorae*. Character states are yellow corolla [0] – black, red corolla [1] – white, purple corolla [2] – gray, and polymorphic for color [3] – stripes. Circles at extant taxa represent character state for species (Table 3.1). Pie charts at each node on the left are the Bayesian posterior probabilities and pie charts on the right are the maximum likelihood probabilities from ancestral state reconstructions. Exact probabilities are available in Appendix E.

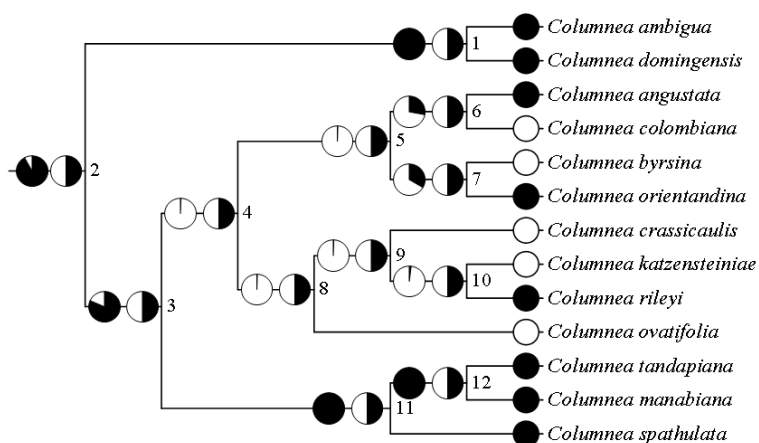


**Figure 3.9 – Ancestral State Reconstruction of Corolla Lobe Color:** Ancestral state reconstructions from Mk1 model and branch length reconstruction mapped onto a

species level phylogenetic tree of section *Angustiflorae*. Character states are same color as corolla [0] – black and different from corolla [1] – white. Circles at extant taxa represent character state for species (Table 3.1). Pie charts at each node on the left are the Bayesian posterior probabilities and pie charts on the right are the maximum likelihood probabilities from ancestral state reconstructions. Exact probabilities are available in Appendix E.

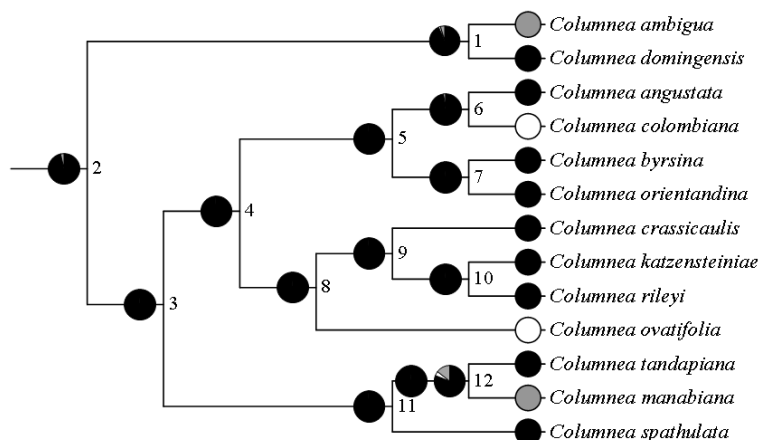


**Figure 3.10 – Ancestral State Reconstruction of Phenology: Ancestral state reconstructions from Mk1 model and branch length reconstruction mapped onto a species level phylogenetic tree of section *Angustiflorae*. Character states are flowering continuously [0] – black, flowering from January to March [1] – white, and flowering from March to October [2] – gray. Circles at extant taxa represent character state for species (Table 3.1). Pie charts at each node on the left are the Bayesian posterior probabilities (BPP) and pie charts on the right are the maximum likelihood probabilities (MLP) from ancestral state reconstructions. Nodes with only one pie chart have equal BPP and MLP values. Exact probabilities are available in Appendix E.**

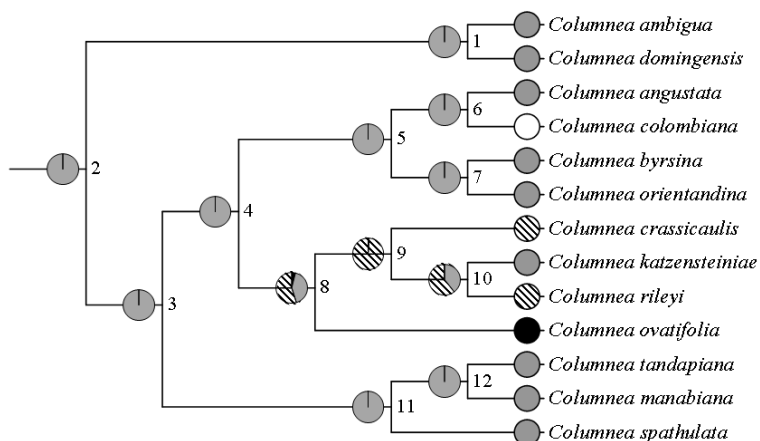


**Figure 3.11 – Ancestral State Reconstruction of Annual Mean Temperature: Ancestral state reconstructions from branch length reconstruction using Simmap 1.5 mapped onto a species level phylogenetic tree of section *Angustiflorae*. Character states are  $< 18.667$  °C [0] – black, 21.225-23.0 °C [1] – white, polymorphic [2] – gray, and  $< 21$  °C [3] – stripes. Circles at extant taxa represent character state for species (Table 3.1). Pie charts at each node represent the Bayesian posterior probability values. Exact probabilities are available in Appendix F.**

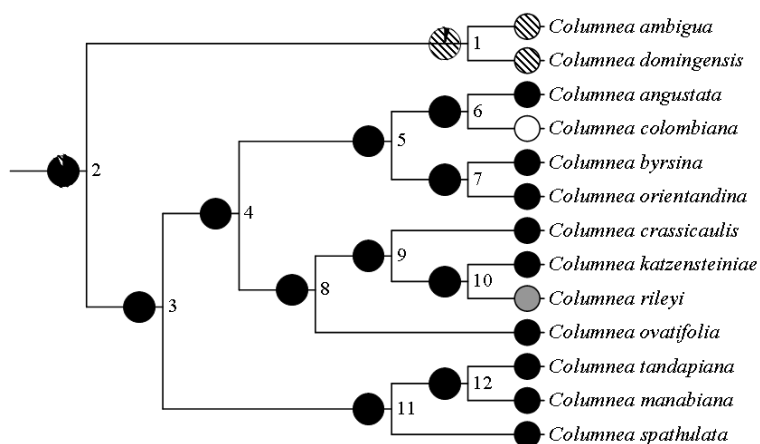


**Figure 3.12 – Ancestral State Reconstruction of Temperature Seasonality: Ancestral state reconstructions from branch length reconstruction using Simmap 1.5 mapped onto a species level phylogenetic tree of section *Angustiflorae*. Character states are polymorphic [0] – black, 265.75-439.5 [1] – white,  $< 439.5$  [2] – gray, and  $> 703.33$  [3] – stripes. Circles at extant taxa represent character state for species (Table 3.1). Pie charts at each node represent the Bayesian posterior probability values. Exact probabilities are available in Appendix F.**

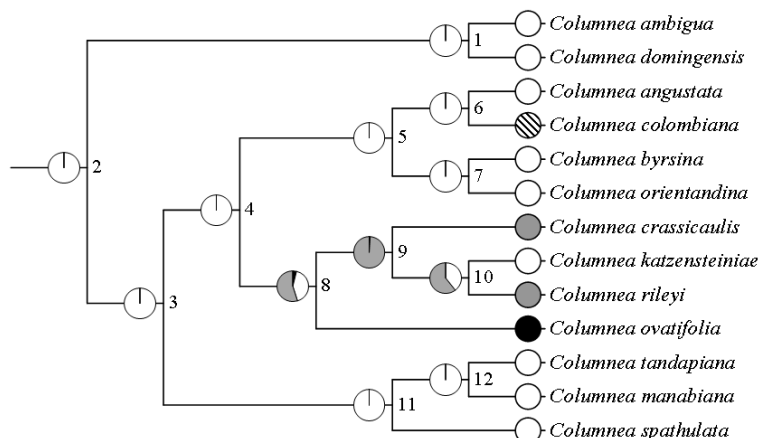


**Figure 3.13 – Ancestral State Reconstruction of Mean Temperature of Wettest, Driest, Warmest, and Coldest Quarters: Ancestral state reconstructions from branch length reconstruction using Simmap 1.5 mapped onto a species level phylogenetic tree of section *Angustiflorae*. Character states are < 18.85 °C [0] – black, polymorphic [1] – white, < 21.5 °C [2] – gray, and > 23.667 °C [3] – stripes for mean temperature of the wettest quarter; < 18.3 °C [0] – black, polymorphic [1] – white, < 20.98 °C [2] – gray, and > 22.633 °C [3] – stripes for mean temperature of the driest quarter; < 19.375 °C [0] – black, polymorphic [1] – white, < 21.85 °C [2] – gray, and > 23.9 °C [3] – stripes for mean temperature of the warmest quarter; < 18.133 °C [0] – black, polymorphic [1] – white, < 20.5 °C [2] – gray, and > 22.433 °C [3] – stripes for mean temperature of the coldest quarter. Though character states are different for each of the four bioclim variables represented on this tree, Bayesian posterior probabilities (BPP) were exactly the same for all four variables at all nodes and scores were the same for all extant species. Circles at extant taxa represent character state for species (Table 3.1). Pie charts at each node represent the BPP values. Exact probabilities are available in Appendix F.**



**Figure 3.15 – Summary of Forces Driving Speciation within Section Angustiflorae: Pictures represent causes of speciation at each node and for individual species. An island represents allopatric speciation; the photosynthesis Z-scheme represents a shift in photosynthetic ability; a bee represents an adaptation to nectar robbing; a hummingbird represents a pollinator shift; a raincloud represents a shift in precipitation; and a sun represents a shift in temperature.**

## APPENDIX A

**Species and Voucher Specimen for Chapter One Phylogenetic Analyses**

Two columns on the right designate how species of *Columnea* were classified by Wiehler (W, 1983; C – genus *Columnea*, D – genus *Dalbergaria*, T – genus *Trichantha*, P – genus *Pentadenia*, B – genus *Bucinellina*) and Kvist and Skog (K&S, 1993; C – section *Columnea*, Co – section *Collandra*, B – section *Bucinellina*, O – section *Ortholoma*, P – section *Pentadenia*, S – section *Stygnanthe*). Species in bold indicate members of section *Stygnanthe* sensu Smith (1994) and an asterisk (\*) indicates a species with a subradially to radially symmetric tubular corolla that was not placed in section *Stygnanthe* by Smith (1994).

Species	Voucher	Herbarium	Locality	W	K&S
<i>Alloplectus hispidus</i> (Kunth.) Mart.	<i>J. L. Clark</i> 7720	US	Ecuador		
<i>Columnea albiflora</i> L. P. Kvist & L. E. Skog	<i>J. L. Clark &amp;</i> <i>J. Rea 8015</i>	UNA	Ecuador	D	Co
<b><i>C. ambigua</i> (Urb.) B. D. Morley</b>	<i>J. Smith 3701</i>	SRP	cultivated, originally Puerto Rico	T	NA
<b><i>C. angustata</i> (Wiehler) L. E. Skog</b>	<i>Amaya M. &amp;</i> <i>J. Smith 625</i>	COL	Brazil	P	S
<b><i>C. angustata</i> (Wiehler) L. E. Skog</b>	<i>J. Smith 1433</i>	WIS	Colombia	P	S
<b><i>C. angustata</i> (Wiehler) L. E. Skog</b>	<i>J. L. Clark</i> 8627	UNA	Panama	P	S
<b><i>C. angustata</i> (Wiehler) L. E. Skog</b>	<i>J. L. Clark et</i> <i>al. 9373</i>	US	Ecuador	P	S
<b><i>C. angustata</i> (Wiehler) L. E. Skog</b>	<i>J. L. Clark et</i> <i>al. 9609</i>	UNA	Ecuador	P	S
<b><i>C. angustata</i> (Wiehler) L. E. Skog</b>	<i>J. L. Clark et</i> <i>al. 9854</i>	UNA	Ecuador	P	S
<b><i>C. angustata</i> (Wiehler) L. E. Skog</b>	<i>J. Smith 2246</i>	WIS	cultivated at SEL	P	S
<i>C. anisophylla</i> DC.	<i>E. Tepe 1081</i>	SRP	Panama	T	O
<i>C. anisophylla</i> DC.	<i>J. L. Clark &amp;</i> <i>J. Rea 8019</i>	UNA	Ecuador	T	O
<i>C. atahualpae</i> J. F. Smith & L. E. Skog	<i>J. L. Clark et</i> <i>al. 8000</i>	UNA	Ecuador	NA	NA
<i>C. bilabiata</i> Seem.	<i>J. L. Clark et</i> <i>al. 11157</i>	UNA	Ecuador	C	C
<i>C. brenneri</i> (Wiehler) B. D. Morley	<i>J. L. Clark &amp;</i> <i>M. Mailloux</i> 7842	UNA	Ecuador	T	O
<i>C. brevipila</i> Urb.	<i>B. Stewart s.</i> <i>n.</i>	SRP	cultivated, originally from Jamaica	C	C

<b>Species</b>	<b>Voucher</b>	<b>Herbarium</b>	<b>Locality</b>	<b>W</b>	<b>K&amp;S</b>
<b><i>C. byrsina</i> (Wiehler) L. P. Kvist &amp; L. E. Skog</b>	<i>J. Smith 3408</i>	SRP	Ecuador	P	S
<b><i>C. byrsina</i> (Wiehler) L. P. Kvist &amp; L. E. Skog</b>	<i>J. L. Clark &amp; O. Meija 6291</i>	UNA	Ecuador	P	S
<b><i>C. byrsina</i> (Wiehler) L. P. Kvist &amp; L. E. Skog</b>	<i>J. L. Clark 2413</i>	US	Ecuador	P	S
<b><i>C. byrsina</i> (Wiehler) L. P. Kvist &amp; L. E. Skog</b>	<i>J. L. Clark et al. 7518</i>	US	Ecuador	P	S
<b><i>C. byrsina</i> (Wiehler) L. P. Kvist &amp; L. E. Skog</b>	<i>H. Wiehler 77122</i>	SEL	cultivated at SEL	P	S
<b><i>C. byrsina</i> (Wiehler) L. P. Kvist &amp; L. E. Skog</b>	<i>T. Croat 94841</i>	MO	Ecuador	P	S
<i>C. calotricha</i> Donn. Sm.	<i>J. Smith et al. 4117</i>	SRP	French Guiana	T	O
<i>C. ciliata</i> (Wiehler) L. P. Kvist & L. E. Skog	<i>J. L. Clark et al. 7508</i>	UNA	Ecuador	T	O
<b><i>C. colombiana</i> (Wiehler) L. P. Kvist &amp; L. E. Skog</b>	<i>J. L. Clark et al. 10024</i>	UNA	cultivated	P	S
<b><i>C. colombiana</i> (Wiehler) L. P. Kvist &amp; L. E. Skog</b>	<i>J. L. Clark 8874</i>	US	cultivated	P	S
<b><i>C. colombiana</i> (Wiehler) L. P. Kvist &amp; L. E. Skog</b>	<i>J. Smith 1126</i>	WIS	cultivated at SEL	P	S
<i>C. consanguinea</i> Hanst.	<i>E. Tepe 1082</i>	SRP	Panama	D	Co
<b><i>C. crassicaulis</i> (Wiehler) L. P. Kvist &amp; L. E. Skog</b>	<i>J. L. Clark 8859</i>	US	cultivated	P	S
<i>C. cruenta</i> B. D. Morley	<i>J. Smith 8606</i>	SRP	cultivated, originally from Panama	D	Co
<i>C. densibracteata</i> L. P. Kvist & L. E. Skog	<i>J. Smith 1972</i>	WIS	Ecuador	D	
<i>C. dielsii</i> Mansf.	<i>J. Smith 1989</i>	WIS	Ecuador	A	A
<i>C. dissimilis</i> C. V. Morton	<i>E. Tepe 1070</i>	SRP	Panama	T	O
<i>C. dodsonii</i> Wiehler	<i>B. Stewart s. n.</i>	SRP	cultivated	C	C
* <i>C. domingensis</i> (Urb.) B. D. Morley	<i>L. Hahn 445</i>	SRP	Dominican Republic	T	NA
<b><i>C. eburnea</i> (Wiehler) L. P. Kvist &amp; L. E. Skog</b>	<i>J. L. Clark et al. 6353</i>	UNA	Ecuador	D	Co
<b><i>C. elongatifolia</i> L. P. Kvist &amp; L. E. Skog</b>	<i>J. L. Clark et al. 10015</i>	UNA	cultivated, originally from Ecuador	T	O
<i>C. ericae</i> Mansf.	<i>J. L. Clark et al. 6920</i>	UNA	Ecuador	D	Co

<b>Species</b>	<b>Voucher</b>	<b>Herbarium</b>	<b>Locality</b>	<b>W</b>	<b>K&amp;S</b>
<i>C. ericae</i> Mansf.	<i>E. Tepe 1570</i>	UNA	Ecuador	D	Co
<i>C. erythrophaea</i> Decne. Ex Houllet	<i>J. Smith 3727</i>	SRP	cultivated	C	C
<i>C. filifera</i> (Wiehler) L. P. Kvist & L. E. Skog	<i>J. L. Clark et al. 7140</i>	UNA	Ecuador	T	O
<i>C. fimbriicalyx</i> L. P. Kvist & L. E. Skog	<i>J. L. Clark et al. 7395</i>	UNA	Ecuador	T	O
<i>C. flexiflora</i> L. P. Kvist & L. E. Skog	<i>J. L. Clark &amp; L. Jost 6968</i>	UNA	Ecuador	T	O
<i>C. gallicauda</i> Wiehler	<i>J. L. Clark 6283</i>	UNA	cultivated	C	C
<i>C. gloriosa</i> Sprague	<i>J. L. Clark et al. 9921</i>	UNA	Ecuador	C	C
* <i>C. grisebachiana</i> Kuntze	<i>J. Smith 10041</i>	IJ	Jamaica	T	NA
<i>C. guianensis</i> C. V. Morton	<i>J. Smith 3711</i>	SRP	Guyana	D	Co
<i>C. guttata</i> Poepp.	<i>J. L. Clark &amp; L. Jost 6974</i>	UNA	Ecuador	D	Co
<i>C. herthae</i> Mansf.	<i>J. L. Clark et al. 11055</i>	UNA	Ecuador	T	O
<i>C. hypocyrthantha</i> (Wiehler) J. F. Smith & L. E. Skog	<i>J. L. Clark &amp; E. Rodriguez 6741</i>	US	Bolivia	P	NA
<i>C. illepida</i> Moore	<i>J. Smith s. n.</i>	SRP	cultivated	T	O
<i>C. illepida</i> Moore	<i>J. L. Clark et al. 11448</i>	UNA	Peru	T	O
<i>C. isernii</i> Cuatrec.	<i>J. Smith 2010</i>	WIS	Ecuador	P	S
<i>C. isernii</i> Cuatrec.	<i>J. L. Clark et al. 6253</i>	UNA	Ecuador	P	S
<b><i>C. katzensteiniae</i> (Wiehler) L. P. Kvist &amp; L. E. Skog</b>	<i>J. L. Clark et al. 7625</i>	UNA	Ecuador	P	S
<i>C. lehmannii</i> Mansf.	<i>J. L. Clark et al. 4960</i>	UNA	Ecuador	T	O
<i>C. lehmannii</i> Mansf.	<i>J. L. Clark et al. 7113</i>	UNA	Ecuador	T	O
<i>C. lophophora</i> Mansf.	<i>J. L. Clark et al. 7888</i>	US	Ecuador	P	S
<i>C. lophophora</i> Mansf.	<i>J. L. Clark et al. 8898</i>	UNA	Ecuador	P	S
<i>C. magnifica</i> Klotzsch ex. Oerst.	<i>J. Smith 8602</i>	SRP	cultivated	C	C
<b><i>C. manabiana</i> (Wiehler) J. F. Sm. &amp; L. E. Skog</b>	<i>Dodson &amp; Dodson 6791</i>	SEL	cultivated at SEL	P	S

<b>Species</b>	<b>Voucher</b>	<b>Herbarium</b>	<b>Locality</b>	<b>W</b>	<b>K&amp;S</b>
<i>C. microphylla</i> Klotsch & Hanst.	<i>J. L. Clark</i> 6261	UNA	cultivated	C	C
<i>C. minor</i> (Hook.) Hanst.	<i>B. Stewart s.</i> <i>n.</i>	SRP	cultivated	T	O
<i>C. minor</i> (Hook.) Hanst.	<i>J. L. Clark s.</i> <i>n.</i>	SRP	Ecuador	T	O
<i>C. minor</i> (Hook.) Hanst.	<i>T. Croat</i> 94778	MO	Ecuador	T	O
<i>C. minutiflora</i> L. P. Kvist & L. E. Skog	<i>J. L. Clark et al.</i> 10832	UNA	Ecuador	T	O
<i>C. minutiflora</i> L. P. Kvist & L. E. Skog	<i>J. L. Clark et al.</i> 7092	US	Ecuador	T	O
<i>C. mira</i> B. D. Morley	<i>J. Smith</i> 2450	WIS	cultivated, originally from Panama	T	O
<b><i>C. moesta</i> Poepp.</b>	<i>J. Smith</i> 1829	WIS	Bolivia	P	NA
<b><i>C. moesta</i> Poepp.</b>	<i>J. L. Clark &amp; M. Zeballos</i> 6850	UNA	Bolivia	P	NA
<b><i>C. moesta</i> Poepp.</b>	<i>J. L. Clark &amp; D. Barrientos</i> 6690	US	Bolivia	P	NA
<b><i>C. moesta</i> Poepp.</b>	<i>J. L. Clark et al.</i> 8211	UNA	Peru	P	NA
* <i>C. moorei</i> C. V. Morton	<i>J. L. Clark</i> 11307	UNA	cultivated	O	NA
<i>C. oblongifolia</i> Rusby	<i>J. Smith</i> 1721	WIS	Bolivia	T	NA
<b><i>C. orientandina</i> Mansf.</b>	<i>J. Smith</i> 3421	SRP	Ecuador	P	S
<b><i>C. orientandina</i> Mansf.</b>	<i>J. L. Clark et al.</i> 9885	UNA	Ecuador	P	S
<b><i>C. orientandina</i> Mansf.</b>	<i>L. Schulte</i> 65	SRP	cultivated	P	S
<b><i>C. ovatifolia</i> L. P. Kvist &amp; L. E. Skog</b>	<i>J. Smith</i> 1921	WIS	Ecuador	P	S
<b><i>C. ovatifolia</i> L. P. Kvist &amp; L. E. Skog</b>	<i>J. L. Clark</i> 8461	US	Ecuador	P	S
<i>C. paramicola</i> (Wiehler) L. P. Kvist & L. E. Skog	no voucher USBRG94529	NA	cultivated	B	B
<i>C. picta</i> H. Karst.	<i>T. Croat</i> 94956	MO	Ecuador	D	Co
<i>C. pulchra</i> (Wiehler) L. E. Skog	no voucher	-	cultivated	T	O
<i>C. pulchra</i> (Wiehler) L. E. Skog	<i>J. L. Clark</i> 6265	US	cultivated	T	O

<b>Species</b>	<b>Voucher</b>	<b>Herbarium</b>	<b>Locality</b>	<b>W</b>	<b>K&amp;S</b>
<i>C. purpusii</i> Standl.	<i>A. Rincon et al.</i> 2302	XAL	Mexico	C	C
<i>C. repens</i> (Hook.) Hanst.	<i>J. Smith</i> 8605	SRP	cultivated, originally from Jamaica	T	NA
<b><i>C. rileyi</i> (Wiehler) J. F. Smith</b>	<i>J. Smith</i> 1944	WIS	Ecuador	P	S
<b><i>C. rileyi</i> (Wiehler) J. F. Smith</b>	<i>J. L. Clark</i> 6263	US	Ecuador	P	S
<b><i>C. rileyi</i> (Wiehler) J. F. Smith</b>	<i>J. L. Clark</i> 7077	US	Ecuador	P	S
<i>C. rubricalyx</i> L. P. Kvist & L. E. Skog	<i>J. L. Clark et al.</i> 11034	UNA	Ecuador	T	O
<i>C. rubricalyx</i> L. P. Kvist & L. E. Skog	<i>T. Croat</i> 95236	MO	Ecuador	T	O
<i>C. sanguinea</i> (Pers.) Hanst.	<i>J. Smith</i> 636	WIS	cultivated	D	Co
<i>C. scandens</i> L.	<i>J. L. Clark &amp; S. G. Clark</i> 6541	UNA	Martinique	C	C
<i>C. schiedeana</i> Schltldl.	<i>J. Smith</i> 288	WIS	cultivated, originally from Mexico	C	C
<i>C. schimpfii</i> Mansf.	<i>J. Smith</i> 8605	SRP	cultivated, originally from Ecuador	D	Co
<i>C. segregata</i> (B. D. Morley) Wiehler	<i>J. L. Clark et al.</i> 10029	UNA	cultivated	T	O
<i>C. sp.</i>	<i>J. L. Clark &amp; N. Harris</i> 7295	SRP	Ecuador		
<b><i>C. spathulata</i> Mansf.</b>	<i>J. Smith</i> 1853	WIS	Ecuador	P	S
<b><i>C. spathulata</i> Mansf.</b>	<i>J. L. Clark et al.</i> 7485	UNA	Ecuador	P	S
<b><i>C. spathulata</i> Mansf.</b>	<i>T. Croat</i> 95254	MO	Ecuador	P	S
<b><i>C. spathulata</i> Mansf.</b>	<i>J. Smith</i> 651	WIS	cultivated at SEL	P	S
<i>C. strigosa</i> Benth.	<i>J. Smith</i> 1200	WIS	Venezuela	P	P
<i>C. strigosa</i> Benth.	<i>T. Croat</i> 94580	MO	Ecuador	P	P
<b><i>C. tandapiana</i> (Wiehler) L.E. Skog &amp; L.P. Kvist</b>	<i>L. Schulte</i> 66	SRP	cultivated	P	S
<b><i>C. tandapiana</i> (Wiehler)</b>	<i>J. L. Clark et</i>	US	Ecuador	P	S

<b>Species</b>	<b>Voucher</b>	<b>Herbarium</b>	<b>Locality</b>	<b>W</b>	<b>K&amp;S</b>
<b><i>L.E. Skog &amp; L.P. Kvist</i></b>	<i>al. 8006</i>				
<i>C. tenella</i> L. P. Kvist & L. E. Skog	<i>M. Amaya M. &amp; J. Smith 603</i>	COL	Colombia	T	O
<i>C. tenensis</i> Wiehler	<i>J. L. Clark et al. 9500</i>	UNA	Ecuador	T	O
<i>C. tenensis</i> Wiehler	<i>J. Smith 3374</i>	SRP	Ecuador	T	O
<i>C. trollii</i> Mansf.	<i>J. Smith 1723</i>	WIS	Bolivia	P	NA
* <i>C. ulei</i> Mansf.	<i>A. Chautems 2803</i>	G	Brazil	T	NA
<b><i>C. ultraviolacea</i> J. F. Smith &amp; L. E. Skog</b>	<i>J. L. Clark &amp; V. Velaz 6603</i>	UNA	Bolivia	NA	NA
<i>C. villosissima</i> Mansf.	<i>E. Tepe 1628</i>	SRP	Ecuador	D	Co
<b><i>C. xiphoidea</i> J. F. Sm. &amp; L. E. Skog</b>	<i>Allard 21300</i>	US	Peru	NA	NA
<i>Corytoplectus capitatus</i> (Hook.) Wiehler	no voucher	-	cultivated		
<i>Corytoplectus speciosus</i> (Poepp.) Wiehler	no voucher, SI 94-268	-	cultivated		
<i>Crantzia cristata</i> (L.) Scopoli	<i>J. L. Clark 6346</i>	US	Martinique		
<i>Crantzia epirotes</i> (Leeuwenb.) J. L. Clark	<i>D. Clarke 10172</i>	US	Guyana		
<i>Crantzia tigrina</i> (Karsten.) J. L. Clark	<i>J. L. Clark 6892</i>	US	Venezuela		
<i>Drymonia coccinea</i> (Aubl.) Wiehler	<i>J. Smith 3373</i>	SRP	Ecuador		
<i>Drymonia pendula</i> (Poepp.) Wiehler	<i>J. Smith 3384</i>	SRP	Ecuador		
<i>Drymonia pilifera</i> Wiehler	<i>E. Tepe 1065</i>	SRP	Panama		
<i>Drymonia serrulata</i> (Jacq.) Mart.	<i>J. Smith 4202</i>	SRP	French Guiana		
<i>Drymonia strigosa</i> (Oerst.) Wiehler	<i>A. Rincon 2301</i>	XAL	Mexico		
<i>Drymonia turrialvae</i> Hanst.	<i>E. Tepe 1063</i>	SRP	Panama		
<i>Drymonia urceolata</i> Wiehler	<i>J. Smith 3416</i>	SRP	Ecuador		
<i>Glossoloma anomalum</i> J. L. Clark	<i>J. Smith 3418</i>	SRP	Ecuador		
<i>Glossoloma grandicalyx</i> (J. L. Clark & L. E. Skog) J. L. Clark	<i>J. Smith 3417</i>	SRP	Ecuador		
<i>Glossoloma martinianus</i> (J. F. Smith) J. L. Clark	<i>J. L. Clark 6101</i>	US	Ecuador		

<b>Species</b>	<b>Voucher</b>	<b>Herbarium</b>	<b>Locality</b>	<b>W</b>	<b>K&amp;S</b>
<i>Glossoloma panamensis</i> (C. V. Morton) J. L. Clark	<i>L. E. Skog et al. 7641</i>	US	cultivated		
<i>Neomortonia nummularia</i> (Hanst.) Wiehler	<i>J. Smith 3944</i>	SRP	cultivated		
<i>Neomortonia rosea</i> Wiehler	no voucher, SI 94-230	-	cultivated		

## APPENDIX B

**Species and Voucher Specimens for Chapter Two Phylogenetic Analyses**

Columns on the right side indicate the partitions that each accession was amplified for. Accessions with the letter F were amplified for the full data set analyses, accessions with the letter R were amplified for the reduced data set, and accessions with an asterisk (\*) indicate accessions that were amplified for seven additional gene regions (*trnK1F-matKR*, *matK1F-1R*, *matK2F-2R*, *G3pdhA*, *G3pdhB*, *idhA*, and *idhB*) to test the ability of the gene regions to identify species level relationships within section *Angustiflorae*.

Species	Voucher	Herbarium	Locality			
Ingroup						
<i>Columnnea ambigua</i> (Urb.) B. D. Morley	<i>J. Smith</i> 3701	SRP	cultivated, originally Puerto Rico	F	R	*
<i>C. angustata</i> (Wiehler) L. E. Skog	<i>Amaya M.</i> & <i>J. Smith</i> 625	COL	Brazil	F		
<i>C. angustata</i> (Wiehler) L. E. Skog	<i>J. Smith</i> 1433	WIS	Colombia	F		
<i>C. angustata</i> (Wiehler) L. E. Skog	<i>J. L. Clark</i> 8627	UNA	Panama	F	R	
<i>C. angustata</i> (Wiehler) L. E. Skog	<i>J. L. Clark</i> <i>et al.</i> 9373	US	Ecuador	F		
<i>C. angustata</i> (Wiehler) L. E. Skog	<i>J. L. Clark</i> <i>et al.</i> 9609	UNA	Ecuador	F		
<i>C. angustata</i> (Wiehler) L. E. Skog	<i>J. L. Clark</i> <i>et al.</i> 9854	UNA	Ecuador	F		
<i>C. angustata</i> (Wiehler) L. E. Skog	<i>J. Smith</i> 2246	WIS	cultivated at SEL	F		
<i>C. byrsina</i> (Wiehler) L. P. Kvist & L. E. Skog	<i>J. Smith</i> 3408	SRP	Ecuador	F	R	
<i>C. byrsina</i> (Wiehler) L. P. Kvist & L. E. Skog	<i>J. L. Clark</i> & <i>O.</i> <i>Meija</i> 6291	UNA	Ecuador	F	R	*
<i>C. byrsina</i> (Wiehler) L. P. Kvist & L. E. Skog	<i>J. L. Clark</i> 2413	US	Ecuador	F	R	
<i>C. byrsina</i> (Wiehler) L. P. Kvist & L. E. Skog	<i>J. L. Clark</i> <i>et al.</i> 7518	US	Ecuador	F		
<i>C. byrsina</i> (Wiehler) L. P. Kvist & L. E. Skog	<i>H.</i> <i>Wiehler</i> 77122	SEL	cultivated at SEL	F		
<i>C. byrsina</i> (Wiehler) L. P. Kvist & L. E. Skog	<i>T. Croat</i> 94841	MO	Ecuador	F	R	
<i>C. colombiana</i> (Wiehler) L. P. Kvist & L. E. Skog	<i>J. L. Clark</i> <i>et al.</i> 10024	UNA	cultivated	F	R	
<i>C. colombiana</i> (Wiehler)	<i>J. L. Clark</i>	US	cultivated	F		

Species	Voucher	Herbarium	Locality		
L. P. Kvist & L. E. Skog	8874				
<i>C. colombiana</i> (Wiehler)	<i>J. Smith</i>	WIS	cultivated at SEL	F	R
L. P. Kvist & L. E. Skog	1126				
<i>C. crassicaulis</i> (Wiehler)	<i>J. L. Clark</i>	US	cultivated	F	R
L. P. Kvist & L. E. Skog	8859				
<i>C. domingensis</i> (Urb.) B. D. Morley	<i>L. Hahn</i> 445	SRP	Dominican Republic	F	R
<i>C. katzensteiniae</i> (Wiehler) L. P. Kvist & L. E. Skog	<i>J. L. Clark et al.</i> 7625	UNA	Ecuador	F	R
<i>C. manabiana</i> (Wiehler) J. F. Sm. & L. E. Skog	<i>Dodson &amp; Dodson</i> 6791	SEL	cultivated at SEL, originally from Ecuador	F	R
<i>C. orientandina</i> Mansf.	<i>J. Smith</i> 3421	SRP	Ecuador	F	
<i>C. orientandina</i> Mansf.	<i>J. L. Clark et al.</i> 9885	UNA	Ecuador	F	R
<i>C. orientandina</i> Mansf.	<i>L. Schulte</i> 65	SRP	cultivated	F	
<i>C. ovatifolia</i> L. P. Kvist & L. E. Skog	<i>J. Smith</i> 1921	WIS	Ecuador	F	R
<i>C. ovatifolia</i> L. P. Kvist & L. E. Skog	<i>J. L. Clark</i> 8461	US	Ecuador	F	
<i>C. rileyi</i> (Wiehler) J. F. Smith	<i>J. Smith</i> 1944	WIS	Ecuador	F	R
<i>C. rileyi</i> (Wiehler) J. F. Smith	<i>J. L. Clark</i> 6263	US	Ecuador	F	
<i>C. rileyi</i> (Wiehler) J. F. Smith	<i>J. L. Clark</i> 7077	US	Ecuador	F	
<i>C. spathulata</i> Mansf.	<i>J. Smith</i> 1853	WIS	Ecuador	F	R
<i>C. spathulata</i> Mansf.	<i>J. L. Clark et al.</i> 7485	UNA	Ecuador	F	R
<i>C. spathulata</i> Mansf.	<i>T. Croat</i> 95254	MO	Ecuador	F	
<i>C. spathulata</i> Mansf.	<i>J. Smith</i> 651	WIS	cultivated at SEL	F	
<i>C. tandapiana</i> (Wiehler) L.E. Skog & L.P. Kvist	<i>L. Schulte</i> 66	SRP	cultivated	F	R
<i>C. tandapiana</i> (Wiehler) L.E. Skog & L.P. Kvist	<i>J. L. Clark et al.</i> 8006	US	Ecuador	F	R
<i>C. ulei</i> Mansf.	A. <i>Chautems</i> 2803	G	Brazil	F	R

Species	Voucher	Herbarium	Locality	
<b>Outgroup</b>				
<i>C. bilabiata</i> Seem.	<i>J. L. Clark et al.</i> 11157	UNA	Ecuador	*
<i>C. brenneri</i> (Wiehler) B. D. Morley	<i>J. L. Clark &amp; M. Mailloux</i> 7842	UNA	Ecuador	F R
<i>C. calotricha</i> Donn. Sm.	<i>J. Smith et al.</i> 4117	SRP	French Guiana	*
<i>C. consanguinea</i> Hanst.	<i>E. Tepe</i> 1082	SRP	Panama	F R
<i>C. dielsii</i> Mansf.	<i>J. Smith</i> 1989	WIS	Ecuador	F R
<i>C. illepida</i> Moore	<i>J. Smith s. n.</i>	SRP	cultivated	F R
<i>C. isernii</i> Cuatrec.	<i>J. L. Clark et al.</i> 6253	UNA	Ecuador	*
<i>C. lophophora</i> Mansf.	<i>J. L. Clark et al.</i> 8898	UNA	Ecuador	F R *
<i>C. microphylla</i> Klotsch & Hanst.	<i>J. L. Clark</i> 6261	UNA	cultivated	F R
<i>C. minor</i> (Hook.) Hanst.	<i>B. Stewart s. n.</i>	SRP	cultivated	F
<i>C. minutiflora</i> L. P. Kvist & L. E. Skog	<i>J. L. Clark et al.</i> 10832	UNA	Ecuador	F R
<i>C. moesta</i> Poepp.	<i>J. Smith</i> 1829	WIS	Bolivia	F
<i>C. moorei</i> C.V. Morton	<i>J. L. Clark</i> 11307	UNA	cultivated	F
<i>C. oblongifolia</i> Rusby	<i>J. Smith</i> 1721	WIS	Bolivia	F R
<i>C. picta</i> H. Karst.	<i>T. Croat</i> 94956	MO	Ecuador	F R
<i>C. purpusii</i> Standl.	<i>A. Rincon et al.</i> 2302	XAL	Mexico	F R
<i>C. rubriacuta</i> (Wiehler) L. P. Kvist & L. E. Skog	<i>J. L. Clark et al.</i> 4975	US	Ecuador	F
<i>C. scandens</i> L.	<i>J. L. Clark &amp; S. G. Clark</i> 6541	UNA	Martinique	*
<i>C. schimpfii</i> Mansf.	<i>J. Smith</i>	SRP	cultivated, originally	*

Species	Voucher	Herbarium	Locality	
	8605		from Ecuador	
<i>C. strigosa</i> Benth.	<i>T. Croat</i> 94580	MO	Ecuador	*
<i>Glossoloma anomalum</i> J. L. Clark	<i>J. Smith</i> 3418	SRP	Ecuador	F
<i>Glossoloma grandicalyx</i> (J. L. Clark & L. E. Skog) J. L. Clark	<i>J. Smith</i> 3417	SRP	Ecuador	F
<i>Glossoloma martinianus</i> (J. F. Smith) J. L. Clark	<i>J. L. Clark</i> 6101	US	Ecuador	F
<i>Glossoloma panamensis</i> (C. V. Morton) J. L. Clark	<i>L. E. Skog et al.</i> 7641	US	cultivated	F

## APPENDIX C

**Latitude and Longitude Data for 493 Herbarium Collection Specimens**

Species	Accession Number	Herbarium	Latitude	Longitude
<i>C. ambigua</i> (Urb.) B. D. Morley	A. A. Heller 4617	US	18°10'20.44"N	66°35'28.57"W
<i>C. ambigua</i> (Urb.) B. D. Morley	B. G. Schubert & H. F. Winters 393	US	18°18'35.14"N	65°47'35.72"W
<i>C. ambigua</i> (Urb.) B. D. Morley	B. M. Boom 6925	US	18° 17' N	65° 47' W
<i>C. ambigua</i> (Urb.) B. D. Morley	B. M. Boom 7972	US	18° 16' N	65° 45' W
<i>C. ambigua</i> (Urb.) B. D. Morley	B. M. Boom 9861	US	18° 07' N	66° 05' W
<i>C. ambigua</i> (Urb.) B. D. Morley	C. M. Taylor & R. Gereau 11857	MO	18° 20' N	65° 50' W
<i>C. ambigua</i> (Urb.) B. D. Morley	C. M. Taylor 11679	MO	18° 20' N	65° 50' W
<i>C. ambigua</i> (Urb.) B. D. Morley	F. Axelrod & P. Chavez 2958	MO	18°14'36.43"N	65°49'16.79"W
<i>C. ambigua</i> (Urb.) B. D. Morley	F. H. Sargent 3170	US, MO	18°12'26.07"N	66°32'11.72"W
<i>C. ambigua</i> (Urb.) B. D. Morley	F. H. Sargent 8137	MO	18°17'39.37"N	65°46'13.26"W
<i>C. ambigua</i> (Urb.) B. D. Morley	J. A. Shafer 3594	US	18°16'42.60"N	65°48'43.49"W
<i>C. ambigua</i> (Urb.) B. D. Morley	N. L. Britton & J. A. Shafer 20016	US	18° 7'45.12"N	66°53'25.56"W
<i>C. ambigua</i> (Urb.) B. D. Morley	N. L. Britton & J. F. Cowell 931	US	18°12'20.86"N	66°35'6.43"W
<i>C. ambigua</i> (Urb.) B. D. Morley	P. Acevedo Rodriguez & J. Alvarez 002987	MO	18° 7'24.16"N	66°31'37.55"W
<i>C. ambigua</i> (Urb.) B. D. Morley	P. Acevedo-Rdgz. 7108	US	18° 16.2' N	65° 49.3' W
<i>C. ambigua</i> (Urb.) B. D. Morley	P. Acevedo-Rdgz. 7923	US	18° 06'56" N	66° 06'11' W
<i>C. ambigua</i> (Urb.) B. D. Morley	Pfeifer et al. 2836	CONN	18°17'27.36"N	65°48'3.38"W
<i>C. ambigua</i> (Urb.) B. D. Morley	R. A. Howard 16815	US, SI, SEL, MO	18°16'33.99"N	65°45'53.43"W
<i>C. ambigua</i> (Urb.) B. D. Morley	R. A. Howard 16828	US	18° 6'49.97"N	66° 3'4.95"W
<i>C. ambigua</i> (Urb.) B. D. Morley	R. J. Wagner 1750	MO	18°16'34.84"N	65°45'52.59"W
<i>C. ambigua</i> (Urb.) B. D. Morley	S. A. Thompson 9995	US	18° 08' N	66° 34' W
<i>C. ambigua</i> (Urb.)	Sintenis 1301	MO	18°16'52.83"N	65°46'58.59"W

B. D. Morley				
<i>C. ambigua</i> (Urb.) B. D. Morley	T. G. Hartley 13321	MO, US, SI, SEL	18°16'34.84"N	65°45'52.59"W
<i>C. ambigua</i> (Urb.) B. D. Morley	W. G. D'Arcy 1859	MO	18° 6'16.66"N	66°46'54.00"W
<i>C. ambigua</i> (Urb.) B. D. Morley	W. G. D'Arcy 1860	MO	18°13'15.00"N	66°35'24.54"W
<i>C. angustata</i> (Wiehler) L. E. Skog	A. Gentry & A. Juncosa 40668	COL, MO	3° 15' N	77° 25' W
<i>C. angustata</i> (Wiehler) L. E. Skog	A. Gentry 18026	MO	0°52'3.37"S	79°26'56.18"W
<i>C. angustata</i> (Wiehler) L. E. Skog	A. Gentry 34920	COL	1°20'20.62"N	78°34'9.40"W
<i>C. angustata</i> (Wiehler) L. E. Skog	A. Gentry et al. 48327	MO	3° 55' N	77° 2' W
<i>C. angustata</i> (Wiehler) L. E. Skog	A. Gentry et al. 70070	US	00° 55' S	78° 35' W
<i>C. angustata</i> (Wiehler) L. E. Skog	A. Gomez et al. 499	SEL	5°19' N	77°17' W
<i>C. angustata</i> (Wiehler) L. E. Skog	A. Hirtz & X. Hirtz 4468	SEL	0°58'16.43"S	77°22'25.36"W
<i>C. angustata</i> (Wiehler) L. E. Skog	A. Hirtz 4473	SEL	0°10'31.88"N	77°16'11.14"W
<i>C. angustata</i> (Wiehler) L. E. Skog	A. Hirtz 9609	SEL	1°20'34.72"S	77°24'10.52"W
<i>C. angustata</i> (Wiehler) L. E. Skog	A. Juncosa 2504	US	5°18'37.56"N	76°19'51.32"W
<i>C. angustata</i> (Wiehler) L. E. Skog	A. S. Hitchcock 21769	MO	1°36'45.48"S	78° 5'40.28"W
<i>C. angustata</i> (Wiehler) L. E. Skog	B. Sparre 15144	US	0°15'19.08"S	79° 9'0.66"W
<i>C. angustata</i> (Wiehler) L. E. Skog	B. Sparre 17099	US	1° 7'11.15"S	79° 9'37.79"W

<i>C. angustata</i> (Wiehler) L. E. Skog	C. Galames et al. 3171	US	08° 33' N	81° 07' O
<i>C. angustata</i> (Wiehler) L. E. Skog	C. H. Dodson & A. Gentry 8916	SEL	3°35'2.65"S	79°50'49.70"W
<i>C. angustata</i> (Wiehler) L. E. Skog	C. H. Dodson & L. B. Thien 1736	SEL	1°10'24.69"S	80°31'56.65"W
<i>C. angustata</i> (Wiehler) L. E. Skog	C. H. Dodson 5667	SEL	0°44'50.84"S	79°25'24.55"W
<i>C. angustata</i> (Wiehler) L. E. Skog	C. H. Dodson 7407	MO, SI, US, SEL	0°16'21.48"S	79° 7'31.22"W
<i>C. angustata</i> (Wiehler) L. E. Skog	C. H. Dodson et al. 16856	SEL	0°53'23.30"N	78°30'17.44"W
<i>C. angustata</i> (Wiehler) L. E. Skog	C. H. Dodson et al. 8447	SEL	3°40'52.82"S	79°47'8.37"W
<i>C. angustata</i> (Wiehler) L. E. Skog	C. H. Dodson et al. 8448	SEL	3°40'52.82"S	79°47'8.37"W
<i>C. angustata</i> (Wiehler) L. E. Skog	D. Neill 11579	US	00° 16' S	80° 12' W
<i>C. angustata</i> (Wiehler) L. E. Skog	D. Neill et al. 5790	US	1° 27' S	78° 06' W
<i>C. angustata</i> (Wiehler) L. E. Skog	E. Asplund 8554	US, SEL	1°24'22.82"S	78°11'33.28"W
<i>C. angustata</i> (Wiehler) L. E. Skog	E. Bello 1548	MO	10° 18' N	84°44' W
<i>C. angustata</i> (Wiehler) L. E. Skog	E. Forero 2111	MO	4°54'57.96"N	76°25'5.09"W
<i>C. angustata</i> (Wiehler) L. E. Skog	E. Forero et al. 3971	COL	4° 10' N	77° 10' W
<i>C. angustata</i> (Wiehler) L. E. Skog	E. Forero et al. 4646	US, MO, COL	4° 42' N	76° 55' W
<i>C. angustata</i>	E. Forero et al.	MO	5° 00' N	76° 44' W

(Wiehler) L. E. Skog	4903			
<i>C. angustata</i> (Wiehler) L. E. Skog	E. Forero et al. 5126	MO	5° 06' N	76° 42' W
<i>C. angustata</i> (Wiehler) L. E. Skog	E. Forero et al. 5528	COL, MO	5° 30-35' N	76° 50-56' W
<i>C. angustata</i> (Wiehler) L. E. Skog	E. Forero et al. 9295	COL	6°33'2.81"N	76°53'36.64"W
<i>C. angustata</i> (Wiehler) L. E. Skog	E. Gudino & R. Moran 1294	US	01° 00' N	78° 35' W
<i>C. angustata</i> (Wiehler) L. E. Skog	E. R. Landa et al. 123	US, COL	7°41'15.71"N	76°36'17.91"W
<i>C. angustata</i> (Wiehler) L. E. Skog	F. Alonso 10235	US	5°18'56.27"N	75°52'51.40"W
<i>C. angustata</i> (Wiehler) L. E. Skog	F. Gonzalez 2331	US	5°25'48.33"N	76°16'32.43"W
<i>C. angustata</i> (Wiehler) L. E. Skog	G. Harling et al. 19617	US	1°27'26.93"S	78° 6'49.24"W
<i>C. angustata</i> (Wiehler) L. E. Skog	G. L. Webster 22927	US	0° 18' S	79° 06' W
<i>C. angustata</i> (Wiehler) L. E. Skog	G. Tipaz et al. 408	US	01° 30' S	78° 00' W
<i>C. angustata</i> (Wiehler) L. E. Skog	H. Lugo S. 1111	US, SI	1°35'18.24"S	77°44'43.08"W
<i>C. angustata</i> (Wiehler) L. E. Skog	H. Lugo S. 1805	US, SI	1°29'28.99"S	78° 3'38.45"W
<i>C. angustata</i> (Wiehler) L. E. Skog	H. Lugo S. 34	US	1°43'19.46"S	77°25'38.00"W
<i>C. angustata</i> (Wiehler) L. E. Skog	H. Lugo S. 4506	US	1°35'21.95"S	77°44'47.82"W
<i>C. angustata</i> (Wiehler) L. E.	H. Lugo S. 5702	US, GB	1°56'35.20"S	77°13'39.57"W

Skog				
<i>C. angustata</i> (Wiehler) L. E. Skog	H. Lugo S. 676	US, SI	1°28'53.85"S	78° 4'1.57"W
<i>C. angustata</i> (Wiehler) L. E. Skog	H. P. Fuchs & L. Zanella 21792	US, SI, MO	5°10'13.49"N	76°11'7.13"W
<i>C. angustata</i> (Wiehler) L. E. Skog	H. Van der Werff et al. 19260	US, MO	03°31'10"S	78°25'53"W
<i>C. angustata</i> (Wiehler) L. E. Skog	H. Wiehler & D. Masterson 79208	SEL	1°25'12.50"S	77°47'28.70"W
<i>C. angustata</i> (Wiehler) L. E. Skog	H. Wiehler & GRF Study Group 86169	US, SEL	0°27'47.96"S	77°51'58.91"W
<i>C. angustata</i> (Wiehler) L. E. Skog	H. Wiehler & GRF Study Group 86224	SEL	0°48'52.12"S	77°37'27.43"W
<i>C. angustata</i> (Wiehler) L. E. Skog	H. Wiehler & GRF Study Group 8665	SEL	1°15'48.70"S	78°33'57.91"W
<i>C. angustata</i> (Wiehler) L. E. Skog	H. Wiehler & GRF Study Group 8801	SEL	2°18'25.42"S	78° 7'1.83"W
<i>C. angustata</i> (Wiehler) L. E. Skog	H. Wiehler & GRF Study Group 8885	SEL	2°22'6.86"S	78°13'1.72"W
<i>C. angustata</i> (Wiehler) L. E. Skog	H. Wiehler & GRF Study Group 9050	SEL	0°52'51.50"N	78°27'52.39"W
<i>C. angustata</i> (Wiehler) L. E. Skog	H. Wiehler & GRF Study Group 9081	US, SEL	0°33'7.91"S	79° 4'53.38"W
<i>C. angustata</i> (Wiehler) L. E. Skog	H. Wiehler & GRF Study Group 9098	SEL	0°29'0.11"S	79°10'10.42"W
<i>C. angustata</i> (Wiehler) L. E. Skog	H. Wiehler & GRF Study Group 93203	SEL	1° 1'17.79"S	77°51'11.61"W
<i>C. angustata</i> (Wiehler) L. E. Skog	H. Wiehler & GRF Study Group 93219	SEL	0°58'59.88"S	77°49'0.12"W
<i>C. angustata</i> (Wiehler) L. E. Skog	H. Wiehler & GRF Study Group 93220	SEL	0°58'59.88"S	77°49'0.12"W

<i>C. angustata</i> (Wiehler) L. E. Skog	H. Wiehler & GRF Study Group 97137	SEL	2°41'41.54"S	77°49'48.58"W
<i>C. angustata</i> (Wiehler) L. E. Skog	H. Wiehler & GRF Study Group 9751	SEL	0°55'60.00"S	79°13'0.00"W
<i>C. angustata</i> (Wiehler) L. E. Skog	H. Wiehler 1176	US	1°29'13.73"S	78° 0'28.64"W
<i>C. angustata</i> (Wiehler) L. E. Skog	H. Wiehler 29	SEL	0°52'49.91"N	78°30'38.29"W
<i>C. angustata</i> (Wiehler) L. E. Skog	H. Wiehler 3351	SEL	0°27'48"S	77°53'33"W
<i>C. angustata</i> (Wiehler) L. E. Skog	H. Wiehler 34	SEL	1°46'37.01"S	79°13'27.44"W
<i>C. angustata</i> (Wiehler) L. E. Skog	H. Wiehler 71124	SEL	0°58'59.88"S	77°49'0.12"W
<i>C. angustata</i> (Wiehler) L. E. Skog	H. Wiehler 7129	SEL	1°23'15.52"S	79°19'59.36"W
<i>C. angustata</i> (Wiehler) L. E. Skog	H. Wiehler 7163	SEL	1°28'57.88"S	78° 0'10.58"W
<i>C. angustata</i> (Wiehler) L. E. Skog	H. Wiehler 79140	SEL	2° 1'51.30"S	79°13'9.97"W
<i>C. angustata</i> (Wiehler) L. E. Skog	H. Wiehler 7997	SEL	0°14'60.00"S	79° 8'60.00"W
<i>C. angustata</i> (Wiehler) L. E. Skog	H. Wiehler 90111	US	0° 5'15.62"N	79°11'17.60"W
<i>C. angustata</i> (Wiehler) L. E. Skog	H. Wiehler 9024	US	0°53'1.39"N	78°30'13.92"W
<i>C. angustata</i> (Wiehler) L. E. Skog	H. Wiehler 95118	SEL	0°41'43.58"S	77°18'2.87"W
<i>C. angustata</i> (Wiehler) L. E. Skog	H. Wiehler 95145	US	1°27'5.82"S	79°16'57.20"W
<i>C. angustata</i>	H. Wiehler 9567	US	0°52'26.56"N	78°27'22.75"W

(Wiehler) L. E. Skog				
<i>C. angustata</i> (Wiehler) L. E. Skog	H. Wiehler 9594	SEL	0°41'43.58"S	77°18'2.87"W
<i>C. angustata</i> (Wiehler) L. E. Skog	H. Wiehler et al. 7276	SEL	3°38'1.52"N	76°49'35.00"W
<i>C. angustata</i> (Wiehler) L. E. Skog	J. A. Duke 15614	US	7°49'4.14"N	77°42'55.49"W
<i>C. angustata</i> (Wiehler) L. E. Skog	J. B. Dataneur et al. 5183	US	1° 12' N	76° 38' W
<i>C. angustata</i> (Wiehler) L. E. Skog	J. B. Watson 331	SEL	0°31'48.51"S	79°27'1.29"W
<i>C. angustata</i> (Wiehler) L. E. Skog	J. Caranqui et al. 821	US	01° 42' S	78° 01' W
<i>C. angustata</i> (Wiehler) L. E. Skog	J. Cuatrecasas & M. Llano 24150	US	5°32'17.45"N	76°37'26.24"W
<i>C. angustata</i> (Wiehler) L. E. Skog	J. Cuatrecasas 21359	F, US	4°28'59.14"N	76°59'17.18"W
<i>C. angustata</i> (Wiehler) L. E. Skog	J. L. Clark & B. Adnepos 50	US, SEL	0° 21' N	79° 44' W
<i>C. angustata</i> (Wiehler) L. E. Skog	J. L. Clark & J. Katzenstein 8322	US	01°42'06"S	77°50'36"W
<i>C. angustata</i> (Wiehler) L. E. Skog	J. L. Clark & J. Katzenstein 8397	US	01°24'16"S	78°11'17"W
<i>C. angustata</i> (Wiehler) L. E. Skog	J. L. Clark & J. Katzenstein 9302	US	01°32'40"S	77°53'53"W
<i>C. angustata</i> (Wiehler) L. E. Skog	J. L. Clark & M. Mailloux 7834	US	01°29'49"S	78°03'42"W
<i>C. angustata</i> (Wiehler) L. E. Skog	J. L. Clark & N. Harris 7232	US	00°49'40"S	77°33'49"W
<i>C. angustata</i> (Wiehler) L. E.	J. L. Clark & V. Duran 6024	US	01°23'08.7"S	78°10'01.2"W

Skog				
<i>C. angustata</i> (Wiehler) L. E. Skog	J. L. Clark 4520	US	00° 08' S	72° 44' W
<i>C. angustata</i> (Wiehler) L. E. Skog	J. L. Clark 4689	US	00° 25' N	79° 45' W
<i>C. angustata</i> (Wiehler) L. E. Skog	J. L. Clark 4747	US	00° 21' N	79° 44' W
<i>C. angustata</i> (Wiehler) L. E. Skog	J. L. Clark 8270	US	00°13'08"S	78°53'53"W
<i>C. angustata</i> (Wiehler) L. E. Skog	J. L. Clark 8627	US	8° 42' N	80° 35' W
<i>C. angustata</i> (Wiehler) L. E. Skog	J. L. Clark 9609	US, SEL	00° 21' N	79° 44' W
<i>C. angustata</i> (Wiehler) L. E. Skog	J. L. Clark 9854	US, SEL	03°09'17"S	78°32'05"W
<i>C. angustata</i> (Wiehler) L. E. Skog	J. L. Clark 9915	US	3°17'51"S	78°33'27"W
<i>C. angustata</i> (Wiehler) L. E. Skog	J. L. Clark et al. 2635	US	00° 01' N	79° 58' W
<i>C. angustata</i> (Wiehler) L. E. Skog	J. L. Clark et al. 2835	US	00° 28' N	79° 43' W
<i>C. angustata</i> (Wiehler) L. E. Skog	J. L. Clark et al. 4959	US	00° 13' N	78° 55' W
<i>C. angustata</i> (Wiehler) L. E. Skog	J. L. Clark et al. 5233	US	00° 44' S	77° 48' W
<i>C. angustata</i> (Wiehler) L. E. Skog	J. L. Clark et al. 5982	US	02° 54'20.2" S	78° 19'41.3" W
<i>C. angustata</i> (Wiehler) L. E. Skog	J. L. Clark et al. 6193	US	1°03'05.2"S	80°39'42.5"W
<i>C. angustata</i> (Wiehler) L. E. Skog	J. L. Clark et al. 7220	US	00°47'49"N	77°35'10"W

<i>C. angustata</i> (Wiehler) L. E. Skog	J. L. Clark et al. 7380	US	00°18'N	78°46'W
<i>C. angustata</i> (Wiehler) L. E. Skog	J. L. Clark et al. 7484	US	00°45'21"N	78°27'98"W
<i>C. angustata</i> (Wiehler) L. E. Skog	J. L. Clark et al. 7797	US	01°23'15"S	78°03'12"W
<i>C. angustata</i> (Wiehler) L. E. Skog	J. L. Clark et al. 8776	US	00°21'N	79°44'W
<i>C. angustata</i> (Wiehler) L. E. Skog	J. L. Clark et al. 9368	US	1°25'10"S	77°59'50"W
<i>C. angustata</i> (Wiehler) L. E. Skog	J. L. Clark et al. 9373	US	01°17'17"S	77°52'54"W
<i>C. angustata</i> (Wiehler) L. E. Skog	J. L. Luteyn & M. Lebron-Luteyn 5820	NY, SEL	1°22'11.75"S	78° 1'4.63"W
<i>C. angustata</i> (Wiehler) L. E. Skog	J. P. Folsom & L. Escobar 10477	US	3°39'18.80"N	76°52'39.36"W
<i>C. angustata</i> (Wiehler) L. E. Skog	J. van Roden et al. 449	US	3° 59' N	76° 57' W
<i>C. angustata</i> (Wiehler) L. E. Skog	J. van Roden 540	US, COL	3° 56' N	77° 10' W
<i>C. angustata</i> (Wiehler) L. E. Skog	L. Holm-Nielsen & S. Jeppesen 469	OV, S	1° 29' S	78° 3' W
<i>C. angustata</i> (Wiehler) L. E. Skog	L. P. Kvist 60325	US	01° 27' S	78° 08' W
<i>C. angustata</i> (Wiehler) L. E. Skog	M. Amaya & J. F. Smith 534	US	5°25'17.11"N	76° 7'50.11"W
<i>C. angustata</i> (Wiehler) L. E. Skog	M. Amaya & L. P. Kvist 402	US	5° 8'14.06"N	76°10'10.70"W
<i>C. angustata</i> (Wiehler) L. E. Skog	M. Amaya & L. P. Kvist 412	US	5°20'22.01"N	76°19'57.49"W
<i>C. angustata</i>	M. Amaya & L. P.	US	5°33'5.10"N	76°17'0.73"W

(Wiehler) L. E. Skog	Kvist 434			
<i>C. angustata</i> (Wiehler) L. E. Skog	M. H. Stone 1168	US	10°15'49.00"N	84°10'58.65"W
<i>C. angustata</i> (Wiehler) L. E. Skog	M. Tirado et al. 1131	US, MO	00° 49' S	78° 45' W
<i>C. angustata</i> (Wiehler) L. E. Skog	M. Tirado et al. 482	US, SEL	00° 43' N	78° 53' W
<i>C. angustata</i> (Wiehler) L. E. Skog	M. Whitten et al. 91276	SEL	0° 2'41.50"S	78°57'34.68"W
<i>C. angustata</i> (Wiehler) L. E. Skog	N. Pitman & M. Bass 874	US	0° 21' N	79° 44' W
<i>C. angustata</i> (Wiehler) L. E. Skog	N. Pitman & M. Bass 998	US	0° 21' N	79° 44' W
<i>C. angustata</i> (Wiehler) L. E. Skog	P. Mendoza-T. et al. 515	US	00° 05' N	78° 55' W
<i>C. angustata</i> (Wiehler) L. E. Skog	P. Mendoza-T. et al. 546	US	00° 13' N	78° 55' W
<i>C. angustata</i> (Wiehler) L. E. Skog	P. Mendoza-T. et al. 555	US, MO	00° 21' N	79° 44' W
<i>C. angustata</i> (Wiehler) L. E. Skog	P. Mendoza-T. et al. 599	US	00° 21' N	79° 43' W
<i>C. angustata</i> (Wiehler) L. E. Skog	R. Fonnegra et al. 1865	MO, US	7°15'0.00"N	76°25'60.00"W
<i>C. angustata</i> (Wiehler) L. E. Skog	R. L. Dressler 5642	SEL	8°42'7.08"N	80°35'2.43"W
<i>C. angustata</i> (Wiehler) L. E. Skog	R. L. Liesner 916	MO, SEL, SI	8°31'41.98"N	81° 8'32.76"W
<i>C. angustata</i> (Wiehler) L. E. Skog	R. W. Dunn 95-04- 136	US	0°18'54.72"S	79° 4'8.18"W
<i>C. angustata</i> (Wiehler) L. E.	R. W. Lent 2551	SEL	9°50'20.51"N	83°42'3.91"W

Skog				
<i>C. angustata</i> (Wiehler) L. E. Skog	S. Diaz 3419	COL	4°56'28.61"N	76°34'9.91"W
<i>C. angustata</i> (Wiehler) L. E. Skog	S. Mori & J. Kallunki 5471	MO, US, SI	7°55'60.00"N	77°43'0.00"W
<i>C. angustata</i> (Wiehler) L. E. Skog	T. B. Croat 49680	US	1°38'4.91"S	77°55'46.89"W
<i>C. angustata</i> (Wiehler) L. E. Skog	T. B. Croat 58926	MO	1° 19' S	77° 51' W
<i>C. angustata</i> (Wiehler) L. E. Skog	W. A. Archer 2053	SEL	5°12'41.74"N	76°39'53.39"W
<i>C. angustata</i> (Wiehler) L. E. Skog	W. Haber & E. Bello 6878	MO	10° 20' N	84°43' W
<i>C. angustata</i> (Wiehler) L. E. Skog	W. Haber & E. Bello 7069	MO	10° 20' N	84° 43' W
<i>C. angustata</i> (Wiehler) L. E. Skog	W. Meier & G. Forbes 12856	US	11°11'N	69°42'O
<i>C. angustata</i> (Wiehler) L. E. Skog	W. Palacios 11496	SEL	0°20'N	79°12'W
<i>C. angustata</i> (Wiehler) L. E. Skog	W. Palacios 11501	SEL	00° 20' N	79° 12' W
<i>C. angustata</i> (Wiehler) L. E. Skog	X. Cornejo & C. Bonifaz 1408	US	01° 30' S	78° 04' W
<i>C. angustata</i> (Wiehler) L. E. Skog	X. Cornejo & C. Bonifaz 323	US	03° 29' S	79° 45' W
<i>C. angustata</i> (Wiehler) L. E. Skog	X. Cornejo & C. Bonifaz 4533	US	02° 06' S	79° 10' W
<i>C. angustata</i> (Wiehler) L. E. Skog	X. Cornejo & C. Bonifaz 6234	US	00° 39' N	78° 59' W
<i>C. angustata</i> (Wiehler) L. E. Skog	X. Cornejo & S. Laegaard 2038	US	00° 15' S	79° 10' W

<i>C. byrsina</i> (Wiehler) L. P. Kvist & L. E. Skog	A. Gentry & G. Shupp 26406	SEL, MO	1° 0'6.97"N	78°13'34.73"W
<i>C. byrsina</i> (Wiehler) L. P. Kvist & L. E. Skog	A. Gentry 34996	COL, US, MO	1° 8' N	77° 58'W
<i>C. byrsina</i> (Wiehler) L. P. Kvist & L. E. Skog	A. Gentry et al. 60328	US	01° 05' N	78° 01' W
<i>C. byrsina</i> (Wiehler) L. P. Kvist & L. E. Skog	A. Hirtz & J. Kent 4556	SEL	0°53'56.22"N	78°32'40.22"W
<i>C. byrsina</i> (Wiehler) L. P. Kvist & L. E. Skog	A. Hirtz 4496	SEL	0°27'21.67"S	77°53'27.49"W
<i>C. byrsina</i> (Wiehler) L. P. Kvist & L. E. Skog	B. B. Klitgaard et al. 606	US	0°24'1.69"S	77°49'6.14"W
<i>C. byrsina</i> (Wiehler) L. P. Kvist & L. E. Skog	C. H. Dodson 17604	US, MO	0°43'N	78°22'W
<i>C. byrsina</i> (Wiehler) L. P. Kvist & L. E. Skog	C. H. Dodson et al. 16836	MO, US, SI	0°54'0.78"N	78°33'39.65"W
<i>C. byrsina</i> (Wiehler) L. P. Kvist & L. E. Skog	C. Luer et al. 3177	SEL	0°27'32.33"S	77°53'45.14"W
<i>C. byrsina</i> (Wiehler) L. P. Kvist & L. E. Skog	C. Luer et al. 4496	SEL	0°27'32.33"S	77°53'45.14"W
<i>C. byrsina</i> (Wiehler) L. P. Kvist & L. E. Skog	C. Restrepo & G. Ramirez 563	US	1°39'51.94"N	77°33'44.75"W
<i>C. byrsina</i> (Wiehler) L. P.	D. Rubio et al. 1692	MO	01°02'N	78°14'W

Kvist & L. E. Skog				
<i>C. byrsina</i> (Wiehler) L. P. Kvist & L. E. Skog	D. Rubio et al. 2203	MO	00°53'N	78°20'W
<i>C. byrsina</i> (Wiehler) L. P. Kvist & L. E. Skog	E. Ferrero et al. 6107	COL	5°47'44.65"N	76°19'36.38"W
<i>C. byrsina</i> (Wiehler) L. P. Kvist & L. E. Skog	G. L. Webster 23237	US	0°25'48"S	77°31'12"W
<i>C. byrsina</i> (Wiehler) L. P. Kvist & L. E. Skog	G. Tipaz et al. 1914	SEL, MO	00°53'N	78°25'W
<i>C. byrsina</i> (Wiehler) L. P. Kvist & L. E. Skog	H. Balslev & E. Madsen 10575	MO, OV, COL, SEL, F	0° 22' S	77° 49' W
<i>C. byrsina</i> (Wiehler) L. P. Kvist & L. E. Skog	H. Balslev 1997	SI, US	0°53'51.54"N	78° 6'58.99"W
<i>C. byrsina</i> (Wiehler) L. P. Kvist & L. E. Skog	H. Wiehler 77122	SEL, US	0°27'32.33"S	77°53'45.14"W
<i>C. byrsina</i> (Wiehler) L. P. Kvist & L. E. Skog	H. Wiehler 79298	SEL	0°10'31.16"S	77°39'56.93"W
<i>C. byrsina</i> (Wiehler) L. P. Kvist & L. E. Skog	H. Wiehler 9095	SEL, US	0° 6'25.68"S	78°52'21.36"W
<i>C. byrsina</i> (Wiehler) L. P. Kvist & L. E. Skog	H. Wiehler 93110	SEL, US, MO	0°56'23.50"N	78°10'43.44"W
<i>C. byrsina</i> (Wiehler) L. P. Kvist & L. E. Skog	H. Wiehler 98156	SEL, US	0°42'59.76"S	77°43'17.05"W

<i>C. byrsina</i> (Wiehler) L. P. Kvist & L. E. Skog	J. Cuatrecasas 22667	US, SI, SEL	3° 9'26.09"N	74°48'8.46"W
<i>C. byrsina</i> (Wiehler) L. P. Kvist & L. E. Skog	J. F. Smith & M. Galeano 1457	WIS	1°10' N	77° 58' W
<i>C. byrsina</i> (Wiehler) L. P. Kvist & L. E. Skog	J. F. Smith & M. Galeano 1505	MO, US, SEL	1° 10' N	77° 58' W
<i>C. byrsina</i> (Wiehler) L. P. Kvist & L. E. Skog	J. F. Smith & M. Galeano 1519	COL, PSO, WIS	1° 10' N	77° 58' W
<i>C. byrsina</i> (Wiehler) L. P. Kvist & L. E. Skog	J. L. Clark & E. Folleco 8539	US	00° 49' N	78° 12' W
<i>C. byrsina</i> (Wiehler) L. P. Kvist & L. E. Skog	J. L. Clark & L. Jost 6992	US	03° 13' S	078° 16' W
<i>C. byrsina</i> (Wiehler) L. P. Kvist & L. E. Skog	J. L. Clark & O. Mejia 6291	SEL, US, MO	00°57'54.3"N	78°13'21.3"W
<i>C. byrsina</i> (Wiehler) L. P. Kvist & L. E. Skog	J. L. Clark 4502	US	00° 11' S	78° 41' W
<i>C. byrsina</i> (Wiehler) L. P. Kvist & L. E. Skog	J. L. Clark et al. 2413	US, MO	00°49'N	78°01'W
<i>C. byrsina</i> (Wiehler) L. P. Kvist & L. E. Skog	J. L. Clark et al. 5969	US	2°57'14"S	78°21'36.4"N
<i>C. byrsina</i> (Wiehler) L. P. Kvist & L. E. Skog	J. L. Clark et al. 6343	SEL, US	0°53'49"N	78°12'33.9"W
<i>C. byrsina</i> (Wiehler) L. P.	J. L. Clark et al. 7518	US	0°45'21"N	78°27'09"W

Kvist & L. E. Skog				
<i>C. byrsina</i> (Wiehler) L. P. Kvist & L. E. Skog	J. L. Clark et al. 7539	US	0°49'51"N	78°28'54"W
<i>C. byrsina</i> (Wiehler) L. P. Kvist & L. E. Skog	J. L. Clark et al. 8460	US	0°49'46"N	78°07'03"W
<i>C. byrsina</i> (Wiehler) L. P. Kvist & L. E. Skog	J. L. Luteyn et al. 13912	US	01° 10' N	77° 55' W
<i>C. byrsina</i> (Wiehler) L. P. Kvist & L. E. Skog	J. L. Zarucchi et al. 5670	US	06° 45' N	76° 23' W
<i>C. byrsina</i> (Wiehler) L. P. Kvist & L. E. Skog	J. L. Zarucchi et al. 5736	MO, US, SI	06° 45' N	76° 24' W
<i>C. byrsina</i> (Wiehler) L. P. Kvist & L. E. Skog	K. von Sneidern 10.IV.1941	OV	1°13'44.24"N	77°58'20.00"W
<i>C. byrsina</i> (Wiehler) L. P. Kvist & L. E. Skog	L. Besse et al. 1633	SEL, US	0°26'15.51"S	77°52'10.28"W
<i>C. byrsina</i> (Wiehler) L. P. Kvist & L. E. Skog	L. Besse et al. 2329	SEL	0°35'46.14"S	77°50'42.77"W
<i>C. byrsina</i> (Wiehler) L. P. Kvist & L. E. Skog	L. Besse et al. 887	SEL	1° 0'42.30"N	78°15'29.31"W
<i>C. byrsina</i> (Wiehler) L. P. Kvist & L. E. Skog	M. T. Madison & L. Besse 7115	SI, SEL	0°36'37.11"N	78° 8'3.46"W
<i>C. byrsina</i> (Wiehler) L. P. Kvist & L. E. Skog	M. T. Madison 3873	SEL	5° 49'0.69"N	76° 25'14.25"W

<i>C. byrsina</i> (Wiehler) L. P. Kvist & L. E. Skog	M. T. Madison et al. 4419	SEL	0°53'3.06"N	78° 5'39.03"W
<i>C. byrsina</i> (Wiehler) L. P. Kvist & L. E. Skog	M. T. Madison et al. 4451	SEL, F	1° 04' N	78° 17' W
<i>C. byrsina</i> (Wiehler) L. P. Kvist & L. E. Skog	M. Tirado et al. 1230	US, MO	0°50'N	78°11'W
<i>C. byrsina</i> (Wiehler) L. P. Kvist & L. E. Skog	P. J. M. Maas & T. Plowman 1838	OV	3°31'0.28"N	76°42'59.99"W
<i>C. byrsina</i> (Wiehler) L. P. Kvist & L. E. Skog	P. Silverstone- Sopkin et al. 9967	MO	0°58'45"S	79°06'53"W
<i>C. byrsina</i> (Wiehler) L. P. Kvist & L. E. Skog	S. A. Thompson & J. A. Rawlins 719	US	0° 56' N	78° 11' W
<i>C. byrsina</i> (Wiehler) L. P. Kvist & L. E. Skog	S. Libenson et al. 30577	MO	1°11'44.64"N	78° 0'55.48"W
<i>C. byrsina</i> (Wiehler) L. P. Kvist & L. E. Skog	T. Nunez et al. 356	MO	01°02'S	80°41'W
<i>C. byrsina</i> (Wiehler) L. P. Kvist & L. E. Skog	W. Palacios 5410	SEL, MO	00°12'S	77°39'W
<i>C. byrsina</i> (Wiehler) L. P. Kvist & L. E. Skog	W. S. Hoover & S. Wormley 1577	MO	00°53'N	78°09'W
<i>C. byrsina</i> (Wiehler) L. P. Kvist & L. E. Skog	X. Londono 240	US	1°12'42.33"N	77°58'56.31"W
<i>C. colombiana</i> (Wiehler) L. P.	E. P. Killip & J. Cuatrecasas 38847	US	6° 0'18.09"N	75°45'15.49"W

Kvist & L. E. Skog				
<i>C. colombiana</i> (Wiehler) L. P. Kvist & L. E. Skog	H. Wiehler 72130	SEL	3°51'50.74"N	76°51'27.35"W
<i>C. colombiana</i> (Wiehler) L. P. Kvist & L. E. Skog	J. W. White & R. H. Warner 74	COL, MO	4°56'33.19"N	77°20'32.97"W
<i>C. crassicaulis</i> (Wiehler) L. P. Kvist & L. E. Skog	A. Hirtz 4500	SEL	0°16'0.13"N	78°34'59.94"W
<i>C. crassicaulis</i> (Wiehler) L. P. Kvist & L. E. Skog	B. R. Ramires P. & A. L. Jojoa B. 5.718	US	1°32'45.31"N	77°13'16.04"W
<i>C. crassicaulis</i> (Wiehler) L. P. Kvist & L. E. Skog	C. H. Dodson et al. 16779	SEL	0°41'48.95"N	78°11'59.02"W
<i>C. crassicaulis</i> (Wiehler) L. P. Kvist & L. E. Skog	C. H. Dodson et al. 6983	SI, SEL	0° 4'59.30"N	78°43'39.25"W
<i>C. crassicaulis</i> (Wiehler) L. P. Kvist & L. E. Skog	C. Luer et al. 4717	SEL, SI	0° 0'44.55"S	78°23'53.82"W
<i>C. crassicaulis</i> (Wiehler) L. P. Kvist & L. E. Skog	G. Harling & L. Andersson 12391	US, SI	0°54'38.96"N	78° 6'18.96"W
<i>C. crassicaulis</i> (Wiehler) L. P. Kvist & L. E. Skog	H. Van der Werff et al. 12307	SEL, US	0° 5'50.40"N	78°39'45.95"W
<i>C. crassicaulis</i> (Wiehler) L. P. Kvist & L. E. Skog	H. Wiehler & GRF Study Group 93164	SEL	0°15'37.50"N	78°33'8.28"W
<i>C. crassicaulis</i> (Wiehler) L. P. Kvist & L. E. Skog	H. Wiehler & GRF Study Group 97172	SEL	0° 3'43.83"N	78°40'55.28"W

<i>C. crassicaulis</i> (Wiehler) L. P. Kvist & L. E. Skog	H. Wiehler & N. H. William 72185	SEL	1°12'6.40"N	77°58'37.77"W
<i>C. crassicaulis</i> (Wiehler) L. P. Kvist & L. E. Skog	H. Wiehler 93128	SEL, US	0°59'3.87"N	78°11'16.13"W
<i>C. crassicaulis</i> (Wiehler) L. P. Kvist & L. E. Skog	R. L. Dressler 4926	SI, SEL	0° 0'8.23"N	78°39'46.32"W
<i>C. crassicaulis</i> (Wiehler) L. P. Kvist & L. E. Skog	St. G. Beck 3043	SEL	16°26'24.00"S	67°31'44.45"W
<i>C. domingensis</i> (Urb.) B. D. Morley	A. Gentry & M. Mejia 50693	MO	18°10'N	71°15'W
<i>C. domingensis</i> (Urb.) B. D. Morley	A. H. Liogier & P. Liogier 22699	NY	18°39'26.46"N	71°29'54.15"W
<i>C. domingensis</i> (Urb.) B. D. Morley	A. H. Liogier 11206	NY, GH	19°34'0.00"N	70°34'0.00"W
<i>C. domingensis</i> (Urb.) B. D. Morley	A. H. Liogier 18055	NY, F	18°55'6.55"N	70°44'57.91"W
<i>C. domingensis</i> (Urb.) B. D. Morley	B. A. H. Liogier 11624	US	18°31'20.47"N	70°17'29.29"W
<i>C. domingensis</i> (Urb.) B. D. Morley	B. A. H. Liogier 12066	US	19° 4'17.40"N	70°37'36.64"W
<i>C. domingensis</i> (Urb.) B. D. Morley	De JS. Jimenez 3033	US	19° 5'18.98"N	70°38'41.98"W
<i>C. domingensis</i> (Urb.) B. D. Morley	E. C. Leonard & G. M. Leonard 15058	US	18°24'53.48"N	73°16'15.97"W
<i>C. domingensis</i> (Urb.) B. D. Morley	E. C. Leonard 3802	US	18°38'48.69"N	71°49'47.61"W
<i>C. domingensis</i> (Urb.) B. D. Morley	E. C. Leonard 4630	US	18°55'30.77"N	70°56'58.02"W

<i>C. domingensis</i> (Urb.) B. D. Morley	E. C. Leonard 8359	US	19°30'42.05"N	72°20'32.97"W
<i>C. domingensis</i> (Urb.) B. D. Morley	E. L. Ekman 1129	US	18°17'8.27"N	71°38'24.54"W
<i>C. domingensis</i> (Urb.) B. D. Morley	E. L. Ekman 12898	US	18°29'25.05"N	70°16'42.62"W
<i>C. domingensis</i> (Urb.) B. D. Morley	E. L. Ekman 79	S, AAH	18°24'0.00"N	74° 1'60.00"W
<i>C. domingensis</i> (Urb.) B. D. Morley	Eggers 2314	KEW	19° 3'1.26"N	70°35'10.25"W
<i>C. domingensis</i> (Urb.) B. D. Morley	G. J. Gastony et al. 244	US	19° 4'38.39"N	70°31'23.53"W
<i>C. domingensis</i> (Urb.) B. D. Morley	G. V. Nash & N. Taylor 1154	US	18°16'54.06"N	72°19'24.97"W
<i>C. domingensis</i> (Urb.) B. D. Morley	H. von Turckhelm 3375	NY	18°54'6.06"N	70°45'5.21"W
<i>C. domingensis</i> (Urb.) B. D. Morley	J. T. Curtis & E. C. Leonard 45	WIS	18°15'N	73°50'W
<i>C. domingensis</i> (Urb.) B. D. Morley	L. H. Bailey 199	US	18°20'58.22"N	72°17'0.70"W
<i>C. domingensis</i> (Urb.) B. D. Morley	L. R. Holdridge 955	US	18°55'19.44"N	70°59'30.89"W
<i>C. domingensis</i> (Urb.) B. D. Morley	M. H. Stone 1136	US	18°25'2.51"N	72°17'56.41"W
<i>C. domingensis</i> (Urb.) B. D. Morley	P. Fuertes 329	US, MO	18°12'21.19"N	71°12'0.27"W
<i>C. domingensis</i> (Urb.) B. D. Morley	R. A. Howard & E. S. Howard 8556	US	18° 4'7.89"N	71°16'35.75"W
<i>C. domingensis</i> (Urb.) B. D. Morley	R. A. Howard 12291	US	18° 8'8.40"N	71°13'11.33"W
<i>C. domingensis</i>	S. A. Thompson et	US	18° 15' N	71° 45' W

(Urb.) B. D. Morley	al. 7592			
<i>C. domingensis</i> (Urb.) B. D. Morley	T. E. Talpey 46	BH	18°25'3.51"N	72°18'0.12"W
<i>C. domingensis</i> (Urb.) B. D. Morley	T. E. Talpey 73	BH	18°42'35.26"N	71°32'3.51"W
<i>C. domingensis</i> (Urb.) B. D. Morley	T. Zanoni & J. Pimentel 26542	NY	18°18'N	71°42.5'W
<i>C. domingensis</i> (Urb.) B. D. Morley	T. Zanoni & M. Mejia 24559	NY	18°20'N	72°16'W
<i>C. domingensis</i> (Urb.) B. D. Morley	T. Zanoni & R. Garcia 30462	NY	18° 18' N	71° 17' W
<i>C. domingensis</i> (Urb.) B. D. Morley	T. Zanoni & R. Garcia 41853	NY	19° 14' N	71° 17' W
<i>C. domingensis</i> (Urb.) B. D. Morley	T. Zanoni et al. 18876	US, MO	18° 07.5' N	71° 13.5' W
<i>C. domingensis</i> (Urb.) B. D. Morley	T. Zanoni et al. 19975	US, MO	19° 04' N	70° 34' W
<i>C. domingensis</i> (Urb.) B. D. Morley	T. Zanoni et al. 38670	US, MO	18° 10' N	71° 12' W
<i>C. domingensis</i> (Urb.) B. D. Morley	T. Zanoni et al. 39209	US, MO	19° 05' N	70° 54' W
<i>C. domingensis</i> (Urb.) B. D. Morley	T. Zanoni et al. 39798	US	18° 42' N	71° 46' W
<i>C. domingensis</i> (Urb.) B. D. Morley	T. Zanoni et al. 41040	US	18° 10' N	71° 13' W
<i>C. domingensis</i> (Urb.) B. D. Morley	W. J. Everdam 280	US	18°46'21.46"N	72°56'4.23"W
<i>C. domingensis</i> (Urb.) B. D. Morley	W. J. Everdam 351	NY, US, GH	18°24'0.00"N	74° 1'60.00"W
<i>C. domingensis</i> (Urb.) B. D.	W. L. Abbott 1583	US	18°12'31.82"N	71°10'43.63"W

Morley				
<i>C. domingensis</i> (Urb.) B. D. Morley	W. L. Abbott 1610	US	18°12'31.82"N	71°10'43.63"W
<i>C. domingensis</i> (Urb.) B. D. Morley	W. L. Abbott 6	US	18°53'26.14"N	70°45'46.97"W
<i>C. domingensis</i> (Urb.) B. D. Morley	W. S. Judd & J. D. Skean Jr 4436	GH	18°20'35.53"N	72°17'15.40"W
<i>C. domingensis</i> (Urb.) B. D. Morley	W. S. Judd et al. 1078	AAH, AAU	18°50'60.00"N	70°33'0.00"W
<i>C. katzensteiniae</i> (Wiehler) L. P. Kvist & L. E. Skog	A. Gentry et al. 22920	US, MO, SI	5°36'50.38"S	78°21'0.02"W
<i>C. katzensteiniae</i> (Wiehler) L. P. Kvist & L. E. Skog	A. Gentry et al. 30858	SI, SEL, MO	3° 8'59.03"S	78°27'15.46"W
<i>C. katzensteiniae</i> (Wiehler) L. P. Kvist & L. E. Skog	B. Sparre 14693	US	0°26'0.48"S	78°43'2.10"W
<i>C. katzensteiniae</i> (Wiehler) L. P. Kvist & L. E. Skog	F. A. Werner 876	US	03° 58' S	79° 04' W
<i>C. katzensteiniae</i> (Wiehler) L. P. Kvist & L. E. Skog	F. Billiet & B. Jadin 6690	MO	00°00'S	78°40'W
<i>C. katzensteiniae</i> (Wiehler) L. P. Kvist & L. E. Skog	G. C. G. Argent & R. B. Burbidge 423	MO	1°24'S	78°12'W
<i>C. katzensteiniae</i> (Wiehler) L. P. Kvist & L. E. Skog	G. Harling & L. Andersson 24524	US	3°38'39.32"S	79°41'6.74"W
<i>C. katzensteiniae</i> (Wiehler) L. P. Kvist & L. E. Skog	H. Wiehler & GRF Expedition 88128	SEL	3°45'6.53"S	78°26'32.75"W
<i>C. katzensteiniae</i>	H. Wiehler et al.	SEL, US	0° 1'25.38"S	78°44'51.54"W

(Wiehler) L. P. Kvist & L. E. Skog	90145			
<i>C. katzensteiniae</i> (Wiehler) L. P. Kvist & L. E. Skog	J. F. Smith 2100	QCA, WIS	3° 0-5' S	78° 30-40' W
<i>C. katzensteiniae</i> (Wiehler) L. P. Kvist & L. E. Skog	J. Homeier & E. Brandes 1218	MO	3°58'S	79°04'W
<i>C. katzensteiniae</i> (Wiehler) L. P. Kvist & L. E. Skog	J. Homeier 1527	MO	3°58'S	79°04'W
<i>C. katzensteiniae</i> (Wiehler) L. P. Kvist & L. E. Skog	J. L. Clark & A. Munoz 6129	SEL, US, MO	00° 25.17' S	79° 00.19' W
<i>C. katzensteiniae</i> (Wiehler) L. P. Kvist & L. E. Skog	J. L. Clark et al. 7625	US	00°13'53"S	78°48'10"W
<i>C. katzensteiniae</i> (Wiehler) L. P. Kvist & L. E. Skog	J. L. Clark et al. 8915	US	04° 46'50"S	79°12'33"W
<i>C. katzensteiniae</i> (Wiehler) L. P. Kvist & L. E. Skog	J. Perea & J. Mateo 3038	MO	05°03'43"S	78°44'49"W
<i>C. katzensteiniae</i> (Wiehler) L. P. Kvist & L. E. Skog	R. W. Dunn 57	US	00°00'57.6"S	78°43'55.0"W
<i>C. manabiana</i> (Wiehler) J. F. Sm. & L. E. Skog	A. Gentry 9625	MO	0° 4'14.87"S	79°19'39.60"W
<i>C. manabiana</i> (Wiehler) J. F. Sm. & L. E. Skog	A. Gentry et al. .72578	MO	01°36'S	80°42'W
<i>C. manabiana</i> (Wiehler) J. F. Sm. & L. E. Skog	A. Gentry et al. 72571	MO	01°36'S	80°42'W
<i>C. manabiana</i> (Wiehler) J. F.	C. Espinoza 58	MO	01°03'53"S	80°53'04"W

Sm. & L. E. Skog				
<i>C. manabiana</i> (Wiehler) J. F. Sm. & L. E. Skog	C. H. Dodson 6791	MO, SEL	0°22'56.37"S	79°46'21.89"W
<i>C. manabiana</i> (Wiehler) J. F. Sm. & L. E. Skog	C. H. Dodson et al. 9170	SEL, US, SI	2°10'55.99"S	79°57'19.69"W
<i>C. manabiana</i> (Wiehler) J. F. Sm. & L. E. Skog	H. Wiehler 87102	SEL	0°29'47.04"S	79°35'32.37"W
<i>C. manabiana</i> (Wiehler) J. F. Sm. & L. E. Skog	J. L. Clark et al. 1588	US, MO	02° 34' S	79° 21' W
<i>C. manabiana</i> (Wiehler) J. F. Sm. & L. E. Skog	J. L. Clark et al. 2487	US	02° 33' S	79° 29' W
<i>C. manabiana</i> (Wiehler) J. F. Sm. & L. E. Skog	X. Cornejo & C. Bonifaz 4591	US	02° 06' S	79° 10' W
<i>C. orientandina</i> Mansf.	E. P. Killip & A. C. Smith 26059	US, SI	11° 4'45.10"S	74°50'1.96"W
<i>C. orientandina</i> Mansf.	G. Pabon & J. Caranqui 309	MO	03°30'26"S	78°25'15"W
<i>C. orientandina</i> Mansf.	H. Wiehler 77123	US, SEL	2°45'27.00"S	78° 1'29.93"W
<i>C. orientandina</i> Mansf.	I. Sanchez Vega & M. Dillon 9023	US	05° 40' S	77° 42' W
<i>C. orientandina</i> Mansf.	J. L. Clark & J. Katzenstein 8282	US, MO	01°23'56"S	78° 16'55"W
<i>C. orientandina</i> Mansf.	J. L. Clark & J. Katzenstein 8294	US	01°32'40"S	77° 53'53"W
<i>C. orientandina</i> Mansf.	J. L. Clark 6264	US	2°15'28.46"S	80° 6'21.14"W
<i>C. orientandina</i> Mansf.	J. L. Clark 9885	US	03°08'36"S	78° 32'13"W
<i>C. orientandina</i> Mansf.	J. L. Clark 9924	US	03°17'51"S	78° 33'27"W
<i>C. orientandina</i> Mansf.	J. L. Clark 9949	US	4° 3'40.66"S	78°57'11.70"W
<i>C. orientandina</i> Mansf.	J. L. Clark et al. 3203	US	04° 05' S	78° 55' W
<i>C. orientandina</i> Mansf.	L. P. Kvist 60424	US, MO	02° 18' S	78° 07' W
<i>C. orientandina</i> Mansf.	L. P. Kvist 60439	US, MO	02° 18' S	78° 07' W

<i>C. orientandina</i> Mansf.	L. P. Kvist et al. 60352	US, SI	01° 16' S	77° 52' W
<i>C. orientandina</i> Mansf.	M. T. Madison & F. R. Coleman 2537	SEL	2°45'27.00"S	78° 1'29.93"W
<i>C. orientandina</i> Mansf.	M. T. Madison et al. 3420	SI	2° 46' S	78° 06' W
<i>C. orientandina</i> Mansf.	P. Nunez V. 14090	MO	13°13'S	70°45'W
<i>C. orientandina</i> Mansf.	T. Montenegro 142	MO	03°31'33"S	78°26'52"W
<i>C. orientandina</i> Mansf.	W. Palacios 12088	MO	01°31'S	77°30'W
<i>C. ovatifolia</i> L. P. Kvist & L. E. Skog	F. Billiet & B. Jadin 6687	MO	00°00'S	78°40'W
<i>C. ovatifolia</i> L. P. Kvist & L. E. Skog	G. Harling & L. Andersson 12316	SI, SEL	0°52'7.96"N	78° 1'5.86"W
<i>C. ovatifolia</i> L. P. Kvist & L. E. Skog	J. F. Smith 1921	QCA, QCNE, WIS	0° 3' N	78°40' W
<i>C. ovatifolia</i> L. P. Kvist & L. E. Skog	J. L. Clark & A. Munoz 6129	US	00° 25.17' S	79° 00.19' W
<i>C. ovatifolia</i> L. P. Kvist & L. E. Skog	J. L. Clark & E. Folleco 8461	US	00° 49'46"S	78°07'03"W
<i>C. ovatifolia</i> L. P. Kvist & L. E. Skog	J. L. Luteyn et al. 8830	SI	0°	78°43' W
<i>C. ovatifolia</i> L. P. Kvist & L. E. Skog	J. Ramos et al. 6025	US	00° 20'41.64"S	78°28'19.92"W
<i>C. ovatifolia</i> L. P. Kvist & L. E. Skog	J. Ramos et al. 7003	US, MO	00° 18'41.4"S	78°34'51.24"W
<i>C. ovatifolia</i> L. P. Kvist & L. E. Skog	J. Ramos et al. 7188	US, MO	00° 19'14.16"S	78°35'24.72"W
<i>C. rileyi</i> (Wiehler) J. F. Smith	H. Wiehler & GRF Expedition 86243	SI, SEL	0°47'58.85"S	77°53'4.50"W
<i>C. rileyi</i> (Wiehler) J. F. Smith	H. Wiehler 97176	US	0° 3'47.74"N	78°41'1.43"W
<i>C. rileyi</i> (Wiehler) J. F. Smith	J. F. Smith 1944	QCA, QCNE,	0° 10' N	78° 45' W

		WIS		
<i>C. rileyi</i> (Wiehler) J. F. Smith	J. L. Clark & A. Munoz 6099	US, MO	00° 25.32' S	78° 57.73' W
<i>C. rileyi</i> (Wiehler) J. F. Smith	J. L. Clark et al. 6180	US	00° 24'14.7"S	78°57'18.1"W
<i>C. rileyi</i> (Wiehler) J. F. Smith	J. L. Clark et al. 7077	US, MO	00° 6'49"N	78°42'10"W
<i>C. rileyi</i> (Wiehler) J. F. Smith	L. Holm-Nielsen et al. 26229	US	00° 25' S	77° 49' W
<i>C. rileyi</i> (Wiehler) J. F. Smith	L. Holm-Nielsen et al. 26744	US	00° 27' S	77° 52' W
<i>C. rileyi</i> (Wiehler) J. F. Smith	T. B. Croat & L. Hannon 93495	US	00° 18'29"S	77°46'55"W
<i>C. rileyi</i> (Wiehler) J. F. Smith	T. B. Croat et al. 87690	US	00° 22'32"S	77°49'01"W
<i>C. spathulata</i> Mansf.	A. Gentry & C. H. Dodson 18027	MO	0° 35' 11" S	79° 21' 53" W
<i>C. spathulata</i> Mansf.	A. Gentry 9625	US	0° 2'7.37"S	79°22'1.59"W
<i>C. spathulata</i> Mansf.	A. Gentry et al. 12164	US, MO	0°13'35.04"S	79° 4'11.32"W
<i>C. spathulata</i> Mansf.	A. Gilli 116	W	0°14'3.59"S	79° 6'35.70"W
<i>C. spathulata</i> Mansf.	B. Hansen et al. 7774	SEL	0°47'37.34"S	79°13'53.72"W
<i>C. spathulata</i> Mansf.	B. Hansen et al. 7850	SEL	0°17'40.37"S	79° 8'58.33"W
<i>C. spathulata</i> Mansf.	B. Hansen et al. 7953	SI, SEL	0°30'3.52"N	79°26'2.02"W
<i>C. spathulata</i> Mansf.	B. Lojtnant & U. Molau 15811	US	0° 34' S	79° 19' W
<i>C. spathulata</i> Mansf.	B. Sparre 17825	US,	0°18'52.50"S	78°57'12.63"W
<i>C. spathulata</i> Mansf.	C. Bonifaz & X. Cornejo 3678	US	03° 41' S	79° 36' W
<i>C. spathulata</i> Mansf.	C. Espinoza 58	US	01° 21' 10.8"S	80°31'49.44"W
<i>C. spathulata</i> Mansf.	C. H. Dodson & A. Gentry 10242	SEL	0°51'44.80"S	79° 6'22.99"W
<i>C. spathulata</i> Mansf.	C. H. Dodson & A. Gentry 12791	US, SEL, MO, SI	0°59'26.75"S	79°12'3.50"W
<i>C. spathulata</i> Mansf.	C. H. Dodson & A. Gentry 9577	US, SEL, MO, SI	0°13'18.44"S	79° 1'24.67"W
<i>C. spathulata</i> Mansf.	C. H. Dodson 5944	SEL	0°18'1.27"S	79°14'1.77"W

<i>C. spathulata</i> Mansf.	C. H. Dodson 5974	SI, SEL	0°53'56.19"S	79°29'9.84"W
<i>C. spathulata</i> Mansf.	C. H. Dodson et al. 8434	SI, SEL	3°37'25.78"S	79°39'27.13"W
<i>C. spathulata</i> Mansf.	C. H. Dodson et al. 8463	SEL	3°38'59.47"S	79°45'0.45"W
<i>C. spathulata</i> Mansf.	C. H. Dodson et al. 8891	SI, MO, SEL	3°32'46.28"S	79°48'5.57"W
<i>C. spathulata</i> Mansf.	C. H. Dodson et al. 9138	SEL, MO, SI	3°35'57.35"S	79°47'8.87"W
<i>C. spathulata</i> Mansf.	C. Jatriva & C. Epling 1183	US, MO, SI	0°14'38.96"S	79° 7'8.86"W
<i>C. spathulata</i> Mansf.	C. Luer et al. 5555	SEL	3°41'0.02"S	79°41'3.55"W
<i>C. spathulata</i> Mansf.	D. R. Simpson & J. Schnuke 461	SI, US	3°56'20.74"S	80°33'3.16"W
<i>C. spathulata</i> Mansf.	D. R. Simpson & J. Schnuke 430	SI	3°56'20.74"S	80°33'3.16"W
<i>C. spathulata</i> Mansf.	E. Forero & R. Jaramillo 2322	US, MO	4°56'43.41"N	76°33'24.48"W
<i>C. spathulata</i> Mansf.	F. A. Michelangeli & M. Alfor 613	US	10°12'41"N	63°22'40"W
<i>C. spathulata</i> Mansf.	F. Fagerlind & G. Wibom 1657	OV, S	0°15'18.30"S	79° 9'27.21"W
<i>C. spathulata</i> Mansf.	F. Fagerlind & G. Wibom 2595	US	0°19'27.30"N	79°28'28.39"W
<i>C. spathulata</i> Mansf.	G. Davidse & A. C. Gonzalex 19450	SI, MO	10° 04' N	64° 14'-16' W
<i>C. spathulata</i> Mansf.	G. Harling & L. Andersson 14460	SI, SEL, US	3°17'31.11"S	79°19'6.52"W
<i>C. spathulata</i> Mansf.	G. Harling & L. Andersson 19245	US	1° 5'55.02"S	79° 9'37.66"W
<i>C. spathulata</i> Mansf.	G. S. Bunting 2637	SEL	10°10'40.19"N	63°29'42.45"W
<i>C. spathulata</i> Mansf.	H. H. Iltis & M. G. Iltis 276	SI, SEL	0° 14' S	79° 14" W
<i>C. spathulata</i> Mansf.	H. H. Iltis & M. G. Iltis 59	WIS	0° 36' S	79° 18' W
<i>C. spathulata</i> Mansf.	H. Van der Werff et al. 12386	US	1°41'9.60"S	79°15'43.05"W
<i>C. spathulata</i> Mansf.	H. Wiehler & GRF Expedition 8648	SEL	3°45'5.57"S	79°41'23.54"W
<i>C. spathulata</i> Mansf.	H. Wiehler & R. Dodson 71312	US, SEL	1° 2'11.93"S	79°28'37.14"W
<i>C. spathulata</i> Mansf.	H. Wiehler 72378	SEL, US	10°13'52.75"N	67°17'5.24"W

<i>C. spathulata</i> Mansf.	H. Wiehler 77135	SEL, US, SI	7°46'0.00"N	70° 9'0.00"W
<i>C. spathulata</i> Mansf.	H. Wiehler 79133	SEL, US	0°53'38.42"S	79° 9'58.08"W
<i>C. spathulata</i> Mansf.	H. Wiehler 79365	SEL, US	0°19'16.40"S	79° 9'15.32"W
<i>C. spathulata</i> Mansf.	H. Wiehler 7972	SEL, US	0°17'32.54"S	78°54'25.32"W
<i>C. spathulata</i> Mansf.	H. Wiehler 8649	SEL, US	3°45'5.57"S	79°41'23.54"W
<i>C. spathulata</i> Mansf.	H. Wiehler 90112	SEL, US	0° 7'0.00"N	79°15'60.00"W
<i>C. spathulata</i> Mansf.	H. Wiehler 9042	SEL, US	0°52'46.92"N	78°27'59.87"W
<i>C. spathulata</i> Mansf.	H. Wiehler 9074	SEL, US	0°53'45.36"N	78°30'12.55"W
<i>C. spathulata</i> Mansf.	H. Wiehler 9082	SEL, US	0°28'30.70"S	79° 9'27.44"W
<i>C. spathulata</i> Mansf.	H. Wiehler 9503	SEL, US	00°48'43.04"N	78°40'25.13"W
<i>C. spathulata</i> Mansf.	H. Wiehler 9775	SEL, US	0°51'29.21"S	79°13'17.89"W
<i>C. spathulata</i> Mansf.	J. A. Steyermark 105926	US	2° 27' 24" N	63° 56' W
<i>C. spathulata</i> Mansf.	J. A. Steyermark & A. J. M. Leeuwenberg 98976	WAG	11°13'25.37"N	69°32'57.44"W
<i>C. spathulata</i> Mansf.	J. A. Steyermark & M. Farinas 90952	US	10°19'59.61"N	67° 8'15.50"W
<i>C. spathulata</i> Mansf.	J. C. Solomon & M. Uehling 12232	MO, US	16° 12' S	67° 47' W
<i>C. spathulata</i> Mansf.	J. C. Solomon 12896	US, MO	16° 03' S	68° 01' W
<i>C. spathulata</i> Mansf.	J. D. Boeke & H. Loyola 2176	NY, SEL, US	2°42'17.75"S	79°23'4.79"W
<i>C. spathulata</i> Mansf.	J. F. Smith 1221	WIS	11° 10' N	69° 41' W
<i>C. spathulata</i> Mansf.	J. F. Smith 1853	QCA, QCNE, WIS	0° 20-25' N	78° 35-55' W
<i>C. spathulata</i> Mansf.	J. F. Smith 1900	QCA, QCNE, WIS	0° 20-25' N	78° 35-55' W
<i>C. spathulata</i> Mansf.	J. F. Smith 1960	QCA, QCNE,	3° 58' S	80° 0'-10' W

		WIS		
<i>C. spathulata</i> Mansf.	J. L. Clark & A. Munoz 6098	US	00° 18.95'S	78° 56.81'W
<i>C. spathulata</i> Mansf.	J. L. Clark 4644	US	00° 21' N	79° 44' W
<i>C. spathulata</i> Mansf.	J. L. Clark 4711	US	00° 25' N	79° 45' W
<i>C. spathulata</i> Mansf.	J. L. Clark 9768	US	00° 21' N	79° 44' W
<i>C. spathulata</i> Mansf.	J. L. Clark 9823	US	2° 42' 41" S	79° 28'35" W
<i>C. spathulata</i> Mansf.	J. L. Clark et al. 2420	US	00° 49' N	78° 01' W
<i>C. spathulata</i> Mansf.	J. L. Clark et al. 2700	US	00° 01'N	79° 58' W
<i>C. spathulata</i> Mansf.	J. L. Clark et al. 2793	US	00° 20'N	79° 28'W
<i>C. spathulata</i> Mansf.	J. L. Clark et al. 2823	US	00° 29'N	79° 41'W
<i>C. spathulata</i> Mansf.	J. L. Clark et al. 4143	US	00° 15' N	79° 48' W
<i>C. spathulata</i> Mansf.	J. L. Clark et al. 6256	US	02°37'46.0"S	79°16'41"W
<i>C. spathulata</i> Mansf.	J. L. Clark et al. 7368	SEL, US	00° 18' N	78° 46' W
<i>C. spathulata</i> Mansf.	J. L. Clark et al. 7482	SEL, US	00°53'24"N	78°30'44"W
<i>C. spathulata</i> Mansf.	J. L. Clark et al. 7485	SEL, US	00°45'21"N	78°27'09"W
<i>C. spathulata</i> Mansf.	J. L. Clark et al. 7530	SEL, US	00°45'21"N	78°27'09"W
<i>C. spathulata</i> Mansf.	J. L. Clark et al. 7532	US	00°49'51"N	78°28'54"W
<i>C. spathulata</i> Mansf.	J. L. Clark et al. 7957	SEL, US	03°39'03"S	79°44'24"W
<i>C. spathulata</i> Mansf.	J. L. Clark et al. 7958	SEL, US	03°39'03"S	79°44'24"W
<i>C. spathulata</i> Mansf.	J. L. Clark et al. 8777	US	00° 21' N	79° 44' W
<i>C. spathulata</i> Mansf.	J. L. Clark et al. 8827	US	00° 21'N	79° 44' W
<i>C. spathulata</i> Mansf.	J. L. Clark et al. 9268	US	03°05'26.49"S	77°52'06.29"W
<i>C. spathulata</i> Mansf.	L. B. Thien 1674	SI, SEL, MO, US	1°48'23.44"S	80°45'27.45"W

<i>C. spathulata</i> Mansf.	L. Besse et al. 1272	SEL, SI	1° 3'19.68"S	80°40'9.63"W
<i>C. spathulata</i> Mansf.	L. Besse et al. 597	SEL	15° 22'41.20" S	68° 30'51.69" W
<i>C. spathulata</i> Mansf.	L. Holm-Nielsen et al. 2972	US	0° 55' S	79° 11' W
<i>C. spathulata</i> Mansf.	L. S. G. Beck 21427	US	16°18'37.67"S	67°35'7.63"W
<i>C. spathulata</i> Mansf.	M. A. Solis 6885	SI, US	1°34'58.85"S	79°10'0.46"W
<i>C. spathulata</i> Mansf.	M. E. Mathias & D. Taylor 5180	US	0°59'12.88"S	79°21'42.07"W
<i>C. spathulata</i> Mansf.	M. T. Madison et al. 4991	SEL	0°52'51.85"N	78°28'6.27"W
<i>C. spathulata</i> Mansf.	O. Haught 2965	US, SI	1° 1'1.45"S	79°28'36.26"W
<i>C. spathulata</i> Mansf.	O. Haught 3408	US	1°22'54.76"S	80°27'56.07"W
<i>C. spathulata</i> Mansf.	P. Mendoza-T. et al. 530	US	00° 05' N	78° 55' W
<i>C. spathulata</i> Mansf.	P. Mendoza-T. et al. 549	US	00° 10' N	78° 55' W
<i>C. spathulata</i> Mansf.	P. Mendoza-T. et al. 591	US	00° 21'N	79° 44'W
<i>C. spathulata</i> Mansf.	P. Mendoza-T. et al. 598	US	00° 21'N	79° 43'W
<i>C. spathulata</i> Mansf.	P. Mendoza-T. et al. 615	US	00° 15'S	78° 45'W
<i>C. spathulata</i> Mansf.	R. Espinesa 1216	SEL	3°52'46.35"S	79°33'24.44"W
<i>C. spathulata</i> Mansf.	R. W. Dunn 95-04- 135	US	0°21'20.17"S	79° 5'44.98"W
<i>C. spathulata</i> Mansf.	S. Mori et al. 14658	US	10°15'N	68° 29'30"W
<i>C. spathulata</i> Mansf.	T. B. Croat 38969	US, MO	0°52'21.42"N	78°26'37.49"W
<i>C. spathulata</i> Mansf.	T. B. Croat 55658	MO, US, SI	0° 16' S	79° 07' W
<i>C. spathulata</i> Mansf.	T. Delinks 504	US	00°08'15"S	80°09'23"W
<i>C. spathulata</i> Mansf.	T. Plowman et al. 13411	F	11° 11' 30" N	69° 41' 00" W
<i>C. spathulata</i> Mansf.	W. Meier & C. Mentel 11860	US	10°37'N	63° 11'W
<i>C. spathulata</i> Mansf.	W. Meier & M. Roeser 1006	US	10°12.5'N	68° 33.5'W

<i>C. spathulata</i> Mansf.	W. Meier & P. Molina 6790	US	10°38'N	63°10'W
<i>C. spathulata</i> Mansf.	W. Meier & R. Struppek 10464	US	10°14'30"N	66° 24'30"W
<i>C. spathulata</i> Mansf.	W. Meier & R. Struppek 13461	US	10°10'30"N	66° 24'W
<i>C. spathulata</i> Mansf.	W. Meier & R. Struppek 10868	US	10°13'30"N	66° 24'W
<i>C. spathulata</i> Mansf.	W. Meier & S. Nehlin 10188	US	10°03'N	66° 53'W
<i>C. spathulata</i> Mansf.	W. Meier 12912	US	10°26'N	66° 51'W
<i>C. spathulata</i> Mansf.	W. Meier 3231	US	10°12.5'N	68° 33'W
<i>C. spathulata</i> Mansf.	W. Meier et al. 14354	US	10°37'N	63° 10'W
<i>C. spathulata</i> Mansf.	W. Meier et al. 7790	US	10°12'30"N	68°33'30"W
<i>C. spathulata</i> Mansf.	W. Meier et al. 8467	US	10°12'30"N	68°33'W
<i>C. spathulata</i> Mansf.	X. Cornejo & C. Bonifaz 1011	US	01° 33'S	80° 38' W
<i>C. spathulata</i> Mansf.	X. Cornejo & C. Bonifaz 4532	US	02° 06'S	79° 10' W
<i>C. spathulata</i> Mansf.	X. Cornejo & C. Bonifaz 5716	US	01° 48'S	80° 47' W
<i>C. spathulata</i> Mansf.	X. Cornejo & C. Bonifaz 6650	US	01° 48'S	80° 47' W
<i>C. spathulata</i> Mansf.	X. Cornejo & C. Bonifaz 939	US	01° 42'S	80° 34' W
<i>C. tandapiana</i> (Wiehler) L.E. Skog & L.P. Kvist	C. Dodson & A. Gentry 9592	SEL, MO	0°19'36.22"S	78°50'58.89"W
<i>C. tandapiana</i> (Wiehler) L.E. Skog & L.P. Kvist	G. Harling & L. Andersson 19225	US	1°10'45.62"S	79° 5'56.12"W
<i>C. tandapiana</i> (Wiehler) L.E. Skog & L.P. Kvist	H. Van der Werff et al. 12298	US, MO	0° 8'54.52"S	78°50'17.79"W
<i>C. tandapiana</i> (Wiehler) L.E. Skog & L.P. Kvist	H. Wiehler & D. Masterson 7954	SEL, US	0° 4'50.31"S	78°47'52.90"W
<i>C. tandapiana</i> (Wiehler) L.E. Skog & L.P. Kvist	H. Wiehler & GRF Expedition 90133	SEL	0° 1'21.72"S	78°51'7.08"W
<i>C. tandapiana</i>	H. Wiehler 97171	SEL, US	0° 3'47.74"N	78°41'1.43"W

(Wiehler) L.E. Skog & L.P. Kvist				
<i>C. tandapiana</i> (Wiehler) L.E. Skog & L.P. Kvist	J. A. Steyermark 52825	US	2°16'52.69"S	79°16'57.98"W
<i>C. tandapiana</i> (Wiehler) L.E. Skog & L.P. Kvist	J. L. Clark & A. Munoz 6106	SEL, US	00°25.17'S	79° 00.19'W
<i>C. tandapiana</i> (Wiehler) L.E. Skog & L.P. Kvist	J. L. Clark 8006	SEL, US	03°33'28"S	79°46'12"W
<i>C. tandapiana</i> (Wiehler) L.E. Skog & L.P. Kvist	J. L. Clark et al. 6168	US	00°25.17'S	79° 00.19'W
<i>C. tandapiana</i> (Wiehler) L.E. Skog & L.P. Kvist	J. L. Clark et al. 6181	US	00°24'14.7"S	78° 57'18.1"W
<i>C. tandapiana</i> (Wiehler) L.E. Skog & L.P. Kvist	J. L. Clark et al. 7076	US, MO	00° 6'49"N	78°42'10"W
<i>C. tandapiana</i> (Wiehler) L.E. Skog & L.P. Kvist	J. Smith 1945	US, SEL	0° 10' N	78°45' W
<i>C. tandapiana</i> (Wiehler) L.E. Skog & L.P. Kvist	M. Madison et al. 3370	SEL	2° 46' S	78°06' W
<i>C. tandapiana</i> (Wiehler) L.E. Skog & L.P. Kvist	P. Silverstone- Sopkin et al. 9967	US	00°58'45"S	79°06'53"W

**APPENDIX D****Extracted Environmental Data for All Herbarium Collection Specimens****as Categorized by SEEVA Analyses**

<b>Bioclim Variable</b>	<b>Range</b>	<i>C. ambigua</i>	<i>C. angustata</i>	<i>C. byrsina</i>	<i>C. colombiana</i>	<i>C. crassicaulis</i>	<i>C. domingensis</i>	<i>C. katzensteiniae</i>	<i>C. manabiana</i>	<i>C. orientandina</i>	<i>C. ovatifolia</i>	<i>C. rileyi</i>	<i>C. spathulata</i>	<i>C. tandapiana</i>
<b>Annual Mean Temperature</b>	< 18.667 °C	0	11	26	0	6	22	14	0	2	12	7	9	11
	18.667-21.225 °C	13	32	23	0	7	9	2	1	6	0	3	24	3
	21.225-23.1 °C	10	43	3	0	0	7	1	4	9	0	0	44	0
	> 23.1 °C	2	69	5	3	0	7	0	6	2	0	0	40	1
<b>Mean Diurnal Range</b>	< 8.7 °C	4	55	6	2	0	0	0	4	0	0	0	49	2
	8.7-9.7 °C	15	48	9	0	4	3	1	6	2	0	3	28	4
	9.7-10.9 °C	6	43	26	0	5	5	6	0	10	6	2	14	7
	> 10.9 °C	0	9	16	1	4	37	10	1	7	6	5	26	2
<b>Isothermality</b>	< 77.75	25	17	2	0	1	43	0	6	3	0	0	28	3
	77.75-84	0	42	3	0	0	2	6	4	10	2	2	56	3
	84-88	0	53	17	1	5	0	10	1	6	6	4	15	9
	> 88	0	43	35	2	7	0	1	0	0	4	4	18	0
<b>Temperature Seasonality</b>	< 265.75 °C	0	24	34	0	12	0	6	0	0	11	4	16	10
	265.75-439.5 °C	0	62	19	3	0	0	8	1	4	0	6	20	3
	439.5-703.33 °C	0	57	3	0	0	0	3	4	13	1	0	47	1
	> 703.33 °C	25	12	1	0	1	45	0	6	2	0	0	34	1
<b>Maximum Temperature of Warmest Month</b>	< 24.925 °C	0	12	31	0	8	13	11	0	2	12	7	10	12
	24.925-27.15 °C	13	37	19	0	4	13	5	2	1	0	3	25	1
	27.15-29.133 °C	8	52	2	0	1	9	1	4	10	0	0	42	1
	> 29.133 °C	4	54	5	3	0	10	0	5	6	0	0	40	1

<b>Bioclim Variable</b>	<b>Range</b>	<i>C. ambigua</i>	<i>C. angustata</i>	<i>C. byrsina</i>	<i>C. colombiana</i>	<i>C. crassicaulis</i>	<i>C. domingensis</i>	<i>C. katzensteiniae</i>	<i>C. manabiana</i>	<i>C. orientandina</i>	<i>C. ovatifolia</i>	<i>C. rileyi</i>	<i>C. spathulata</i>	<i>C. tandapiana</i>
<b>Minimum Temperature of Coldest Month</b>	< 12.533 °C	2	9	21	0	7	30	13	0	1	12	8	12	8
	12.533-15.4 °C	19	25	24	0	4	8	3	1	7	0	2	19	6
	15.4-17.933 °C	4	53	7	0	2	5	1	4	9	0	0	44	0
	> 17.933 °C	0	68	5	3	0	2	0	6	2	0	0	42	1
<b>Temperature Annual Range</b>	< 10.575 °C	0	58	14	2	4	0	0	3	0	0	0	37	2
	10.575-11.45 °C	0	64	12	0	3	0	1	2	4	1	3	32	5
	11.45-12.84 °C	14	27	21	0	2	0	5	5	8	7	5	23	6
	> 12.84 °C	11	6	10	1	4	45	11	1	7	4	2	25	2
<b>Mean Temperature of the Wettest Quarter</b>	< 18.85 °C	0	10	28	0	7	18	13	0	2	12	9	10	11
	18.85-21.5 °C	7	42	21	0	6	12	3	1	6	0	1	21	3
	21.5-23.667 °C	13	46	5	0	0	6	1	3	10	0	0	40	0
	> 23.667 °C	5	57	3	3	0	9	0	7	1	0	0	46	1
<b>Mean Temperature of the Driest Quarter</b>	< 18.3 °C	6	9	21	0	7	27	12	0	1	12	5	9	10
	18.3-20.98 °C	16	26	27	0	6	8	4	1	3	0	5	27	4
	20.98-22.633 °C	3	52	4	0	0	4	1	4	11	0	0	46	0
	> 22.633 °C	0	68	5	3	0	6	0	6	4	0	0	35	1
<b>Mean Temperature of the Warmest Quarter</b>	< 19.375 °C	0	9	28	0	8	16	13	0	2	12	9	9	12
	19.375-21.85 °C	8	41	21	0	5	14	3	1	5	0	1	24	2
	21.85-23.9 °C	12	44	3	0	0	6	1	3	10	0	0	41	0
	> 23.9 °C	5	61	5	3	0	9	0	7	2	0	0	43	1

<b>Bioclim Variable</b>	<b>Range</b>	<i>C. ambigua</i>	<i>C. angustata</i>	<i>C. byrsina</i>	<i>C. colombiana</i>	<i>C. crassicaulis</i>	<i>C. domingensis</i>	<i>C. katzensteiniae</i>	<i>C. manabiana</i>	<i>C. orientandina</i>	<i>C. ovatifolia</i>	<i>C. rileyi</i>	<i>C. spathulata</i>	<i>C. tandapiana</i>
<b>Mean Temperature of the Coldest Quarter</b>	< 18.133 °C	2	10	22	0	7	27	13	0	2	12	7	8	10
	18.133-20.5 °C	15	32	25	0	6	8	3	1	4	0	3	25	4
	20.5-22.433 °C	8	41	5	0	0	4	1	5	11	0	0	39	0
	> 22.433 °C	0	72	5	3	0	6	0	5	2	0	0	45	1
<b>Annual Precipitation</b>	< 1578.5 mm	0	14	12	0	5	28	8	6	2	6	0	45	1
	1578.5-2294.2 mm	9	22	18	1	6	16	4	3	4	5	3	30	6
	2294.2-2888.3 mm	9	35	12	0	0	1	4	2	8	1	5	36	7
	> 2888.3 mm	7	84	15	2	2	0	1	0	5	0	2	6	1
<b>Precipitation of the Wettest Month</b>	< 253.5 mm	1	13	20	0	6	30	9	4	5	5	0	33	0
	253.5-331 mm	17	13	21	1	6	12	5	2	9	6	6	25	3
	331-429.75 mm	7	52	9	0	1	3	3	3	1	1	3	27	10
	> 429.75 mm	0	77	7	2	0	0	0	2	4	0	1	32	2
<b>Precipitation of the Driest Month</b>	< 29 mm	0	26	12	0	5	12	2	9	1	5	0	54	4
	29-53 mm	0	26	7	0	4	30	5	2	0	6	3	39	4
	53-136.43 mm	24	25	27	1	4	3	7	0	4	1	2	22	6
	> 136.43 mm	1	78	11	2	0	0	3	0	14	0	5	2	1
<b>Precipitation Seasonality</b>	< 25	4	75	17	1	0	0	9	0	15	1	4	3	0
	25-44	15	25	31	2	4	9	0	0	3	2	1	18	1
	44-70.5	6	18	7	0	9	36	7	0	0	8	5	26	10
	> 70.5	0	37	2	0	0	0	1	11	1	1	0	70	4

<b>Bioclim Variable</b>	<b>Range</b>	<i>C. ambigua</i>	<i>C. angustata</i>	<i>C. byrsina</i>	<i>C. colombiana</i>	<i>C. crassicaulis</i>	<i>C. domingensis</i>	<i>C. katzensteiniae</i>	<i>C. manabiana</i>	<i>C. orientandina</i>	<i>C. ovatifolia</i>	<i>C. rileyi</i>	<i>C. spathulata</i>	<i>C. tandapiana</i>
<b>Precipitation of the Wettest Quarter</b>	< 697 mm	1	13	20	0	5	33	8	4	4	5	0	33	0
	697-921.67 mm	9	15	20	1	6	12	6	2	10	6	6	26	3
	921.67-1184.5 mm	15	49	10	0	2	0	3	3	1	1	3	28	8
	> 1184.5 mm	0	78	7	2	0	0	0	2	4	0	1	30	4
<b>Precipitation of the Driest Quarter</b>	< 116.6 mm	0	22	8	0	4	18	1	10	1	5	0	55	4
	116.6-198.43 mm	1	30	10	0	5	25	5	1	0	3	2	41	3
	198.43-492 mm	23	24	26	1	4	2	8	0	8	4	5	14	7
	> 492 mm	1	79	13	2	0	0	3	0	10	0	3	7	1
<b>Precipitation of the Warmest Quarter</b>	< 486 mm	0	22	18	1	2	20	8	4	5	4	0	41	1
	486-698.38 mm	9	23	21	0	5	25	4	1	10	3	4	14	1
	698.38-1022 mm	16	44	10	1	6	0	5	2	2	5	6	21	7
	> 1022 mm	0	66	8	1	0	0	0	4	2	0	0	41	6
<b>Precipitation of the Coldest Quarter</b>	< 158 mm	0	27	3	0	2	30	2	9	1	5	0	47	1
	158-382 mm	13	22	5	0	3	15	8	1	2	7	3	40	9
	382-829 mm	12	24	32	1	6	0	5	1	12	0	4	24	4
	> 829 mm	0	82	17	2	2	0	2	0	4	0	3	6	1

## APPENDIX E

**Maximum Likelihood Probability (MLP) and Bayesian Posterior Probability (BPP)  
Results from Ancestral State Reconstructions of Morphological Characters Using  
Both the Branch Length Model (BL) in Simmap 1.5 Analyses and Mk1 Model in  
Mesquite v. 2.75 Analyses for all Character States (Ch. State)**

Character	Ch. State	Node 1		Node 2		Node 3		Node 4	
		BL	Mk1	BL	Mk1	BL	Mk1	BL	Mk1
<b>Habit</b>	Pr(0)	0.336093	0.33333333	0.334178	0.33333333	0.334366	0.33333333	0.333345	0.33333333
	Pr(1)	0.331951	0.33333333	0.332597	0.33333333	0.332098	0.33333333	0.332023	0.33333333
	Pr(2)	0.331957	0.33333333	0.333225	0.33333333	0.333536	0.33333333	0.334632	0.33333333
<b>Leaf Isophylly</b>	Pr(0)	0.835732	0.50000000	0.623619	0.50000000	0.484461	0.50000000	0.010329	0.50000000
	Pr(1)	0.164268	0.50000000	0.376381	0.50000000	0.515539	0.50000000	0.989671	0.50000000
<b>Lamina Surface Area</b>	Pr(0)	0.43232	0.84372972	0.667414	0.87225388	0.909036	0.89955136	0.999858	0.92745508
	Pr(1)	0.56768	0.15627028	0.332586	0.12774612	0.090964	0.10044864	0.000142	0.07254492
<b>Adaxial Pubescence</b>	Pr(0)	0.999949	0.99226725*	0.99766	0.99006834*	0.999733	0.99419857*	0.999986	0.99848980*
	Pr(1)	0.000051	0.00773275	0.00234	0.00993166	0.000267	0.00580143	0.000014	0.00151020
<b>Abaxial Pubescence</b>	Pr(0)	0.040757	0.03761109	0.014849	0.01154453	0.000033	0.00070907	0.000007	0.00024352
	Pr(1)	0.959243	0.96238891*	0.985151	0.98845547*	0.999967	0.99929093*	0.999993	0.99975648*
<b>Abaxial Coloration</b>	Pr(0)	0.999989	0.99312237*	0.998129	0.98808357*	0.999734	0.99193813*	0.999991	0.99844366*
	Pr(1)	0.000008	0.00210179	0.00064	0.00302484	0.00006	0.00147238	0.000007	0.00038334
	Pr(2)	0.000001	0.00207121	0.000132	0.00287293	0.000006	0.00127756	0	0.00023825
	Pr(3)	0.000002	0.00270463	0.001099	0.00601866	0.0002	0.00531193	0.000002	0.00093474
<b>Petiole Length</b>	Pr(0)	0.000443	0.33333333	0.082095	0.33333333	0.204778	0.33333333	0.933693	0.33333333
	Pr(1)	0.999557	0.33333333	0.917851	0.33333333	0.795221	0.33333333	0.0663	0.33333333
	Pr(2)	0.000001	0.33333333	0.000054	0.33333333	0.000001	0.33333333	0.000006	0.33333333
<b>Inflorescence</b>	Pr(0)	0.005591	0.54493802	0.013053	0.29041264	0.000598	0.20571980	0.005057	0.19834718

Character	Ch. State	Node 1		Node 2		Node 3		Node 4	
		BL	Mk1	BL	Mk1	BL	Mk1	BL	Mk1
<b>Number</b>	Pr(1)	0.994409	0.45506198	0.986947	0.70958736	0.999402	0.79428020	0.994943	0.80165282
<b>Floral Bract Size</b>	Pr(0)	0.363259	0.62693651	0.63971	0.55078089	0.902338	0.55562474	0.994281	0.57126170
	Pr(1)	0.636671	0.22960890	0.359872	0.31087851	0.097648	0.33319572	0.005714	0.32435572
	Pr(2)	0.00007	0.14345458	0.000418	0.13834060	0.000013	0.11117954	0.000005	0.10438258
<b>Corolla to Calyx Ratio</b>	Pr(0)	0.999909	0.66172817	0.996729	0.609145497	0.999362	0.62450568	0.967257	0.62342224
	Pr(1)	0.000091	0.33827183	0.003271	0.3908545	0.000638	0.37549435	0.032743	0.37657776
<b>Calyx Margin</b>	Pr(0)	0.005891	0.22548332	0.473183	0.54176321	0.944673	0.63566307	0.967779	0.6386422
	Pr(1)	0.994109	0.77451668	0.526817	0.45823679	0.055327	0.36433693	0.032221	0.361357795
<b>Corolla Length</b>	Pr(0)	0.00005	0.00472694	0.002231	0.00695983	0.000245	0.00423008	0.006263	0.00585462
	Pr(1)	0.99995	.99527306*	0.997769	0.99304017*	0.999755	0.99576992*	0.993737	0.99414538*
<b>Corolla Color</b>	Pr(0)	0.998858	0.32705859	0.608628	0.24903233	0.034205	0.23524106	0.002723	0.23119221
	Pr(1)	0.000007	0.22203762	0.001122	0.2306541	0.000016	0.2182115	0.000194	0.21307141
	Pr(2)	0.000001	0.22260971	0.000181	0.23559757	0.000001	0.22743773	0.000005	0.22445093
	Pr(3)	0.001134	0.22829408	0.390069	0.28471599	0.965778	0.31910971	0.997078	0.33128545
<b>Corolla Lobe Color</b>	Pr(0)	0.999424	0.5	0.920454	0.5	0.815725	0.5	0.00491	0.5
	Pr(1)	0.000576	0.5	0.079546	0.5	0.184275	0.5	0.99509	0.5
<b>Phenology</b>	Pr(0)	0.96427	0.93335155	0.98847	0.96955478	0.999976	0.99068860*	0.999722	0.99131966*
	Pr(1)	0.000142	0.02050742	0.000851	0.01444038	0.000014	0.00694644	0.000277	0.0074762
	Pr(2)	0.035588	0.04614103	0.01068	0.01900483	0.00001	0.00236496	0.000001	0.00120413

Character	Ch. State	Node 5		Node 6		Node 7		Node 8	
		BL	Mk1	BL	Mk1	BL	Mk1	BL	Mk1
<b>Habit</b>	Pr(0)	0.332758	0.33333333	0.333045	0.33333333	0.332608	0.33333333	0.332918	0.33333333
	Pr(1)	0.331944	0.33333333	0.328798	0.33333333	0.334021	0.33333333	0.331659	0.33333333
	Pr(2)	0.335298	0.33333333	0.338157	0.33333333	0.333371	0.33333333	0.335424	0.33333333
<b>Leaf Isophylly</b>	Pr(0)	0.022833	0.50000000	0.000855	0.49999999	0.991152	0.50000000	0.000143	0.50000000
	Pr(1)	0.977167	0.50000000	0.999145	0.50000001	0.008848	0.50000000	0.999857	0.50000000
<b>Lamina Surface Area</b>	Pr(0)	0.99984	0.92421476*	0.989319	0.87701277	0.999864	0.92115961*	0.999996	0.98627764*
	Pr(1)	0.00016	0.07578524	0.010681	0.12298723	0.000136	0.07884039	0.000004	0.01372236
<b>Adaxial Pubescence</b>	Pr(0)	0.999998	0.99955229*	0.999996	0.99949172*	0.999977	0.99670817*	0.999988	0.99933316*
	Pr(1)	0.000002	0.00044771	0.000004	0.00050828	0.000023	0.00329183	0.000012	0.00066684
<b>Abaxial Pubescence</b>	Pr(0)	0.000003	0.00014170	0.000004	0.00024111	0.000023	0.00165862	0.000152	0.00238900
	Pr(1)	0.999997	0.99985830*	0.999996	0.99975889*	0.999977	0.99834138*	0.999848	0.997610998*
<b>Abaxial Coloration</b>	Pr(0)	0.999979	0.99865233*	0.999997	0.99955182*	0.996416	0.96527797*	1	0.99978861*
	Pr(1)	0.000021	0.00082768	0.000002	0.00019286	0.003576	0.02562700	0	0.00006634
	Pr(2)	0	0.00020028	0	0.00012080	0.000004	0.00450812	0	0.00006191
	Pr(3)	0	0.00031971	0	0.00013452	0.000004	0.00458691	0	0.00008314
<b>Petiole Length</b>	Pr(0)	0.914765	0.33333333	0.040214	0.33333333	0.997744	0.33333333	0.935227	0.33333333
	Pr(1)	0.084749	0.33333333	0.904944	0.33333333	0.00222	0.33333333	0.064771	0.33333333
	Pr(2)	0.000486	0.33333333	0.054841	0.33333333	0.000036	0.33333333	0.000001	0.33333333
<b>Inflorescence</b>	Pr(0)	0.000081	0.07747771	0.000005	0.03091461	0.000033	0.08312606	0.682411	0.44034781

Character	Ch. State	Node 5		Node 6		Node 7		Node 8	
		BL	Mk1	BL	Mk1	BL	Mk1	BL	Mk1
<b>Number</b>	Pr(1)	0.999919	0.92252229*	0.999995	0.96908539*	0.999967	0.91687394*	0.317589	0.55965219
<b>Floral Bract Size</b>	Pr(0)	0.999959	0.67170947	0.996746	0.68999700	0.999959	0.69000782	0.894302	0.45909902
	Pr(1)	0.000022	0.19127305	0.000144	0.11879997	0.000034	0.17015726	0.105679	0.47981088
	Pr(2)	0.00002	0.13701748	0.003109	0.19120303	0.000007	0.13983492	0.000019	0.06109007
<b>Corolla to Calyx Ratio</b>	Pr(0)	0.993517	0.70412442	0.999982	0.8191104	0.989211	0.62885076	0.141156	0.44753968
	Pr(1)	0.006483	0.29587558	0.000018	0.180889596	0.010789	0.37114924	0.858844	0.55246032
<b>Calyx Margin</b>	Pr(0)	0.034026	0.39959092	0.000074	0.11152671	0.082697	0.43543442	0.999779	0.960689798
	Pr(1)	0.965974	0.60040908	0.999926	0.88847329	0.917303	0.56456558	0.000221	0.0393102
<b>Corolla Length</b>	Pr(0)	0.000096	0.000682636	0.000004	0.000358889	0.000023	0.0021506	0.627045	0.26683448
	Pr(1)	0.999904	0.99931736*	0.999996	0.996411111*	0.999977	0.997849396*	0.372955	0.73316552
<b>Corolla Color</b>	Pr(0)	0.011726	0.20914736	0.000075	0.15841546	0.604927	0.235939	0.059598	0.23942139
	Pr(1)	0.004382	0.20503428	0.000009	0.15704762	0.267461	0.24512142	0.005695	0.18570219
	Pr(2)	0.000005	0.2075836	0	0.15695586	0.000037	0.22853503	0.001251	0.23578495
	Pr(3)	0.983888	0.38106001	0.999916	0.52758106	0.127575	0.29040455	0.933456	0.336909147
<b>Corolla Lobe Color</b>	Pr(0)	0.015219	0.5	0.279305	0.5	0.333698	0.5	0.000046	0.5
	Pr(1)	0.984781	0.5	0.720695	0.5	0.666302	0.5	0.999954	0.5
<b>Phenology</b>	Pr(0)	0.99868	0.98398558*	0.979158	0.91437805*	0.999952	0.98426368*	0.992225	0.96578901*
	Pr(1)	0.001319	0.01435269	0.020823	0.079545297	0.000043	0.01096435	0.007768	0.3127227
	Pr(2)	0.000001	0.00166172	0.000018	0.00607662	0.000005	0.00477197	0.000007	0.00293873

Character	Ch. State	Node 9		Node 10		Node 11		Node 12	
		BL	Mk1	BL	Mk1	BL	Mk1	BL	Mk1
<b>Habit</b>	Pr(0)	0.336581	0.33333333	0.345215	0.33333333	0.338089	0.33333333	0.336258	0.33333333
	Pr(1)	0.333814	0.33333333	0.328449	0.33333333	0.330877	0.33333333	0.331871	0.33333333
	Pr(2)	0.329605	0.33333333	0.326336	0.33333333	0.331034	0.33333333	0.331871	0.33333333
<b>Leaf Isophylly</b>	Pr(0)	0.001483	0.50000000	0.231048	0.50000000	0.997155	0.50000000	0.99977	0.50000000
	Pr(1)	0.998517	0.50000000	0.768952	0.50000000	0.002845	0.50000000	0.00023	0.50000000
<b>Lamina Surface Area</b>	Pr(0)	0.999997	0.99341957*	0.999994	0.99388757*	0.338166	0.36284545	0.449164	0.45927197
	Pr(1)	0.000003	0.00658043	0.000006	0.00611243	0.661834	0.63715455	0.550836	0.54072803
<b>Adaxial Pubescence</b>	Pr(0)	0.999926	0.99819755*	0.997206	0.98138383*	0.965714	0.71172887	0.998275	0.90833573*
	Pr(1)	0.000074	0.00180245	0.002794	0.01861617	0.034286	0.28827113	0.001725	0.09166427
<b>Abaxial Pubescence</b>	Pr(0)	0.004983	0.01574713	0.000144	0.00217601	0.00002	0.00162683	0.000048	0.00696659
	Pr(1)	0.995017	0.98425287*	0.999856	0.99782399*	0.99998	0.99837317*	0.999952	0.99303341*
<b>Abaxial Coloration</b>	Pr(0)	1	0.99987508*	0.999999	0.99974955*	0.693832	0.31386829	0.159681	0.16024494
	Pr(1)	0	0.00004130	0	0.00008345	0.042862	0.08186122	0.755186	0.31952160
	Pr(2)	0	0.00004094	0	0.00008341	0.004094	0.07370515	0.073564	0.27898571
	Pr(3)	0	0.00004268	0	0.00008359	0.259211	0.53056534	0.011569	0.24124774
<b>Petiole Length</b>	Pr(0)	0.166581	0.33333333	0.179216	0.33333333	0.529661	0.33333333	0.994003	0.33333333
	Pr(1)	0.833419	0.33333333	0.820782	0.33333333	0.470331	0.33333333	0.005995	0.33333333

Character	Ch. State	Node 9		Node 10		Node 11		Node 12	
		BL	Mk1	BL	Mk1	BL	Mk1	BL	Mk1
	Pr(2)	0	0.33333333	0.000002	0.33333333	0.000009	0.33333333	0.000003	0.33333333
<b>Inflorescence Number</b>	Pr(0)	0.659907	0.41828026	0.000182	0.12592752	0.000057	0.09436142	0.000071	0.14892673
	Pr(1)	0.340093	0.58171974	0.999818	0.87407248	0.999943	0.90563858*	0.999929	0.85107327
<b>Floral Bract Size</b>	Pr(0)	0.000111	0.16097020	0.000006	0.05720867	0.560086	0.23862077	0.873718	0.36551408
	Pr(1)	0.999889	0.80290309	0.999993	0.92053536	0.43821	0.62214151	0.074069	0.32711025
	Pr(2)	0	0.03612671	0	0.02225596	0.001704	0.13923772	0.052213	0.30737567
<b>Corolla to Calyx Ratio</b>	Pr(0)	0.255236	0.48818103	0.999769	0.75167856	0.998834	0.70949996	0.987951	0.54079172
	Pr(1)	0.744764	0.51181897	0.000231	0.24832144	0.001166	0.29050004	0.012049	0.45920828
<b>Calyx Margin</b>	Pr(0)	0.999996	0.98948469*	0.999992	0.99540711*	0.999877	0.90244704	0.99985	0.90592255*
	Pr(1)	0.000004	0.01051531	0.000008	0.00459289	0.000123	0.09755296	0.00015	0.09407745
<b>Corolla Length</b>	Pr(0)	0.513779	0.26337983	0.000144	0.03491852	0.000062	0.00226934	0.000048	0.100813257
	Pr(1)	0.486221	0.73662017	0.999856	0.96508148*	0.999938	0.99773066*	0.999952	0.99186743*
<b>Corolla Color</b>	Pr(0)	0.85742	0.29104108	0.070492	0.18397094	0.04008	0.20096286	0.998069	0.25830879
	Pr(1)	0.029841	0.18253245	0.21245	0.18603405	0.000052	0.19960206	0.000014	0.24478794
	Pr(2)	0.097485	0.28618906	0.716082	0.46249844	0.000006	0.0012108	0.000002	0.24480693
	Pr(3)	0.015253	0.2402374	0.000975	0.16749657	0.959863	0.39931403	0.001916	0.25209633
<b>Corolla Lobe Color</b>	Pr(0)	0.000296	0.5	0.019558	0.5	0.997192	0.5	0.99985	0.5
	Pr(1)	0.999704	0.5	0.980442	0.5	0.002808	0.5	0.00015	0.5

Character	Ch. State	Node 9		Node 10		Node 11		Node 12	
		BL	Mk1	BL	Mk1	BL	Mk1	BL	Mk1
Phenology	Pr(0)	0.999979	0.99467189*	0.999999	0.99837184*	0.999925	0.97806805*	0.996581	0.80920635
	Pr(1)	0.000021	0.00459138	0.000001	0.001104863	0.000009	0.00845001	0.00007	0.04537186
	Pr(2)	0.000001	0.000736734	0.000001	0.00052333	0.000066	0.01348194	0.003349	0.14542179

## APPENDIX F

**Bayesian Posterior Probability Results for Ancestral State Reconstructions of  
Climatic Variables Using the Branch Length Model in Simmap 1.5 Analyses for all  
Character States (Ch. State)**

<b>Climate Variable</b>	<b>Ch. State</b>	<b>Node 1</b>	<b>Node 2</b>	<b>Node 3</b>	<b>Node 4</b>	<b>Node 5</b>	<b>Node 6</b>
<b>Annual Mean Temperature</b>	Pr(0)	0.000001	0.000069	0.000002	0.000122	0.000006	0.000002
	Pr(1)	0.000001	0.000036	0.000001	0.000025	0.000272	0.009692
	Pr(2)	0.999991	0.999546	0.999973	0.998212	0.999661	0.990289
	Pr(3)	0.000007	0.00035	0.000024	0.001641	0.000062	0.000018
<b>Temperature Seasonality</b>	Pr(0)	0.040876	0.936305	0.999975	0.999999	0.999971	0.990289
	Pr(1)	0.000005	0.000222	0	0.000001	0.000028	0.009692
	Pr(2)	0.000005	0.000209	0	0	0	0.000002
	Pr(3)	0.959115	0.063264	0.000025	0	0.000001	0.000018
<b>Mean Temperature of Wettest Quarter</b>	Pr(0)	0.000001	0.000069	0.000002	0.000122	0.000006	0.000002
	Pr(1)	0.999991	0.999546	0.999973	0.998212	0.999661	0.990289
	Pr(2)	0.000007	0.00035	0.000024	0.001641	0.000062	0.000018
	Pr(3)	0.000001	0.000036	0.000001	0.000025	0.000272	0.009692
<b>Mean Temperature of Driest Quarter</b>	Pr(0)	0.000001	0.000069	0.000002	0.000122	0.000006	0.000002
	Pr(1)	0.999991	0.999546	0.999973	0.998212	0.999661	0.990289
	Pr(2)	0.000007	0.00035	0.000024	0.001641	0.000062	0.000018
	Pr(3)	0.000001	0.000036	0.000001	0.000025	0.000272	0.009692
<b>Mean Temperature of Warmest Quarter</b>	Pr(0)	0.000001	0.000069	0.000002	0.000122	0.000006	0.000002
	Pr(1)	0.999991	0.999546	0.999973	0.998212	0.999661	0.990289
	Pr(2)	0.000007	0.00035	0.000024	0.001641	0.000062	0.000018
	Pr(3)	0.000001	0.000036	0.000001	0.000025	0.000272	0.009692
<b>Mean Temperature of</b>	Pr(0)	0.000001	0.000069	0.000002	0.000122	0.000006	0.000002

<b>Climate Variable</b>	<b>Ch. State</b>	<b>Node 1</b>	<b>Node 2</b>	<b>Node 3</b>	<b>Node 4</b>	<b>Node 5</b>	<b>Node 6</b>
<b>Coldest Quarter</b>	Pr(1)	0.999991	0.999546	0.999973	0.998212	0.999661	0.990289
	Pr(2)	0.000007	0.00035	0.000024	0.001641	0.000062	0.000018
	Pr(3)	0.000001	0.000036	0.000001	0.000025	0.000272	0.009692
<b>Precipitation of Coldest Quarter</b>	Pr(0)	0.77392	0.975283	0.999985	0.999987	0.999959	0.990289
	Pr(1)	0.049754	0.010435	0.000012	0.000012	0.000003	0.000018
	Pr(2)	0.000087	0.000244	0	0.000001	0.000037	0.009692
	Pr(3)	0.176239	0.014037	0.000003	0	0	0.000002

<b>Character</b>	<b>Ch. State</b>	<b>Node 7</b>	<b>Node 8</b>	<b>Node 9</b>	<b>Node 10</b>	<b>Node 11</b>	<b>Node 12</b>
<b>Annual Mean Temperature</b>	Pr(0)	0.000001	0.038148	0.000035	0.000007	0.000001	0.000001
	Pr(1)	0.000009	0.000088	0	0.000007	0.000001	0.000001
	Pr(2)	0.999985	0.413924	0.009801	0.395795	0.999992	0.999989
	Pr(3)	0.000005	0.547839	0.990163	0.604191	0.000007	0.000009
<b>Temperature Seasonality</b>	Pr(0)	0.999985	0.999999	0.999994	0.9992	0.999996	0.999989
	Pr(1)	0.000009	0	0	0.000001	0	0.000001
	Pr(2)	0.000001	0	0.000005	0.000791	0	0.000001
	Pr(3)	0.000005	0	0.000001	0.000007	0.000003	0.000009
<b>Mean Temperature of Wettest Quarter</b>	Pr(0)	0.000001	0.038148	0.000035	0.000007	0.000001	0.000001
	Pr(1)	0.999985	0.413924	0.009801	0.395795	0.999992	0.999989
	Pr(2)	0.000005	0.547839	0.990163	0.604191	0.000007	0.000009
	Pr(3)	0.000009	0.000088	0	0.000007	0.000001	0.000001

<b>Character</b>	<b>Ch. State</b>	<b>Node 7</b>	<b>Node 8</b>	<b>Node 9</b>	<b>Node 10</b>	<b>Node 11</b>	<b>Node 12</b>
<b>Mean Temperature of Driest Quarter</b>	Pr(0)	0.000001	0.038148	0.000035	0.000007	0.000001	0.000001
	Pr(1)	0.999985	0.413924	0.009801	0.395795	0.999992	0.999989
	Pr(2)	0.000005	0.547839	0.990163	0.604191	0.000007	0.000009
	Pr(3)	0.000009	0.000088	0	0.000007	0.000001	0.000001
<b>Mean Temperature of Warmest Quarter</b>	Pr(0)	0.000001	0.038148	0.000035	0.000007	0.000001	0.000001
	Pr(1)	0.999985	0.413924	0.009801	0.395795	0.999992	0.999989
	Pr(2)	0.000005	0.547839	0.990163	0.604191	0.000007	0.000009
	Pr(3)	0.000009	0.000088	0	0.000007	0.000001	0.000001
<b>Mean Temperature of Coldest Quarter</b>	Pr(0)	0.000001	0.038148	0.000035	0.000007	0.000001	0.000001
	Pr(1)	0.999985	0.413924	0.009801	0.395795	0.999992	0.999989
	Pr(2)	0.000005	0.547839	0.990163	0.604191	0.000007	0.000009
	Pr(3)	0.000009	0.000088	0	0.000007	0.000001	0.000001
<b>Precipitation of Coldest Quarter</b>	Pr(0)	0.999985	0.998741	0.99998	0.999999	0.999996	0.999989
	Pr(1)	0.000005	0.001257	0.00002	0	0.000003	0.000009
	Pr(2)	0.000009	0.000002	0	0	0	0.000001
	Pr(3)	0.000001	0.000001	0	0	0	0.000001